

## DOCTOR OF PHILOSOPHY

### Experimental investigation of emission from a light duty diesel engine utilizing urea spray SCR system

Tamaldin, Noreffendy

*Award date:*  
2010

*Awarding institution:*  
Coventry University

[Link to publication](#)

#### General rights

Copyright and moral rights for the publications made accessible in the public portal are retained by the authors and/or other copyright owners and it is a condition of accessing publications that users recognise and abide by the legal requirements associated with these rights.

- Users may download and print one copy of this thesis for personal non-commercial research or study
- This thesis cannot be reproduced or quoted extensively from without first obtaining permission from the copyright holder(s)
- You may not further distribute the material or use it for any profit-making activity or commercial gain
- You may freely distribute the URL identifying the publication in the public portal

#### Take down policy

If you believe that this document breaches copyright please contact us providing details, and we will remove access to the work immediately and investigate your claim.

# **Experimental Investigation of Emission from a Light Duty Diesel Engine Utilizing Urea Spray SCR system**

By  
**Noreffendy Tamaldin**

**PhD**

**June 2010**



The work contained within this document has been submitted  
by the student in partial fulfilment of the requirement of their course and award



EXPERIMENTAL INVESTIGATION OF  
EMISSION FROM A LIGHT DUTY  
DIESEL ENGINE UTILIZING  
UREA SPRAY SCR SYSTEM

NOREFFENDY TAMALDIN, M.Eng.

A thesis submitted in partial fulfilment of the University's requirements for the  
Degree of Doctor of Philosophy

JUNE 2010

## ACKNOWLEDGEMENTS

This thesis is the culmination of over three years of research at AEARG (Automotive Engineering Applied Research Group), Coventry University. It is over three years of which I have survived only through the help and understanding of many people. I would like to thank them here. First and foremost, I would like to express my appreciation to the AEARG director who is also my supervisor Professor S.F. Benjamin for offering me this enriching opportunity and experience to pursue my Ph.D. I would also like express my gratitude for his untiring patience and encouragement when obstacles and difficulties arise, guidance in my research, and for his good example that urges me to progress academically and personally.

I would also like to convey my invaluable thanks to Dr. C. A. Roberts, for her indispensable guidance and kind support, her involvement in the project, continuous advice, support and useful discussions. Without all of these, this work may not have been completed. Special thank Dr. A.J. Alimin for training me on setting up and running the test bed, analyzers and the Froude control system. To Dr S. Quadri for calibration and setting up the Ricardo air flow meter. To Mr. R. Gartside, thank you for his help during the commissioning of the engine, test bed and the engine control system. To Mr E. Larch for the engine ECU programming and Gredi setup. To Mr S. Goodall (Brico) for his technical advice. The technical help and assistance from, Mr C. Thorneycroft, Mr. S Allitt, Mr. C. Roebuck and the late Mr. K.Smith are also appreciated and acknowledged.

I am indebted to UTeM and MOHE (Ministry of Higher Education), Malaysia for providing the financial support throughout my study and the following companies: Jaguar Land Rover, Johnson Matthey Catalyst and Faurecia, for their technical provisions for the experimental works.

I cannot end without thanking my family on whose constant encouragement and love I have relied throughout my study, especially my parents, Tamaldin Bahardin and Zaiton Husin for their love and emotional support. My gratitude also goes to my Faculty Dean, Professor Dr Md. Razali Ayob, for believing in me and his continuous moral support to make sure I complete my study.

Last but not least, my deepest love and appreciation to my dearest wife, Maseidayu Zolkiffili and my wonderful kids, Ameer Husaini and Amaar Zuhasny, for their passion and suffering being with me in the challenging weather and life in the UK throughout my study. They are all the reason I continue improving myself being a better person for a better life.



## ABSTRACT

Stringent pollutant regulations on diesel-powered vehicles have resulted in the development of new technologies to reduce emission of nitrogen oxides (NO<sub>x</sub>). The urea Selective Catalyst Reduction (SCR) system and Lean NO<sub>x</sub> Trap (LNT) have become the two promising solutions to this problem. Whilst the LNT results in a fuel penalty due to periodic regeneration, the SCR system with aqueous urea solution or ammonia gas reductants could provide a better solution with higher NO<sub>x</sub> reduction efficiency.

This thesis describes an experimental investigation which has been designed for comparing the effect NO<sub>x</sub> abatement of a SCR system with AdBlue urea spray and ammonia gas at 5% and 4% concentration. For this study, a SCR exhaust system comprising of a diesel particulate filter (DPF), a diesel oxidation catalyst (DOC) and SCR catalysts was tested on a steady state, direct injection 1998 cc diesel engine. It featured an expansion can, nozzle and diffuser arrangement for a controlled flow profile for CFD model validation. Four different lengths of SCR catalyst were tested for a space velocity study. Chemiluminescence (CLD) based ammonia analysers have been used to provide high resolution NO, NO<sub>2</sub> and NH<sub>3</sub> measurements across the SCR exhaust system. By measuring at the exit of the SCR bricks, the NO and NO<sub>2</sub> profiles within the bricks were found. Comparison of the measurements between spray and gas lead to insights of the behaviour of the droplets upstream and within the SCR bricks.

From the analysis, it was deduced that around half to three quarters of the droplets from the urea spray remain unconverted at the entry of the first SCR brick. Approximately 200 ppm of potential ammonia was released from the urea spray in the first SCR brick to react with NO<sub>x</sub>. The analysis also shows between 10 to 100 ppm of potential ammonia survived through the first brick in droplet form for cases from NO<sub>x</sub>-matched spray input to excess spray. Measurements show NO<sub>x</sub> reduction was complete after the second SCR bricks. Experimental and CFD prediction showed breakthrough of all species for the short brick with gas injection due to the high space velocity. The long brick gas cases predictions gave reasonable agreement with experimental results. NO<sub>2</sub> conversion efficiency was found higher than NO which contradicts with the fast SCR reaction kinetics.

Transient response was observed in both cases during the NO<sub>x</sub> reduction, ammonia absorption and desorption process. From the transient analysis an estimate of the ammonia storage capacity of the bricks was derived. The amount of ammonia slippage was obtained through numerical integration of the ammonia slippage curve using an excel spreadsheet. Comparing the time constant for the spray and gas cases, showed a slightly faster time response from the gas for both NO<sub>x</sub> reduction and ammonia slippage.

## TABLE OF CONTENTS

CHAPTER	TITLE	PAGE
	ACKNOWLEDGEMENTS.....	ii
	ABSTRACT.....	iii
	TABLE OF CONTENTS.....	iv
	LIST OF TABLES .....	x
	LIST OF FIGURES .....	xi
	LIST OF ABBREVIATIONS AND SYMBOLS.....	xiv
	LIST OF APPENDICES .....	xx
<b>CHAPTER 1 : INTRODUCTION .....</b>		<b>1</b>
1.0 Background of Air pollution. ....		1
1.1.1 History of Pollution .....		1
1.1.2 Diesel Emission Regulation. ....		3
1.2 Motivation of this thesis .....		4
1.2.1 Aims and Objectives.....		4
1.2.2 Thesis Organisation.....		5
<b>CHAPTER 2 LITERATURE REVIEW.....</b>		<b>6</b>
2.0 Diesel After-treatment on NO <sub>x</sub> Emission Overview .....		6
2.1 Principle of Operation: Selective Catalyst Reduction (SCR).....		6
2.2 Diesel Oxidation Catalyst (DOC) and Diesel Particulate Filter (DPF).....		8
2.2.1 Effect of NO <sub>2</sub> /NO ratio on NO <sub>x</sub> conversion.....		12
2.3 SCR Catalyst types.....		13
2.3.1 Platinum catalysts .....		13
2.3.2 Vanadia Titania Catalysts .....		14
2.3.3 Zeolite Catalyst.....		14

2.3.3.1 High Temperature Zeolite .....	14
2.3.3.1 Low temperature Zeolite .....	15
2.3.4 Comparison of SCR catalysts.....	16
2.4 SCR reductants .....	17
2.4.1 Aqueous Ammonia.....	17
2.4.2 Anhydrous ammonia.....	20
2.5 Challenges in automotive SCR. ....	20
2.5.1 Ammonia slip .....	21
2.5.2 Uniform mixing of Urea. ....	21
2.5.4 Space velocity .....	22
2.5.5 Light duty diesel engine study .....	22
2.5.6 Urea spray droplet modelling .....	22
<b>CHAPTER 3: RESEARCH METHODOLOGY .....</b>	<b>25</b>
3.0 Introduction .....	25
3.1 Engine Commissioning and Setup .....	25
3.1.1 Engine Commissioning and Setup for Steady State Test. ....	25
3.1.2 Engine Dynamometer .....	27
3.1.3 Engine mass flow rate measurement .....	27
3.2 Final SCR Exhaust build and commissioning. ....	28
3.2.1 SCR Exhaust Fabrications and Specifications. ....	30
3.2.2 DPF-DOC assembly.....	30
3.2.3 SCR Catalysts Assembly.....	31
3.2.4 Urea Spray Mixing Chamber .....	32
3.2.5 Instrumentation module assembly.....	33
3.2.6 Long and short diffuser assembly .....	34
3.2.7 Bypass pipe assembly. ....	34
3.2.8 DPF Monitoring and Preconditioning .....	34

3.2.10 SCR Catalyst Monitoring and Preconditioning.....	35
3.3 EXSA 1500 NOx Analyser Setup .....	35
3.3.1 EXSA 1500 Specifications and Resolutions .....	35
3.3.2 Gas requirements and Calibration Gases .....	36
3.3.3 NOx measurement procedure .....	37
3.4 Ammonia analyser MEXA 1170Nx .....	38
3.4.1 MEXA1170Nx Specification and Resolution.....	39
3.4.2 MEXA 1170Nx Gas Requirements and Calibration. ....	40
3.4.3 MEXA 1170Nx Working Principles .....	43
3.4.3a Working Principle of Chemiluminescence (CLD).....	43
3.4.3b Interference of CO <sub>2</sub> and H <sub>2</sub> O.....	44
3.4.3c Measurement of NOx.....	44
3.4.4 NOx measurement in NH <sub>3</sub> mode. ....	45
3.4.5 NO <sub>2</sub> measurement in NO <sub>2</sub> mode.....	45
3.5 ETAS Lambda Meter.....	46
3.6 Urea Spray Setup .....	47
3.6.1 Urea Spray Calibration .....	48
3.6.2 Urea Spray Pulse Length Setting Procedure .....	49
3.6.3 Engine NOx Out Mapping .....	49
3.6.4 The Urea Spray Layout and Experimental Procedure .....	52
3.6.5 Spray Setting and Cleaning Procedures. ....	54
3.6.6 Deposit build up on Spray.....	56
3.6.7 Cleaned Spray inspection.....	57
3.7 NH <sub>3</sub> Gas Experimental Setup.....	59
3.7.1 NH <sub>3</sub> Gas Supply and Nozzle Location. ....	59
3.7.2 Gas flow meter and pressure gauge. ....	60
3.7.3 NH <sub>3</sub> gas experimental layout. ....	61

3.7.4 NH <sub>3</sub> Gas Experimental Procedure. ....	62
3.8 NO/NO <sub>2</sub> measurement for DPF-DOC arrangement. ....	63
3.8.1 DOC-DPF configuration. ....	63
3.8.2 DPF-DOC configuration. ....	64
3.9 Measurement using various sampling probe length. ....	66
3.10 Problems associated with the MEXA Analyser ....	68
3.11 Final measurement strategies. ....	73
3.12 Summary of final experimental procedures. ....	76
3.13 Example of measurements strategy applied ....	77
<b>CHAPTER 4: EXPERIMENTAL RESULTS AND DISCUSSIONS .....</b>	<b>79</b>
4.0 Experimental results: Introduction .....	79
4.1.0 Urea spray studies: General overview .....	79
4.1.1 Urea spray studies: Upstream Measurements (1 and 4 SCR bricks) .....	80
4.1.2 Urea spray studies: Downstream Measurements (1 and 4 SCR bricks).....	80
4.1.3 Urea spray studies: Deduced value.....	81
4.1.4 Urea sprays studies: Ammonia levels. ....	81
4.1.5 Measurement with Urea Spray and 1 SCR bricks. ....	82
4.1.6 Measurement with Urea Spray and 4 SCR bricks. ....	83
4.2 Ammonia gas studies: General Overview .....	84
4.2.1 Ammonia gas studies: upstream measurements. (1 and 4 SCR bricks).....	84
4.2.2 Ammonia gas studies: downstream measurements. (1 and 4 SCR bricks).....	85
4.2.3 Ammonia gas studies: Deduced values.....	85
4.2.4 Ammonia gas studies: Ammonia levels .....	86
4.2.5 Measurement with 5% Ammonia Gas and 1 SCR brick. ....	87
4.2.6 Measurement with 5% Ammonia Gas and 2 SCR bricks.....	87
4.2.7 Measurement with 5% Ammonia Gas and 3 SCR bricks.....	88
4.2.8 Measurement with 5% Ammonia Gas and 4 SCR bricks.....	89

4.2.9 Measurement with 4% Ammonia Gas and 1 SCR bricks.....	90
4.3 Analysis of measurement results against ammonia input/potential ammonia input.....	91
4.4 Analysis of spray compared to gas.....	92
4.5 Analysis of insight behaviour of droplet from the urea spray. ....	93
4.5.1 Ammonia released from urea spray upstream of the SCR bricks.....	93
4.5.2 Ammonia released from urea spray within the 4 SCR bricks.....	94
4.5.3 Ammonia passing through 1 SCR brick in droplets form. ....	94
4.6 Analysis of NO and NO <sub>2</sub> conversion efficiency and ammonia slip. ....	95
4.6.1 NO conversion efficiency .....	96
4.6.2 NO <sub>2</sub> conversion efficiency.....	97
4.6.3 Comparison of NO and NO <sub>2</sub> conversion.....	98
4.6.4 Ammonia slip. ....	99
4.7 CFD modelling analysis comparison with measurements. ....	100
4.7.1 CFD data comparison with ammonia gas injection for 1 SCR and 4 SCR bricks.....	101
4.8 Comparison of CFD prediction with NO <sub>2</sub> , NO and NH <sub>3</sub> at the SCR exit.....	102
4.8.1 CFD prediction comparison of NO <sub>2</sub> with measurement results.....	102
4.8.2 CFD prediction comparison of NO with measurement results.....	103
4.8.3 CFD prediction comparison of NH <sub>3</sub> with measurement results.....	103
4.8.4 Overall remark from CFD comparison with measurements. ....	104
4.9 Transient analysis in the investigation.....	105
4.9.1 Transient analysis of 4 SCR bricks with 4% NH <sub>3</sub> gas.....	105
4.9.1.1 Time constants for gas. ....	108
4.9.2 Transient analysis of 4 SCR brick with urea spray.....	109
4.9.2.1 Time constants for urea spray. ....	111
4.9.3 Comparison of the urea spray and ammonia gas transients.....	111
4.10 Summary of the experimental and simulation results. ....	112

<b>CHAPTER 5 CONCLUSIONS AND FUTURE WORK .....</b>	<b>114</b>
5.0 Conclusions and Future work: Introduction. ....	114
5.1 DPF-DOC arrangement.....	114
5.2 Experimental techniques. ....	114
5.3 Behaviour of urea droplet from spray. ....	115
5.4 Space velocity and resident time effect.....	115
5.5 Transient observation and storage. ....	115
5.6 Significant of findings in chapter 4.....	116
5.7 Contributions to the knowledge .....	116
5.8 Recommendation for Future Work.....	117
5.8.1 Improved gas analyser to measure NO <sub>x</sub> in presence of ammonia.....	117
5.8.2 Spray dosing system.....	117
5.8.3 Cleaning of spray or continuous spraying.....	118
5.8.4 Improved warm up and system using sequential program. ....	118
5.8.5 Signal trigger improvement with level differentiation of spray pulses and gas settings. ....	118
5.8.6 Investigation of effect of spray angle and positions.....	118
5.8.7 Moving from 1D to 3D flow .....	118
5.8.8 Transient study (acceleration and deceleration).....	119
5.8.9 Engine Mass flow rate measurement and logging.....	119
<b>REFERENCES .....</b>	<b>120</b>
<b>APPENDICES .....</b>	<b>134</b>

## LIST OF TABLES

TABLE	TITLE	PAGE
1.1.2	Evolution of European emission regulations (reproduced from DieselNet 2010).....	3
2.3.1	Various SCR Catalyst Temperature range. ....	16
3.1.1	Diesel Engine specification used for investigation (Ford 2FM series) .....	26
3.2.2	Detail specification of the DOC catalyst.....	31
3.2.3	Detail specification of the SCR catalyst.....	32
3.3.1	Technical Specifications of EXSA 1500 Common gas analyser [Extracted from the Horiba Ltd, EXSA 1500 operating manual Oct 2004] .....	36
3.4.2	Gas Requirement for MEXA-1170Nx Analyser. ....	40
3.8.1	NO/ NO <sub>2</sub> ratio based on DOC-DPF assembly. ....	64
3.10a	MEXA analyser performance when measuring a mixture of NO, NO <sub>2</sub> and NH <sub>3</sub> .....	72
3.11a	Measurement strategy when using Horiba MEXA 1170Nx ammonia analyser.....	75
3.11b	Experimental test matrix with urea spray and NH <sub>3</sub> gas.....	76
4.1.5	Summary of Result: Urea Spray with 1 SCR. ....	82
4.1.6	Summary of Result: Urea Spray with 4 SCR. ....	83
4.2.5	Summary of Result: 5% Ammonia Gas with 1 SCR. ....	87
4.2.6	Summary of Result: 5% Ammonia Gas with 2 SCR. ....	88
4.2.7	Summary of Result: 5% Ammonia Gas with 3 SCR. ....	89
4.2.8	Summary of Result: 5% Ammonia Gas with 4 SCR. ....	90
4.2.9	Summary of Result: 4% Ammonia Gas with 1 SCR.....	91
4.6.1	Space velocity for SCR bricks used in the investigation. ....	97
4.9.3	Comparison of the 4% gas with urea spray transient analysis. ....	112



## LIST OF FIGURES

FIGURE	TITLE	PAGE
1.1.1	Increasing popularity of diesel powered vehicle in the United Kingdom (reproduced from SMMT Motor Industry Fact 2010).....	2
1.1.2	Euro 6 (2014) LDD NO <sub>x</sub> regulations compared to US Tier 2 Bin 5 and California SULEV (Bin2). [Johnson T.V. 2009].....	4
2.1	SCR system configurations with open loop urea SCR system [DieselNet 2005].....	8
2.2	Wall-Flow DPF [reproduced from Heck 2009] .....	9
2.2a	Possible architecture for NO <sub>x</sub> /PM control.....	10
2.2b	Schematic of an advance diesel after treatment system architecture compared in Gurupatham et al (2008) .....	10
2.2c	Advance diesel after treatment system with SCRF concepts [Guo et al 2010] .....	11
2.2.1a	Effect of NO <sub>2</sub> /NO ratio on NO <sub>x</sub> conversion in V <sub>2</sub> O <sub>5</sub> /TiO <sub>2</sub> catalyst .....	12
2.2.1b	Effect of NO <sub>2</sub> from DOC on NO <sub>x</sub> conversion.....	13
2.3	Comparison of SCR catalyst operating temperature windows [Walker 2005].....	16
2.4.1a	Urea solution freezing point [BASF 2003].....	19
2.4.1b	Urea solution 32.5% decomposition [BASF 2003].....	19
3.1.1	The 2FM series engine with Injection Control Unit (ICU) and Engine Control Unit (ECU) on Froude Consine AG150 engine dynamometer.....	26
3.1.4	Ricardo mass flow meter measuring engine Mass Flow Rate (MFR).....	28
3.2	Final assembly of the SCR exhaust system.....	29
3.2.1	The suspended exhaust from a square metal frame.....	30
3.2.4	The Urea spray mixing chamber.....	32
3.2.5	Instrumentation modules location along the SCR exhausts system.....	33
3.3.2	EXSA 1500 NO <sub>x</sub> analyzer gas piping configuration.....	37
3.4	The MEXA-1170Nx NH <sub>3</sub> analyzer unit.....	39
3.4.2	Gas piping Layout for MEXA-1170NX ammonia analyzer.....	41
3.3.4	Process flow of MEXA-1170NX daily operation and calibration.....	42
3.4.4	NH <sub>3</sub> mode of MEXA-1170NX analyzer.....	45
3.4.5	NO <sub>2</sub> mode of MEXA-1170NX analyzer.....	46
3.5	ETAS LA4 Lambda meter used to measure O <sub>2</sub> before and after the SCR catalysts.....	47
3.6	Schematic of a manual urea spray system.....	47

3.6.1	Calibration chart of mass flow rate (mg/s) against spray pulse length (ms) [courtesy Dr C.A. Roberts].....	48
3.6.2	Chart showing estimated urea/AdBlue (g/s) required against engine NOx out (ppm)....	49
3.6.3a	Engine NOx out based on load BMEP (bars), speed (RPM) and EGR ON.....	50
3.6.3b	Exhaust Mass Flow (g/s) based on load, BMEP (bars), speed (RPM) and EGR ON.....	50
3.6.4a	Urea AdBlue injector testing prior to experimental with spray system.....	52
3.6.4b	Urea Spray injector and supply pipes and wiring in place.....	53
3.6.4d	Urea spray system experimental layout.....	54
3.6.5a	Spray cleaning procedures flow chart.....	55
3.6.6	White deposit build up and ultrasonic cleaning.....	56
3.6.6e	Manual cleaning of injector sleeve with tweezers.....	57
3.6.7	Final visual inspection of fully cleaned injector.....	58
3.7.1b	NH <sub>3</sub> gas injection nozzle.....	60
3.7.2	Gas flow meter reading as a guide. ....	61
3.7.3	NH <sub>3</sub> gas experimental layout.....	62
3.8.1	Initial configuration with DOC-DPF assembly.....	64
3.8.2	Final DPF-DOC assembly.....	65
3.9a	Variation of sampling probe length for profile measurement.....	66
3.9b	Long (55 mm) sampling probe.....	67
3.9c	Medium (25 mm) sampling probe.....	67
3.9d	Check point with medium sampling probe for gas measurement.....	68
3.10a	Rubber seal disintegrate in the SUM NOx converter.....	69
3.10.1b	Paper based finger filter located at the back of MEXA 1170Nx ammonia analyser.....	69
3.10c	Spherical carbon compact NOx converter.....	70
3.10d	New glassy carbon NOx converter.....	70
3.10e	A typical example of erroneous measurement of NOx in present of ammonia.....	71
3.13	Example of engine log from 5% ammonia gas with 1 scr brick.....	78
4.1a	Typical example of erroneous measurement of NOx in present of ammonia.....	78
4.3	Summary of measurement with 1 and 4 SCR bricks.....	92
4.5.1	Ammonia released from spray upstream of the SCR bricks.....	93
4.5.2	Ammonia released from urea spray within 4 SCR bricks.....	94
4.5.3	Ammonia passing through 1 SCR brick in droplets form. ....	95
4.6.1	NO conversion with respect to SCR length.....	96
4.6.2	NO <sub>2</sub> conversion with respect to SCR length.....	98

4.6.3	Comparison of NO and NO <sub>2</sub> conversion efficiency.....	99
4.6.4	Ammonia slip against potential ammonia input with respect to SCR brick length.....	100
4.7.1a	CFD and data comparison for species level at exit from 1 SCR brick.....	101
4.7.1b	CFD and data comparison for species levels at exit from 4 SCR bricks.....	101
4.8.1	Simulations of NO <sub>2</sub> against measurements at SCR exit. ....	102
4.8.2	Simulations of NO against measurements at SCR exit. ....	103
4.8.3	Simulations of NH <sub>3</sub> against measurements at SCR exit. ....	104
4.9.1	Sample of transient response in 4 SCR bricks with 4% NH <sub>3</sub> gas.....	105
4.9.1a	Transient analysis for 4% gas with 4 SCR.....	106
4.9.2	Transient analysis for urea spray with 4 SCR.....	109

## LIST OF ABBREVIATIONS AND SYMBOLS

$\alpha$	-	Alpha – ratio of $\text{NH}_3$ : $\text{NO}_x$
$\lambda$	-	Ratio between actual AFR and stoichiometric AFR
ACEA	-	European Automobile Manufacturers Association
AdBlue	-	Registered trademark for AUS32 (Aqueous Urea Solution 32.5%)
AEARG	-	Automotive Engineering Applied Research Group, Coventry University
AFR	-	Air Fuel Ratio
$\text{Al}^{+3}$	-	Aluminium cations
$\text{Al}_2(\text{SO}_4)_3$	-	Aluminium Sulfate
$\text{Al}_2\text{O}_3$	-	Aluminium Oxide
AMI	-	AdBlue supplier - Agrolinz Melamine International (Austria)
Anatase	-	One of the three mineral forms of titanium dioxide, the other two being brookite and rutile. It is always found as small, isolated and sharply developed crystals, and like rutile, a more commonly occurring modification of titanium dioxide, it crystallizes in the tetragonal system.
ARB	-	Air Resource Board
ASAM	-	Association for Standardization of Automation and Measuring Systems
AUS32	-	Aqueous Urea Solution 32.5% by weight.
BaO	-	Barium Oxide is a white Hygroscopic Compound Formed by the Burning of Barium in Oxygen.
BASF	-	AdBlue supplier, German Chemical Company, Badische Anilin und Soda Fabrik (Baden Anilin and Soda Factory)
Bhp-hr	-	Brake horse power-hour (typical unit for emission in the United States)

BMEP	-	Brake Mean Effective Pressure (bar)
BSP	-	British Standard Pipe Taper thread
CAE	-	Computer Aided Engineering
CAFE	-	Corporate Average Fuel Economy
CAL	-	Calibration
CAN	-	Controller Area Network (computer network protocol and bus standard designed to allow microcontrollers and devices to communicate with each other and without a host computer.)
CARB	-	California Air Resource Board
CEFIC	-	European Chemical Industry Council
CFD	-	Computational Fluid Dynamics
CLD	-	Chemiluminescence Detector
CNG	-	Compressed Natural Gas is a fossil fuel substitute for gasoline (petrol), diesel, or propane fuel.
CO	-	Carbon Monoxide
CO <sub>2</sub>	-	Carbon Dioxide
CRT	-	Continuously Regenerating Technology filter
Cu	-	Copper
DEF	-	Diesel Exhaust Fluid
DIN 70070	-	German Industrial Standard on Specification of SCR Urea Grade, (DIN- Deutsches Institut für Normung. German Institute for Standardization)
DOC	-	Diesel Oxidation Catalysts
DPF	-	Diesel Particulate Filters
dSPACE	-	A software package integrated with Matlab Simulink use to control the throttle body of an engine.

ECE R49	-	European Cycle Emission Revision 49
ECU	-	Engine Control Unit
EEC(CED)	-	European Commission Directive
EGR	-	Exhaust Gas Recirculation
EMS	-	Engine Management System
EPA	-	Environmental Protection Agency, United States
ESC	-	European Steady Cycle
FAN MOG		Fleet Average Non-methane Organic Gases
FBC	-	Fuel Borne Catalyst
GHG	-	Green House Gases
GREDI	-	Engine ECU calibration software from Kleinknecht Automotive GmbH
GVWR	-	Gross Vehicle Weight Rating
H <sub>2</sub> O	-	Water
HC	-	Hydrocarbon
HLDT	-	Heavy light-duty trucks
HNCO	-	Isocyanic Acid
ICU	-	Injection Control Unit
JAMA	-	Japan Automobile Manufacturers Association
JARI	-	Japan Automotive Research Institute
kW	-	Kilowatt (Power)
LDD	-	Light Duty Diesel
LDT	-	Light Duty Truck
LDV	-	Light Duty Vehicles

LEV	-	Low Emission Vehicle
LEV II	-	Low Emission Vehicle II
LLDT	-	Light light-duty Trucks
LNT	-	Lean NOx Trap
LPG	-	Liquid Petroleum Gas
MAF	-	Intake air Mass Air Flow
MECA	-	Manufacturer of Emissions Control Association
MKT	-	Market
MLW	-	Maximum Laden Weight
MoO <sub>3</sub>	-	Molybdenum trioxide
N <sub>2</sub>	-	Nitrogen gas
NAAQS	-	National Ambient Air Quality Standard
NGV	-	Natural Gas Vehicle
NH <sub>2</sub>	-	Amines are organic compounds and functional groups that contain a basic nitrogen atom with a lone pair
NH <sub>3</sub>	-	Ammonia
NH <sub>4</sub>	-	Ammonium cation (also known as ionized ammonia)
NMHC	-	Non-methane Hydro Carbon. All Hydrocarbons excluding methane.
NMOG	-	Non- methane Organic Gases. All Hydrocarbons and Reactive Oxygenated Hydrocarbon Species such as Aldehydes, but excluding Methane
NOx	-	Nitrogen Oxides ( NO and NO <sub>2</sub> )
NPT	-	National Pipe Thread Tapered Thread (NPT) is a U.S. standard for tapered threads.
O <sub>2</sub>	-	Oxygen gas

O <sub>3</sub>	-	Ozone
OEHHA	-	The Office of Environmental Health Hazard Assessment (California EPA)
OGU	-	Ozone Generator Unit
Pb	-	Lead
PEL	-	Permissible Exposure Level
PM	-	Particulate Matters
ppm	-	Parts per million
Pt	-	Platinum
PZEV	-	Partial Zero Emission Vehicle.
RPM	-	Speed in Revolution per Minute
Rutile	-	Mineral composed primarily of titanium dioxide, TiO <sub>2</sub> .
SAE	-	Society of Automotive Engineers
SAE J1088	-	SAE J1088 - Test Procedure for the Measurement of Gaseous Exhaust Emissions From Small Utility Engines
SCR	-	Selective Catalyst Reduction
SCRf	-	Combination of SCR and DPF with SCR washcoat on a DPF (Ford Motor)
SMMT	-	Society of Motor Manufacturers and Traders, UK Limited.
SO <sub>2</sub>	-	Sulphur Dioxides
SO <sub>3</sub>	-	Sulphur Trioxides
SOF	-	Organic Fraction of Diesel Particulates
STAR-CD	-	A CFD software package from CD-Adapco
SULEV	-	Super Ultra Low Emission Vehicle
SUV	-	Sport Utility Vehicle



T&E	-	Transport and Environment
TiO <sub>2</sub>	-	Titanium Dioxide
TLEV	-	Transitional Low Emission Vehicle.
ULEV	-	Ultra Low Emission Vehicle
UN ECE	-	United Nation European Cycle Emission
US, EPA	-	United States, Environmental Protection Agency
V <sub>2</sub> O <sub>5</sub>	-	Vanadium Oxides
VGT	-	Variable Geometry Turbocharger
VPU	-	Vacuum Pump Unit
WHTC	-	World Harmonized Transient Cycle
WO <sub>3</sub>	-	Tungsten trioxide
ZSM-5	-	Zeolite Sieve of Molecular Porosity (or Zeolite Socony Mobil)-5. It is a synthetic zeolite.

## LIST OF APPENDICES

APPENDIX Reference section numbered in thesis	TITLE	PAGE
3.1.1	Power curve for Ford 2.0 cc diesel engine	A-1
3.1.3	Ricardo mass flow meter calibration	A-2
3.2	Supplied parts for SCR exhaust build	A-3
3.2b	List of drawing for SCR exhaust system	A-4
3.4.1	MEXA 1170Nx specification	A-5
3.5	Lambda sensor LA4 connection configuration	A-6
3.6.2	Potential ammonia released from urea spray calculation	A-7
3.7a	Calibration chart for NH <sub>3</sub> gas flow rate using glass float	A-8
3.7b	Calibration chart for NH <sub>3</sub> gas flow rate using stainless steel float	A-9
3.7.1	Summary of gas flow rate with 4% and 5% ammonia in balance N <sub>2</sub>	A-10
3.7.1a	Calculation of gas flow rate with 4% ammonia in N <sub>2</sub> with steel float	A-11
3.7.1b	Calculation of gas flow rate with 4% ammonia in N <sub>2</sub> with glass float	A-12
3.7.1c	Calculation of gas flow rate with 5% ammonia in N <sub>2</sub> with steel float	A-13
3.7.1d	Gas flow setting/spray setting vs. ammonia level produced	A-14
4.0	List of appendices from chapter 4 : Experimental Results	B-1
4.1.5	Result from Urea spray : 1 SCR	B-2
4.1.5b	SUM in and SUM out average for 1 SCR with spray	B-3
4.1.6	Result from Urea spray : 4 SCR	B-4
4.1.6b	SUM in and SUM out average for 4 SCR with spray	B-5
4.2.5	Result from 5% Gas : 1 SCR	B-6
4.2.5b	NO dw 1SCR 5% : manual log from MEXA	B-6b
4.2.6	Result from 5% Gas : 2 SCR	B-7
4.2.7	Result from 5% Gas : 3 SCR	B-8
4.2.8	Result from 5% Gas : 4 SCR	B-9
4.2.9	Result from 4% Gas : 1 SCR	B-10
4.9.1a	Excel numerical integration – 4% gas 4 SCR	B-11
4.9.2a	Excel numerical integration – Urea spray 4SCR	B-12
5.0	Publication : SAE World Congress April 2010 Experimental Study of SCR in a Light-Duty Diesel Exhaust to Provide Data for Validation of a CFD Model Using the Porous Medium Approach (SAE 2010-01-1177)	C-1

## CHAPTER 1: INTRODUCTION

### 1.0 Background of Air pollution.

At present, there are many sources of air pollution from the combustion of fossil fuel for power plants, factories, office building, transportation and other. Air pollution can have a large negative impact on human health and the environment. The United States environmental protection agency (EPA) has identified six common pollutants including Ozone ( $O_3$ ), Particulate Matter (PM), Carbon Monoxide (CO), Sulphur Dioxide ( $SO_2$ ), Lead (Pb) and Nitrogen Oxides (NO<sub>x</sub>). The sum of nitric oxide (NO) and NO<sub>2</sub> is commonly called nitrogen oxides or NO<sub>x</sub>. Over the past decade, NO<sub>x</sub> emissions have become one of the concerns due to its health impact to human. Various studies have been conducted by numerous agencies around the world to evaluate the negative impact of NO<sub>x</sub> emission to human health. The World Health Organization (**WHO, 2002**) estimated that around 2.4 million people die every year linked to causes directly attributable to air pollution. A study at Birmingham University also revealed a strong correlation between deaths by pneumonia and traffic emissions in England. (**Knox, E.G. 2008**)

#### 1.1.1 History of Pollution

The environmental impact of automotive pollution has led governments to enforce automotive manufacturers to reduce quantities of tail-pipe emissions. Developments of the modern automotive catalytic converter and engine management systems have been in response to these requirements. There are an increasing number of vehicles in the world today with an estimate at around 800 million [**Preschern et al, 2001**]. The history of the new vehicle population over a ten year period in the United Kingdom shows the growing popularity of diesel powered vehicles over petrol since 2003. This is shown in figure 1.1.1. The rise of fuel prices and the advantages of diesel-powered vehicles in term of fuel efficiency have driven this trend.



Figure 1.1.1 Increasing popularity of diesel powered vehicle in the United Kingdom (reproduced from SMMT Motor Industry Fact 2010)

### **1.1.2 Diesel Emission Regulation.**

Diesel Emission control began in the mid 1980's when the United States, Environmental Protection Agency (EPA) and California Air Resource Board (CARB) starting to consider emission from on road vehicles. It started after a growing popularity of diesel engine patented by Rudolf Diesel in 1892 for replacing steam engines. In the past, only Carbon Monoxide (CO) and Hydrocarbon (HC) emission from gasoline engines were regulated [Heck, 2009].

The Three-Way catalytic (TWC) converter technology that has been successfully used on spark ignition internal combustion engines operating at stoichiometric air-fuel ratio (typically fuelled by petrol but also sometimes fuelled by LPG, CNG, or ethanol) since the middle 1980s will not function at  $O_2$  levels in excess of 1.0%, and do not function well at levels above 0.5%. Since diesels operate with excess oxygen, TWC cannot be utilized to reduce  $NO_x$  and alternative after treatment technology must be used.

In developed countries, automobiles must comply with statutory emission regulation to stay road-worthy. These are measured over a standard drive-cycle, typical of mixed driving conditions. A summary of the evolution of European emissions standards shows that future legislation will place even tighter restrictions on automotive emissions with Euro 6 NO<sub>x</sub> level at only 0.08 g/km. The evolution of European emission regulations is shown in the table 1.1.2.

Table 1.1.2 Evolution of European emission regulations (reproduced from **DieselNet 2010**)

Future legislation cannot be achieved in a cost-effective manner with current diesel after treatment technology; consequently, the prospect of reducing emissions without substantially increasing vehicle cost is attractive to manufacturers. Therefore, significant efforts have been driven to further improve the diesel after treatment. Automotive manufacturers have been tested with reducing NO<sub>x</sub> emissions especially for the latest Euro 6, US Bin 5 and California SULEV regulations.

Figure 1.1.2 Euro 6 (2014) LDD NOx regulations compared to US Tier 2 Bin 5 and California SULEV (Bin2). (Johnson T.V. 2009)

## **1.2 Motivation of this thesis**

The main motivation in this investigation is that the collaborating automotive manufacturers working with the Automotive Engineering Applied Research Group (AEARG) at Coventry University are required to find a cost effective diesel after treatment system to further reduce NOx pollution from light duty diesel powered passenger cars.

### **1.2.1 Aims and Objectives**

The thesis aims and objectives are:

- To investigate the SCR performance on a Light Duty Diesel (LDD) engine.

Most of the current SCR investigations are focused on Heavy Duty Diesel (HDD) engines. This investigation will provide information on the light duty diesel segment.

- To utilize zeolite in the SCR exhaust system.

Relatively few studies have been conducted on zeolite catalysts. Historically vanadium catalysts have been used for SCR.

- To develop a unique test facility and provide a database for CFD validation.

The SCR exhaust system built in this investigation provides an excellent opportunity for assessing the performance of simulation models.

- To develop a simplified controlled SCR exhaust system with real engine on test bed.

Most of SCR investigations use laboratory reactor and very little information is available from SCR system on real engine test beds. The experience gained in this investigation will be useful for future development.

### 1.2.2 Thesis Organisation

The organization of the thesis corresponds to the four objectives above.

**Chapter 2** reviews current understanding of SCRs and examines the relation between NO<sub>x</sub> reduction and NO/NO<sub>2</sub> ratio.

**Chapter 3** addresses the setting up of experiments, instrumentation and test protocol in order to achieve the objectives above.

**Chapter 4** presents and discusses the results obtained from the ammonia gas and urea spray experiments.

Finally, **Chapter 5** summarizes the contribution of this research to new knowledge and future work is proposed.

## CHAPTER 2: LITERATURE REVIEW

### 2.0 Diesel After-treatment for NOx reduction

Recent advancement in diesel after-treatment has identified two key promising technologies for reducing diesel emission which are the Lean NOx Trap (LNT) and Selective Catalyst Reduction (SCR) [Spurk et al., 2007]. Despite much research, improvements are needed in conversion efficiency across wider temperature ranges.

Alimin et al., (2006) explored the performance of an LNT at the Automotive Engineering Applied Research Group (AEARG), Coventry University. Whilst good NOx reduction was achieved the LNT system results in a fuel penalty due to regeneration period where rich combustion is needed to purge the trap. In contrast, the SCR system provides an alternative solution without an associated fuel penalty.

### 2.1 Principle of Operation: Selective Catalyst Reduction (SCR)

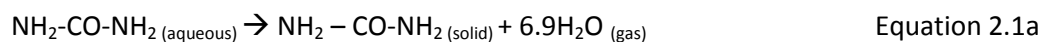
Selective catalytic reduction (SCR) is a means of removing nitrogen oxides, through a chemical reaction between the exhaust gases, a (reductant) additive, and a catalyst. Beeck et al., (2006) suggested the use of gaseous or liquid reductant (most commonly urea or AdBlue) to be added to a stream of exhaust gas and absorbed onto a SCR catalyst. The reductant reacts with NOx in the exhaust stream to form harmless H<sub>2</sub>O (vapour) and N<sub>2</sub>.

Three main processes involved in the SCR technology involve thermal decomposition, hydrolysis and three NOx reduction SCR reactions. The three SCR reactions involved are Fast SCR, Standard SCR and Slow SCR reaction.

Koebel, M. et al., (2000) and Yim, S.D. et al., (2004) suggested that thermal decomposition occurred as the urea water solution is injected in the hot exhaust stream as below.



Urea droplets from the spray exchange mass, momentum and energy with surroundings hot exhaust gases leading to vaporization of water.



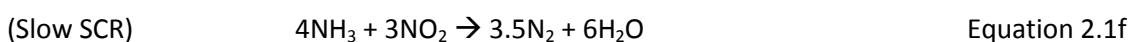
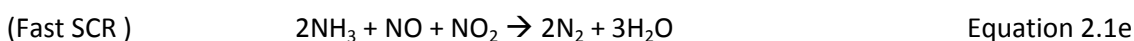
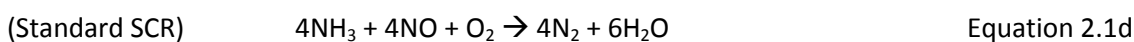
**Schaber et al., (2004)** reported that the Solid urea left from equation 2.1a started melting at 133°C and undergoes thermolysis to form ammonia and Isocyanic acid as follows:



**Yim S.D. et al., (2004)** also suggested the hydrolysis of Isocyanic acid is facilitated by high temperatures at around 400°C in the presence of a SCR catalyst. The Isocyanic acid which is stable in gas form undergoes hydrolysis to form ammonia and carbon dioxide as shown in equation 2.1c.



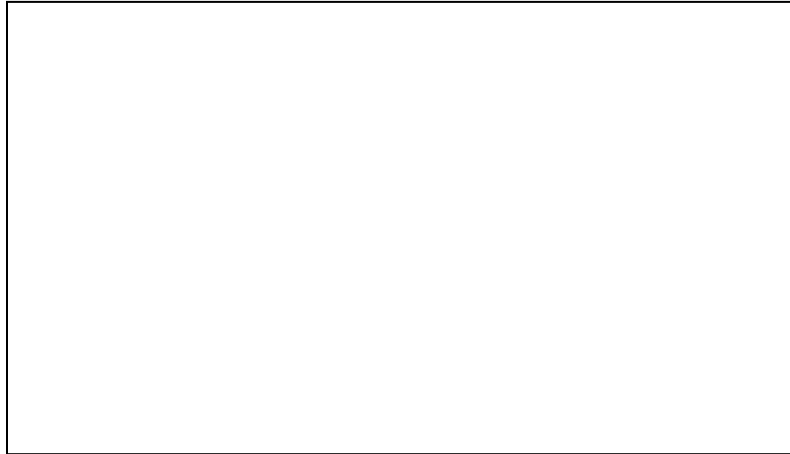
**Olsson et al., (2008)** reported once the  $\text{NH}_3$  gas is available, the three NOx reduction SCR reactions take place depending on the NOx source. The standard SCR using NO, Fast SCR with NO,  $\text{NO}_2$  and slow SCR with only  $\text{NO}_2$  as follows:



**Amon et al., (2004)** reported good NOx conversion efficiency with the SCR system in both stationary and transient test cycle of Japanese, European and US test cycle.

**Tennison et al., (2004)** investigations on light duty SCR with zeolite showed good NOx conversion level of over 90% for cold start FTP-75 and over 80% for the US06 cycle. A closed couple DOC was used to convert a portion of NO to  $\text{NO}_2$ . It was suggested that a mixture of NO and  $\text{NO}_2$  enhanced low temperature NOx conversion in light duty application.

Various SCR configurations have been used by different researchers and ongoing development is still underway especially for light duty application. A typical urea SCR schematic for heavy duty is shown in figure 2.1



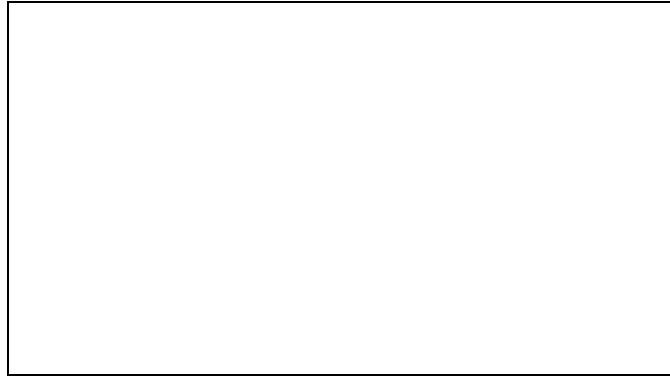
**Figure 2.1 SCR system configurations with open loop urea SCR system [DieselNet 2005].**

## **2.2 Diesel Oxidation Catalyst (DOC) and Diesel Particulate Filter (DPF)**

Diesel Oxidation catalyst and particulate filter have been widely used for PM removal in diesel applications. DOC is one of the oldest technologies originated from the early two way catalyst for controlling CO, HC and PM. DOC works by oxidizing unburned species of fuel in the exhaust to harmless products such as  $\text{CO}_2$  and  $\text{H}_2\text{O}$ . DOCs come in metallic or ceramic through honeycomb substrates coated with an oxidizing catalyst such as platinum, palladium or both due to low temperature activity for HC conversions [MECA 2007]. Johnson T.V., (2010) highlighted the usage of DOC as being used in more vehicles than any other emission control device. Their critical present for the proper functioning of DPF and  $\text{eNOx}$  system was also reviewed and continuously evolving.

Diesel Particulate Filters (DPF) are devices which remove diesel particulate matter (PM) or soot from the exhaust gas of diesel engines. It works by forcing the particulate matter to flow through a wall flow ceramic honeycomb filter. The filters have alternate open and closed channel as illustrated in figure 2.2. The exhaust gases contained PM or soot will enter the open channel, and gaseous  $\text{CO}_2$  and  $\text{H}_2\text{O}$  will pass through the wall. Dry carbon soot particle size

larger than the monolith wall are trapped until the pressure drop across the DPF become too high.



**Figure 2.2 Wall-Flow DPF (reproduced from Heck 2009)**

However DPFs have limited capability and will eventually fully clog, therefore they need to be periodically regenerated by combustion of the trapped PM. The soot requires a minimum temperature of  $500^{\circ}\text{C}$  for ignition in the absence of a catalyst which the engine exhaust does not frequently or reliably reach. Additional steps or mechanism are needed to clean up the trapped PM, reduce the back pressure and restart the trapping cycle. (Heck 2009)

**Konstandopoulos et al., (2000)** suggested three methods of facilitating the DPF regeneration in order to maintain the satisfactory performance of DPF. They involved active, external and passive regeneration. The active regeneration involved changing the operation of the diesel engine while the passive approach involved modification of the trap composition. External regeneration would be possible with the introduction of an external system to heat up the trap.

**Magdi et al., (1999)** evaluated the performance of DOCs and DPFs coupled with SCR system and reported excellent results for PM emission. SCR with DOC can achieve PM emission of  $0.05 \text{ g/bhp-hr}$  and combined PM,  $\text{NO}_x$  and NHMC of less than  $1.5 \text{ g/bhp-hr}$ . DPF technology further reduced the PM emissions below  $0.01 \text{ g/bhp-hr}$ . **Beeck et al., (2006)** reviewed possible conflict from integration of SCR with DPF technologies based on pure thermal and catalyzed DPF regeneration as shown in figure 2.2a. The benefit of Fuel Borne Catalyst (FBC) was also highlighted which provides flexible thermal management allowing fast and complete DPF regeneration.



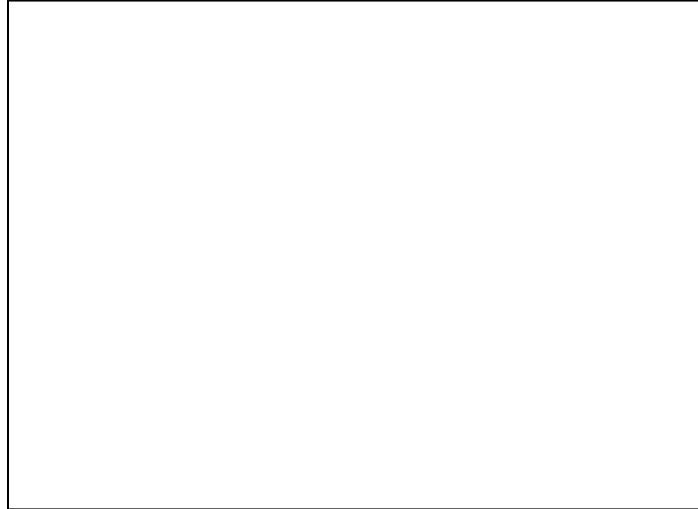
**Figure 2.2a Possible architecture for NO<sub>x</sub>/PM control (Beeck et al. 2006)**

**Gurupatham et al., (2008)** compared the integrated DOC-SCR-DPF, DOC-DPF-SCR and close coupled DOC-DPF-SCR as shown in figure 2.2b. The DPF forward system shows better PM active regeneration due to being closer to the engine and greater passive regeneration of DOC by NO<sub>2</sub>. However, DPF forward system disadvantage includes substantially delay of hot gas downstream reducing its SCR light off and the reduction of NO<sub>2</sub> by SCR reactions because of soot oxidation by NO<sub>2</sub> in the DPF. The close coupled DOC-DPF improved warm up time of DPF and SCR for cold start.

**Figure 2.2b Schematic of an advance diesel after treatment system architecture compared in Gurupatham et al., (2008)**

**Guo G. et al., (2010)** introduced an SCR washcoat with wall flow on DPF called SCRF together with traditional SCR catalyst in light duty diesel application to perform NO<sub>x</sub> and PM reduction

simultaneously. However low washcoat loading on SCRF due to backpressure concern, cause the NO<sub>x</sub> reduction efficiency lower than SCRF placed upstream of SCR catalyst.



**Figure 2.2c Advance diesel after treatment system with SCRF concepts (Guo et al., 2010)**

**Gieshoff et al., (2001)** discovered that the SCR catalyst is affected by the unburned diesel fuel therefore suggested a DOC be placed upstream to remove unburned hydrocarbon. **Koebel (2002) and Koebel (2001)** also highlighted an increased NO<sub>2</sub> level can be realized by placing an oxidation catalyst which promotes oxidation of NO. The oxidation catalyst placed upstream of the urea injection point decreased V<sub>2</sub>O<sub>5</sub> light off temperature to as low as 150°C. The disadvantages of this was an increased oxidation of sulphur dioxide and sulfate PM which result from using fuels of higher sulphur content and an increased of ammonium nitrate formation at temperature below 200°C.

**Lambert et al., (2006)** proposed to move the SCR upstream of the DPF to handle cold start issues for passenger car. Many automotive manufacturers have announced SCR systems for their latest SUVs and LDTs with undisclosed system configuration especially regarding the actual location of the SCR catalyst.

### 2.2.1 Effect of $\text{NO}_2/\text{NO}$ ratio on $\text{NO}_x$ conversion.

**Chandler (2000)** suggested that the composition of exhaust gases emission are mostly of NO (from 85-95%) and small quantity of  $\text{NO}_2$  (5-15%). It was reported that increasing the  $\text{NO}_2$  fraction in the feed gas can improve low temperature activity of the  $\text{V}_2\text{O}_5$  as shown in figure 2.2.1a

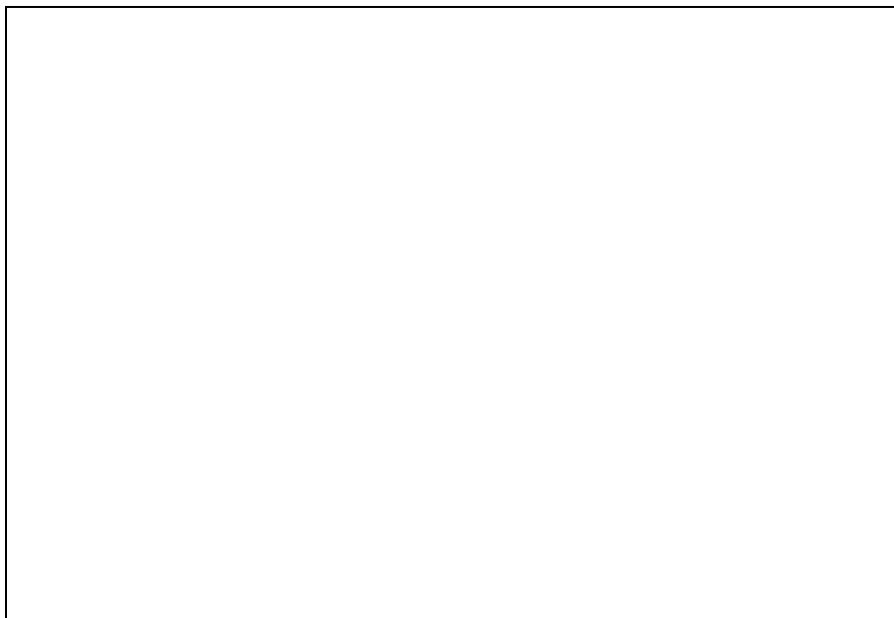


**Figure 2.2.1a Effect of  $\text{NO}_2/\text{NO}$  ratio on  $\text{NO}_x$  conversion in  $\text{V}_2\text{O}_5/\text{TiO}_2$  catalyst (Chandler, 2000)**

**Gieshoff (2001)** also reported similar performance with  $\text{Cu}/\text{ZSM-5}$  and other low temperature zeolite based catalysts. **Narayanaswamy et al., (2008)** simulated  $\text{NO}_2/\text{NO}$  ratios up to three and implied good conversion over zeolite with excess  $\text{NO}_2$ .

The significance of excess  $\text{NO}_2$  particularly over zeolite at lower temperature was discussed by **Rahkamaa-Tolonen et al., (2005)** who stated that excess  $\text{NO}_2$  will enhance the SCR reactions. **Takada et al., (2007)** also show good  $\text{NO}_x$  conversion with high  $\text{NO}_2$  level (> 50%) in their modelling of reactions over zeolite at a temperature range from 500 to 550 K. **Devadas et al., (2006)** also supported excess  $\text{NO}_2$  particularly over zeolite and reported best performance at  $\text{NO}_2/\text{NO}_x$  ratio of 75% which is much higher than the generally accepted optimum 50%.

However **Cooper (2003)** suggested that the amount of  $\text{NO}_2$  must be optimised by suitable sizing and formulation of the oxidation catalyst. If the  $\text{NO}_2$  level are too high,  $\text{NO}_x$  conversion efficiency decreases as shown by the red dash line and circles in figure 2.2.1b



**Figure 2.2.1b Effect of  $\text{NO}_2$  from DOC on  $\text{NO}_x$  conversion (Cooper 2003).**

**Cooper (2003)** also suggested a large Pt loading Oxidation catalyst to increase the  $\text{NO}_2/\text{NO}$  ratio to nearly 5 (over 80%  $\text{NO}_2$  in  $\text{NO}_x$ ) at around  $280^\circ\text{C}$ . As a result, the  $\text{NO}_x$  conversion deteriorated significantly due to depletion of ammonia since the required NO was substituted by  $\text{NO}_2$  as shown in red line in figure 2.2.1b.

### 2.3 SCR Catalyst types

The formulation of catalyst is important for the SCR reaction to take place. Three SCR catalysts commonly used are platinum, vanadium and zeolite.

#### 2.3.1 Platinum catalysts

The historical development of the SCR technology discovered that  $\text{NH}_3$  can react selectively with  $\text{NO}_x$  to produce elemental  $\text{N}_2$  over platinum catalyst in excess oxygen [**Heck 2009**]. **Heck (1993)**

suggested that the first SCR catalyst discovered was platinum but with limited usage due to low temperature activity. The effective temperature window for platinum was found from 175 to 250°C [DieselNet 2005]. Due to its poor activity at higher temperature, the other base metal like vanadium and zeolite catalysts were found to be effective at higher temperature windows.

### 2.3.2 Vanadia Titania Catalysts

**Bosch and Janssen (1988)** suggested  $V_2O_5/Al_2O_3$  catalysts be used for operating temperature higher than 250°C but restricted to sulphur free application due to deactivation of the catalyst from alumina reaction with  $SO_3$  forming  $Al_2(SO_4)_3$ . The nonsulphating  $TiO_2$  carrier was recommended for the  $V_2O_5$ . **Amon and Keefe (2001)** reported extensive studies of  $V_2O_5$  catalyst supported on  $TiO_2$  and  $WO_3$  added for HD diesel in Europe with numerous on highway studies. **Lambert et al., (2006)** highlighted problem with vanadium catalyst which quickly deactivated at high temperatures above 600°C therefore suggested zeolite catalyst. The recommended temperature window for vanadium is from 300 to 450°C [DieselNet 2005].

### 2.3.3 Zeolite Catalysts

Zeolite catalysts were developed to cover a wider range of temperature windows over platinum and vanadium based catalysts. **Byrne et al., (1992)** suggested zeolite based catalyst to further extend the operating temperature above 350°C. However two type of zeolite catalysts were developed to cover high and low temperature windows. The high temperature zeolite covers temperature windows from 350 to 600°C while the low temperature zeolite covers 150 to 450°C [DieselNet 2005]

#### 2.3.3.1 High Temperature Zeolite

**Chen (1995)** identified mordenite as the first zeolite active SCR catalyst. Common mordenites have a well defined crystalline structure with  $SiO_2: Al_2O_3$  ratio of 10. It was not possible to describe them in details as manufacturers keep their catalyst formulation undisclosed. Typically the zeolite catalysts are exchanged with metal and iron-exchanged zeolite were found useful in SCR application.



**Heck (1994)** found that zeolite can operate up to 600°C and in the presence of NO<sub>x</sub>, ammonia was not oxidised to NO<sub>x</sub> therefore its NO<sub>x</sub> conversion continually increases with temperature. Therefore the upper temperature limit for this type of zeolite catalysts may be determined by catalyst durability rather than selectivity. It was suggested that this type of zeolite catalysts may be prone to stability problems at high temperature with the presence of water vapour. For excessive temperature above 600°C in a high water content zeolite tends to deactivate by dealumination where Al<sup>+3</sup> ion in the SiO<sub>2</sub>-Al<sub>2</sub>O<sub>3</sub> migrated out of the structure leading to permanent deactivation and in extreme cases collapsed the crystalline structure.

**Lambert et al., (2006)** suggested the importance of thermal durability of zeolite catalysts particularly with the integration with DPF with forced regeneration. The zeolite catalyst is capable of withstanding temperature above 650°C and brief exposure to temperature of 750 - 850°C. **Theis (2009)** recommended Fe-zeolite catalyst for NO<sub>x</sub> control at high temperature from 400-600°C. **Giovanni et al., (2007)** found Fe-zeolite have higher NO<sub>x</sub> conversion above 350°C with no significant N<sub>2</sub>O produced and suggested not to exceed 925°C

### 2.3.3.1 Low temperature Zeolite

**Gieshoff (2001) and Spurk et al., (2001)** suggested that a different type of low temperature zeolite catalyst could be developed for mobile engine application. In the 1990s, research was conducted for the formulation of Cu-exchanged ZSM-5 zeolite also known as a lean-NO<sub>x</sub> catalyst. The Cu/ZSM-5 was active in reducing NO<sub>x</sub> within a temperature range of 200 to 400°C but with insufficient thermal durability. This led to a new formulation by modifying the ion-exchanging of zeolite to undisclosed transition metals. The normal NO<sub>x</sub> reducing activity for this catalyst was low and the final low temperature zeolite was thermally stable up to 650°C. This formulation has been designed specifically for NO<sub>2</sub> gases which significantly improved its NO<sub>x</sub> conversion and extended the temperature window with NO<sub>x</sub> reduction efficiency better than 90% over a temperature range of 150-500°C.

**Theis (2009)** also suggested Cu-Zeolite catalysts as more effective for NO<sub>x</sub> control at low temperature in the range of 200 to 400°C. **Giovanni et al., (2007)** again found Cu-zeolite to have higher NO<sub>x</sub> conversion at temperature below 350°C with significant N<sub>2</sub>O produced and suggested not to exceed 775°C

### 2.3.4 Comparison of SCR catalysts.

The basis of SCR catalyst comparison is mainly on the operating temperature windows. Each of the catalysts has their own limitations and problems and are continuously redeveloped for further improvement in term of NO<sub>x</sub> conversion efficiency and thermal durability.

**Schmieg et al., (2005)** summarized the performance comparison of Cu-zeolite and Fe-zeolite with vanadium based catalyst to provide useful guidance in the design and operation of urea SCR NO<sub>x</sub> reduction systems. The effect of NO: NO<sub>2</sub> ratio on steady state NO<sub>x</sub> reduction on a typical diesel exhaust temperature of 150 to 500°C was investigated. Transient measurements were performed to determine the impact of NH<sub>3</sub>: NO<sub>x</sub> ratio and NH<sub>3</sub> storage on catalyst and HC and sulphur poisoning effect.

**Hamada (2005)** reported new formulations with bi-functional catalyst design to simultaneously reduce NO<sub>x</sub> and oxidize the NH<sub>3</sub> slip as well as CO and HC. **Walker (2005)** compared the SCR catalyst temperature windows for NO<sub>x</sub> reduction with ammonia and summarized them in figure 2.3. Continuous effort on catalyst formulation is progressing toward wider temperature windows, thermal durability, NO<sub>x</sub> conversion and cost.



**Figure 2.3 Comparison of SCR catalyst operating temperature windows (Walker 2005)**

## 2.4 SCR reductants

Two most commonly used SCR reductants are anhydrous ammonia and aqueous ammonia or urea. Pure anhydrous ammonia is extremely toxic and difficult to safely store, but needs no further conversion to operate within an SCR. It is typically favored by large industrial SCR operators. Aqueous ammonia must be hydrolyzed in order to be used, but it is substantially safer to store and transport than anhydrous ammonia. Urea is the safest to store, but requires conversion to ammonia through thermal decomposition in order to be used as an effective reductant [DieselNet 2005].

The aqueous ammonia is also known as AdBlue, Urea Water Solution (UWS) and Diesel Exhaust Fluid (DEF) depending on manufacturers. **Eberhard (1994)** introduced the use of solid urea but it has received very little acceptance. **Hoffman (1996)** suggested an alternative to urea using carbamate salt such as ammonium carbamate,  $\text{NH}_2\text{COONH}_4$ . **Kelly et al., (2006)** reported various amines evaluated as SCR reductants which could potentially be generated from diesel fuel and nitrogen.

**Alkemade et al., (2006)** reviewed the best reductant to be used for SCR system. While ammonia offer slightly better performance, its toxicity and handling difficulty remain the biggest concern. Urea is not as effective but safer to handle which has made it the popular choice for automotive manufacturers. **Sullivan et al., (2005)** suggested in both form of ammonia it has to be extremely pure due to the fact that impurities can clog the catalyst. An SCR catalyst typically requires frequent cleaning even with pure reductants as the reductants can cake the inlet surface of the catalyst when the exhaust gas stream temperature is too low for the SCR reaction to occur. Research in to reductant technology is continuing and a wide variety of alternative reductant have been explored especially the one with wide availability and a distribution infrastructure in place. [US EPA 2006]

### 2.4.1 Aqueous Ammonia

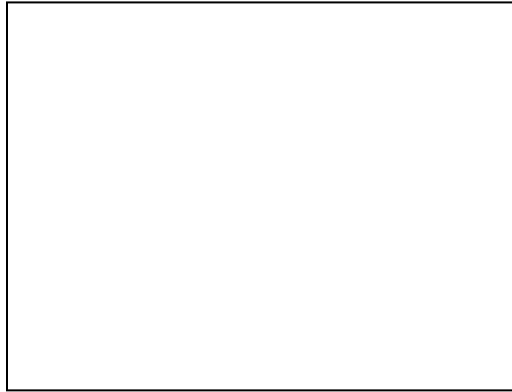
Aqueous ammonia or water solutions urea remained the preferred choice for SCR application due to safe handling and commercial availability. AdBlue is a registered trademark for AUS32

(aqueous Urea solution 32.5% by weight) It is a solution of high purity urea (32.5%) in demineralised water (67.5%) used as a supplementary operating fluid (reducing agent) in diesel powered vehicles using selective catalytic reduction (SCR) to improve exhaust emissions. AUS32 is primarily produced in Europe by BASF and AMI, however many other companies manufacture their own similar solution in varying quantities. **[BASF 2003]**

AUS32 is carried onboard the vehicle in a tank separate to the fuel system and is sprayed into the engine exhaust gases in a special catalytic converter. A typical SCR system uses an amount of AUS32 equivalent to approximately 3 to 5% of the vehicle fuel consumption. In order to ensure effective working of the SCR system, care must be taken to ensure purity of the catalyst and reducing agent. Any small contaminant can severely reduce the SCR system performance. The manufacturing quality control for AUS32 solutions is governed by DIN standard 70070 **[Focus on Catalysts (8), 2, 2005]**

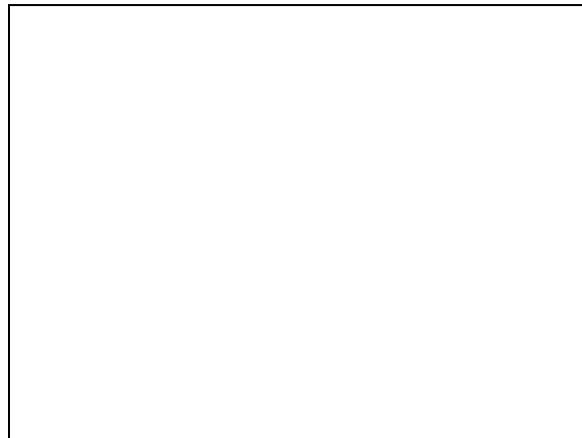
SCR systems using AdBlue are currently fitted to many trucks and buses manufactured by Mercedes Benz, Volvo Trucks, DAF Trucks and Iveco, however AdBlue usage as reducing agent is hindered by its relative availability. Schemes are underway in Europe but to lesser extents in Australasia and North America to improve the network distributors for AdBlue and other SCR additive. Internet based tool have been developed to map the locations of AUS32 filling stations reflecting plans for small scale use of SCR system in private vehicle as well as corporate fleets **[Focus on Catalysts(2), 3, 2006]**.

The typical aqueous urea solutions for SCR system concentration at 32.5% form an eutectic solution characterized by the lowest crystallization point of  $-11^{\circ}\text{C}$ . The eutectic solution is advantages due to equal concentrations in liquid and solid phases during crystallization. With even partial freezing of the solution in the urea tanks, crystallization would not change the concentration of the urea solution fed to the SCR system **[BASF 2003]**.



**Figure 2.4.1a Urea solution freezing point [BASF 2003].**

The 32.5% urea solution is a colourless liquid with a faint alkaline reaction. The freshly prepared solutions have a pH of 9 to 9.5. In solution the urea decomposes slowly in room temperature into ammonia and  $\text{CO}_2$ . When the solution is heated, the rate of decomposition increases additionally producing biuret [BASF 2003].



**Figure 2.4.1b Urea solution 32.5% decomposition [BASF 2003].**

**Fang and DaCosta (2003)** highlighted possible side reactions from decomposition of urea in HDD application. **Koebel et al., (2000)** also presented problem related to urea during start up due to its freezing point at  $-11^{\circ}\text{C}$  which cause it to be heated if the surrounding temperature is lower.

Problem associated with urea spray have triggered for alternative solution to supply ammonia gas to the SCR system. **Elmoe et al., (2006)** suggested solid ammonia storage using  $\text{Mg}(\text{NH}_3)_6\text{Cl}_2$  which has high ammonia density very close to urea solution. **Taturr et al., (2009)** also provide alternative to urea with the use of ammonium carbamate  $[(\text{NH}_2\text{-CO}_2)\text{-(NH}_4)]$  in HD diesel which is capable to supply ammonia by heating at a capacity 3 to 4 times more than urea. Therefore, other alternatives than urea to supply ammonia to the SCR system are continuously explored.

#### 2.4.2 Anhydrous ammonia.

The term anhydrous ammonia refers to the absence of water in the material. Ammonia gas is a compound consisting of nitrogen and hydrogen,  $\text{NH}_3$ . It is a colourless gas with pungent odour. Ammonia is widely used in agricultures and contributes significantly to the nutritional needs of terrestrial organisms as by serving as food and fertilizer. The liquid boiling temperature is at  $-33.34^\circ\text{C}$  and it solidifies at  $-77.7^\circ\text{C}$  to white crystals therefore the must be stored under high pressure or low temperature [**BOC datasheet 2005**].

Although widely used, ammonia gas is classified as toxic and dangerous for the environment. The US EPA has established a guideline for Permissible exposure level (PEL) of 50 ppm in an 8 hours weighted average. Anhydrous ammonia also corrodes copper and zinc containing alloy, therefore brass fittings must be avoided in handling the gas and liquid ammonia can also attack rubber and certain plastics [**Yost D.M., 2007**]

Recent development in SCR technology considers readily available ammonia gas rather than aqueous ammonia solution. Ammonia in gas form can be supplied using a special storage container or specially design ammonia storage system.

### 2.5 Challenges in automotive SCR.

**Johnson T.V. (2010)** reviewed various research efforts in optimizing the SCR system and highlighted DP placement with regards to SCR, non urea ammonia systems, mixed zeolite catalyst development and fundamental understanding on issues such as ammonia storage, sulphur impact and reaction mechanism. Development on LNT-SCR system where the LNT is

calibrated to generate ammonia for the SCR was also discussed. Despite promising NO<sub>x</sub> conversion with the SCR system, many other grey areas need attention to further improve the system.

### 2.5.1 Ammonia slip

Ammonia slip remains the undesired emission in the SCR system. It can be described as ammonia that exits the SCR system unreacted. **Huennikes et al., (2006)** suggested 3 ways the injected urea can lead to NH<sub>3</sub> slipping out of the SCR catalyst. It involved the incomplete SCR reaction due to NH<sub>3</sub>: NO<sub>x</sub> ratio higher than NO<sub>x</sub> conversion efficiency, the release of stored ammonia from SCR catalyst and the incomplete decomposition of urea before reaching the SCR catalyst. **Girard et al., (2007)** also reported NH<sub>3</sub> slippage as a result of high NH<sub>3</sub>: NO<sub>x</sub> ratio (called alpha). It was suggested reducing the alpha value less than one at low temperature where the ideal alpha is equal to one.

### 2.5.2 Uniform mixing of Urea.

The urea injection quality and mixing are complex and critically important. In real engine testing such as in this study, uncertainties existed over the uniform mixing of the urea spray with the exhaust gases. **Gorbach et al., (2009)** introduced urea mixers for mixing of urea droplets from sprays and saw system efficiencies vary from 60 to 95% depending on ammonia distribution across the catalyst. The urea mixer comes in a variety of types ranging from wire mesh designs to vanes and honeycomb. **Breedlove et al., (2008)** suggested the use of different nozzle designs to provide different droplet quality with range of characteristics at different injection stages.

### 2.5.3 Spray effect on temperature

**Johannessen et al., (2008)** reported that the sprayed urea in exhaust stream reduced the exhaust gas temperature by 10-15°C therefore diminished the NO<sub>x</sub> conversion efficiency especially in the low temperature region. **Way (2008)** also reported problem with urea injection

at low temperature (less than 190°C) where incomplete evaporation of urea and solid deposit build-up occurred in the exhaust system.

#### 2.5.4 Space velocity

**Koebel et al., (2001)** described problem faced by the SCR system in automotive application due to low exhaust gas temperature and short resident time due to space constraints in LD Diesel application. The problem leads to the reduced performance of SCR systems resulting from incomplete thermolysis of urea before entering the SCR catalyst. It is reported that only 50% of urea decomposed at 400°C and even lower than 15% at 255°C.

#### 2.5.5 Light duty diesel engine study

**Fisher et al., (2004)** reported successful adaptation of the SCR system by European truck manufacturers to comply with Euro 4 and 5 standards. **Beeck et al., (2006)** suggested that the urea SCR system integration seems quite easy on HDD application but it is much more difficult with the confine space in LDD such as passenger cars. Many researchers have focussed on real engine tests with HDD application and the light duty engine test is progressing slowly. **Spurk et al., (2007)** highlighted cold start problem with passenger cars and suggested formulation of dedicated low temperature active SCR catalysts. It was suggested that the SCR catalyst need to show wider operating windows. However the SCR system complexity in light duty remained disadvantages and need further optimization.

#### 2.5.6 SCR modelling

A literature review was undertaken and compiled as part of an internal report (private communication, Dr C. A. Roberts (2009). The objective is to validate the CFD model against engine data from this study. The earlier kinetic scheme reviewed was a very simple scheme of



**Snyder and Subramaniam (1998), Chatterjee et al., (2005), Tronconi et al., (2005) and Chi et al., (2005)** later derived other kinetic schemes.

**Chatterjee et al., (2005)** comment on the limitations of simplified surface reaction models, especially in the case of extruded catalysts; however, it was stated that their model accounts for intra-porous diffusion and was appropriate for coated as well as extruded catalysts. Their initial reactor experiments for intrinsic chemistry were carried out over the temperature range of 150 to 450 °C. This scheme gives a reaction rate for only the standard SCR reaction and become obsolete due to more complete scheme that follows.

**Tronconi et al., (2005)** presented a kinetic analysis of the standard SCR reaction and further extended it to gain more fundamental insight into the catalytic kinetics and mechanism prevailing in the low temperature region. This would be interesting especially for mobile applications. In particular transient reactive experiments have shown that a decrease of the ammonia gas phase concentration temporarily enhanced the NO conversion. They also suggested an inhibiting effect of ammonia that could play a non-negligible role in the SCR reaction.

The scheme by **Chi et al., (2005)** also provided full SCR reactions with constants similar to Tronconi et al. scheme but includes more reactions. One of the main significant differences between the two schemes was in the standard SCR reaction rate. The Chi et al. scheme suggested that the rate is directly proportional to the ammonia concentration which this dependent does not present in the Tronconi et al. scheme.

A vanadium scheme due to **Chi et al., (2005)** has been used with significant differences between this scheme and a new scheme for Zeolite catalyst published by **Chatterjee et al., (2007)**. The zeolite scheme does not include the slow SCR reaction but does include an NO oxidation reaction. The comparison on both schemes shows Zeolite possessing slightly higher values on Ammonia adsorption, Ammonia desorption, Ammonia Oxidation and Standard SCR reaction. There are significant differences on the fast SCR rate between the two schemes which suggest that the rate calculated using the information from **Chi et al.,** may be not accurate.

Finally the scheme **Olsson et al., (2008)** which considers Cu-Zeolite and emphasis on ammonia adsorption and desorption,  $\text{NH}_3$  oxidation, NO oxidation, standard SCR, rapid SCR,  $\text{NO}_2$  SCR and  $\text{N}_2\text{O}$  formation. Good agreement was obtained using this scheme therefore this zeolite scheme remained to be used for the SCR CFD model in this study (**Tamaldin et al. 2010**).

To this end a programme has been initiated with AEARG to provide a simulation tool that describes the behaviour of a SCR system for light-duty application using zeolite catalysts. This thesis describes an engine test bed programme designed to provide data for model validation. Chapter 3 describe development of the test rig.

## CHAPTER 3: RESEARCH METHODOLOGY

### 3.0 Introduction

The details of the engine commissioning and experimental procedures for the steady state tests are given in this chapter. This includes the engine, exhaust and analysers' preparation, the technical aspect, measurement and calibration of the equipment. The urea SCR spray system and the ammonia gas injection system will also be covered along with the calibration charts required. Several precautions and cleaning procedure will also be included especially for the urea SCR spray system. The final assembly of the SCR exhaust system will be covered and also the final experimental matrix for measuring the exhaust gases upstream and downstream of the SCR brick.

### 3.1 Engine Commissioning and Setup

The original plan was to use a Ford 4FM series diesel engine with a new transient engine test bed. Some time was spent to commission this engine with a new transient engine dynamometer within the university. Due to various problems with commissioning the 4FM series involving ECU (Engine Control Unit), wiring harness and diesel injectors, a 2FM series diesel engine used during recent Lean NO<sub>x</sub> Trap (LNT) studies was configured to run steady state tests for this investigation on a EC (Eddy Current) dynamometer

#### 3.1.1 Engine Commissioning and Setup for Steady State Test.

The recent Lean NO<sub>x</sub> Trap project within AEARG (Automotive Engineering Applied Research Group) Coventry University used a 2FM series diesel engine equipped with VGT and EGR, an Injection Control Unit (ICU) and an Engine Control Unit (ECU). This engine is also equipped with common rail injection system with a high pressure fuel pump, an intercooler and an engine management system (EMS) programmed through dSPACE, GREDI and a throttle body to control the intake air to the engine. The throttle body was controlled by dSPACE using a customized application based on Matlab Simulink. The application software was capable of controlling the timing for main, pilot and post injection and also controlling the opening and closing of the throttle body. GREDI was the monitoring software which reads the ECU and displays the value of parameters needed on a host computer. Any parameter changed through dSPACE was recorded in GREDI alongside with the Froude Consine test bed host computer. All the software and hardware was supplied by Ford

including the license for dSPACE, GREDI and Matlab Simulink. At a later stage of this project the EMS capability from dSPACE and GREDI was disabled due to technical failure of the ECU. Another ECU was programmed for this 2FM series diesel engine and the previous control of the throttle body for regeneration purpose was disabled. Therefore this project focussed only on steady state testing using pre-programmed engine settings. The exhaust back pressure was also monitored as an indicator for the DPF cleaning process. The 2FM configuration is shown in figure 3.1.1

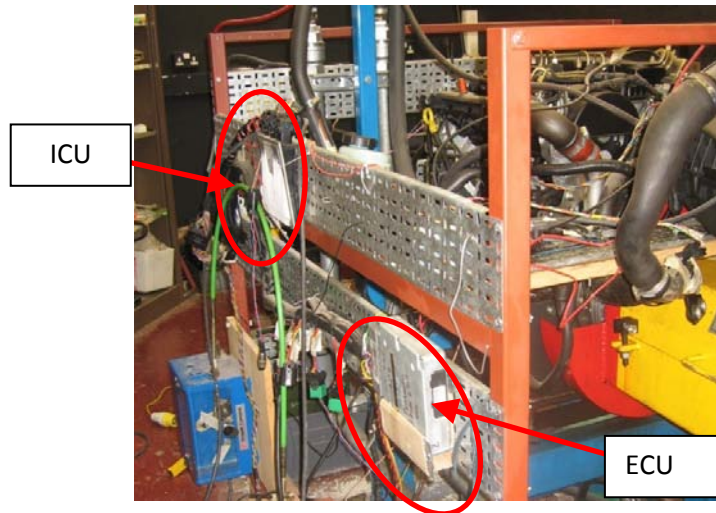


Figure 3.1.1 The 2FM Series Engine with Injection Control Unit (ICU) and Engine Control Unit (ECU) on Froude Consine AG150 engine dynamometer.

The specification of the diesel engines is shown in table 3.1.1 and the power curve for this engine is supplied in the appendix 3.1.1

Table 3.1.1 Diesel Engine specification used for investigation (Ford 2FM series)

Items	Description
Engine capacity	1998 cc / 121.9 cu in
Bore	86.0 mm / 3.39 in
Stroke	86.0 mm / 3.39 in
Compression ratio	18.2:1
Number of cylinders	Inline 4, 16 valves
Firing order	1-3-4-2
Rated power output	96.9 kW / 130.0 bhp at 3800 rpm
Rated torque	330 Nm / 243.4 ft lbs at 1800 rpm
Ignition type	Common rail, diesel fuelled, direct injection system

### 3.1.2 Engine Dynamometer

The engine dynamometer was an Eddy Current (EC) AG150 from Froude Consine rated at 150 kW (200 BHP) and 500 Nm (370 lb-ft) torque with maximum speed of 8000 rpm. The AG series is also known as the air gap range of eddy current dynamometers which has been designed to be compact, robust and allow easy maintenance. The dynamometer is fitted with oil injected half couplings at either end of a non-magnetic stainless steel shaft which is supported in grease lubricated, deep groove ball bearings.

The dynamometer casing houses twin magnetising coils that produce a retarding controllable magnetic field that resists the applied torque. Heat generated in this process is dissipated by cooling water. Rotation of the casing is resisted by a precision strain gauge load cell that gives accurate measurement of total input torque, measurement accuracy of  $\pm 0.25\%$  of full rated torque and a speed measurement accuracy of  $\pm 1$  RPM. The dynamometer has low inertia, bi-directional motion and high reliability.

### 3.1.3 Engine mass flow rate measurement

The engine mass flow rate was measured using a Ricardo mass flow meter coupled with a digital manometer. Prior to testing the flow meter was calibrated in the flow lab within the university. The Ricardo mass flow meter was connected to a pre-calibrated nozzle on an air flow rig (figure 3.1.3). A digital manometer was connected to the Ricardo mass flow meter and the air flow supply was varied. The air pressure drop was recorded for every air flow rate supplied and a calibration chart was produced for use on the engine. The arrangement used for air flow meter calibration is shown in figure 3.1.3 and the calibration chart is shown in Appendix 3.1.3.

Figure 3.1.3 Ricardo mass flow meter calibration [Courtesy of S. Quadri]

On the engine the mass flow rate was measured with a Testo digital manometer in mmH<sub>2</sub>O and later converted to gram/seconds and was recorded throughout the investigation. The Ricardo mass flow meter configuration with digital manometer is shown in figure 3.1.4

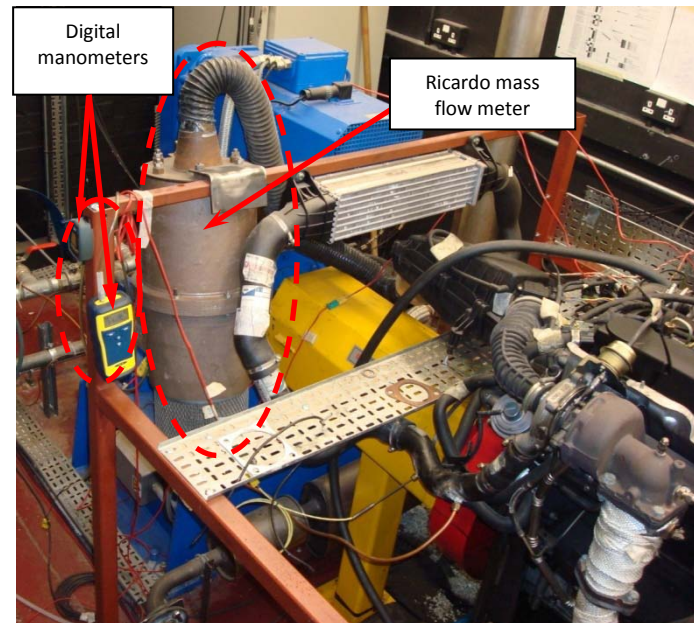


Figure 3.1.4 Ricardo mass flow meter measuring engine Mass Flow Rate (MFR)

### 3.2 Final SCR Exhaust build and commissioning.

The Selective Catalyst Reduction (SCR) exhaust system was built based on the parts supplied by EMCON Technologies Incorporated and catalysts supplied by Johnson Matthey and the finalized drawing agreed in a quarterly review meeting at Coventry University. The details of the parts supplied are listed in appendix 3.2. The SCR exhaust system comprises a Diesel Particulate Filter (DPF), Diesel Oxidation Catalyst (DOC), expansion chamber and nozzle, a narrow angled diffuser, SCR catalyst, bypass pipe and instrumentation modules. Figure 3.2 shows a schematic of the final assembly. It has been designed in such a way so to provide approximately 1D flow for comparison with a 1D computational model. Details of the components are discussed later.

From the engine exhaust manifold outlet, the exhaust was connected to the Diesel Oxidation Catalyst (DOC) for NO, CO and HC oxidation. Diesel oxidation catalysts can reduce emissions of particulate matter (PM) from 15 to 30 percent while hydrocarbons (HC) and carbon monoxide (CO) by over 90 percent within temperature interval of 20 to 30 °C(45). These processes can be described by the following chemical reactions.



HC are oxidized to form carbon dioxide and water vapour. The reaction in equation 3.2a represents two processes: the oxidation of gas phase HC and the oxidation of organic fraction of diesel particulates (SOF) compounds. Reaction in equation 3.2b describes the oxidation of carbon monoxide to carbon dioxide. Since carbon dioxide and water vapour are considered harmless, the above reactions bring an obvious emission benefit. The most significant contribution of the DOC is to oxidize incoming NO to NO<sub>2</sub> which allow fast SCR reaction to reduce NO<sub>x</sub> as described in the equation 3.2c



Therefore, the arrangement where DPF and DOC were designed in this investigation was crucial to provide sufficient NO/NO<sub>2</sub> ratio for optimum SCR reaction. The first instrumentation module was connected to the DOC to accommodate the EXSA, MEXA analyser, lambda sensor and thermocouples for measuring the exhaust emissions downstream of the DPF and DOC and also monitoring exhaust temperature.

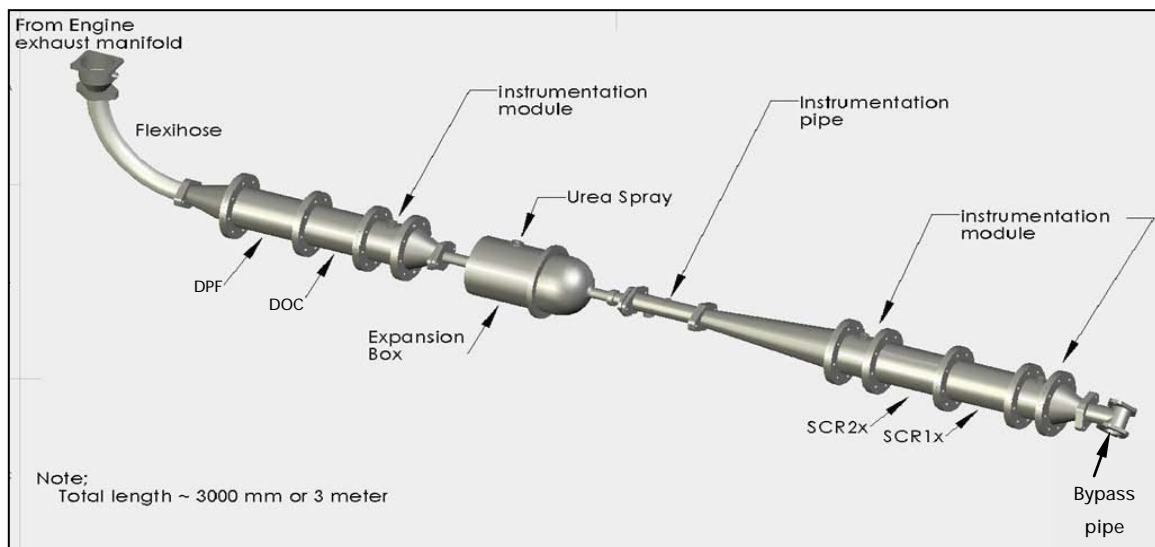


Figure 3.2 Final Assembly of the SCR Exhaust System.

### 3.2.1 SCR Exhaust Fabrications and Specifications.

The SCR exhaust fabrication took place at various facilities across the university, the local fabrication workshop at the university and also at the collaborating companies facilities of EMCON Technology and Johnson Matthey.



Figure 3.2.1 The suspended exhaust from a square metal frame.

The complete SCR exhaust system was suspended horizontally from a metal square frame with cable wire as shown in figure 3.2.1. Sealing gaskets were placed in between each component. The gasket used was a high temperature resistance type in order to prevent gas leakage from the exhaust system. Some minor adjustment was necessary in the final SCR exhaust assembly because of the restricted space within the cell.

### 3.2.2 DPF-DOC assembly.

The first component of the exhaust system comprises of DPF coupled with DOC. In the initial plan the DPF and DOC were to be connected in a vertical position but they were later repositioned due to cell constraints and laid horizontally as in figure 3.2. A final assembly front view and isometric view drawing is shown in appendix 3.2b. A draining plug was fitted underneath the expansion box which houses the spray assembly. Two DOC configurations were available for this investigation; a single DOC of diameter 115 mm and length 95 mm and a double DOC of the same diameter but of length 190 mm. This is shown in the DOC assembly drawing in appendix 3.2b. The details of DPF assembly are also shown in the DPF assembly drawing of appendix 3.2b. The detail specification of the DOC is shown in table 3.2.2.



Table 3.2.2 Detail specification of the DOC catalyst

Diameter	118.4 mm with 115 mm exposed in rig
Length	Single = 91 mm, Volume approximately 1 litre Double = 182 mm, Volume approximately 2 litre
Cell Density	400 cpsi
Cell Pitch	1.27 mm
Substrate	NGK HoneyCeram
Wall Thickness	0.11 mm [4.3 thou(UK),4.3 mil (USA)]
Open frontal area (non-washcoated)	83.4%
Bulk density of substrate	0.29 g/cc (290 kg/m <sup>3</sup> )
Washcoat thickness	0.085 mm
Washcoated channel dimension	1.076 mm
Washcoat loading (assuming washcoat density = 1350 kg/m <sup>3</sup> )	158.7 kg/m <sup>3</sup>

### 3.2.3 SCR Catalysts Assembly

The SCR catalyst assembly has been designed to accommodate four SCR configurations in this investigation. An assembly consisting of a single brick measuring 115 mm in diameter and of length 92.5 mm was available. Two double bricks of diameter 115 mm and length 185 mm were also available. A blank SCR with the same dimension as the single and double bricks configurations was also used. This SCR assembly is shown in appendix 3.2b. The single SCR can, two double SCR cans and the blank SCR can allowed single, double, triple and quadruple SCR configurations to be tested. The detailed specification of the SCR catalyst is shown in table 3.2.3.

Table 3.2.3 Detail specification of the SCR catalyst

Diameter	118.4 mm with 115 mm exposed in rig
Length	Single = 91 mm, Volume approximately 1 litre Double = 182 mm, Volume approximately 2 litres Triple = 273 mm, Volume approximately 3 litres Quadruple = 364 mm, Volume approximately 4 litres
Cell Density	400 cpsi
Cell Pitch	1.27 mm
Substrate	NGK HoneyCeram
Wall Thickness	0.11 mm [4.3 thou(UK),4.3 mil (USA)]
Open frontal area (non-washcoated)	83.4%
Bulk density of substrate	0.29 g/cc (290 kg/m <sup>3</sup> )
Washcoat thickness	0.089 mm
Washcoated channel dimension	1.072 mm
Washcoat loading (assuming washcoat density = 1350 kg/m <sup>3</sup> )	166.6 kg/m <sup>3</sup>

### 3.2.4 Urea Spray Mixing Chamber.

The Urea spray mixing chamber consists of a combination of a short 50 mm pipe and a 200 mm diameter by 200 mm long plenum, attached to a bell shaped converging nozzle as shown in figure 3.2.4. The urea spray mixing chamber was designed to allow uniform mixing of urea droplets in the presence of hot exhaust flow from the engine.

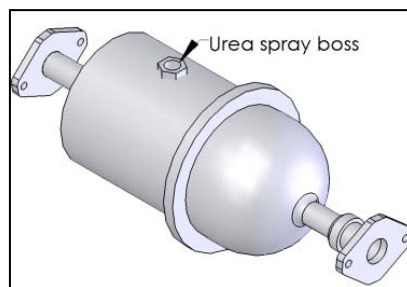


Figure 3.2.4 The Urea spray mixing chamber.

The mixing chamber has a urea spray boss fitted on top and a tiny drainage plug at the bottom. In the event of running the test with urea spray, the chamber would house the spray injector unit while with the  $\text{NH}_3$  gas test the boss was plugged to prevent gas leakage.

### 3.2.5 Instrumentation module assembly.

Four instrumentation modules were fabricated and assembled. Two of the modules were of diameter 115mm and of length 110 mm. A third had a diameter of 115 mm and was 90 mm long and a fourth had a diameter of 50 mm was of length 200 mm. The modules were used to house the analysers, thermocouples and lambda sensors. The two 110mm long modules were placed after the DPF-DOC assembly and before the SCR assembly and the 90 mm long module was placed after the SCR assembly. The 50 mm by 200 mm pipe was placed after the mixing chamber before the long diffuser. This pipe provided an alternative placement for Urea spray Injector. The instrumentation modules arrangement is as shown in figure 3.2.5.

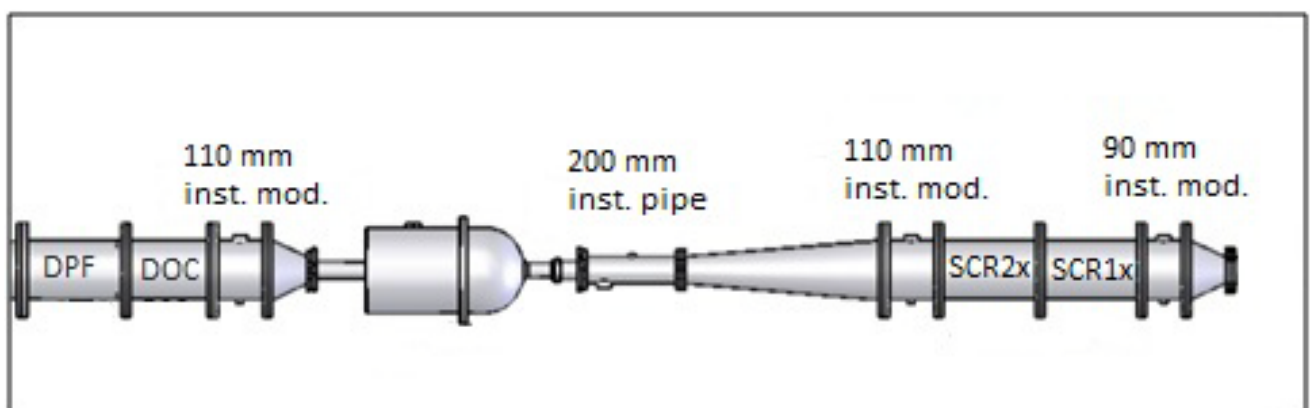


Figure 3.2.5 Instrumentation modules location along the SCR exhaust system.

Bosses were fabricated to accommodate the urea spray system, lambda sensors, analysers, thermocouples and pressure sensors in the instrumentation modules, urea expansion box and the end of the exhaust system. 1/8 inch BSP fittings were used for thermocouples and 1/4 inch NPT fittings for the Horiba analysers. These ports could be capped during the engine calibration process. Cleaning of the bosses was required after assembly using respective thread taps. This was done to remove any welding residue left on the bosses to ensure proper fitting for the instrumentation.

### 3.2.6 Long and short diffuser assembly

Four cones were used with different length and cone angles. The longest cone was 410 mm long with a half cone angle of  $4.5^{\circ}$  while the shortest cone was 90 mm long with a half cone angle of  $19.9^{\circ}$ . The inlet and exit cones both were 150 mm long with half cone angles of  $12.2^{\circ}$ . The most important cone in this assembly was the long diffuser cone. This cone was placed after the spray assembly and before the SCR assembly. This was designed to provide an approximate uniform one dimensional flow from the nozzle to the front face of the SCR catalyst.

### 3.2.7 Bypass pipe assembly.

The system was designed to have the option of a bypass system, but it was not used in the experiments described in this thesis so the pipes were capped. Pressure tapping was installed at the cap for measuring the exhaust backpressure for the system. The bypass T-joint with pressure tapping is shown in figure 3.2.7.



Figure 3.2.7 Capped T-joint with pressure tapping.

### 3.2.8 DPF Monitoring and Preconditioning

The DOC, DPF and SCR catalysts were supplied by Johnson Matthey along with technical data and procedure for monitoring and preconditioning. As the engine ran an increase in backpressure indicated that the DPF was being loaded with soot. Hence during the project the DPF was periodically cleared by blowing it out using a high pressure air supply. With a DPF system, it is important to avoid uncontrolled regeneration especially under severe conditions such when the engine load is rapidly reduced. This could result in damage to the DPF due to overheating especially when there the DPF is heavily loaded with soot. Throughout the experiment, close monitoring of the temperature and pressure across the SCR exhaust was undertaken using the thermocouples placed at various locations across the exhaust. Monitoring and data logging was done using the Froude Consine Texcel v10 software.

### **3.2.10 SCR Catalyst Monitoring and Preconditioning**

In the beginning of this test programme, the engine was run for sometime and it is assumed that the bricks were effectively de-greened.

### **3.3 EXSA 1500 NOx Analyser Setup**

The EXSA 1500 NOx Analyser was supplied by Horiba Instruments limited. The operation of this analyser is described in the operating manual and is targeted for measuring emissions from small engines ranging from two or four stroke gasoline and also diesels. It is capable of measuring CO, CO<sub>2</sub>, NOx, O<sub>2</sub> and THC simultaneously. This equipment is compatible with the SAE J1088 (R) standard. The standard is a SAE recommended practice and Test Procedure for the Measurement of Gaseous Exhaust Emissions from Small Utility Engines. In this investigation, the EXSA 1500 NOx analyser was used mainly to measure the engine out NOx level in the first instrumentation module as shown in figure 3.3.2. The EXSA 1500 was also used to measure NO in other locations of the SCR exhaust system based on the test matrix.

#### **3.3.1 EXSA 1500 Specifications and Resolutions**

The EXSA 1500 utilizes a cross flow type Non Dispersive Infra Red (NDIR) sensor at normal temperature for measuring CO and CO<sub>2</sub>. For measurement of NO and NOx, a chemiluminescence detector (CLD) is used while O<sub>2</sub> is measured with a single coil type magnetic pressure. THC on the other hand is measured using a heating type Flame Ionization Detector (FID). The specification of EXSA 1500 is given in the table 3.3.1.

Table 3.3.1 Technical Specifications of EXSA 1500 Common gas analyser.

[Extracted from the Horiba Ltd, EXSA 1500 operating manual Oct 2004]

Detection Target:	Gasoline engine (2-stroke, 4-stroke) exhaust, GM diesel engine exhaust gas
Detection:	CO/CO <sub>2</sub> :NDIR - Non Dispersive Infra Red Detector NO/ NO <sub>x</sub> :CLD - Chemiluminescence Detector O <sub>2</sub> :MPD – Magnetic Pressure Detector THC :HFID - Heated Flame Ionization Detector
Measurable Ranges Used	CO: 0~5000ppm CO <sub>2</sub> : 0~20 % vol. THC: 0~500 ppm C NO <sub>x</sub> : 0~1000 ppm O <sub>2</sub> : 0~25 % vol. AFR: 10-20 $\lambda$ : 0.5 – 2.5
Repeatability:	±1 % of Full Scale
90% percent respond:	15 seconds

### 3.3.2 Gas requirements and Calibration Gases

A total of six gases and compressed air at a pressure of approximately 1.2 bars are required for the operation and calibration of EXSA 1500 analyser. The gases are NO/NO<sub>x</sub>, CO/CO<sub>2</sub>, O<sub>2</sub>, N<sub>2</sub>, H<sub>2</sub>/He and Air mix. The EXSA 1500 NO<sub>x</sub> analyser gas piping configuration is shown in figure 3.3.2

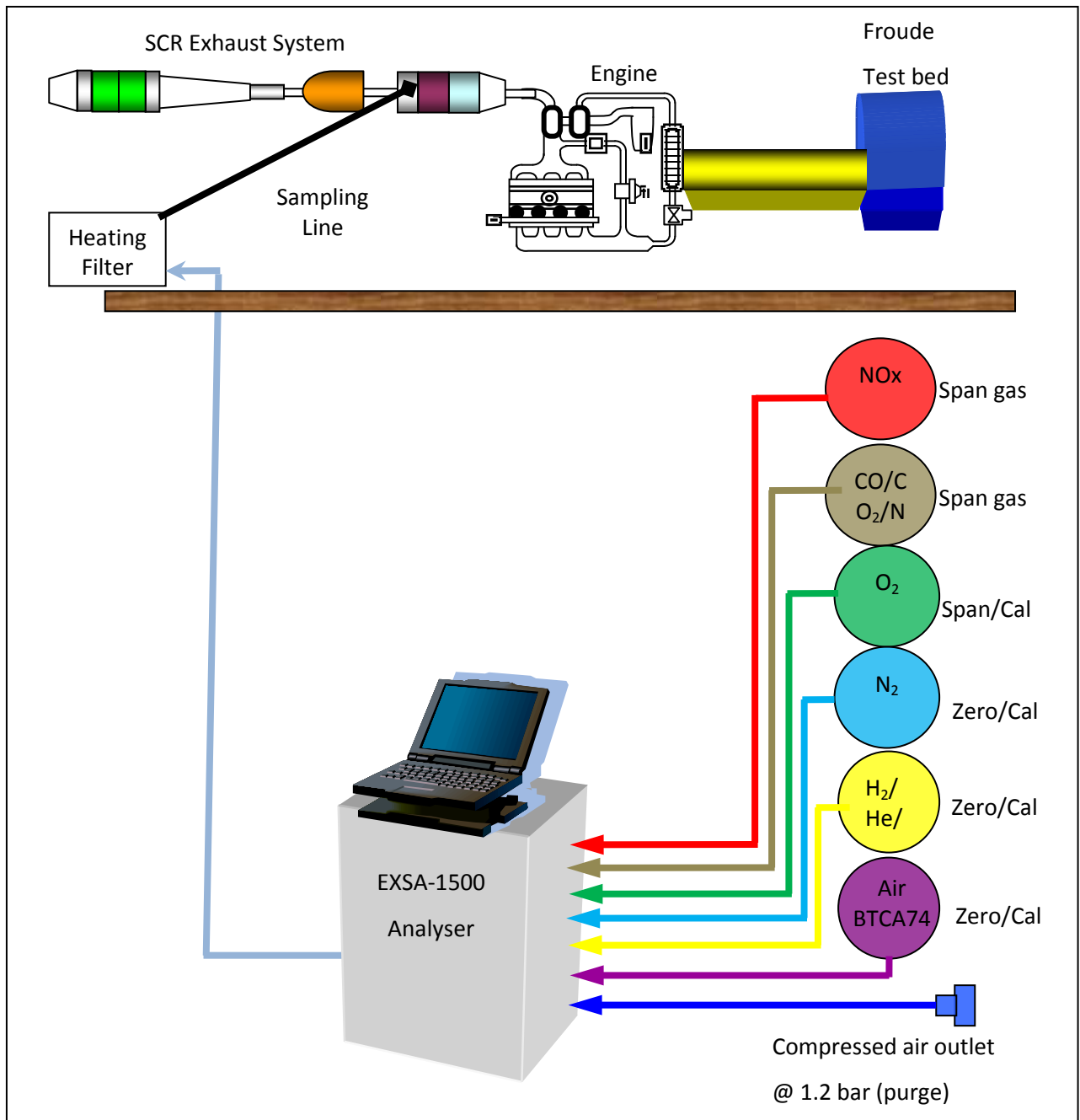


Figure 3.3.2 EXSA 1500 NOx analyser gas piping configuration.

### 3.3.3 NOx measurement procedure

Once all the gas network connections had been made, the gas bottles were opened and maintained at a pressure of 1.2 bars. After the EXSA 1500 analyser had been switched on and warmed up, the calibration was completed. The hot hose temperature must reach around 191°C before the calibration can be done. The Ozone Generator Unit (OGU) must be switched on when the NOx analyser is used. The FUEL switch must be set to “MANU” position to ignite the FID from the EXSA

main console. The ignite button needs to be pressed and it is necessary to wait until the alarm light from the display goes out. Then, the FUEL switch must be switched to AUTO after the ignition had completed. The appropriate CO, CO<sub>2</sub>, NO<sub>x</sub>, THC, O<sub>2</sub> range must be selected. In this investigation, the NO<sub>x</sub> range was selected from 0 to 1000 ppm and the O<sub>2</sub> range from 0 to 20%. The rest of the species were not needed for this investigation but are recorded as reference values.

The hot line was connected to the heating filter before reaching the exhaust sampling location. The sampling line was 40 mm in diameter and had a maximum sampling flow rate of 3 litres per minute. The recommended sampling line length was 6 meters but in the setup used here a 12 meter long sampling line was used. Therefore a heating filter unit was used to ensure the sampling line was maintained at 191°C throughout the experiment. The response time for this equipment was rated around 23 seconds for a standard 6 meters long sampling line. **[EXSA 1500 Operating manual version Oct. 2004]**

The engine also needed a warm up time. It took the engine approximately 45 to 60 minutes to fully warm up until the last instrumentation module toward the end of exhaust reached 300°C. Once the analyser was fully warmed up, calibrated and the engine warm up was completed, the analyser was put on to measure and the data logged either from the Froude Texcel main logger or within the built in data logger in the EXSA main unit. Throughout the investigation, the Froude Texcel data logger was used as the main data logger for synchronization with the MEXA. The temperatures, lambda sensors, spray or gas trigger and engine condition (Speed and BMEP) were also recorded by the Froude Texcel data logger.

In most of the cases, the EXSA 1500 sampling point remained on the first instrument module where the exhaust had passed the DPF and DOC before entering the mixing chamber where the urea spray or gas was injected. The EXSA 1500's capability of measuring NO and NO<sub>x</sub> also allowed it to be used as a backup for the MEXA analyser for measuring NO and NO<sub>2</sub>. Once the NO and NO<sub>x</sub> were measured the NO<sub>2</sub> value could be deduced from both readings.

### **3.4 Ammonia analyser MEXA 1170Nx**

The Horiba MEXA-1170Nx is one of the instruments capable of measuring ammonia and NO<sub>x</sub> simultaneously as described in the operating manual **[MEXA 1170Nx user manual, 2006]**. This instrument uses dual Chemiluminescence detectors (CLD) and an oxidation catalyst to measure



ammonia. Optionally, this product can measure NO<sub>x</sub> and NO<sub>2</sub> simultaneously with a simple setting change from the front control panel. The MEXA-1170NX main unit, which consists of an analyser unit, houses the CLD detectors, a control unit and a vacuum pump unit (VPU) is shown in figure 3.4



Figure 3.4 The MEXA-1170Nx NH<sub>3</sub> Analyser Unit

As compared to the EXSA, the MEXA sampling line used 60 mm diameter tubing and the maximum sampling rate was at 5 litres per minute. The effective sampling rate was slightly lower at around 3 litres per minute due to the filter assembly being placed upstream of the analyser. The filters protect the analyser from any unwanted HC soot entering the system. The response time for the MEXA was stated as being around a maximum of 1.5 seconds.

#### **3.4.1 MEXA1170Nx Specification and Resolution.**

The MEXA-1170NX analyser is claimed to be capable of measuring NH<sub>3</sub> in real time with high sensitivity using twin CLD detectors with an NH<sub>3</sub> oxidizing oven. In theory, by means of two heated-type Chemiluminescence (CLD) detectors with an NH<sub>3</sub> oxidizing oven, either NH<sub>3</sub> or NO<sub>2</sub> can be measured with high sensitivity in real time by calculation of the difference of NO readings from two detectors (one without a converter). It also features the capability of measuring NH<sub>3</sub> and NO<sub>x</sub>, or (optionally) NO<sub>2</sub>, NO and NO<sub>x</sub>, and should be suitable for the experiment as it can take direct exhaust measurement without having a cooling unit and water removal. The analyser performance and resolution is shown in section d of appendix 3.4.1 while section a through c describes its physical, accessories and configurations. The commissioning was performed by Horiba at the AEARG,

Coventry University site. Compressed air regulators were also installed next to the HBF-722H heating filter inside the test cell for purging the analyser.

### 3.4.2 MEXA 1170Nx Gas Requirements and Calibration.

The various gases needed to operate the MEXA-1170Nx are shown in table 3.4.2 below.

Table 3.4.2 Gas Requirement for MEXA-1170 NX Analyser.

Name	Specification	Supply pressure	Note
Zero gas	Nitrogen 100 %	100 kPa $\pm$ 10 kPa	At calibration 3 L / min
Span gas	NO in Balance N <sub>2</sub> 900 ppm	100 kPa $\pm$ 10 kPa 200 bar	At calibration 3 L / min
NH <sub>3</sub> gas	Ammonia in balance N <sub>2</sub> 95 ppm	100 kPa $\pm$ 10 kPa 200 bar	At oxidation catalyst check; 3 L / min
Ozonator gas	Oxygen 100%	100 kPa $\pm$ 10 kPa	At standby 0.7 L / min
Purge gas	N <sub>2</sub>	100 kPa $\pm$ 10 kPa	At purge 5 L / min

Gas regulators were installed for the NO bottle (in balance N<sub>2</sub>) and the ammonia bottle (in balance N<sub>2</sub>). Precautions were taken while installing both regulators especially for the ammonia bottle which used a left hand thread at the regulator and bottle outlet. Compressed air was used as the purge gas instead of N<sub>2</sub>. A dust filter and oil filter or mist catcher was installed as well. The gas piping layout is shown in figure 3.4.2.

The calibration of the MEXA analyser was performed before and after each sampling. After completing the calibration prior to testing, a gas bottle with 900 ppm NO was used to validate the analyser measurement. If the calibration was successful, then the experiment proceeded. If not, the MEXA analyser was recalibrated and validated or sent for minor service. Gas measurements are expressed as parts per million (ppm). This unit expresses the concentration of a pollutant as the ratio of its volume if segregated pure, to the volume of the air in which it is contained.

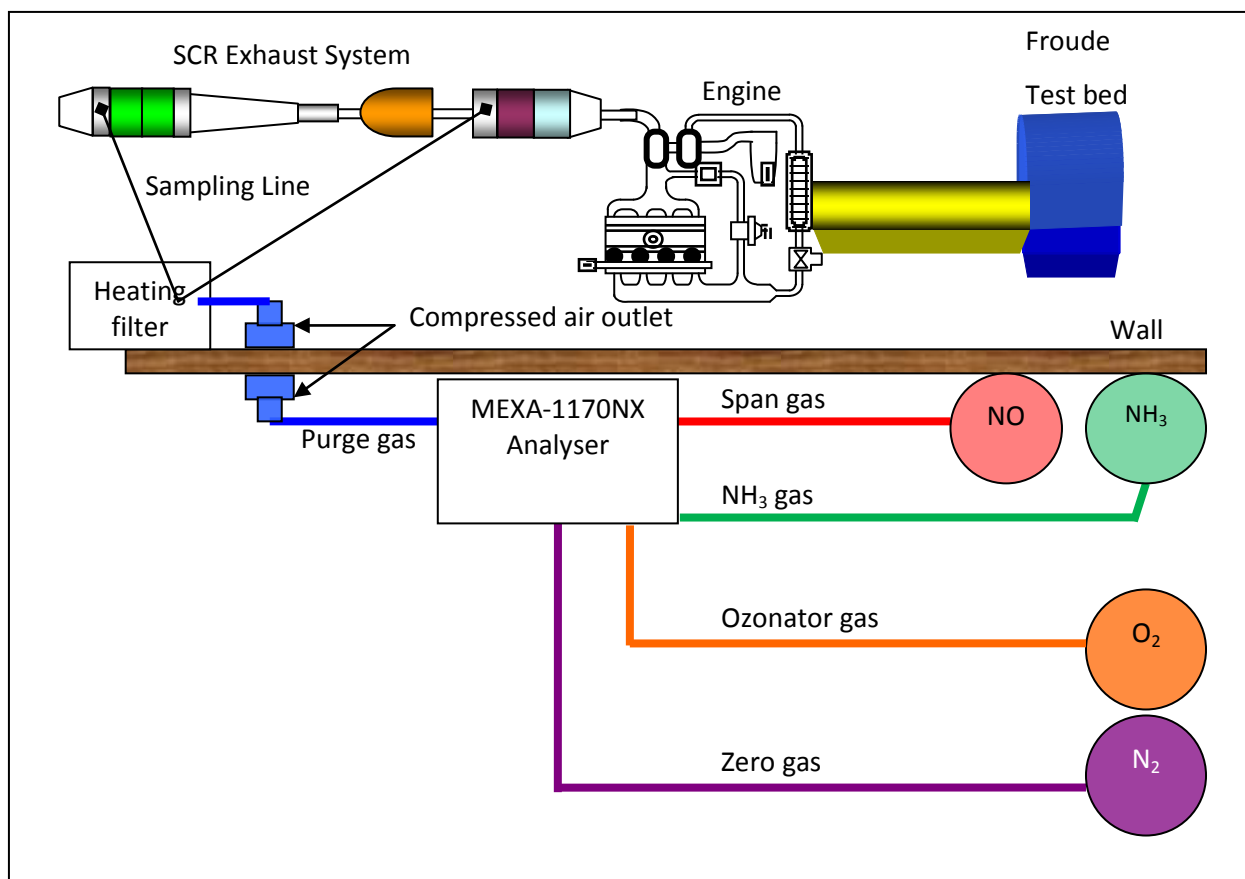


Figure 3.4.2 Gas piping Layout for MEXA-1170Nx Ammonia analyser

The calibration gas concentration was set to one range depending on the calibration bottle supplied. The range was set by pressing the CAL key. When the calibration process was completed, the analyser efficiency was recorded and monitored. Typically the calibration was done before and after every test run to monitor the integrity of the results. At any time, when the efficiency dropped less than 80% for any of the analyser units, the results were disregarded and the supplier was contacted to rectify the problem. The filter was also changed for every 4 hours of testing for protection of the analyser.

A custom operational procedure and calibration were implemented for this investigation according to the basic guidelines from Horiba. This was due to various failures faced throughout the investigation based on the standard operation and calibration procedure. Even though the action was considered very costly it was necessary for early detection of the failure at any stage of the experiment. Therefore, the  $\text{NH}_3$  oxidation catalyst efficiency check was performed before and after each test by running the calibration with an ammonia bottle. For the NO efficiency check, the procedure was undertaken weekly according to recommendation by Horiba. A daily operation and calibration procedure is summarized in figure 3.3.4.

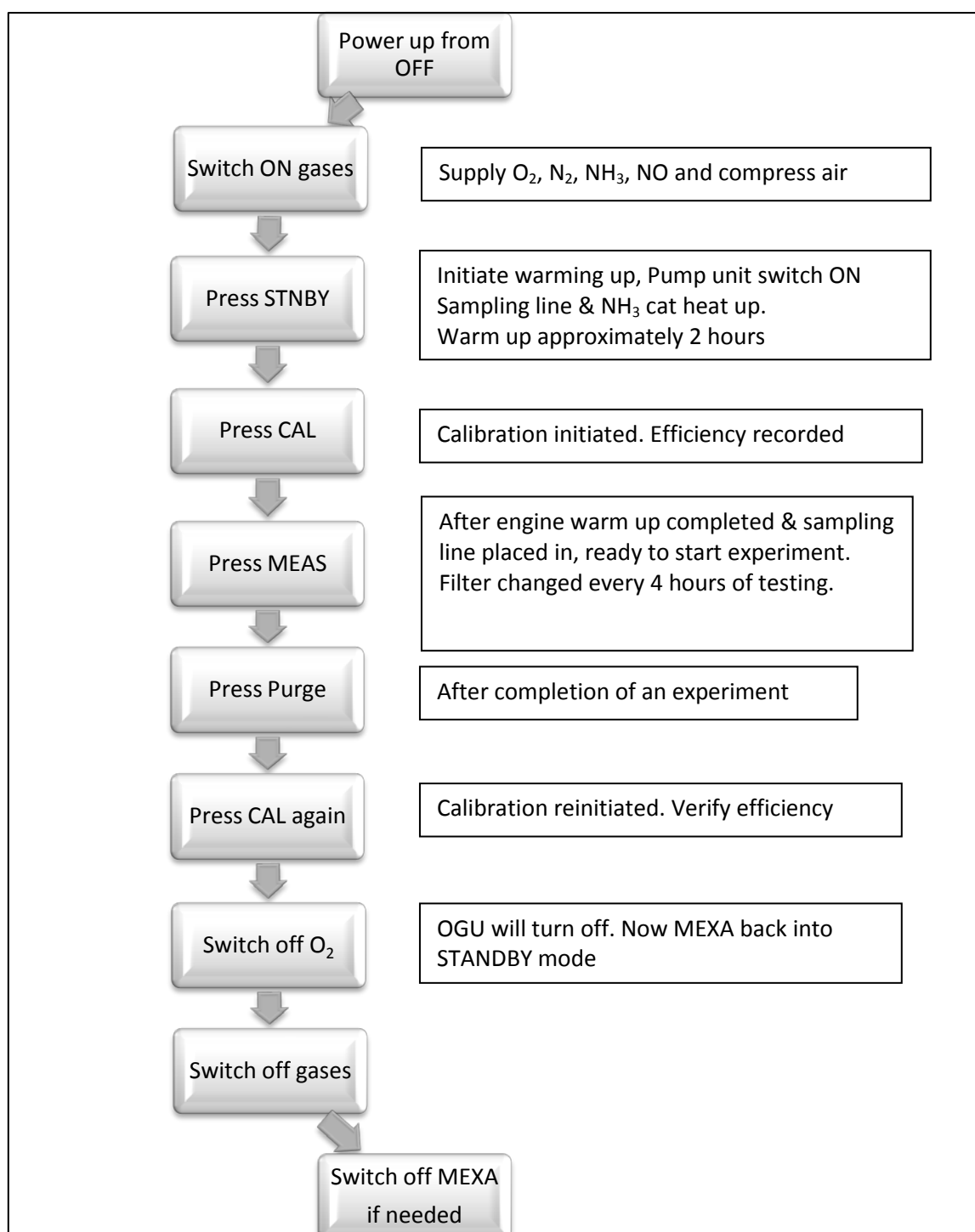
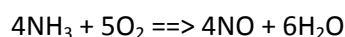


Figure 3.3.4 Process Flow of MEXA-1170NX Daily Operation and Calibration.

### 3.4.3 MEXA 1170Nx Working Principles

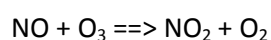
The MEXA-1170NX is the NH<sub>3</sub> measuring unit combining NO (NO<sub>x</sub>) detector based on the Chemiluminescence (CLD) method and the oxidation catalyst. The sample gas is divided into two lines. One line (SUM line) would go through the catalyst inside the oxidation furnace at around 850° C. The other line (NO<sub>x</sub> line) would skip the oxidation furnace. At the catalyst, NH<sub>3</sub> is oxidized into NO by the reaction as follows:



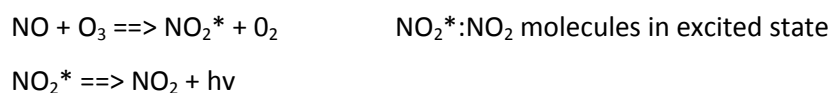
Since the oxidation efficiency in the oxidized catalyst is not 100%, the measured value is compensated using the confirmed oxidation efficiency value. The unit is equipped with an adjustment function to minimize the response gap between detectors in each line that may cause error at drastic concentration change. The analyser is capable of switching between two modes. By default in the NO<sub>2</sub> mode the oxidation catalyst would be turned off but optionally could be turned on for fast switching option. The carbon converter is gradually consumed by reduction process and requires periodic replacement.

#### 3.4.3a Working Principle of Chemiluminescence (CLD)

The details of CLD working principles are described in the MEXA 1170Nx user manual [Horiba MEXA 1170Nx operating manual 2004]. CLD is widely used as the measurement method of NO and NO<sub>x</sub> in exhaust gases from engines because it is highly sensitive to NO and is not easily interfered by other components. When sample gas containing NO is mixed with ozone (O<sub>3</sub>) gas in a reactor, NO is oxidized and is transformed to NO<sub>2</sub> as shown in the reaction:



Some of the formed NO<sub>2</sub> molecules here is in excited state, which means its energy is higher than normal. Excited NO<sub>2</sub> molecules release excitation energy as light when returning to the ground state following these reactions:



This phenomenon is called Chemiluminescence, and the light intensity is directly proportional to the quality of NO molecules before the reaction. Thus, NO concentration in the sample can be estimated by measuring the amount of radiated light.

### 3.4.3b Interference of CO<sub>2</sub> and H<sub>2</sub>O

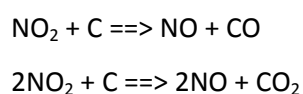
Also noted from the MEXA 1170Nx user manual is the effect from interference of CO<sub>2</sub> and H<sub>2</sub>O to the measurements. Some of excited NO<sub>2</sub> molecules lose excitation energy by collision with another molecule before returning to the ground state by emitting light. In this case, NO<sub>2</sub> returns to ground state, but chemiluminescence does not occur as shown in reaction;



The probability of energy loss depends on the kind of the collision opponent, and the species and concentrations of co-existing gas components may affect NO sensitivity of the CLD method. The probability of energy loss by CO<sub>2</sub> and H<sub>2</sub>O is larger than that by N<sub>2</sub> and O<sub>2</sub> in the components of typical engine exhaust gas. Therefore the change of CO<sub>2</sub> and H<sub>2</sub>O concentration in the sample tends to cause the change of NO sensitivity. In general, to lessen the interference of CO<sub>2</sub> and H<sub>2</sub>O inside of a reactor is maintained to a low pressure condition.

### 3.4.3c Measurement of NO<sub>x</sub>

Based on the working principles of CLD described in MEXA 1170Nx user manual, it is obvious that the NO<sub>2</sub> originally included in a sample cannot be measured by CLD, because it does not cause chemiluminescence. To measure the NO<sub>2</sub>, it is converted to NO using NO<sub>x</sub> converter before measurement. This is shown in the following reactions:



From the above reaction, it is clearly seen that carbon (C), which is the main substance of the NO<sub>x</sub> converted is being consumed by the reduction process. Therefore, as mention earlier, the periodic check and replacement of the NO<sub>x</sub> converter is required.

### 3.4.4 NO<sub>x</sub> measurement in NH<sub>3</sub> mode.

The MEXA1170Nx detects by using a chemiluminescence detector (CLD) which can only detect NO. In this mode the ammonia is converted to NO as illustrated in figure 3.4.4. Therefore, the top line in figure 3.4.4 will display SUM which is the total of all NO and converted NO from Ammonia. The

second line will display only the NO<sub>x</sub> measurement and thus the last display in the analyser show the deduced ammonia by subtraction of SUM to the NO<sub>x</sub> measurement earlier.

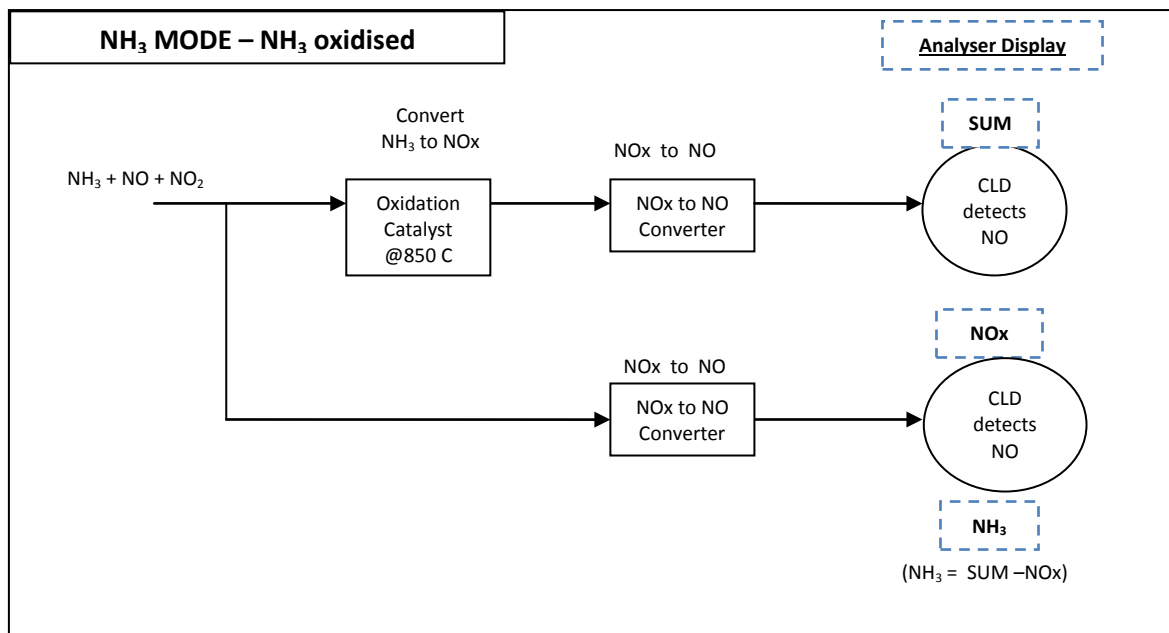
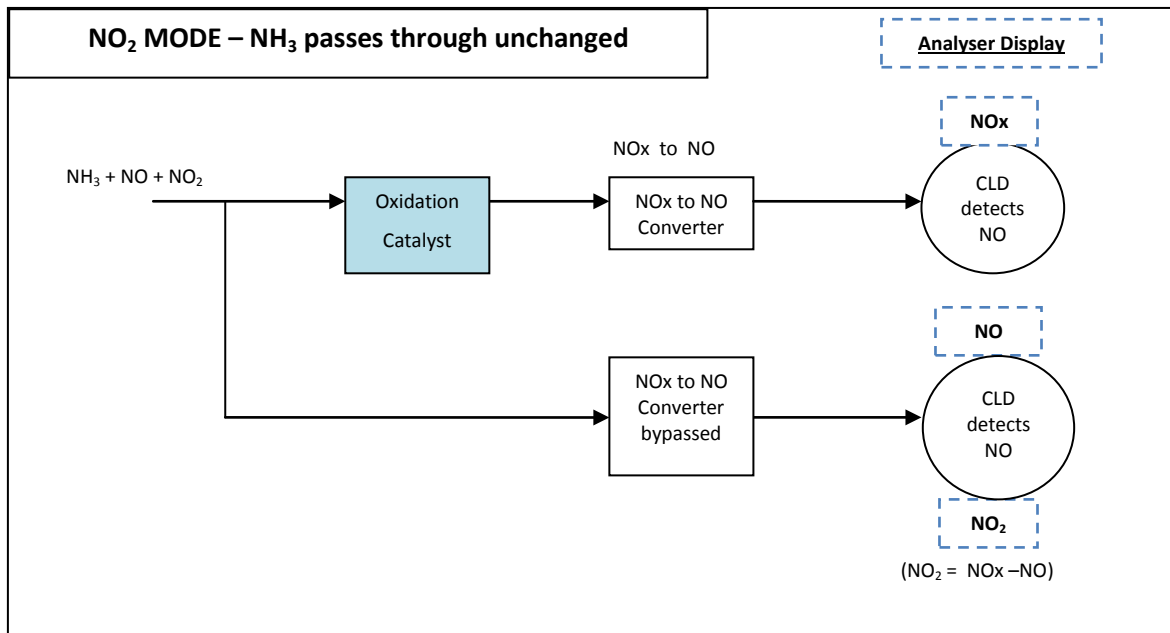


Figure 3.4.4 NH<sub>3</sub> mode of MEXA-1170NX analyser

### 3.4.5 NO<sub>2</sub> measurement in NO<sub>2</sub> mode.

In the NO<sub>2</sub> mode, the NH<sub>3</sub> catalyst is not utilized. It can be switched off or leaving it ON for fast switching mode. In the first line of the analyser in figure 3.4.5, the exhaust gases will pass through the oxidation catalyst unchanged. Then, any NO<sub>x</sub> will be converted to NO before being detected by the CLD detector. Any NO will be detected directly by the CLD. Therefore, the analyser will display NO<sub>x</sub> in the first line. In the second line, the NO<sub>x</sub> to NO converter will be bypassed, therefore the CLD only detect NO and displayed by the analyser. Finally, the analyser only display NO<sub>2</sub> deduced from NO<sub>x</sub> in the first line to the NO in the second line as shown in figure 3.4.5

Figure 3.4.5 NO<sub>2</sub> mode of MEXA-1170NX analyser

### 3.5 ETAS Lambda Meter

In this investigation, the ETAS LA4 lambda meter was used to measure O<sub>2</sub> at any of the instrumentation modules along the SCR exhaust system. In most cases it was used to measure O<sub>2</sub> across the SCR catalysts. The attributes of the LA4 Lambda Meter are described in the operating manual [ETAS LA4 User's Guide, 2005]. The manual describes the LA4 lambda meter as a high-precision measuring device for emission levels. It allows determining lambda values, oxygen content, and Air/Fuel ratio, as well as the internal resistance, pump current, and heater voltage of the LSU lambda sensor. The LA4 is designed for exhaust gas measurements on gasoline, diesel and gas engines.

Based on the output signals from Bosch LSU broadband lambda probes, the measurement results can be calculated either by means of an analytical method that considers fuel properties and ambient conditions or by characteristic curves. The measured value was continuously displayed on the built-in LCD and periodically recorded manually as required. The device conducts a self-test after being powered on using an internal reference. An optimized heater control ensures that the sensor quickly reaches its operating temperature while preventing overheating damages, even at highly fluctuating exhaust gas temperatures and different supply voltages. The advantages of using this device is that it provides a wide measurement range of lambda, oxygen content and air/fuel ratio. In this investigation, two units of LA4 Lambda meter were used as a standalone unit but the data were



logged to the Froude Texcel program. The LA4 lambda meters used in the experiment are shown in figure 3.5. The LA4 wiring configuration is shown in appendix 3.5.



Figure 3.5 ETAS LA4 Lambda meter used to measure  $O_2$  before and after the SCR catalysts

### 3.6 Urea Spray Setup

The spray injector unit was a prototype manufactured by Hilite International Incorporated and it is a customized standalone unit. The spray is a heavy duty spray and the dosing of urea was done manually by setting up the spray frequency and pulse length. The configuration of the Hilite urea spray system is illustrated in figure 3.6. For this program, manual operation of the spray system was considered adequate since only steady state testing was performed. The inlet pressure for this system was fixed at 5 bars

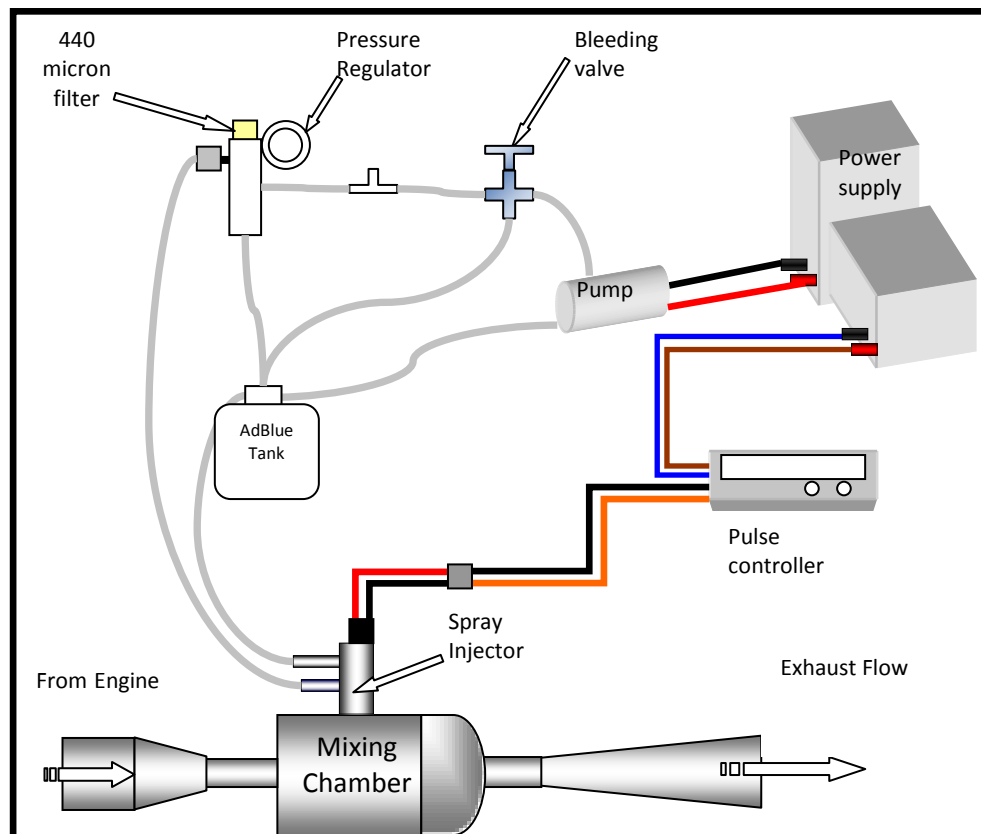


Figure 3.6 Schematic of a manual Urea spray system.

### 3.6.1 Urea Spray Calibration

Prior to running with AdBlue solution, the spray system was calibrated and characterised to measure the flow rate using water. Based on the measurement obtained, a calibration chart was developed as shown in figure 3.6.1. The chart shows the mass flow rate (mg/s) against pulse length (ms) at frequency of 5 Hz. In this chart, the line with circles shows the data calibration with water while the line with triangle shows the urea spray.

The differences between the two lines are due to the different of specific gravity between water and AdBlue solution. The AdBlue, at specific gravity of 1.09 is denser than water, resulting to higher mass flow rate. Periodically, a hydrometer was used to measure the specific gravity of the AdBlue solution. This will ensure that the AdBlue solution does not change due to storage within the vicinity of the test cell. Using the calibration chart gave a general idea of which pulse length in milliseconds should be used with respect to the NO<sub>x</sub> level and engine mass flow rate produced at a specific engine load (BMEP) and speed (RPM).

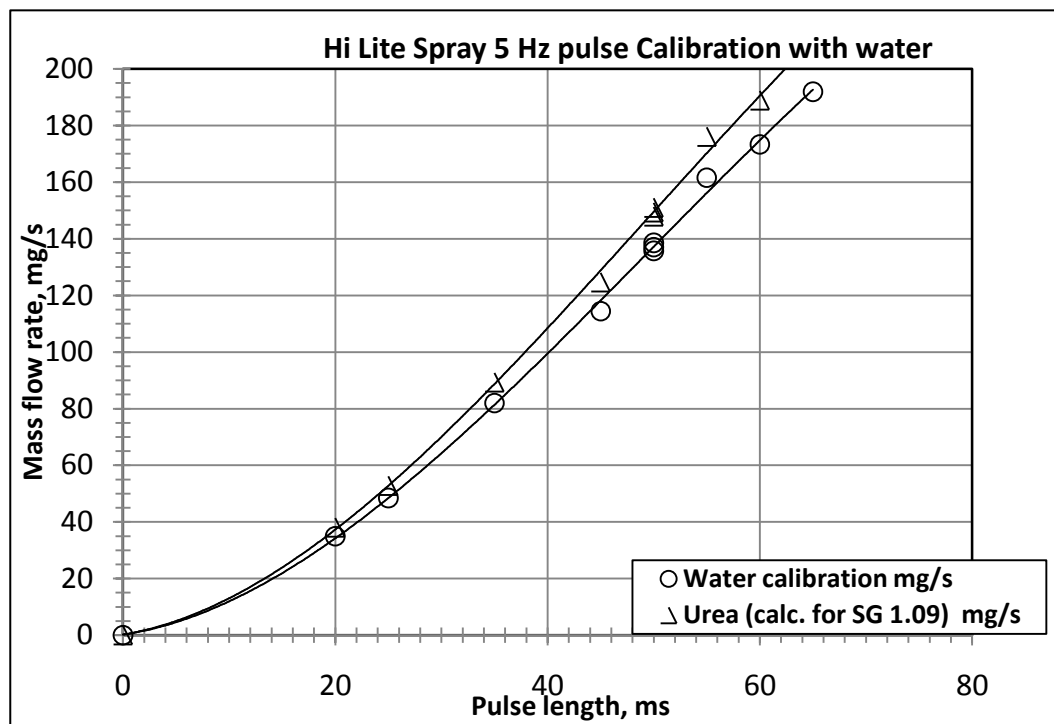


Figure 3.6.1 Calibration chart of Mass flow rate (mg/s) against  
Spray Pulse length (ms) [courtesy Dr C.A. Roberts]

### 3.6.2 Urea Spray Pulse Length Setting Procedure

To determine a suitable spray pulse length the urea spray injector calibration chart as shown in figure 3.6.1 was used. Starting from 28 ms pulse length, the urea mass flow rate is found around 63.2 mg/s. At engine speed of 1500 rpm and 6 bars BMEP, the exhaust mass flow rate was measured around 28.5 grams/seconds. Using this information, the potential ammonia gas produce at this setting was worked out to be around 695 ppm as shown in appendix 3.6.2.

Repeating this procedure for various engine speeds from 1500 to 2500 rpm and load from 2 to 8 bar gives various exhaust mass flow rate ranging from 10 to 100 grams/seconds. As a result chart of the estimated required urea dosage against NOx was established as shown in figure 3.6.2

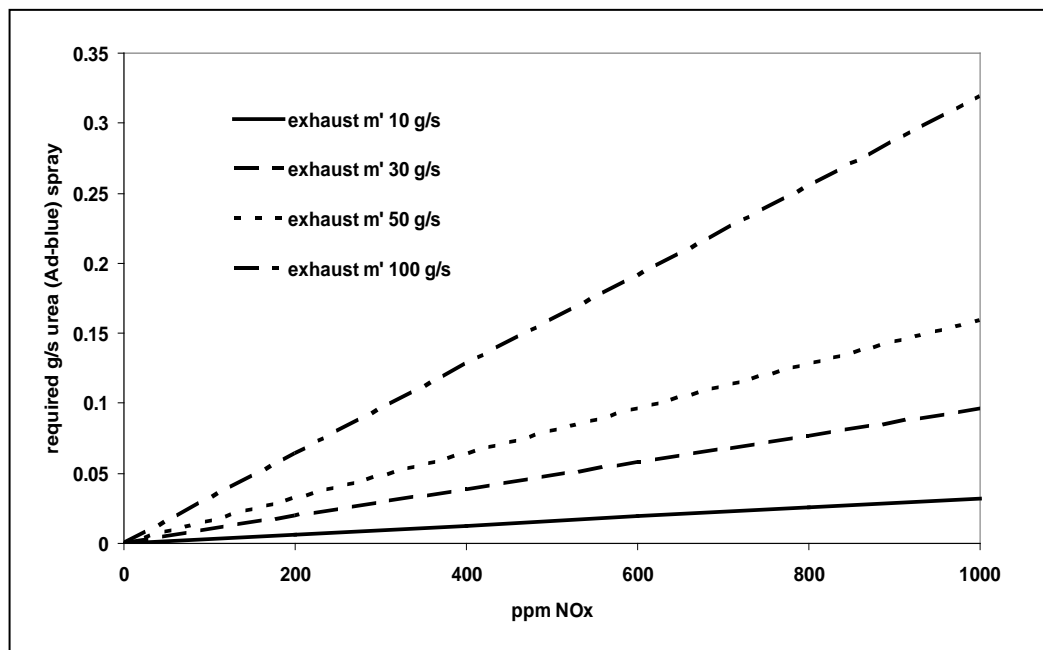


Figure 3.6.2 Chart showing estimated Urea/AdBlue (g/s) required against engine NOx out (ppm)

### 3.6.3 Engine NOx Out Mapping

Prior to selecting the appropriate spray dosage, the engine NOx out level mapping was also produced. This was achieved by running the engine at different Speed (RPM) and Load/BMEP (bar). The engine mass flow rates were recorded manually as the engine speed varied from 1500 rpm to 2500 rpm and BMEP from 2 to 8 bars. The NOx levels were measured using the MEXA 1170Nx and

EXSA 1500 analysers. Figure 3.6.3a and 3.6.3b provide a general engine mapping showing the engine NO<sub>x</sub> out and mass flow rate at various engine Speed (RPM) and load, BMEP (bar).

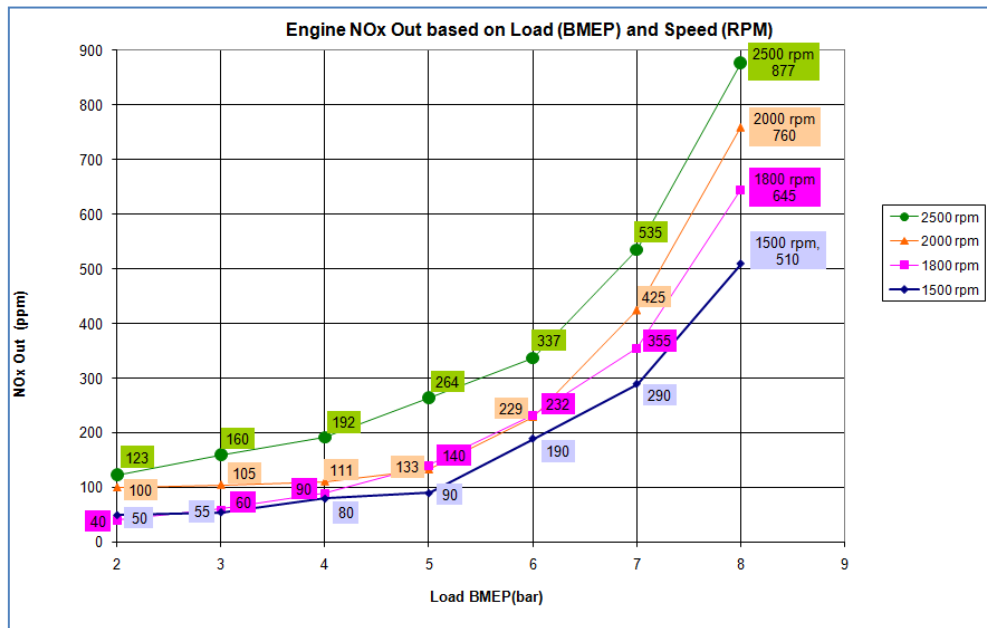


Figure 3.6.3a Engine NO<sub>x</sub> out based on Load BMEP (bars), Speed (RPM) and EGR ON

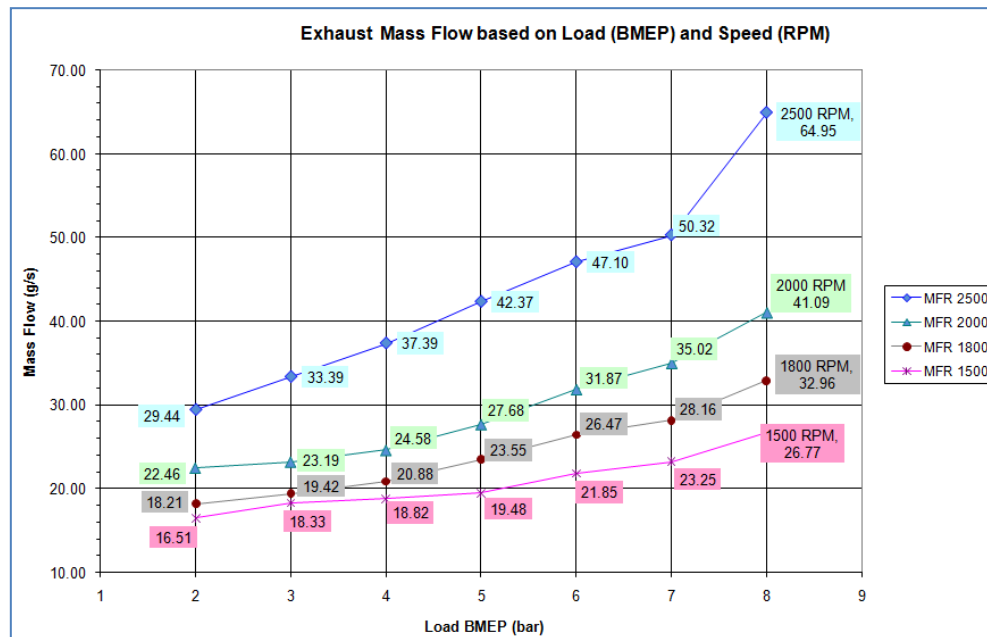


Figure 3.6.3b Exhaust Mass Flow (g/s) based on Load, BMEP (bars), Speed (RPM) and EGR ON.

Based on the fact that the urea spray injector was for heavy duty applications, the lowest possible spray injector setting was utilized for this investigation. It was at 24 ms which is expected to produce about 550 ppm ammonia gas for the SCR reaction ( refer to calculation in appendix 3.6.2 ) In order to match the lowest urea pulse rate at 24 ms, the NO<sub>x</sub> out level must be in the range of 530 to 550

ppm. Therefore in the general NO<sub>x</sub> out mapping (figure 3.6.3a) the engine condition at 1800 rpm and BMEP 8 bars was appropriate at that time. Due to high fuel consumption at 1800 rpm and BMEP 8 bars, the EGR feature was switched off in order to increase the NO<sub>x</sub> level produced by the engine. The low engine speed is preferable based on lower fuel consumption which allows longer testing period with various urea spray and ammonia gas settings. Switching off the EGR also improved the NO-NO<sub>2</sub> ratio as detailed in section 3.8.2.

Therefore another engine NO<sub>x</sub> out mapping was produce by running the engine at 1500 rpm with EGR off whilst varying the load BMEP from 2 to 8 bars with exhaust mass flow rate recorded. As a result the new engine mapping at 1500 rpm was produced as shown in figure 3.6.3c. From this engine mapping, the desirable engine condition was chosen as 1500 rpm and BMEP 6 bars with a mass flow rate of 28.5 g/s.

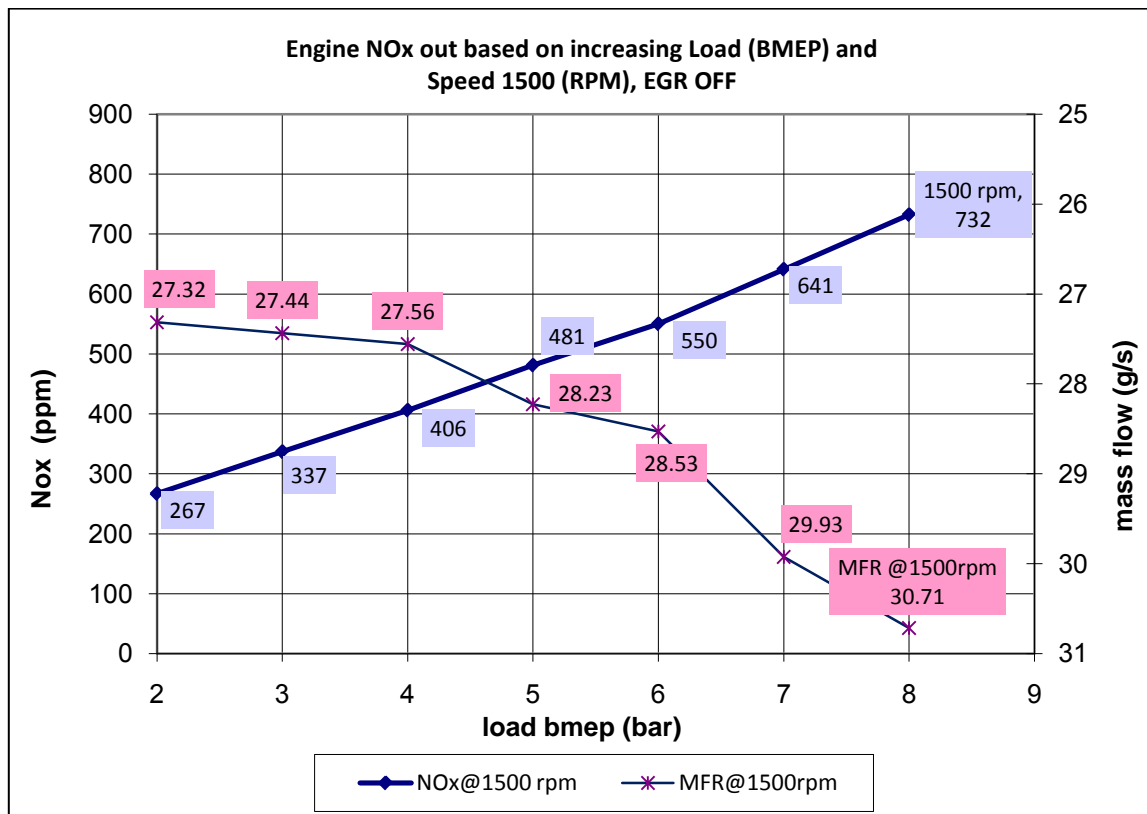


Figure 3.6.3c Exhaust Mass Flow (g/s) based on Load, BMEP (bars), Speed (RPM) and EGR OFF.

### 3.6.4 The Urea Spray Layout and Experimental Procedure

The urea spray pump and the pulse controller were powered by their individual power supply. The pump feeds the AdBlue solution from the tank through the pressure regulator to the spray. The

spray pulse length was controlled using the pulse controller, from 28 ms upwards. The spray was originally designed for heavy duty so this was the minimum working range setting in the experiment. The spray frequency remained at 5 hertz throughout the experiment. The pulse length was increased at 2 ms increments in the experiment. The engine and both analysers were first warmed up. Next, analyser calibrations were completed. The engine was set at 1500 rpm and BMEP of 6 bars. Once the exhaust temperature had stabilised at 300 °C at the last instrumentation module, then the engine warm up stage had completed. During the engine warm up, the urea spray was checked and calibrated outside of the exhaust. Whilst this was being undertaken, the urea injector bosses were blanked off to avoid exhaust gas leakage.

The spray was clamped on a stand and all the piping was connected as shown in figure 3.6.4a and the power supply and the pulse controller were switched on. Normally, the spray would not start spraying immediately and required a few seconds. The urea AdBlue solution would start dripping and eventually spray into the bucket. Once a uniform spraying pattern was achieved, the spray could be plugged back in its location in the exhaust system. If the spray was clogged, then a spray cleaning procedure would take place as described in section 3.6.5. After cleaning, the spray trial would be repeated in the bucket to ensure that cleaning had fixed the clogging problem.



Figure 3.6.4a Urea AdBlue Injector testing prior to experimental with spray system.

Once the clogging issue had been resolved, the spray testing procedure could proceed as per the test program. The spray unit was carefully re-assembled into the exhaust making sure that it was not over tightened. A torque wrench was available for this procedure and a torque setting of no more than 10 Nm was applied. This was a very important procedure as over tightening the assembly could damage the thread causing the spray to fail. The urea AdBlue pipes line and wiring were routed clear of the hot exhaust, see figure 3.6.4b.

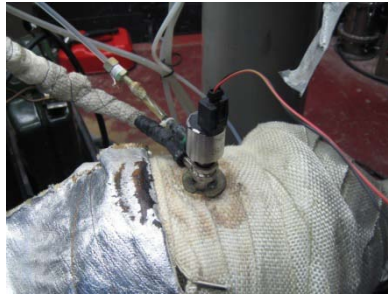


Figure 3.6.4b Urea Spray injector and supply pipes and wiring in place.

Once the spray injector was placed at the mixing chamber, the only indication that the spray was working properly was by monitoring NO<sub>x</sub> level reduction. In this case, the MEXA analyser sampling line must be placed downstream of the SCR. If the NO<sub>x</sub> level remains the same for more than one minute then the experiment was stopped and the spray was rechecked on the stand and probably cleaned. During the engine warm up and after the spray had been cleaned and checked on the stand with the bucket, it was found best practice not to leave the spray injector in the exhaust without spraying.

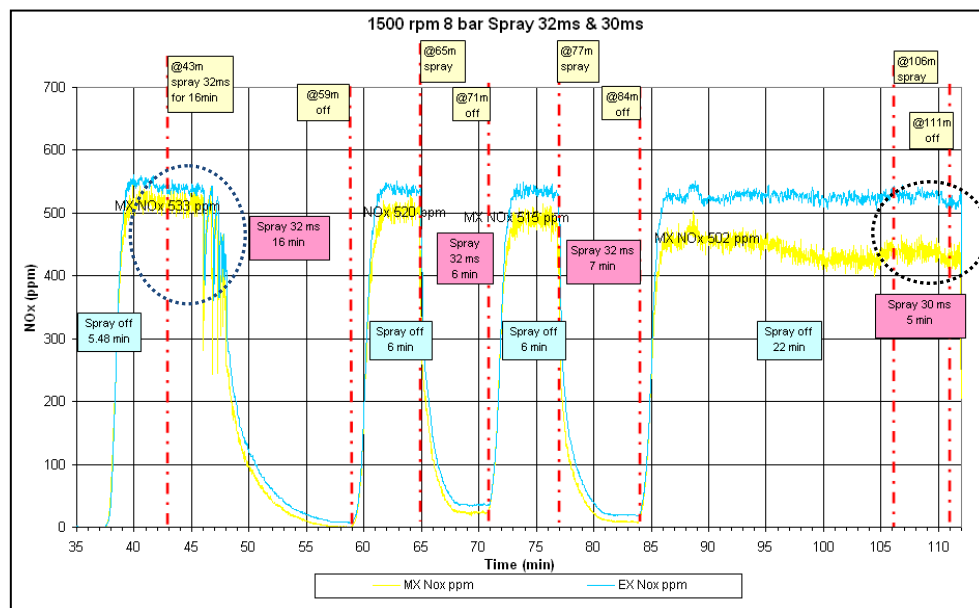
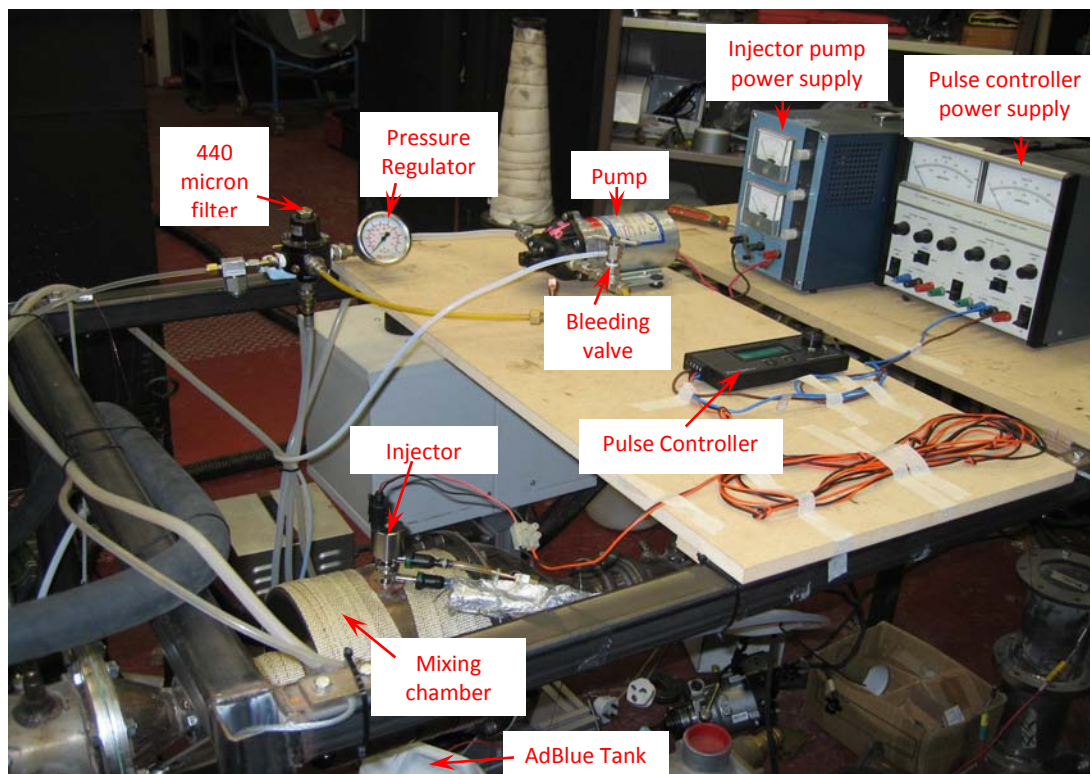


Figure 3.6.4c Spray Injector failure.

This was because the hot exhaust flow had a tendency to bake the urea AdBlue residue left within the spray injector assembly causing the injector not to work properly. The best practice was found to place the urea injector in the mixing chamber and start the experiment immediately, certainly within five minutes of insertion. Longer waiting times before the experiments started would increase the chances of spray failure.

Examples of spray failure are circled in the 43<sup>rd</sup> and 105<sup>th</sup> minutes of figure 3.6.4c. In the 43<sup>rd</sup> minutes, the spray failed to open in the first 4 minutes but later open intermittently for another 3 minutes but managed to properly open after the 7<sup>th</sup> minute. In this case, the spray was previously stopped for about 5.48 minutes. Later in the 105<sup>th</sup> minute, the spray was previously stopped for a period of 22 minutes. At this point, the spray totally failed to open even after running for about 5 minutes. Once all the necessary precaution and injector testing were performed, then the experiment with the urea spray system is ready as the layout shown in figure 3.6.4d.



**Figure 3.6.4d Urea spray system Experimental Layout.**

### 3.6.5 Spray Setting and Cleaning Procedures.

Due to various problems related to the use of urea AdBlue with the spray injector, a customized spray setting and cleaning procedures was developed. These procedures involved visual inspection and cleaning with either warm water or ultrasonic cleaning and also drying with compressed air and a paper towel. These procedures are described in the flow chart in figure 3.6.5a. Periodically, the interior of the spray and the urea piping was cleaned by flushing through with warm water. This was done by substituting the urea AdBlue solution with warm water and running the spray.



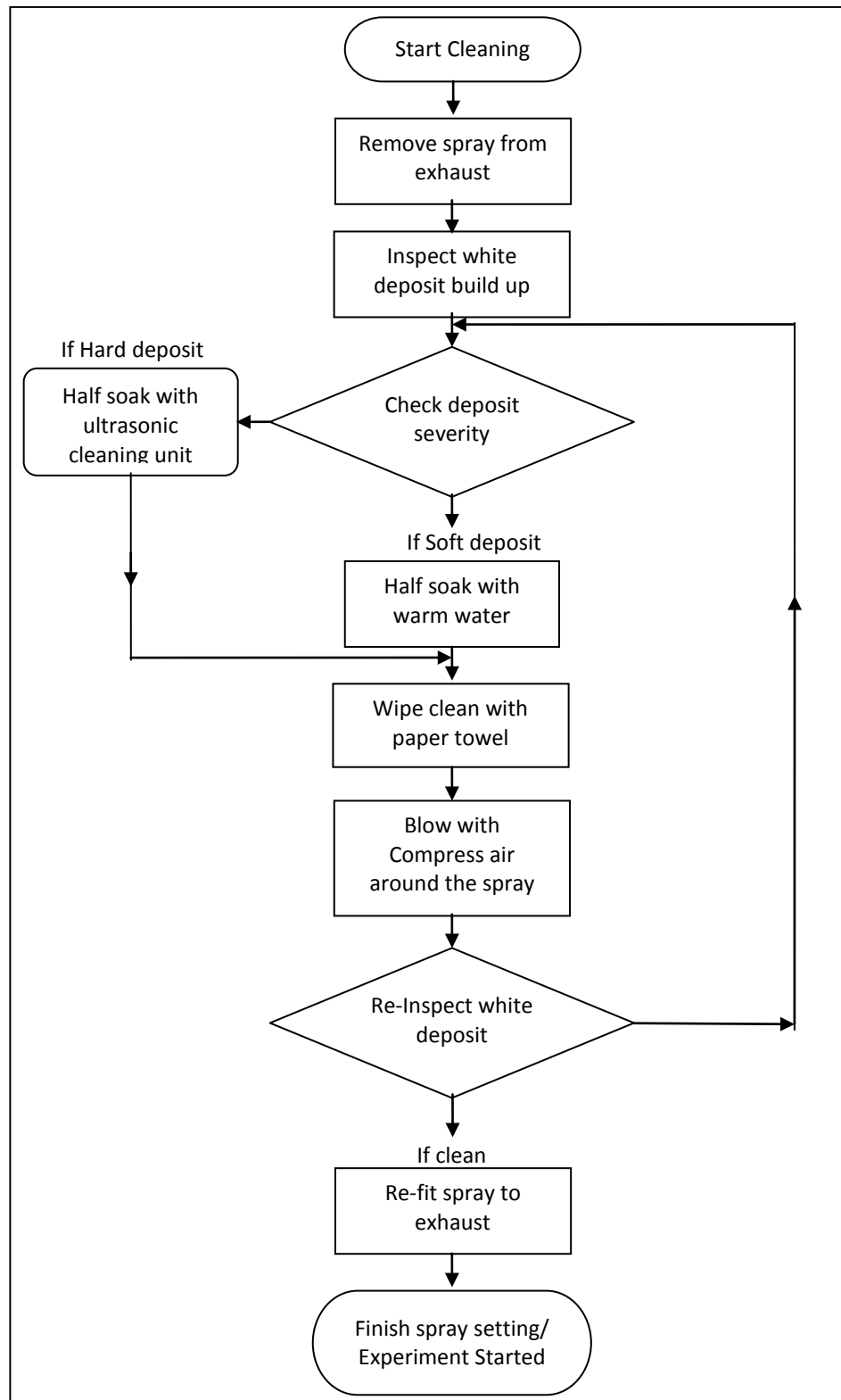


Figure 3.6.5a Spray Cleaning Procedures flow chart

### 3.6.6 Deposit build up on Spray

The AdBlue urea solution has a tendency to crystallize when exposed to the air. This produced a white deposit build up around the spray and tubes. Some of this white deposit hardened if exposed to high temperature in the exhaust stream in the range of 250° to 400°C. Under some conditions melamine formation occurred inside the spray injector opening. Some examples of these white deposits are shown in figure 3.6.6a and 3.6.6b. When this happened, cleaning the spray by soaking with warm water may not be suitable and an ultrasonic cleaning unit was needed.



Figure 3.6.6 White deposit build up and ultrasonic cleaning

The use of the ultrasonic cleaning unit is subject to special attention in order to protect the electrical contact point of the spray unit. The spray unit was disassembled from the main unit and the outer cover sleeve and the removable part were submerged in the ultrasonic cleaning unit as shown in figure 3.6.6d. The cleaning normally took approximately two minutes. If necessary, the procedure was repeated. For the main unit with electrical parts, only the mechanical part of the spray was submerged in the ultrasonic cleaning as shown in figure 3.6.6c and the electrical contact point

remained above the water level at all times. Once the cleaning was completed the spray unit was dried completely using compressed air. Further inspection was needed to ensure none of the electrical parts were exposed to water or any debris from the crystallized AdBlue solution. Sometimes certain parts of the spray injector cleaning could be done manually using tweezers. This procedure depends on the hardness of the deposit formed. An example in this case is shown in figure 3.6.6e



Figure 3.6.6e Manual cleaning of injector sleeve with tweezers.

### 3.6.7 Cleaned Spray inspection

Final visual inspection was needed after the cleaning procedures were completed. The areas to be inspected were the main injector sleeve, the injector opening, the supply inlet and outlet and also the complete assembly as shown in figure 3.6.7. The cleaned sleeve is shown in figure 3.6.7a while figure 3.6.7b shows the main injector opening. Clean inlet and outlet supply lines are shown in figure 3.6.7c. The overall inspection of the spray injector required looking for any debris around the main assembly of the spray as shown in figure 3.6.7d.

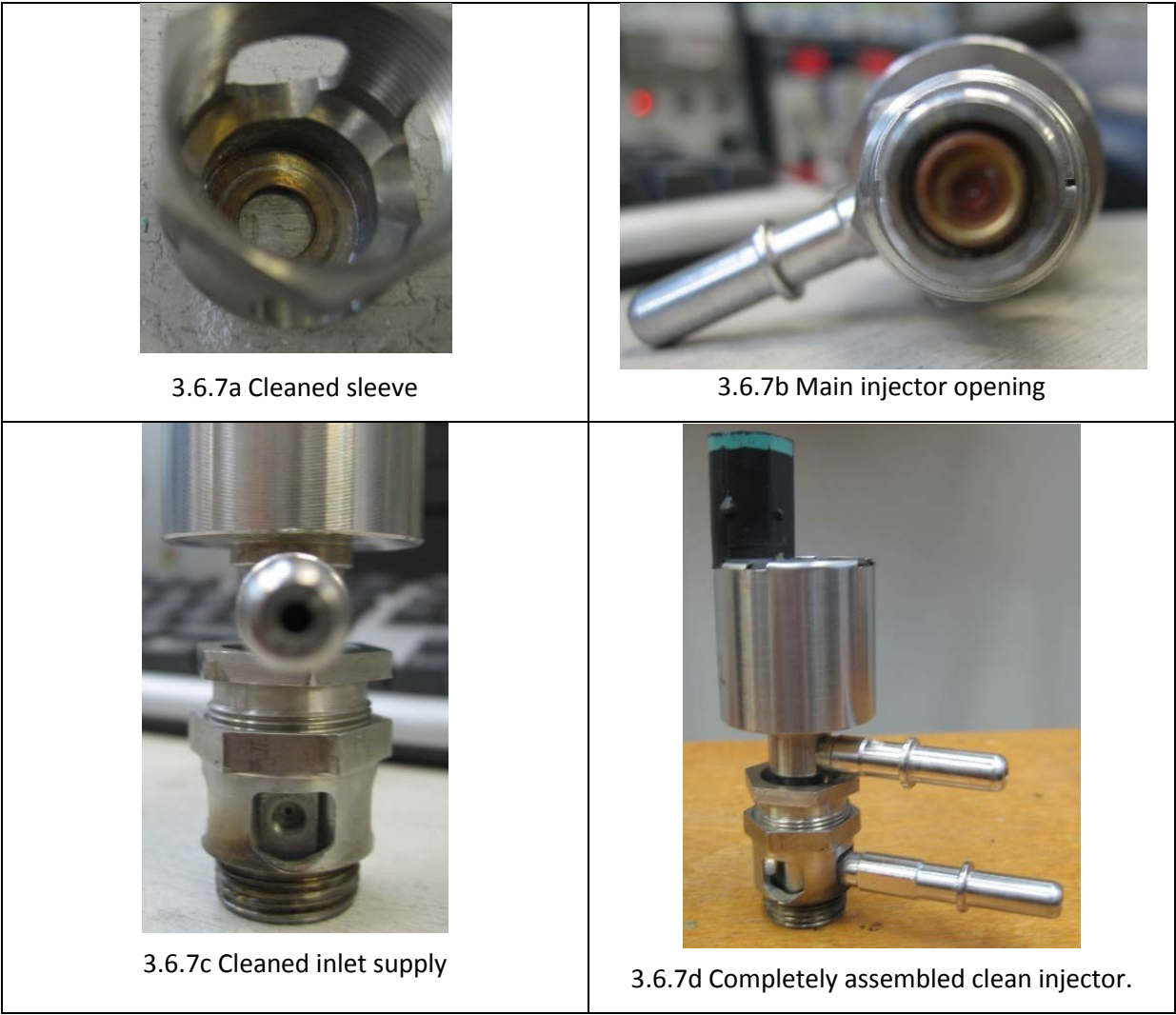


Figure 3.6.7 Final visual inspection of fully cleaned injector

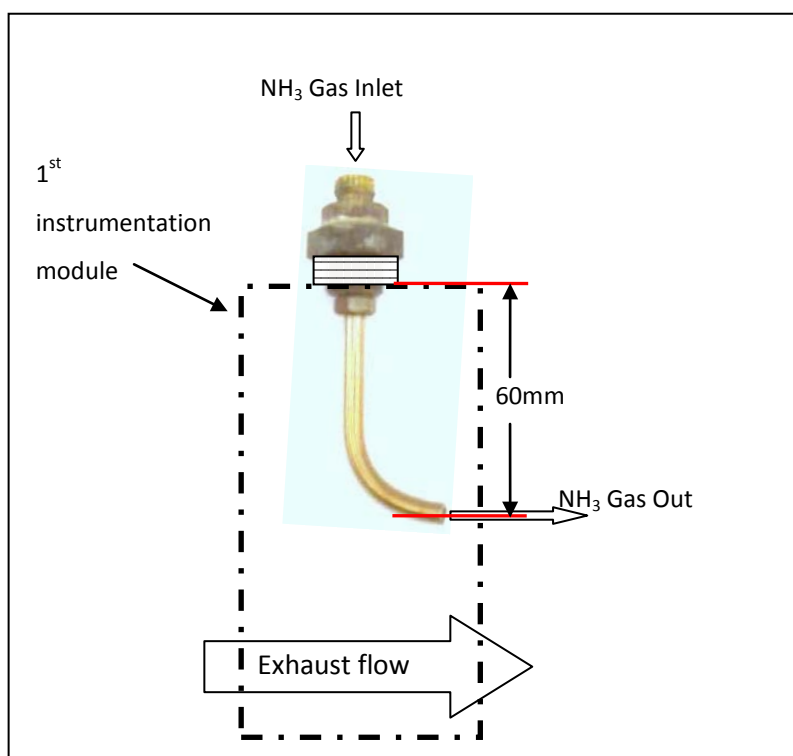
### 3.7 NH<sub>3</sub> Gas Experimental Setup

As a comparison with the AdBlue Urea Spray experiment, NH<sub>3</sub> gas at 4% and 5% concentration, the balance being N<sub>2</sub>, was used. The gas experiment was conducted in order to isolate NH<sub>3</sub> species from urea decomposition processes. In the urea spray experiment, it was expected that the urea droplets would be converted to NH<sub>3</sub> gas. The phase changed and the time taken for it to decompose in the exhaust system before reacting with the SCR catalyst is difficult to predict. Using NH<sub>3</sub> gas should provide information as to SCR performance when 100 % of the urea droplet had transformed to gas phase. When compared to the urea spray experiments it should also provide insight into droplet behaviour.

#### 3.7.1 NH<sub>3</sub> Gas Supply and Nozzle Location.

Initially the test was done utilizing gas bottles containing 4% NH<sub>3</sub>, the balance being N<sub>2</sub> gas, however only approximately 4 to 6 hours of testing was possible. To reduce costs and extend the testing time, a 5% NH<sub>3</sub> gas was later introduced. The flow rate was lowered about 20% from the 4% gas in order to get similar concentration in ppm. Gas was injected into the exhaust stream at the first instrumentation module in the same location as the EXSA 1500 sampling point.

A nozzle with a J-shape was fabricated of internal diameter 4 mm and 6 mm outside diameter. Since the pipe diameter of the instrumentation module was 120 mm, the nozzle was designed such that it measured 60 mm from the wall; the centre of the pipe. The nozzle was also pointed to the direction of the flow. Before connecting the nozzle with the NH<sub>3</sub> gas supply, the nozzle was carefully inserted in the instrumentation module and turned to face the mixing chamber. As the NH<sub>3</sub> gas reached the mixing chamber, it was expected that it would mixed uniformly with the exhaust gases. Then it would continue flowing through the long diffusing cone, as an approximate one dimensional flow, eventually reaching the SCR catalysts for reduction with NO<sub>x</sub>. The gas injector geometry is shown in figure 3.7.1b

Figure 3.7.1b NH<sub>3</sub> Gas Injection Nozzle.

### 3.7.2 Gas flow meter and pressure gauge.

A needle valve was used to control gas flow rate into the exhaust stream and a rotameter – type flow meter measured the rate. The reading on the flow meter was calibrated to ensure an appropriate amount of NH<sub>3</sub> gas was injected. There were two floats available on the flow meter, a glass float and a stainless steel float. The glass float was more sensitive and less dense but was limited to a maximum flow rate of 24 litres per minute. The stainless steel float was denser and suitable for higher flow rate while capable of measuring up to a maximum of 44 litres per minute.

To establish the gas flow rate, measurements must be taken by observing the position of the centre of the float on a graduated scale. The scale ranged from 0 to 150 mm at increments of 10 mm. Readings were converted to flow rate using a calibration chart for air with the appropriate float as shown in appendix 3.7a and 3.7b. Flow rate was controlled using the dial at the bottom of the flow meter. The pressure within the line was monitored by reading the pressure gauge. The gas flow

meter readings were taken manually and the changes of flow rate were marked by pressing the voltage signal trigger.

The voltage signal trigger was a switch wired to the Froude Texcel data logger which helps to identify the change of gas flow rate used. Therefore any changes of NO<sub>x</sub> and NH<sub>3</sub> levels were clearly visible and differentiated on the Texcel control panel. Actually, the measurements with gas flow meter as shown in figure 3.7.2 were used only as a guide. The actual NH<sub>3</sub> mass flow was calculated from the measured ppm and exhaust flow rate.

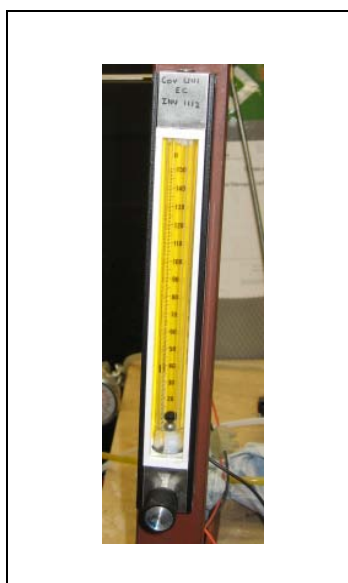
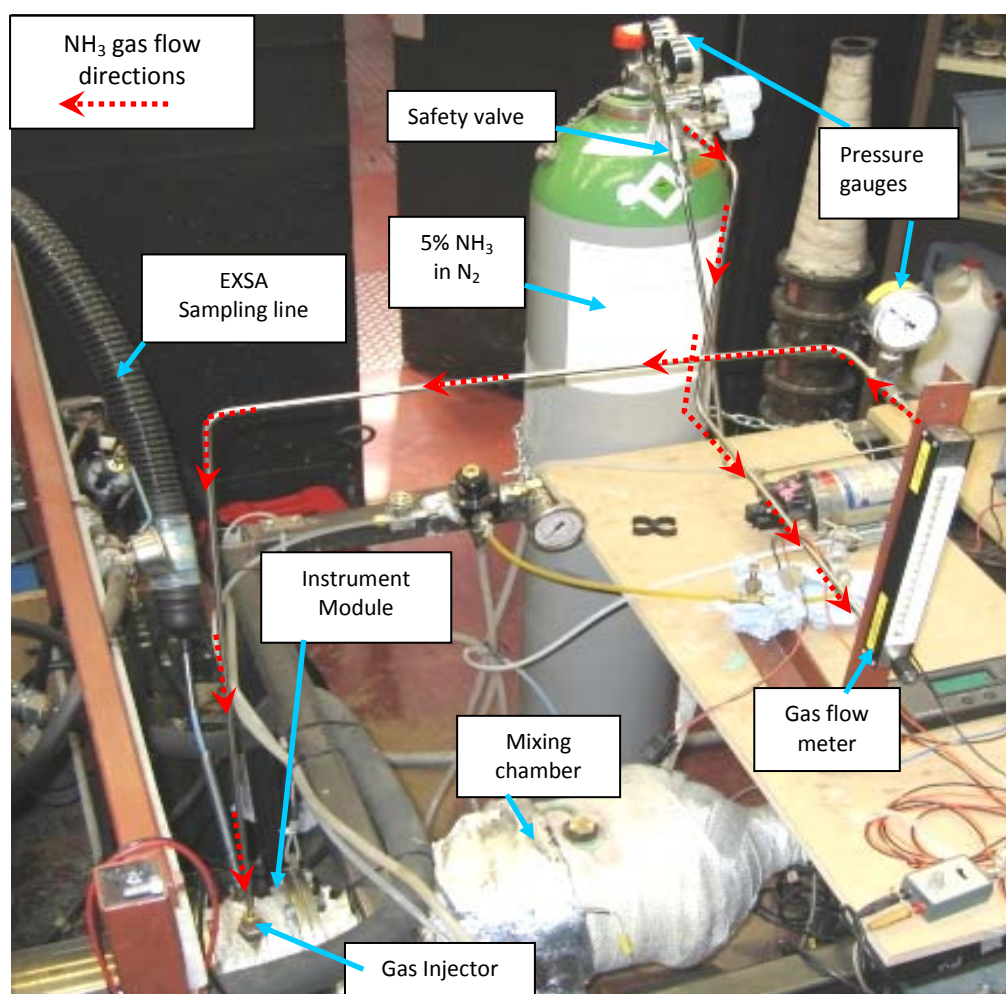


Figure 3.7.2 Gas flow meter reading as a guide.

### 3.7.3 NH<sub>3</sub> gas experimental layout.

The 5% NH<sub>3</sub> gas was used and connected to the exhaust stream in the 1<sup>st</sup> instrumentation module. Stainless steel pipes were used due to the nature of NH<sub>3</sub> which has a tendency to stick on every surface especially on materials such as Teflon. The pressure in the line was fixed to 1 bar and a vented safety valve was connected to the air extraction system on the roof of the engine test cell. A pressure gauge was connected to the flow meter and the pressure recorded throughout to ensure gas flow rate can be accurately calculated. NH<sub>3</sub> gas setup is shown in figure 3.7.3



Figure 3.7.3 NH<sub>3</sub> Gas Experimental Layout

#### 3.7.4 NH<sub>3</sub> Gas Experimental Procedure.

The procedures followed when using gas were similar to those when using urea. With the NH<sub>3</sub> gas, the procedures were much simpler and cleaner but appropriate precautions were necessary including ventilation in the engine cell. Basically, after the engine and analysers had warmed up, the NH<sub>3</sub> gas bottle was switched on. The pressure within the gas bottle and the pipes were adjusted to be at approximately 1 bar. If there was any leakage in the gas piping, the pressure would drop and required necessary action.



The valve was opened on the flow meter and the rate adjusted by noting the position of the glass float. The readings based on the glass float were recorded together with the pressure gauge readings in the pipe line. The  $\text{NH}_3$  and  $\text{NO}_x$  measurements were logged within the Froude Texcel system. The engine mass flow rate readings were also taken from the Ricardo air flow meter. Various sampling locations were used depending on the test matrix, see later in section 3.11. Once the experiment was completed, the air flow meter dial and the gas bottle regulator were turned off. The engine and analysers were cooled down and turned off. Finally the results were plotted and the recorded readings were compiled and are shown in the results section of Appendix 4.

### **3.8 $\text{NO}/\text{NO}_2$ measurement for DPF-DOC arrangement.**

SCR performance depends on the  $\text{NO}/\text{NO}_2$  ratio and this is determined by the DPF/DOC arrangement. Measurements were taken upstream and downstream of the DPF/DOC components. The  $\text{NO}$  to  $\text{NO}_2$  ratio is very important for the SCR reduction reaction due to the  $\text{NO}_2$  involvement as one of the main reductants in the SCR reaction. Initially, as recommended by the catalyst supplier, the DPF/DOC configuration was DOC followed by DPF. However, during the preliminary  $\text{NO}$  and  $\text{NO}_2$  ratio study, it was observed that the amount of  $\text{NO}_2$  produced was not at the appropriate level for optimal SCR performance. So, the alternative configuration was also investigated.

#### **3.8.1 DOC-DPF configuration.**

In the early stage of this investigation, the DOC-DPF was used as the configuration upstream of the Spray and SCR catalyst. The exhaust pipe was connected first to the DOC and then the DPF assembly. The function of the DOC is primarily to oxidize a fraction of the engine out  $\text{NO}$  to  $\text{NO}_2$ . The primary function of the DPF is to trap soot particles and so protect the downstream components, the SCR catalysts. The experiment was conducted at an engine condition of 1500 rpm and BMEP of 6 bars with the EGR and VGT running as normal. The engine was warmed up as per the normal procedure and the MEXA analyser was calibrated prior to sampling.

The EXSA  $\text{NO}_x$  analyser was occasionally used to measure  $\text{NO}$  and  $\text{NO}_x$  for comparison. The sampling points were at the engine out and downstream of DOC-DPF bricks as shown in figure 3.8.1. Before running the experiment, the DPF was taken out for cleaning with compressed air.  $\text{NO}_x$  and  $\text{NO}$  measurement were obtained upstream of the DOC at the same location. The sampling probe was then moved to the second location downstream of the DOC-DOF assembly and  $\text{NO}$  and  $\text{NO}_2$  was

recorded. The results are as shown in table 3.8.1 for an engine conditions of 1500 rpm and 6 bars and temperature of 350 to 420 °C.

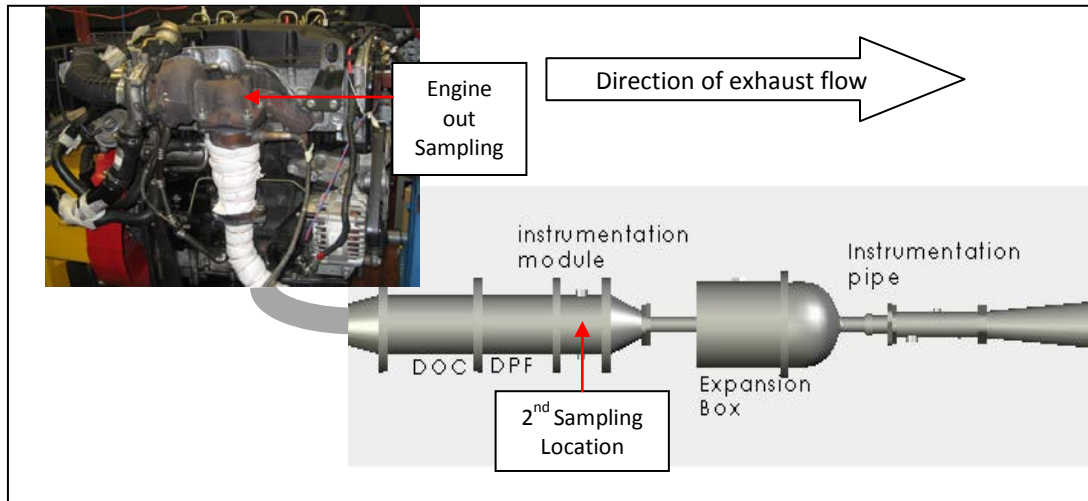


Figure 3.8.1 Initial configuration with DOC-DPF assembly.

Based on the NO<sub>x</sub> and NO measurements, the NO<sub>2</sub> values were deduced and NO/NO<sub>2</sub> ratio was established. From table 3.8.1, the NO<sub>2</sub> level before the DOC-DPF assembly was approximately 0 %. Downstream of the DOC-DPF assembly, only 10 % of NO<sub>x</sub> was NO<sub>2</sub>. This was considered too low for optimal performance of the SCR. It was assumed that soot in the DPF was reducing some of the NO<sub>2</sub> from the DOC back to NO

Sampling Location	NO <sub>x</sub> (ppm)	NO (ppm)	NO <sub>2</sub> (ppm)	NO <sub>2</sub> /NO <sub>x</sub> percentage
Upstream DOC-DPF	392	392	0	0 %
Downstream DOC-DPF	415	372	43	10 %

Table 3.8.1 NO/ NO<sub>2</sub> ratio based on DOC-DPF assembly.

### 3.8.2 DPF-DOC configuration.

The experiment was repeated with the DPF and DOC reversed as in figure 3.8.2. The DPF will still be expected to protect the SCR by trapping soot.

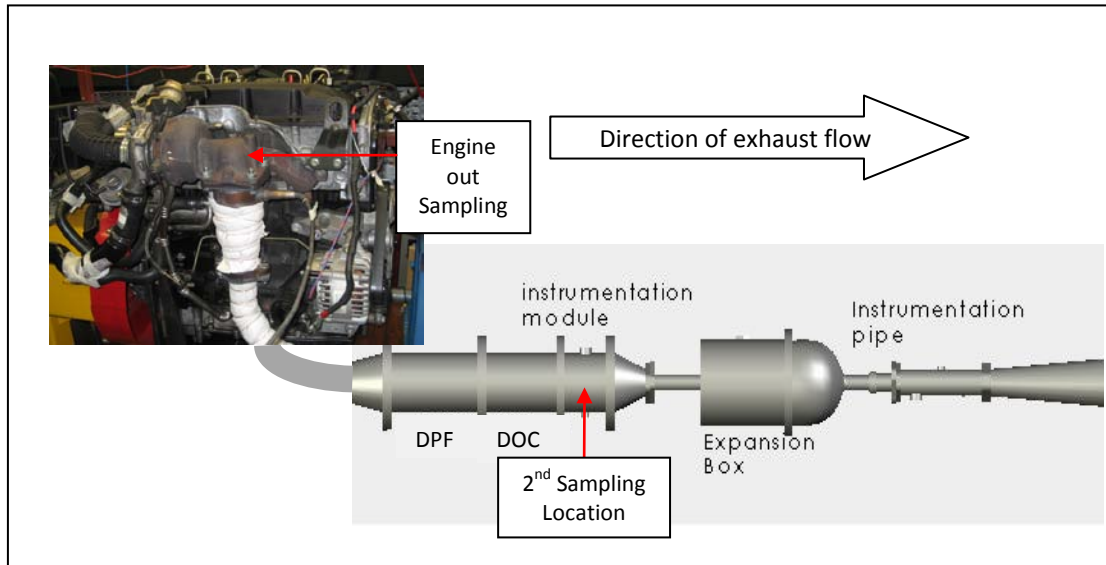


Figure 3.8.2 Final DPF-DOC assembly

Using this configuration, the NO and NO<sub>2</sub> levels were measured. The results are tabulated in table 3.8.2 and show an improved NO<sub>2</sub> level at approximately 40%.

Table 3.8.2 NO/NO<sub>2</sub> ratio based on DPF-DOC assembly

Sampling Location	NO <sub>x</sub> (ppm)	NO (ppm)	NO <sub>2</sub> (ppm)	NO <sub>2</sub> /NO <sub>x</sub> percentage
Upstream DPF-DOC	412	404	8	1.9 %
Downstream DPF-DOC	433	255	178	40 %

Based on these results the second configuration was adopted. The NO<sub>2</sub> to NO<sub>x</sub> ratio of about 40% was considered more desirable for this investigation. However, in most literature reviewed a higher ratio is recommended for good NO<sub>x</sub> conversion. Narayanaswamy et al. (2008) simulated NO/NO<sub>2</sub> ratio up to 0.25/0.75 and implied good conversion over zeolite with excess NO<sub>2</sub>. The significance of excess NO<sub>2</sub> over zeolite at lower temperature was discussed by Rahkamaa-Tolonen et al. (2005) to enhance SCR reactions. Devadas et al. (2006), Takada et al. (2007) and Chatterjee et al. (2007) all agreed that higher NO<sub>2</sub>/NO<sub>x</sub> ratios (> 50%) give good conversion of NO<sub>x</sub>.

In order to further increase the NO<sub>2</sub> level for this experiment, the EGR was turned off. This resulted in higher engine out NO<sub>2</sub> levels as shown in table 3.8.3 below. The NO<sub>2</sub>/NO ratio supplied to the SCR system in the experiments was thus generally about 60% NO<sub>2</sub> and 40% NO. The NO<sub>2</sub>/NO ratio from

the engine was about 20% NO<sub>2</sub> to 80% NO. This configuration was finalized and used throughout the investigation.

Table 3.8.3 NO/NO<sub>2</sub> ratio based on DPF-DOC assembly with EGR off.

Sampling Location	NO <sub>x</sub> (ppm)	NO (ppm)	NO <sub>2</sub> (ppm)	NO <sub>2</sub> /NO <sub>x</sub> percentage
Upstream DPF-DOC	525	420	105	20 %
Downstream DPF-DOC	530	205	325	60 %

### 3.9 Measurement using various sampling probe length.

Prior to designing the experimental test matrix, a brief investigation of various sampling probe lengths was also conducted. The assumption throughout was that the flow was essentially one dimensional within the SCR. To assess the validity of this assumption, measurements were taken inside the exhaust pipe using 3 different lengths of sampling probes. The sampling probe was connected directly to the end of the heated line from the MEXA 1170Nx. Based on the inside diameter of the instrumentation module (120 mm), the centre stream was 60 mm from the pipe wall. The three sampling probes used were at 55 mm, 25 mm and 10 mm from the wall as shown in figures 3.9a, b and c.



Figure 3.9a Variation of sampling probe length for profile measurement

Experiments were conducted using 4% NH<sub>3</sub> gas. The experiments were conducted at engine speed of 1500 rpm and BMEP of 6 bars. The quadruple SCR catalyst was used. Initially the NO<sub>x</sub> measurement was taken upstream of the SCR catalyst without injecting NH<sub>3</sub> gas. Then, the MEXA sampling probe was moved to the location downstream of the SCR catalyst and NH<sub>3</sub> gas was injected. The analyser

was thus placed to measure  $\text{NH}_3$  or  $\text{NO}_x$  slippage after the SCR. The same procedure was used for all probes.

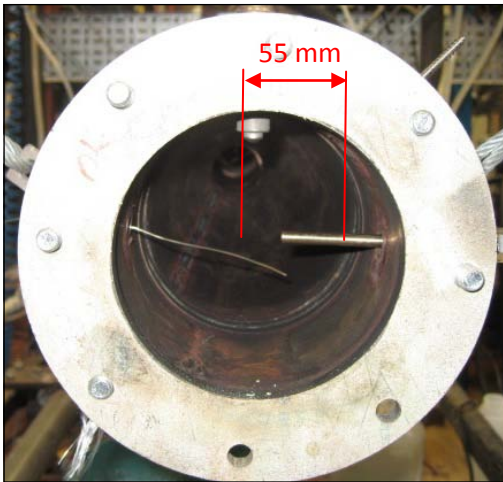


Figure 3.9b Long (55 mm) sampling probe

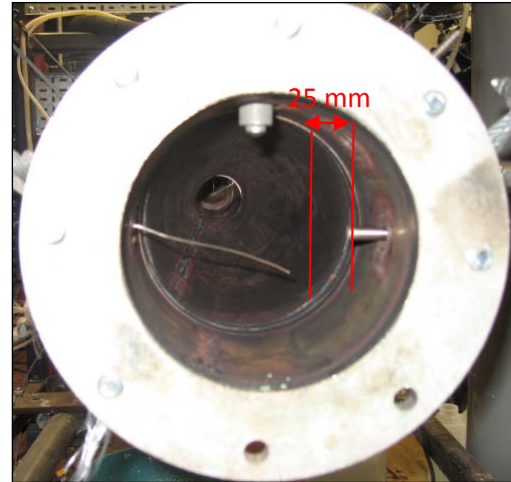


Figure 3.9c Medium (25 mm) sampling probe

The comparison of results between the medium length probe and the long probe at a setting of 100 mm of the glass float are tabulated in table 3.9.

Table 3.9 Profile Measurements inside the exhaust stream.

Date/ Probe length	SCR brick	Glass float mm	Gas Pressure psi	$\text{NO}_x$ in upstream SCR	$\text{NH}_3$ in upstream SCR	$\text{NH}_3$ out downstream SCR	$\text{NO}_x$ out downstream SCR
16jun/ 55 mm	4	100	1.2	579	510	6	150
24Jun/ 25 mm	4	100	1.2	576	535	7	128
24Jun/ 25 mm	4	100	1.2	576	534	5	125

From table 3.9,  $\text{NO}_x$  in and  $\text{NH}_3$  out measurement do not show much variation between long (55 mm) and medium (25 mm) sampling probe. The slight variation is due to the  $\text{NH}_3$  distribution being non-uniform upstream and hence  $\text{NO}_x$  consumption is not uniform downstream. A plot of results for the long sampling probe measurements at various gas flow rates are shown by the blue line in figure 3.9d. The two measurements using the medium sampling probe are shown in green.

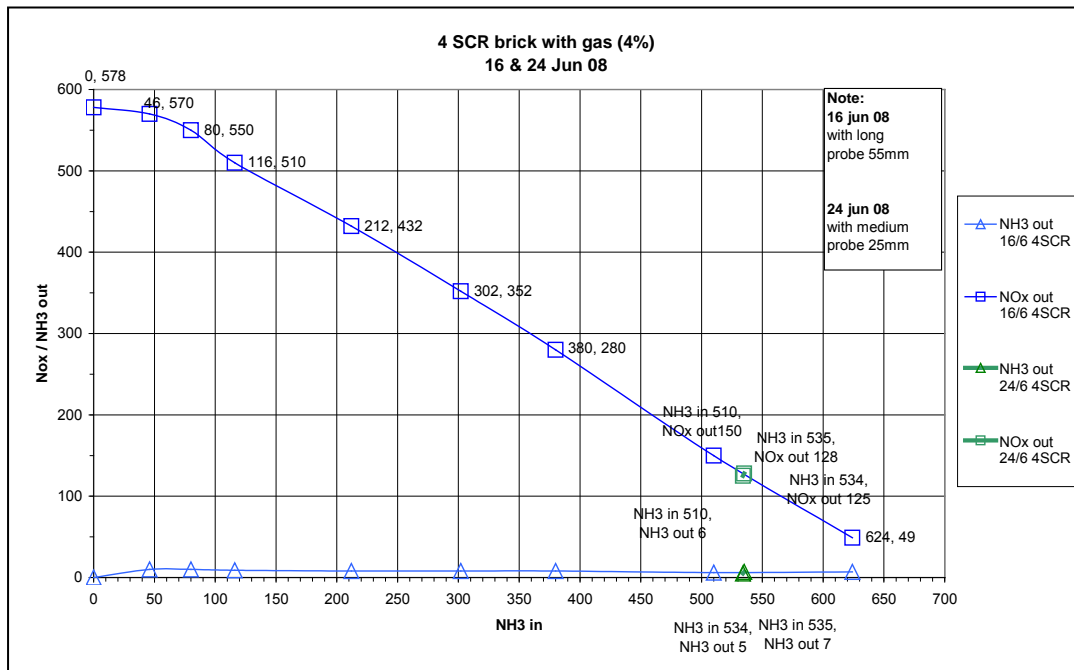


Figure 3.9d Check point with medium sampling probe for gas measurement.

The result shows that the medium sampling probe on the MEXA ammonia analyser was producing similar result as the long sampling probe. So it was concluded that the sampling probe length inside the exhaust assembly does not have much impact on the measurement of the NO<sub>x</sub> and NH<sub>3</sub> level in the exhaust flow. As a result of this, the experiment with the short probe (10 mm) was not necessary for the investigation. Therefore all further measurements used the long probe.

### 3.10 Problems associated with the MEXA Analyser

In the early stage of the investigation, the MEXA ammonia analyser failed several times when measuring NO<sub>x</sub> or NH<sub>3</sub> with the presence of high ammonia concentration or urea. Five types of failures occurred involving rubber seal disintegration, sample line blockage, NO<sub>x</sub> converter failure, NH<sub>3</sub> oxidation catalyst poisoning and NH<sub>3</sub>, NO<sub>2</sub> reaction on the NO<sub>x</sub> converter.

Disintegration of the rubber seal for the NO<sub>x</sub> converter (in the SUM line of the converter) resulted in leakage of the sampling gas flow from the sampling line to the converter unit. This was detected during NO<sub>x</sub> calibration when measuring lower NO<sub>x</sub> readings from the NO<sub>x</sub> calibration bottle. Replacing the rubber seal required a minor service to be performed on the analyzer. A sample of the rubber seal failure is shown in figure 3.10.1a. At this point, the damaged rubber seal was replaced

with a new rubber seal whilst the use of a high temperature PTFE seal was under investigation by the Horiba Corporation.

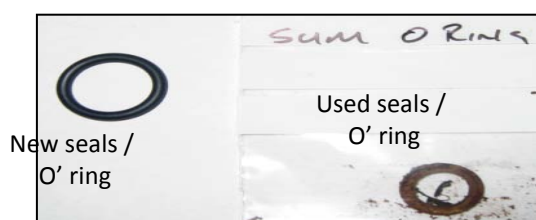


Figure 3.10a Rubber seal disintegrate in the SUM NOx converter.

The second most common failure was line blockage, resulting in the analyser failing to calibrate. During one of the services, deposit build up inside the pipeline to the converter was observed. The blockage was easily cleaned and removed. It was believed that the white deposit was coming from surviving urea droplets penetrating the MEXA analyser sampling line filter. Some of the urea droplets have a tendency to change form to a white deposit when the temperature changes. Urea droplets should evaporate and release  $\text{NH}_3$  in the exhaust, but some evidently survived and were sucked into the MEXA sampling probe and subsequently cooled within the sampling line. This observation was reported to the Horiba research centre for further investigation.

To resolve this problem, a paper based finger filter had to be replaced for approximately four hours of sampling. This will prevent any surviving urea droplet from passing through the sampling line and penetrating the crucial element of the MEXA analyser and also preventing sampling line blockage. The paper based finger filter is located at the back of the main unit of MEXA analyser as shown in figure 3.10b

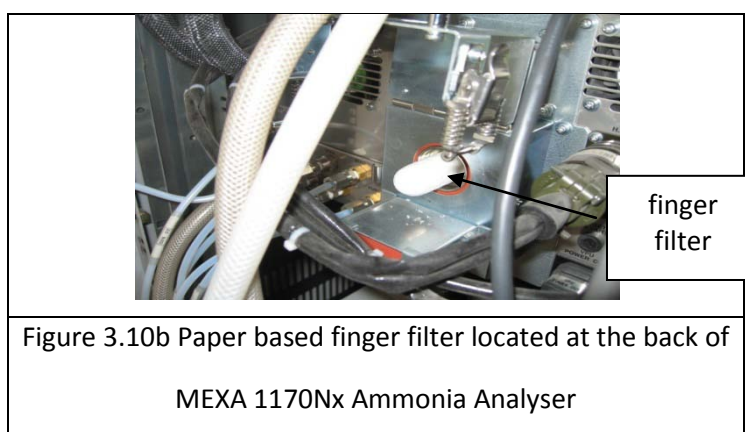


Figure 3.10b Paper based finger filter located at the back of  
MEXA 1170Nx Ammonia Analyser

The most severe problem was due to NOx converter failure. In this failure, the carbon converter used for converting NOx to NO had disintegrated into dust or a powder type material. Initially, a spherically shape carbon compacted NOx converter was supplied as shown in figure 3.10c. The



converter benefited from a large surface area for the reaction which converts NO<sub>x</sub> to NO prior to detection by the CLD analyser unit. It was suspected that some of the unconverted urea droplets survived the exhaust stream and got into the converter, attacking the carbon.

A new glassy carbon for the NO<sub>x</sub> converter, shown in fig 3.10d was used to fix this problem. It features a crystal structure which benefits from low surface area and greater poison resistance. The glassy carbon converter was gradually consumed each time reaction took place in the NO<sub>x</sub> oxidation catalyst. The efficiency of the NO<sub>x</sub> converter must remain at 90% or higher. Once the efficiency drops below 90%, it needs replacing. A gas divider is needed for the NO<sub>x</sub> efficiency check and certified Horiba engineers are trained to perform the efficiency check.

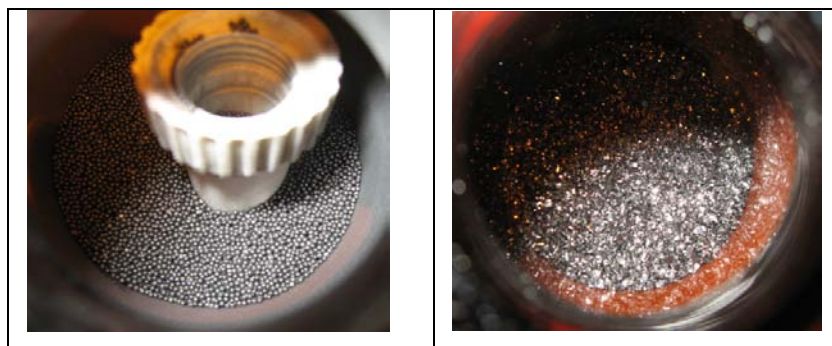


Figure 3.10c Spherical carbon compact NO<sub>x</sub> converter

Figure 3.10d New Glassy Carbon NO<sub>x</sub> Converter

The NH<sub>3</sub> oxidation catalyst poisoning was one of the crucial factors which delayed this investigation. The function of the NH<sub>3</sub> oxidation catalyst is to oxidize all NH<sub>3</sub> gas to NO to be detected by the CLD detector. It was first detected during the daily NH<sub>3</sub> catalyst efficiency check. The NH<sub>3</sub> catalyst efficiency check was performed by running the analyser calibration at the beginning and the end of each test. During this check, the NH<sub>3</sub> catalyst efficiency was found to be below 80%. At this point the NH<sub>3</sub> measurement is no longer considered acceptable and the oxidation catalyst needs replacing.

It was believed that some of the surviving urea droplets were attacking the NH<sub>3</sub> oxidation catalyst. The NH<sub>3</sub> efficiency check was easier to perform as compared to the NO<sub>x</sub> converter efficiency check. It only needs the NH<sub>3</sub> gas bottle at 95 ppm and the NH<sub>3</sub> efficiency was checked daily throughout the investigation. The daily NH<sub>3</sub> efficiency check was included as part of the testing procedure. The final problem identified with the MEXA was the occurrence of reaction between NO<sub>2</sub> and NH<sub>3</sub> on the NO<sub>x</sub> converter which lead to errors in the measurement of these species.



The measurement of NO, NO<sub>2</sub> and NH<sub>3</sub> were performed at the inlet and exit of the SCR catalysts as described by the test matrix shown in table 3.11b. Due to some interference with the NO<sub>x</sub> and NH<sub>3</sub> measurements in the NO<sub>x</sub>/NH<sub>3</sub> mode and NO<sub>x</sub> and NO<sub>2</sub> in the NO/NO<sub>2</sub> mode, some basic assumption had to be made. The assumption covered the reliability of the measurements taken with respect to the measurement modes selected. In the NO<sub>x</sub>/NH<sub>3</sub> mode, only the SUM measurements were correct while the NO<sub>x</sub> measurements were too low and the NH<sub>3</sub> measurements were too high in the presence of Ammonia.

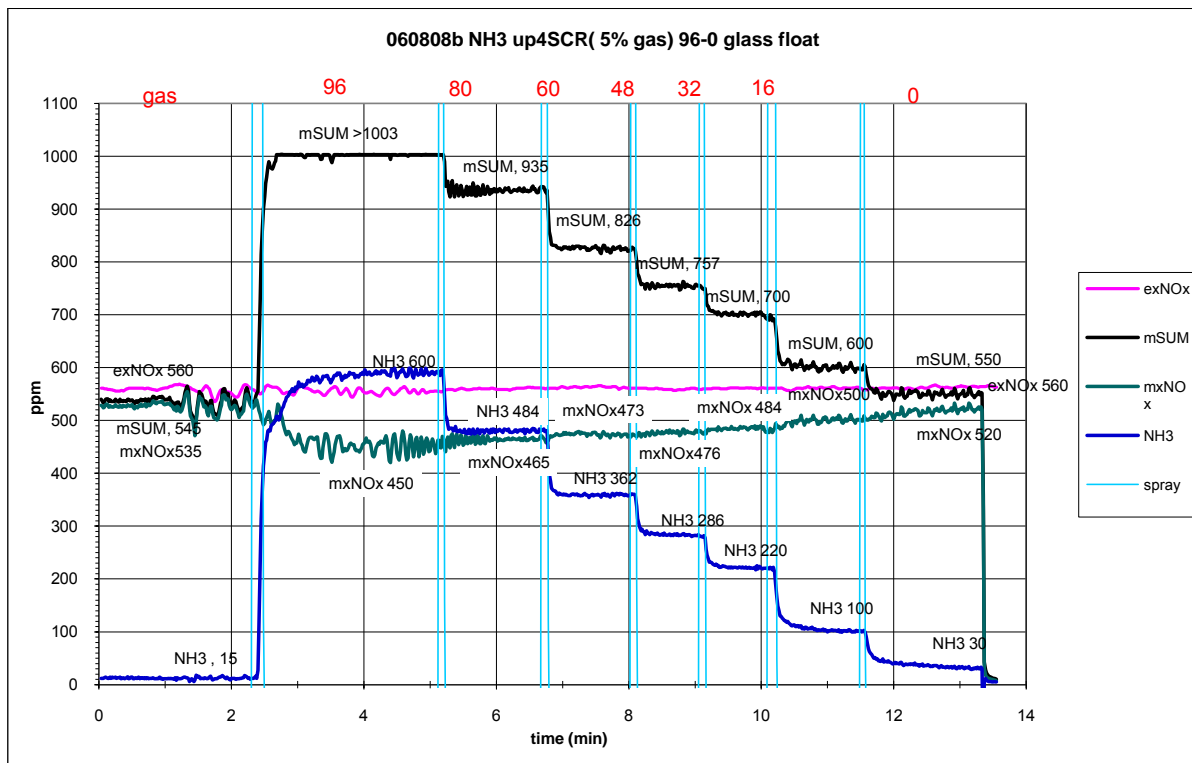


Figure 3.10e A typical example of erroneous measurement of NO<sub>x</sub> in presence of Ammonia.

The typical erroneous measurement of NO<sub>x</sub> in presence of ammonia is shown by the green line in figure 3.10e. In this example, the NO<sub>x</sub> measurement was taken upstream of the SCR brick using the NH<sub>3</sub> mode of the MEXA analyser. At the same time, EXSA analyser was also used to measure NO<sub>x</sub>, but upstream of the gas injection, shown by the pink line in figure 3.10e.

The spray trigger was denoted by the vertical light blue lines, which indicates the changes of gas injection setting. As the gas injection started from the second to the fifth minutes, the NO<sub>x</sub> level shows decreasing values (green line) as the ammonia level rises (blue line). In the absence of ammonia, using the EXSA analyser upstream of the gas injection shows the NO<sub>x</sub> level remains

unchanged. This interference can be seen for all measurements of NO<sub>x</sub> in presence of ammonia. This phenomenon was also supported by the finding of **Sandip et al., (2007)** where, Chemiluminescence (CLD) based analyser lead to erroneous NO<sub>x</sub> measurements. They also develop a way to cure this problem using an ammonia scrubber which prevents the interference of NO<sub>2</sub> with ammonia and poisoning effect of the converter catalysts in CLD NO<sub>x</sub> analyser. At the time of this investigation, the use of ammonia scrubbers was still under evaluation by Horiba. Therefore, a special measurement strategy was developed later discussed in section 3.11 in order to measure NO<sub>x</sub> and NH<sub>3</sub> in the presence of high concentration of ammonia.

Meanwhile, in the NO/NO<sub>2</sub> mode of the MEXA analyser, only NO measurements were correct while SUM and NO<sub>2</sub> measurements were too low. These erroneous measurements were due to reaction between NH<sub>3</sub> and NO<sub>2</sub> on the NO<sub>x</sub> converters in both lines of the analyser. Instead of simply converting NO<sub>2</sub> to NO, the reaction of NO<sub>2</sub> with NH<sub>3</sub> to produce N<sub>2</sub> causes low NO<sub>x</sub> reading in NO<sub>x</sub>/NH<sub>3</sub> mode.

It also caused erroneous NO<sub>x</sub> and NO<sub>2</sub> reading in the NO/NO<sub>2</sub> mode. The SUM measurements in NO<sub>x</sub>/NH<sub>3</sub> mode represent the measurement of the total NH<sub>3</sub> + NO + NO<sub>2</sub>. At a later stage, the SUM readings were used to deduce the NO<sub>x</sub> and NH<sub>3</sub> and later to NO<sub>2</sub> by deduction method. The analyser performance when measuring a mixture of NO, NO<sub>2</sub> and NH<sub>3</sub> are summarized in table 4.1a below.

Table 3.10a MEXA analyser performance when measuring a mixture of NO, NO<sub>2</sub> and NH<sub>3</sub>

	<b>SUM(NO+NO<sub>2</sub>+NH<sub>3</sub>)</b>	<b>NO<sub>x</sub></b>	<b>NH<sub>3</sub></b>
NO <sub>x</sub> /NH <sub>3</sub> mode	Correct	Incorrect – too low	Incorrect – too high
	<b>SUM (NO<sub>x</sub>)</b>	<b>NO</b>	<b>NO<sub>2</sub></b>
NO/NO <sub>2</sub> mode	Incorrect – too low	Correct	Incorrect – too low

Considering the MEXA analyser limitation in measuring the emission in this investigation, careful interpretations are needed to analyze the results. Therefore a total of seven set of positive results have been identified and categorized according to the type of ammonia injected and the number of SCR brick utilized. The remaining of the measurements was considered as loss and discarded from the analysis of the results. Two sets of result were obtained from urea spray test comprises of single SCR brick and four SCR bricks. Four sets were from the 5% ammonia gas test which includes one through four bricks. Only one set of results were available from the 4% ammonia gas test.

### 3.11 Final Measurement Strategies.

As stated above due to the interference between  $\text{NO}_2$  and  $\text{NH}_3$  on the  $\text{NO}_x$  converter erroneous measurements resulted when  $\text{NH}_3$  was present in the gas stream. To circumvent this problem a measurement strategy was derived which enable measurements of all three gas,  $\text{NO}$ ,  $\text{NO}_2$  and  $\text{NH}_3$  to be obtained upstream and downstream of the SCR. The EXSA was used to measure engine out emissions upstream of the DPF/DOC. The MEXA was used upstream and downstream of the SCR.

The following measurement strategy was used to interpret the MEXA analyser readings. The  $\text{NO}$  and  $\text{NO}_2$  measurements upstream of the SCR were made in the absence of ammonia and it was assumed that gas phase reactions prior to the SCRs were negligible. Therefore these readings were also valid in the presence of ammonia. The SUM reading from the analyser in the  $\text{NO}_x/\text{NH}_3$  mode in the presence of ammonia was valid, so the ammonia level could be found by manual subtraction.

In the presence of ammonia slip, downstream of the SCR brick only  $\text{NO}$  measurement is correct and reliable. However the readings of the SUM upstream minus the SUM downstream gives a measure of  $(\text{NH}_3 + \text{NO}_x)$  consumed by the SCR bricks. Furthermore, an assumption can be made that  $\text{NO}_x$  and ammonia are mainly consumed on a mol/mol basis during the SCR reactions.

Using this assumption neglects ammonia oxidation and the slow SCR reaction, but is valid as a first approximation for the temperature range of around  $300^\circ\text{C}$  in this investigation. Therefore, half of  $(\text{NH}_3 + \text{NO}_x)$  consumed is either ammonia or  $\text{NO}_x$  consumed.  $\text{NO}$  consumed is available directly from

the difference between upstream and downstream measurements. Finally,  $\text{NO}_2$  consumed is found from the difference between  $\text{NO}_x$  consumed and  $\text{NO}$  consumed.

From the direct measurement of  $\text{NO}$  downstream, the slip of  $(\text{NH}_3 + \text{NO}_2)$  is found by subtraction of  $\text{NO}$  from the measurements of SUM ( $\text{NH}_3 + \text{NO}_2 + \text{NO}$ ). In the case of 4% and 5% ammonia gas in  $\text{N}_2$  injection, the input level can be determined from a calibrated flow meter and the known exhaust mass flow rate. This information can be used to check upstream measurements. For urea spray injection, the potential ammonia injected can be determined from the spray mass flow rate.

By comparison of this with the measured ammonia upstream of the SCR will indicate the mass of spray that has released its ammonia between the spray point and the emissions measurement location. The magnitude of the potential SUM upstream (potential  $\text{NH}_3 + \text{NO} + \text{NO}_2$ ) minus the measured SUM downstream should indicate the total consumption of all species ( $\text{NH}_3 + \text{NO} + \text{NO}_2$ ) in the SCR bricks. This condition is valid with the assumption that no droplets pass through the SCRs.

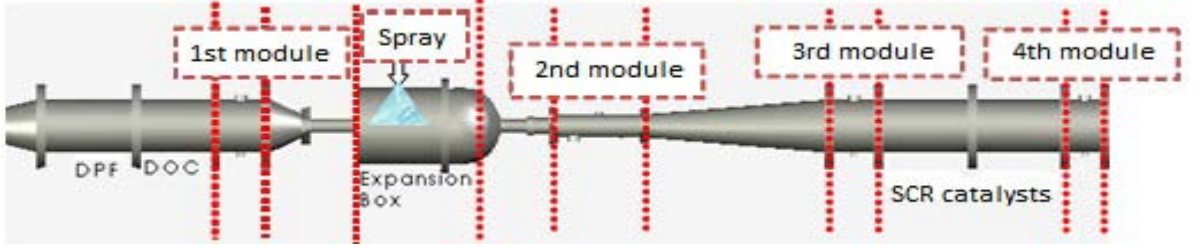
The comparison between urea injection and  $\text{NH}_3$  gas injection in the 1 SCR case would generally give some idea of what happened to the droplets within the SCR brick. Finally the tests were carried out for 1, 2, 3 and 4 SCRs with ammonia gas injection but only 1 SCR and 4 SCR test cases were implemented using urea spray. All of the measurements were made as a function of ammonia level input. The measurement capability of the MEXA analyzer in the investigation is summarized in table 3.11a.

Table 3.11a Measurement strategy when using Horiba MEXA 1170Nx Ammonia analyzer

Location Measure	NH <sub>3</sub> Gas case Sampling Upstream SCR	NH <sub>3</sub> Gas Case Sampling Downstream SCR	Spray Case Sampling Upstream SCR	Spray Case Sampling Downstream SCR
SUM = (NH <sub>3</sub> +NO+NO <sub>2</sub> )	OK	OK	OK	OK
NH <sub>3</sub>	Subtraction (SUM-NOx)	OK If low NH <sub>3</sub> slip	Subtraction (Potential SUM-NOx)	OK If low NH <sub>3</sub> slip
NOx	Measure with gas off	OK If low NH <sub>3</sub> slip	Measure upstream of spray with spray off	OK If low NH <sub>3</sub> slip
NO	Measure with gas off	OK If low NH <sub>3</sub> slip	Measure upstream of spray with spray off	OK If low NH <sub>3</sub> slip
NO <sub>2</sub>	Measure with gas off	OK If low NH <sub>3</sub> slip	Measure upstream of spray with spray off	OK If low NH <sub>3</sub> slip

Note: Downstream measurements with high NH<sub>3</sub> levels ideally need an ammonia scrubber which was not available for MEXA at the time of this study.

These restrictions, have resulted in different measurements mode (either NH<sub>3</sub>/NOx or NO<sub>2</sub>/NO) to be conducted in separate environments. After the final measurement strategies have been fully develop the sampling locations of EXSA and MEXA analysers along the SCR exhaust system were finalized. The experiment was carried out according to the test matrix shown in table 3.11b.

Table 3.11b Experimental Test Matrix with urea spray and NH<sub>3</sub> gas


	Up DPF	1 <sup>st</sup> module	Spray /Gas	2 <sup>nd</sup> module	3 <sup>rd</sup> module	SCR Bricks length	4 <sup>th</sup> module
Test A	EXSA	Capped	Spray	capped	Lambda1 MEXA1	Single (1x) 91 mm	Lambda2 MEXA2
Test B	EXSA	capped	Spray	capped	Lambda1 MEXA1	Quad (4x) 364 mm	Lambda2 MEXA2
Test 1	EXSA	NH <sub>3</sub> gas	Capped	capped	Lambda1 MEXA1	Single (1x) 91 mm	Lambda2 MEXA2
Test 2	EXSA	NH <sub>3</sub> gas	Capped	capped	Lambda1 MEXA1	Double (2x) 182 mm	Lambda2 MEXA2
Test 3	EXSA	NH <sub>3</sub> gas	Capped	capped	Lambda1 MEXA1	Triple (3x) 273 mm	Lambda2 MEXA2
Test 4	EXSA	NH <sub>3</sub> gas	Capped	capped	Lambda1 MEXA1	Quad (4x) 364 mm	Lambda2 MEXA2

### 3.12 Summary of Final Experimental Procedures.

Despite of all the obstacles experienced in the investigation, remedial action was taken and a series of test procedures was adopted in order to ensure a valid and consistent result throughout. The final experimental procedures implemented in the investigation are summarized as follows:

- Allow engine warm up for engine condition of 1500 rpm and load of 6 bars BMEP until the exhaust temperature in final module reached 300 °C.
- Record exhaust mass flow rate for every gas or urea injection settings used.
- Measure O<sub>2</sub> upstream and downstream of SCR bricks.
- Allow EXSA and MEXA calibrations to be completed before and after each test. MEXA efficiency check needs to be maintained for internal oxidation catalyst to be above 90% at all time and the NO<sub>x</sub> converter efficiency was assumed to be 100%
- Measure NO<sub>x</sub> out from engine using EXSA NO<sub>x</sub> Analyser downstream of DOC.
- Measure NO, NO<sub>2</sub>, NO<sub>x</sub> upstream of the SCR using MEXA Analyser
- For urea injection, check spray outside the mixing chamber prior to fitting within the SCR exhaust system. Spray pulse rate setting range from 24 to 36 ms.

- Inject Gas (4% or 5%) in the first module or Urea in the expansion box for uniform mixing upstream of SCR.
- Adjust gas flow rate from 0 to 120 mm for 4% and 0 to 96 mm for 5% gas. For urea injection, pulse rate setting used is from 24 to 36 ms.
- Measurements of all species must be allowed to reach a steady value before changing to a different urea spray or ammonia gas injection settings.
- Measure NO<sub>x</sub>, NH<sub>3</sub> upstream of SCR using MEXA Analyser
- Measure NO, NO<sub>x</sub> and NH<sub>3</sub> downstream of SCR using MEXA Analyser.
- Vary the SCR bricks length from 91 mm in length, four were available, then repeat the measurement upstream and downstream of SCR with 2x, 3x and 4x SCR.

### 3.13 Example of measurements strategy applied

All the measurements obtained in this study are given in full in Appendix 4. Each graph in appendix 4 has a code name derived from the details of the experiment and the date on which it was performed. The code name is printed at the top of each graph. Appendix 4.0 has a list of contents at the beginning which should enable each experiment to be found. For example, “9jul08b NH<sub>3</sub> dw 1SCRL” is a measurement trace obtained on 9/7/2008 of NH<sub>3</sub> downstream of the 1 SCR, and L refers to LHS of the original plot

An example of the test with 5% ammonia gas injected upstream of 1 SCR brick is selected and the engine log is shown in figure 3.13. In this engine log, the MEXA analyser was used upstream of the SCR in NH<sub>3</sub> mode measuring SUM, NO<sub>x</sub> and NH<sub>3</sub> as described earlier in section 3.4.4. The EXSA analyser was measuring NO<sub>x</sub> upstream of the 5% gas injection point to provide the engine NO<sub>x</sub> out. The code name for this test “12aug08 bNH<sub>3</sub> up1SCR 5% L2” refers to the engine log data 120808b nh3 up1scr, which refers to the actual date the test was performed.

The code “b” refers to the second data log after the engine warm up and analysers calibration had been completed, which had a code “a”. The name NH<sub>3</sub> up1SCR 5% L2 refers to the NH<sub>3</sub> mode of MEXA analyser with sampling location upstream of the SCR brick with the 5% ammonia gas injected. This whole test was performed from high gas injection rate setting to low, then low to high, and again high to low. The code L2 refers to the final high to low gas injection setting from the overall engine log from time 17<sup>th</sup> to 25<sup>th</sup> minute.

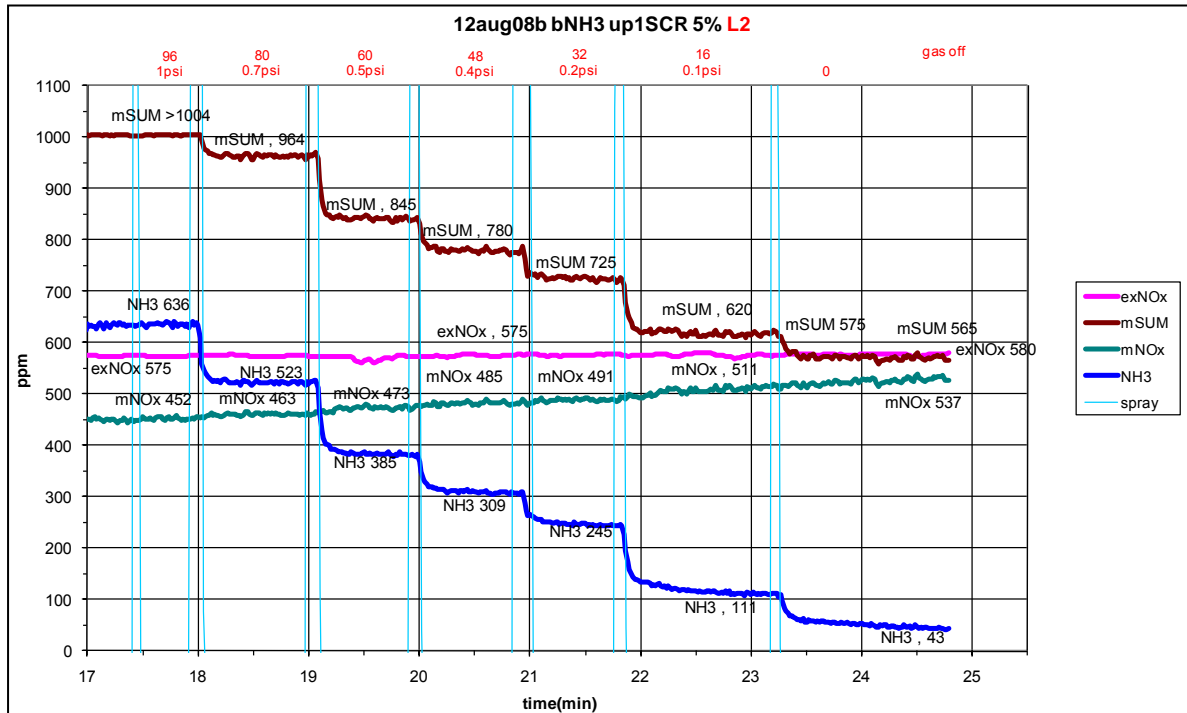


Figure 3.13 Example of engine log from 5% ammonia gas with 1 SCR brick.

From the figure 3.13 above, the engine NO<sub>x</sub> out from EXSA showed a consistent 575 to 580 ppm (labelled exNO<sub>x</sub>) from the 17<sup>th</sup> to 25<sup>th</sup> minute shown by the trace in pink. The changes of gas setting were indicated by the vertical light blue line. Starting from gas injection setting at 96 mm (see appendix 3.7.1c for details), the SUM reading was showing over (noted by >1004), the NH<sub>3</sub> reading was 636 ppm (in blue) and mNO<sub>x</sub> (from MEXA) was 452 ppm in green. As previously described, the NO<sub>x</sub> reading from MEXA was taken with the gas off. As the gas injection setting was reduced in steps from 96 to 80, 60, 48, 32, 16 and finally 0, the SUM and NH<sub>3</sub> level also reduces accordingly.

At each gas injection setting, the SUM and NH<sub>3</sub> readings were allowed to settle down to steady state for about a minute before the next gas injection setting was selected. The SUM trace is shown in brown. This methodology of systematic variation of settings and allowance of sufficient time for the analyzer reading to reach steady state was applied to all measurements in this study. The results are all presented and discussed in the next chapter.



## CHAPTER 4: EXPERIMENTAL RESULTS AND DISCUSSIONS

### 4.0 Experimental results: Introduction

In this chapter, the experimental results are obtained based on the experimental methodology described in chapter 3. These tests include the use of urea spray, 5% and 4%  $\text{NH}_3$  gas. The urea spray experiments were performed with a single and quadruple SCR bricks. For the 5%  $\text{NH}_3$  gas, experiments were conducted by varying the SCR bricks from single up to quadruple bricks. The experiment with 4%  $\text{NH}_3$  gas was carried out with only a single SCR brick. The data were obtained from these experiments using the MEXA analyser by sampling upstream and downstream of the SCR bricks. Information about  $\text{NO}_2$  and  $\text{NH}_3$  levels could be obtained by analysis described in the following sections. Most of the tests were carried out under steady state conditions, but this chapter also discusses some aspects of transient behaviour. Finally the features of the SCR process revealed by the measurements are discussed.

#### 4.1.0 Urea spray studies: General overview

The main difference between the gas and the spray studies is the upstream  $\text{NH}_3$  level. In the gas studies, the upstream  $\text{NH}_3$  was readily available whilst for the spray studies; the upstream  $\text{NH}_3$  was potentially available from the decomposition of the urea. Each urea molecule within the droplets must first decompose into an ammonia molecule and an HCNO (iso-cyanic acid molecule). This occurs at temperature of approximately 130 to 137 °C.

The iso-cyanic acid molecule must then react with water to produce a further ammonia molecule. This hydrolysis reaction is more likely to occur on a catalyst surface rather than in the gas phase, and will be more rapid at higher temperatures. Therefore the upstream deduced measurement of ammonia in these studies is only part of the ammonia potentially available for the SCR reactions on the catalyst bricks. From the known spray pulse length setting, the spray calibration and the known exhaust mass flow rate, the “potential ammonia” introduced into the exhaust in ppm can be calculated, see Appendix 3.6.2

#### 4.1.1 Urea spray studies: Upstream Measurements (1 and 4 SCR bricks)

At the location upstream of the SCR bricks with the MEXA in  $\text{NH}_3/\text{NO}_x$  mode the following equation applies,

$$\text{SUM upstream} = [\text{NH}_3 + \text{NO} + \text{NO}_2]$$

Thus, for potential values,

$$\text{Pot SUM upstream} = [\text{potential NH}_3 + \text{NO} + \text{NO}_2]$$

Pot SUM is calculated from the potential ammonia and from NO and  $\text{NO}_2$  measurement taken when the spray was off. The  $\text{NO}_x$  upstream is measured without the spray injection and is assumed to remain the same when the spray is injected due to the assumption that the gas phase reactions are negligible. The NO upstream can be measured, even with the presence of ammonia using the MEXA analyser in NO/ $\text{NO}_2$  mode. Similarly, the assumption is made that no gas phase reactions occur.

#### 4.1.2 Urea spray studies: Downstream Measurements (1 and 4 SCR bricks)

The measurement with the MEXA in  $\text{NH}_3/\text{NO}_x$  mode downstream of the SCR bricks will give the SUM downstream, which effectively represent the  $\text{NH}_3$ , NO and  $\text{NO}_2$  coming out from the SCR bricks. Thus,

$$\text{SUM downstream} = [\text{NH}_3 + \text{NO} + \text{NO}_2]$$

The  $\text{NO}_x$  downstream can generally be measured only with the spray off, unless the ammonia slip is very minimal. In the spray experiments, in all cases, the ammonia slip was significant. This is because the spray was designed for heavy duty vehicles and would not operate effectively at lower urea flow setting. Therefore, all of the experiments with the spray were carried out under excess spray conditions. The NO downstream could be measured even in the presence of ammonia slip by using MEXA in the NO/ $\text{NO}_2$  mode. The  $\text{NH}_3$  downstream reading is erroneous with the MEXA when the ammonia slip level is significantly above zero, which occurred in most of the experiments with spray.

However,

$$[\text{SUM} - \text{NO}] = [\text{NH}_3 + \text{NO}_2].$$

Thus, the two useful pieces of downstream information are the NO levels and  $[\text{NH}_3 + \text{NO}_2]$  levels and would be useful for CFD validation.

#### 4.1.3 Urea spray studies: Deduced value.

To deduce  $\text{NH}_3$ , and  $\text{NO}_2$ , it was necessary to use the difference between the potential SUM upstream and the SUM downstream in this case. Therefore, using the following equation

$$\text{Pot SUM upstream} - \text{SUM downstream} = [\text{NH}_3 + \text{NO} + \text{NO}_2] \text{ consumption in the catalyst.}$$

The implication of this is the assumption that SUM downstream is the true measurement of the ammonia gas plus the  $\text{NO}_x$  with no droplets or  $\text{HNCO}$  passing through the catalyst. This assumption may not be true for the 1 SCR, where ammonia in droplet form (or possibly as  $\text{HNCO}$ ) at the catalyst exit is unaccounted for. But, it should however be true for the 4 SCR bricks case. It is again reasonable to assume that these species can only be consumed if they react with one another, and that they react on a mol  $\text{NH}_3$  per mol  $\text{NO}_x$  basis. It also neglects non mol to mol reactions and ammonia oxidation. There may be also additional reactions with urea by products that are neglected. Therefore,

$$\frac{1}{2} [\text{NH}_3 + \text{NO} + \text{NO}_2] \text{ consumed} = \text{NH}_3 \text{ consumed} = \text{NO}_x \text{ consumed}$$

$\text{NO}$  consumed can be found directly from

$$[\text{NO upstream} - \text{NO downstream}]$$

Hence,

$$\text{NO}_2 \text{ consumed} = [\text{NO}_x \text{ consumed} - \text{NO consumed}]$$

#### 4.1.4 Urea sprays studies: Ammonia levels upstream of SCR bricks.

In getting the ammonia levels, the calibrated spray pulse length setting and the knowledge of the exhaust mass flow rate can be used to calculate the potential ammonia level in ppm at location upstream of the SCR. This can be compared with the deduced value obtained from  $[\text{SUM} - \text{NO}_x]$ . The difference between the levels would give an indication of how many of the droplets have released their ammonia between the spray injection point and the gas analysis measurement point upstream of the SCR. The 1 SCR and 4 SCR cases give remarkably different amounts of ammonia released from the droplets upstream of the SCR. It is not immediately apparent why this should happen, as the temperatures in the two experiments were very much similar and the main difference was the SCR resistance to the flow. This is further discussed in section 4.5.1.

#### 4.1.5 Measurement with Urea Spray and 1 SCR brick.

Table 4.1.5 summarizes the test results associated with urea spray and 1 SCR brick. Potential ammonia release from the urea spray was also calculated. The NH<sub>3</sub> reading upstream from MEXA was recorded and clearly does not represent the correct NH<sub>3</sub> values. The SUM readings previously introduced in section 4.1.1 have been recorded from several set SUM readings and the average values were used in this table compiled from data shown in appendix 4.1.5b. Upstream of SCR, direct measurement of SUM, NO, NO<sub>x</sub> and NH<sub>3</sub> were tabulated in the table. For downstream measurements, only SUM, NO and NH<sub>3</sub> were obtained directly from MEXA.

Table 4.1.5 Summary of Result: Urea Spray with 1 SCR. (all measurements in ppm)

<b>Results for urea spray (1 SCR)</b>												
Temp upstream	573 K											
Temp downstream	574 K											
O2 upstream	9.70%											
O2 downstream	7.90%											
1 SCR												
Spray pulse length (ms) -->		Description	0	24	26	28	30	32	34	36	Refn	Guide
Potential	up 1SCR	Potential NH3	0	552	614	696	818	888	960	1042	calc	A
Potential	up 1SCR	Potential SUM	505	1057	1119	1201	1323	1393	1465	1547	Pot(nh3+nox)	B
MEXA	up 1SCR	SUM	550	645	680	700	723	734	754	761	avg sum	C
MEXA, Spray off	up 1SCR	NO	196	196	196	196	196	196	196	196	070708a	D
MEXA, Spray off	up 1SCR	NOx	505	505	505	505	505	505	505	505	090708c	E
Calculated	up 1SCR	NO2	309	309	309	309	309	309	309	309	nox-no	F
MEXA Reading	up 1SCR	NH3	21	210	250	290	310	320	345	385	090708c	G
Deduced ammonia	up 1SCR	SUM-NOx	45	140	175	195	218	229	249	256	sum-nox	C-E=H
MEXA	dw 1SCR	*SUM(excludes drops)	539	495	564	607	661	732	797	863	avg sum	I
MEXA	dw 1SCR	NO	200	137	139	139	140	140	140	140	070708b	J
MEXA Reading	dw 1SCR	NH3	21	222	312	395	450	513	614	680	090708b	K
NH3 + NO2	dw 1SCR	SUM-NO	339	358	425	468	521	592	657	723	calc	I-J=L
NH3 + NOx consumed	across 1 SCR	Potential SUM-SUM (*)	-34	562	555	594	662	661	668	684	calc	B-I=M
(*) Value too large because downstream sum was too small as it excluded drops												
Note: Plotted against potential ammonia supplied												
	Pot NH3 up		0	552	614	696	818	888	960	1042		A
up - down, 1SCR	SUM-SUM 1SCR		-34	562	555	594	662	661	668	684		M
1SCR spray	NOx or NH3 consumed		-17	281	278	297	331	331	334	342		M/2=N
1SCR spray	NO consumed		-4	59	57	57	56	56	56	56		D-J=O
1SCR spray	NO2 consumed		-13	222	221	240	275	275	278	286		N-O=P
concentration table	pot NH3 up		0	552	614	696	818	888	960	1042		A
Deduced ammonia	upstream 1SCR	SUM-NOx	45	140	175	195	218	229	249	256		H
Downstream	NH3		17	271	337	399	487	558	626	700		A-N
	NOx		522	224	228	208	174	175	171	163		E-N
	NO		200	137	139	139	140	140	140	140		D-O
	NO2		322	87	88.5	69	34	34.5	31	23		F-P

Three columns on the right side of table 4.1.5 give reference to the actual data log in appendix 4, provide a guide on how to read the table and refer to related appendix for the data in respective rows.

#### 4.1.6 Measurement with Urea Spray and 4 SCR bricks.

The test results with urea spray and 4 SCR bricks are summarized in the table 4.1.6. The same methodology used for Urea Spray with 1 SCR was utilised in this test. The main differences from the 1 SCR case is the NO<sub>x</sub> reading downstream of the SCR. Clearly in this test, excess ammonia from urea spray have reduced all of NO<sub>x</sub> but posses another problem in the system. The undesired NH<sub>3</sub> slippages have been detected and further analysis in the section 4.1.6 will discuss this in depth.

Table 4.1.6 Summary of Result: Urea Spray with 4 SCR. (all measurements in ppm)

<b>Results for urea spray (4 SCRs)</b>												
Temp upstream	592 K											
Temp downstream	582 K											
O2 upstream	9.30%											
O2 downstream	7.90%											
4 SCRs												
Spray pulse length (ms) -->			0	24	26	28	30	32	34	36	Refn	Guide
Potential	up 4SCR	Pot NH3	0	552	614	696	818	888	960	1042	calc	A
Potential	up 4SCR	Pot SUM	510	1062	1124	1206	1328	1398	1470	1552	nh3+nox	B
MEXA	up 4SCR	SUM	544	797	813	837	858	878	904	908	avg sum	C
MEXA, Spray off	up 4SCR	NO	200	200	200	200	200	200	200	200	240708b	D
MEXA, Spray off	up 4SCR	NOx	510	510	510	510	510	510	510	510	240708b	E
Calculated	up 4SCR	NO2	310	310	310	310	310	310	310	310	calc	F
MEXA Reading	up 4SCR	NH3	38	318	346	381	405	434	466		240708b	G
Deduced ammonia	up 4SCR	SUM-NOx	34	287	303	327	348	368	394	398	240708b	C-E=H
MEXA	dw 4SCR	SUM	539	78	128	181	242	304	367	424	avg sum	I
MEXA	dw 4SCR	NO	205	30	5	1	1	1	2		20708c	J
Measured	dw 4SCR	NH3	0	79	136	167	225	310	375		230708b	K
NH3 + NO2	dw 4SCR	SUM-NO	334	48	123	180	241	303	365	424	calc	I-J=L
Total consumed	across 4 SCRs	Pot SUM-SUM	-29	984	996	1025	1086	1094	1103	1128	calc	B-I=M
Note: Plotted against potential ammonia supplied												
	Pot NH3 up		0	552	614	696	818	888	960	1042		A
up - down, 4SCR	Pot SUM-SUM 4 SCR		-29	984	996	1025	1086	1094	1103	1128		M
4SCR spray	NOx or NH3consumed		-15	492	498	512.5	543	547	551.5	564		M/2=N
4SCR spray	NO consumed		-5	170	195	199	199	199	198	200		D-J=O
4SCR spray	NO2 consumed		-9.5	322	303	313.5	344	348	353.5	364		N-O =P
concentration table	pot NH3 up		0	552	614	696	818	888	960	1042		A
Deduced ammonia	ups 4SCR	SUM-NOx	34	287	303	327	348	368	394	398		H
Downstream	NH3		14.5	60	116	183.5	275	341	408.5	478		A-N
	NOx		525	18	12	-2.5	-33	-37	-41.5	-54		E-N
	NO		205	30	5	1	1	1	2	0		D-O
	NO2		320	-12	7	-3.5	-34	-38	-43.5	-54		F-P

At the bottom of table 4.1.6 some of the NO<sub>x</sub> and NO<sub>2</sub> reading were showing negative values due to experimental error in this study using the methodology described earlier in the range of around +/- 55 ppm. The NO<sub>2</sub> measurements were not measured directly but derived using the methodology described in section 4.1. It is believed that the negative values reflect the magnitude of the errors resulting from these assumptions, but do not affect the general conclusions discussed later.

## **4.2 Ammonia gas studies: General Overview**

The test with 5% and 4% ammonia gas provide a comparison of SCR reaction in the form of gas as compared to aqueous ammonia solution. The ammonia input level can be determined from known exhaust mass flow rate and a calibrated flow meter. The advantages using ammonia gas is obviously to accelerate the SCR reaction to reduce NO<sub>x</sub> and eliminate the complication with the use of urea spray. The analyser response to the measurements also improved and also reduced analyser break down due to urea droplets penetrating the sampling lines and internal components of the analyser. Five cases are presented in this investigation involving four 5% tests and one 4% test.

### **4.2.1 Ammonia gas studies: upstream measurements. (1 and 4 SCR bricks)**

The measurements taken for the 4% and 5% ammonia gas were the SUM upstream and downstream of the SCR and the NO upstream and downstream of the SCR. The SUM in NO<sub>x</sub>/NH<sub>3</sub> mode of the MEXA follows the equation below:

$$\text{SUM upstream} = [\text{NH}_3 + \text{NO} + \text{NO}_2] \text{ upstream}$$

The NO<sub>x</sub> measurements upstream were obtained in the absence of ammonia gas injection and were assumed unchanged when ammonia gas was injected. This assumes that the gas phase reactions were negligible. In the MEXA NO/NO<sub>2</sub> mode, the NO measurements upstream, even in the presence of ammonia, should be the same as without the ammonia gas injection as the converter is bypassed. Similarly, the assumption made was no gas phase reactions occurred. Therefore, the NO<sub>2</sub> upstream can be deduced from NO<sub>x</sub>-NO and had the same value regardless of amount of ammonia injected. The NH<sub>3</sub> measurements recorded upstream were erroneous but the correct ammonia level could be obtained by calculation of SUM-true NO<sub>x</sub>.

#### 4.2.2 Ammonia gas studies: downstream measurements. (1 and 4 SCR bricks)

The SUM measurements downstream of the SCR bricks were also valid using the MEXA in NO<sub>x</sub>/NH<sub>3</sub> mode similar to the upstream measurements. The SUM measurement downstream is given as the equation below:

$$\text{SUM downstream} = [\text{NH}_3 + \text{NO} + \text{NO}_2] \text{ downstream}$$

NO<sub>x</sub> measurements downstream are only valid with no ammonia gas injection present or with very minimal ammonia slip. If the latter was true, for cases with more than 1 SCR bricks, then the measured NO<sub>x</sub> level downstream was additional information available in these cases. The NO measurements downstream were always valid using the MEXA in the NO/NO<sub>2</sub> mode even with the presence of ammonia slip. The NO<sub>2</sub> values downstream with gas off can be deducted from NO<sub>x</sub>-NO and it is also available for cases where gas injection dosing was very low and where ammonia slip was minimal. The NH<sub>3</sub> downstream measurements were erroneous with the MEXA at any ammonia levels significantly above zero. However, the following equation is true:

$$[\text{SUM-NO}] = [\text{NH}_3 + \text{NO}_2].$$

Therefore the two useful pieces of downstream data are the NO levels and [NH<sub>3</sub>+NO<sub>2</sub>] levels and these could be used for CFD model validation. The NO<sub>2</sub> levels downstream are also available for the low dose cases where approximately zero ammonia slips occurred.

#### 4.2.3 Ammonia gas studies: Deduced values.

The gaseous consumption in the catalyst could be easily obtained via deductions by the following equation:

$$\text{SUM upstream} - \text{SUM downstream} = [\text{NH}_3 + \text{NO} + \text{NO}_2] \text{ consumption in the catalyst.}$$

Reasonably, it is safe to assume that these species can only be consumed in the SCR if NO<sub>x</sub> reacts with NH<sub>3</sub>. Furthermore, it is reasonable to assume that a mol of NH<sub>3</sub> reacts with a mol of NO<sub>x</sub> thus neglecting non-mol to mol reactions and ammonia oxidation.

Consequently,

$$\frac{1}{2} [\text{NH}_3 + \text{NO} + \text{NO}_2] \text{ consumed} \approx \text{NH}_3 \text{ consumed} \approx \text{NO}_x \text{ consumed}$$

Therefore, the NO consumed can be found directly from,

$$[\text{NO upstream} - \text{NO downstream}]$$

and similarly the NO<sub>2</sub> consumed from,

$$\text{NO}_2 \text{ consumed} = [\text{NO}_x \text{ consumed} - \text{NO consumed}]$$

#### 4.2.4 Ammonia gas studies: Ammonia levels

From the calibrated gas flow meter setting used, together with the knowledge of the exhaust mass flow rate, the injected ammonia level in ppm upstream of the SCR can be calculated. This is shown in the appendices 3.7.1a to d. Then, this information can be compared with the deduced value obtained from [SUM-NO<sub>x</sub>]



#### 4.2.5 Measurement with 5% Ammonia Gas and 1 SCR brick.

The test results for 5% ammonia gas with 1 SCR brick are shown in table 4.2.5. In this table only SUM and NO readings were directly obtained from the MEXA measurements upstream and downstream of the SCR brick. The NO<sub>x</sub> value upstream was assumed constant due to no ammonia gas present during the measurement.

Table 4.2.5 Summary of Result: 5% Ammonia Gas with 1 SCR. (all measurements in ppm)

Results for 5% NH <sub>3</sub> in N <sub>2</sub> gas and 1SCR												
Temp upstream	596 K											
Temp downstream	582 K											
O <sub>2</sub> upstream	8.8%											
O <sub>2</sub> downstream	7.6%											
1 SCR												
Flowmeter setting (glass float) →			0	16	32	48	60	80	96	Refn	Guide	Apdx
MEXA	up	SUM	575	620	725	780	845	964	1088	120808b	A	4.2.5
MEXA, Gas off	up	NO	230	230	230	230	230	230	230	210808c	B	4.2.5
MEXA, Gas off	up	NO <sub>x</sub>	539	539	539	539	539	539	539	120808b	C	4.2.5
Calculated	up	NO <sub>2</sub>	309	309	309	309	309	309	309	calc	C-B=D	
MEXA Reading	up	NH <sub>3</sub>	52	111	245	309	385	523	636	120808b	E	4.2.5
Deduced ammonia	up	SUM-NO <sub>x</sub>	36	81	186	241	306	425	549	calc	A-C=F	
MEXA	down	SUM	578	513	470	476	495	579	669	120808c	G	4.2.5
MEXA	down	NO	214.13	188.86	162.26	155.61	150.29	147.63	155.61	avg NO	H	4.2.5b
MEXA Reading	down	NH <sub>3</sub>	38	46	82	114	168	279	389	120808c	I	4.2.5
NH <sub>3</sub> + NO <sub>2</sub>	down	SUM-NO	363.87	324.14	307.74	320.39	344.71	431.37	513.39	calc	G-H=J	
NH <sub>3</sub> + NO <sub>x</sub> consumed	up - down	SUM-SUM	-3	107	255	304	350	385	419	calc	A-G=K	
			0	16	32	48	60	80	96			
			575	620	725	780	845	964	1088		A	
	NH <sub>3</sub>		36	81	186	241	306	425	549		F	
up - down, 1SCR	SUM-SUM 1SCR		-3	107	255	304	350	385	419		K	
up - down, 1SCR 5%	NO <sub>x</sub> or NH <sub>3</sub> consumed		-1.5	53.5	127.5	152	175	192.5	209.5		K/2=L	
up - down, 1SCR 5%	NO consumed		15.87	41.14	67.74	74.39	79.71	82.37	74.39		B-H=M	
up - down, 1SCR 5%	NO <sub>2</sub> consumed		-17.37	12.36	59.76	77.61	95.29	110.13	135.11		L-M=N	
concentration table	NH <sub>3</sub> up		0	16	32	48	60	80	96			
Deduced ammonia	up 1SCR	SUM-NO <sub>x</sub>	36	81	186	241	306	425	549		F	
Downstream	NH <sub>3</sub>		37.5	27.5	58.5	89.0	131.0	232.5	339.5		F-L	
	NO <sub>x</sub>		540.5	485.5	411.5	387.0	364.0	346.5	329.5		C-L	
	NO		214.1	188.9	162.3	155.6	150.3	147.6	155.6		B-M	
	NO <sub>2</sub>		326.4	296.6	249.2	231.4	213.7	198.9	173.9		D-N	

#### 4.2.6 Measurement with 5% Ammonia Gas and 2 SCR bricks.

The test results with 5% ammonia gas and 2 SCR are presented in the table 4.2.6. In this test, similar method as the 1 SCR was utilised but this time with 2 SCR bricks. The MEXA analyser was measuring NO<sub>x</sub> and NH<sub>3</sub> and SUM upstream and downstream of the 2 SCR bricks. At this stage, the NO data was not recorded downstream, therefore restricting the analysis to only NO<sub>x</sub> and NH<sub>3</sub> consumed. The information on NO and NO<sub>2</sub> consumed could have become available with the NO data downstream

of the 2 SCR. This is mainly due to time constraint involving the relocation of the engine test bed. Therefore the analysis associated with NO and NO<sub>2</sub> for the 2 SCR bricks cannot be performed. The analysis done on this test case only focussed on the NO<sub>x</sub> and NH<sub>3</sub> consumed by the 2 SCR bricks.

Table 4.2.6 Summary of Result: 5% Ammonia Gas with 2 SCR. (all measurements in ppm)

Results for 5% NH3 in N2 gas and 2 SCRs													
Temp upstream	592 K												
Temp downstream	581 K												
O2 upstream	9.1%												
O2 downstream	7.7%												
2 SCRs													
Flowmeter setting (glass float) -->			0	16	32	48	60	80	96	Refn	Guide	Apdx	
MEXA	up	SUM	567	608	710	770	824	935	1052	110808b	A	4.2.6	
MEXA	up	NO	231	231	231	231	231	231	231	210808c	B	4.2.6	
MEXA, Gas off	up	NOx	542	542	542	542	542	542	542	110808b	C	4.2.6	
Calculated	up	NO2	311	311	311	311	311	311	311	110808b	C-B=D	4.2.6	
MEXA Reading	up	NH3	31	98	218	282	352	482	589	110808b	E	4.2.6	
Deduced ammonia	up	SUM-NOx	25	66	168	228	282	393	510	calc	A-C =F		
MEXA	down	SUM	556	476	361	297	226	101	14	110808c	G	4.2.6	
MEXA	down	NO	231							210808c	H	4.2.6	
MEXA,OK-low NH3	down	NOx	548	470	354	297	224	100	9	110808c	I	4.2.6	
Calculated	down	NO2	317							calc	I-H=J		
MEXA Reading	down	NH3	6	6	7	4	3	3	4	110808c		4.2.6	
NH3 + NO2	down	SUM-NO	325							calc	G-H=K		
Deduced NH3	down	SUM-NOx	8	6	7	0	2	1	5	calc	G-I=L		

#### 4.2.7 Measurement with 5% Ammonia Gas and 3 SCR bricks.

The test results with 5% ammonia gas and 3 SCR bricks are summarized in table 4.2.7. For the 3 SCR bricks, similar test was performed and data was recorded accordingly. The NO and NO<sub>2</sub> data downstream was also unavailable therefore restrict further analysis.

Table 4.2.7 Summary of Result: 5% Ammonia Gas with 3 SCR. (all measurements in ppm)

Results for 5% NH3 in N2 gas and 3 SCR's												
Temp upstream	595K											
Temp downstream	584K											
O2 upstream	9.0%											
O2 downstream	7.7%											
3 SCR's												
Flowmeter setting (glass float) -->			0	16	32	48	60	80	96	Refn	Guide	Apdx
MEXA	up	SUM	583	628	729	777	835	956	1080	070808b	A	4.2.7
MEXA	up	NO	231							210808c	B	4.2.6
MEXA, Gas off	up	NOx	550	550	550	550	550	550	550	070808b	C	4.2.7
Calculated	up	NO2	319							calc	C-B=D	
MEXA Reading	up	NH3	32	104	236	295	371	500	618	070808b	E	4.2.7
Deduced ammonia	up	SUM-NOx	33	78	179	227	285	406	530	calc	A-C =F	
MEXA	down	SUM	566	490	373	309	244	95	11	070808c	G	4.2.7
MEXA	down	NO	231							210808c	H	4.2.6
MEXA,OK-low NH3	down	NOx	553	480	360	305	238	91	7	070808c	I	4.2.7
Calculated	down	NO2	322							calc	I-H=J	
MEXA Reading	down	NH3	10	10	9	7	5	2	1	070808c		4.2.7
NH3 + NO2	down	SUM-NO	335							calc	G-H=K	
Deduced NH3	down	SUM - NOx	13	10	13	4	6	4	4	calc	G-I=L	
			5% gas 3 SCR									
			0	16	32	48	60	80	96			
			583	628	729	777	835	956	1080		A	
	NH3		33	78	179	227	285	406	530		F	
up - down, 3SCR	SUM-SUM 3SCR		17	138	356	468	591	861	1069		A-G=M	
up - down, 3SCR	NOx or NH3 consumed		8.5	69	178	234	296	431	535		M/2=N	
	NOx Downstream		542	481	372	316	255	120	15.5		C-N	

#### 4.2.8 Measurement with 5% Ammonia Gas and 4 SCR bricks.

The test results with 5% ammonia gas and 4 SCR bricks are summarized in table 4.2.8. The final set of test with 5% ammonia gas was with the 4 SCR bricks. Similar to the 5% and 1 SCR tests, a complete set of tests were available including NO<sub>x</sub>, NH<sub>3</sub> and NO for further analysis. So, the NO<sub>x</sub>, NH<sub>3</sub>, NO and NO<sub>2</sub> consumed within the 4 SCR bricks was obtained using the method previously described.

Table 4.2.8 Summary of Result: 5% Ammonia Gas with 4 SCR. (all measurements in ppm)

Results for 5% NH <sub>3</sub> in N <sub>2</sub> gas and 4 SCRs												
Temp upstream	594 K											
Temp downstream	584 K											
O <sub>2</sub> upstream	9.1%											
O <sub>2</sub> downstream	7.9%											
4 SCRs												
Flowmeter setting (glass float) -->			0	16	32	48	60	80	96	Refn	Guide	Apdx
MEXA	up	SUM	550	600	700	757	826	935	1050	060808b	A	4.2.8
MEXA	up	NO	213	213	212	212	210	210	207	060808c	B	4.2.8
MEXA, Gas off	up	NO <sub>x</sub>	527	527	527	527	527	527	527	060808b	C	4.2.8
Calculated	up	NO <sub>2</sub>	314	314	315	315	317	317	320	calc	C-B=D	
MEXA Reading	up	NH <sub>3</sub>	30	100	220	286	362	484	600	060808b	E	4.2.8
Deduced ammonia	up	SUM-NO <sub>x</sub>	23	73	173	230	299	408	523	calc	A-C =F	
MEXA	down	SUM	550	472	353	283	217	87	8	060808e	G	4.2.8
MEXA	down	NO	214	170	122	100	75	25	2	060808d	H	4.2.8
MEXA,OK-low NH <sub>3</sub>	down	NO <sub>x</sub>	536	460	344	275	210	83	4	060808e	I	4.2.8
Calculated	down	NO <sub>2</sub>	322	290	222	175	135	58	2	calc	I-H=J	
MEXA Reading	down	NH <sub>3</sub>	14	11	10	8	6	4	3	060808e		4.2.8
NH <sub>3</sub> + NO <sub>2</sub>	down	SUM-NO	336	302	231	183	142	62	6	calc	G-H=K	
Deduced NH <sub>3</sub>	down	SUM-NO <sub>x</sub>	14	12	9	8	7	4	4	calc	G-I=L	
NH <sub>3</sub> + NO <sub>x</sub> consumed	up - down	SUM-SUM	0	128	347	474	609	848	1042	calc	A-G=M	
5% gas 4 SCR												
			0	16	32	48	60	80	96			
			550	600	700	757	826	935	1050		A	
			23	73	173	230	299	408	523		F	
up - down, 4SCR	SUM-SUM 4SCR		0	128	347	474	609	848	1042		A-G=N	
up - down, 4SCR 5%	NO <sub>x</sub> or NH <sub>3</sub> consumed		0	64	174	237	305	424	521		N/2=O	
up - down, 4SCR 5%	NO consumed		-1	43	90	112	135	185	205		B-H=P	
up - down, 4SCR 5%	NO <sub>2</sub> consumed		1	21	84	125	170	239	316		O-P=Q	
concentration table	NH <sub>3</sub> up		0	16	32	48	60	80	96			
Deduced ammonia	up 4SCR	SUM-NO <sub>x</sub>	23	73	173	230	299	408	523		F	
Downstream	NH <sub>3</sub>		23	9	-1	-7	-6	-16	2		F-O	
	NO <sub>x</sub>		527	463	354	290	223	103	6		C-O	
	NO		214	170	122	100	75	25	2		B-P	
	NO <sub>2</sub>		313	293	232	190	148	78	4		D-Q	

#### 4.2.9 Measurement with 4% Ammonia Gas and 1 SCR bricks.

The test results with 4% ammonia gas and 1 SCR brick are summarized in table 4.2.9. The 4% and 1 SCR test was conducted in a similar way as the 5% and 1 SCR. The main difference is the ammonia gas injection flow meter setting used. For the 4% ammonia gas test, the flow meter setting used was higher. Later it was discovered that the 4% ammonia gas was unsuitable for the test due to short testing capability. On average the 4% ammonia gas bottle can be utilized for approximately 4 hours of testing. The potential ammonia injected with the 4% and 5% is summarized in appendix 3.10.4.

Table 4.2.9 Summary of Result: 4% Ammonia Gas with 1 SCR. (all measurements in ppm)

<b>Results for 4% NH<sub>3</sub> in N<sub>2</sub> gas</b>												
Temp upstream		592 K										
Temp downstream		573 K										
O <sub>2</sub> upstream		9.50%										
O <sub>2</sub> downstream		8.30%										
1 SCR												
Flowmeter setting (steel float) -->			0	40	50	60	75	100	120	Refn	Guide	Apdx
MEXA	up	SUM	592	824	914		1118	1360	1580	100608b	A	4.2.9
MEXA, Gas off	up	NO	209	209	209	209	209	209	209	100608c	B	4.2.9
MEXA, Gas off	up	NO <sub>x</sub>	565	565	565	565	565	565	565	100608b	C	4.2.9
Calculated	up	NO <sub>2</sub>	356	356	356	356	356	356	356	calc	D	
MEXA Reading	up	NH <sub>3</sub>	28	364	461		703	971	1200	100608b	E	4.2.9
Deduced ammonia	up	SUM-NO <sub>x</sub>	27	259	349		553	795	1015	calc	A-C=F	
MEXA	down	SUM	579	449	471		600	869	1121	100608b2	G	4.2.9
MEXA	down	NO	208		148		149	149	152	100608d	H	4.2.9
MEXA Reading	down	NH <sub>3</sub>	14	42.9	169		333	625	836	100608b2	I	4.2.9
NH <sub>3</sub> + NO <sub>2</sub>	down	SUM-NO	371		323		451	720	969	calc	G-H=J	
NH <sub>3</sub> + NO <sub>x</sub> consumed	up - down	SUM-SUM	13	375	443		518	491	459	calc	A-G=K	
4% gas 1 SCR												
			0	40	50	60	75	100	120			
			592	824	914		1118	1360	1580		A	
	NH <sub>3</sub>		27	259	349		553	795	1015		F	
up - down, 1SCR	SUM-SUM 1SCR		13	375	443		518	491	459		K	
up - down, 4% 1SCR	NO <sub>x</sub> or NH <sub>3</sub> consumed		6.5	188	222		259	246	230		K/2=L	
up - down, 4% 1SCR	NO consumed		1	50	61		60	60	57		B-H=M	
up - down, 4% 1SCR	NO <sub>2</sub> consumed		5.5	138	161		199	186	173		L-M=N	
concentration table	NH <sub>3</sub> up		0	40	50	60	75	100	120			
Deduced ammonia	up 1SCR	SUM-NO <sub>x</sub>	27	259	349		553	795	1015		F	
Downstream	NH <sub>3</sub>		21	72	128		294	550	786		F-L	
	NO <sub>x</sub>		559	378	344		306	320	336		C-L	
	NO		208	159	148		149	149	152		B-M	
	NO <sub>2</sub>		351	219	196		157	171	184		D-N	

### 4.3 Analysis of measurement results against ammonia input/potential ammonia input.

In order to summarize the results in this investigation, the detail measurements of NO<sub>x</sub>, NO, NO<sub>2</sub> and NH<sub>3</sub> entering and exiting the SCR is needed. From this information the species consumed within the SCR brick can be analysed. As previously shown in the previous sections (4.1.5 to 4.1.6 and 4.2.5 to 4.2.9) the NO, NO<sub>2</sub>, NO<sub>x</sub> and NH<sub>3</sub> data are only available for the 1 and 4 SCR bricks. The 2 and 3 brick cases lack NO information downstream therefore cannot be used to analyse the NO and NO<sub>2</sub> species consumed within the SCR. In this analysis, the results from 1 SCR and 4 SCR of the 4%, 5% gas and urea spray are plotted with respect to the ammonia input or potential ammonia input for urea spray. Figure 4.3 shows the summary of measurement with 1 and 4 SCR bricks for urea spray, 4% and 5 % gas.

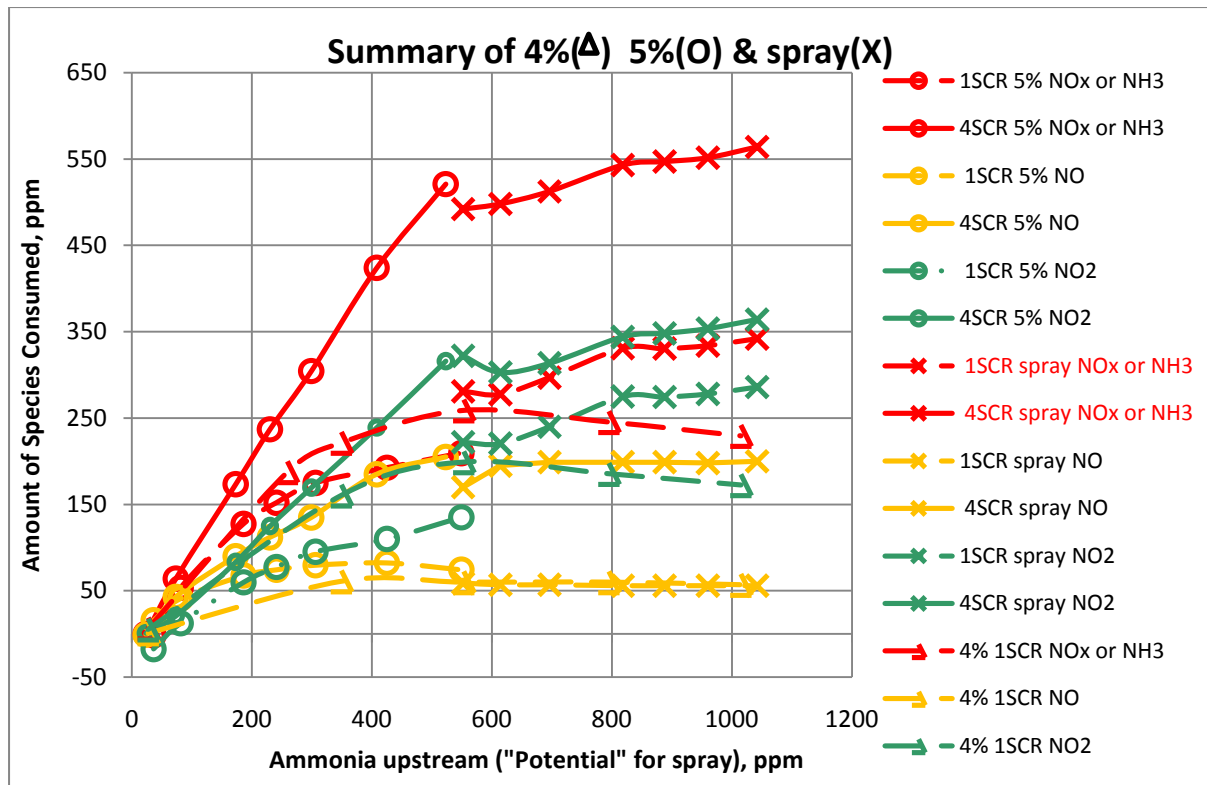


Figure 4.3 Summary of measurement with 1 and 4 SCR bricks.

From figure 4.3, it is observed that the 5% gas tests were performed at low ammonia input to avoid excessive ammonia slip. The spray tests were completed at high potential ammonia input levels due to the spray unit being intended for heavy duty application but it was used at its lower range setting for this investigation. The 4% gas tests on the 1 SCR brick covered the entire range. Unfortunately the 4% gas tests did not investigate 4 SCR.

#### 4.4 Analysis of spray compared to gas

From figure 4.3 the 4 SCR test results for 5% gas (o-marker) matched fairly the spray results (x-marker) at around 500 to 600 ppm ammonia input. The 1 SCR test results for NO shows good agreement between 4% gas ( $\Delta$ ), 5% gas (o) and urea spray (x). The  $\text{NO}_2$  and  $\text{NH}_3$  level after one SCR with spray shows higher values and do not agree with the 4% gas results. The reason for this is because droplets from urea spray are able to survive through one brick and this is not accounted for in the methodology applied in this investigation. It is unlikely that HNCO will survive passage through 1 SCR bricks as hydrolysis is rapid.

The differences between the one SCR spray and 4% gas can be utilised to deduce how much  $\text{NH}_3$  exits from one SCR brick in droplet (i.e. non-gaseous ammonia) form. This is considered as one of the most significant finding in the investigation and will be discussed later.

#### 4.5 Analysis of droplet behaviour.

In this section the analysis of ammonia released from the urea spray is discussed. Section 4.5.1 discusses ammonia release from urea spray upstream of the SCR for both 1 SCR and 4 SCR cases. Section 4.5.2 discusses ammonia released within the 4 SCR bricks. Finally section 4.5.3 discusses ammonia passing through the 1 SCR brick in droplet form.

##### 4.5.1 Ammonia released from urea spray upstream of the SCR bricks.

In order to analyse the droplet behaviour upstream of the SCR, the information from potential ammonia from the spray (see appendix 4.1.5) and the deduced ammonia from the upstream measurements of 1 SCR and 4 SCR bricks are used (see table 4.1.5 and 4.1.6). This information is plotted against the potential ammonia input from the spray in figure 4.5.1.

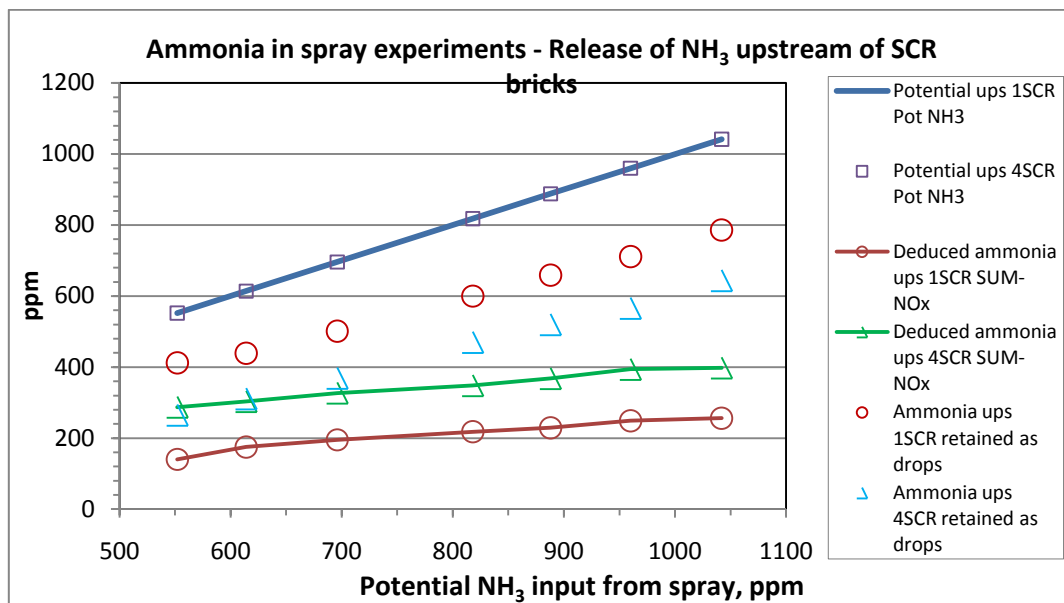


Figure 4.5.1 Ammonia released from spray upstream of the SCR bricks

From figure 4.5.1, it is observed that from half to three quarters of the droplets from the urea spray remained in droplet form, or possibly as  $\text{HNCO}$  at the inlet of the first SCR bricks. This is obtained from deduction of the potential ammonia upstream to the deduced ammonia upstream of the brick. The 1 SCR and 4 SCR results vary due to experimental variation. The SUM values represent a series of experiments performed at various times using the same method.

#### 4.5.2 Ammonia released from urea spray within the 4 SCR bricks

In order to analyse this, the measurements of ammonia gas entering and consumed in the 4 SCR brick are needed. Figure 4.5.2 shows the ammonia released from the spray within the 4 SCR bricks.

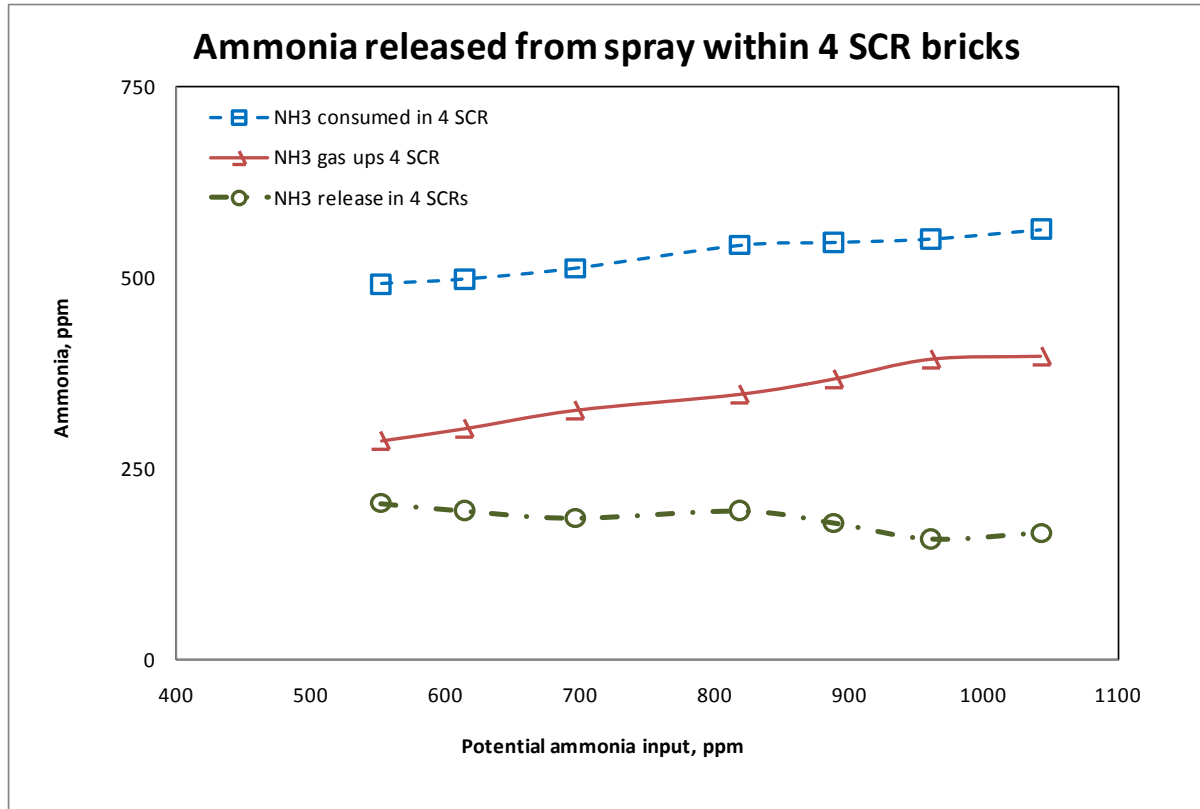


Figure 4.5.2 Ammonia released from urea spray within 4 SCR bricks.

From figure 4.5.2, the differences between the ammonia consumed by the 4 SCR and the ammonia released upstream of the 4 SCR gives the ammonia released within the 4 SCR bricks. It is observed that approximately 200 ppm or less ammonia is being released within the bricks to be consumed by the SCR reactions. It also shows that, as the spray injection flow rates increases, the ammonia released within the bricks reduced possibly as a result of lower brick temperatures. This is probably due to the excess spray cooling the SCR bricks.

#### 4.5.3 Ammonia passing through 1 SCR brick in droplets form.

In this analysis, the results from NO<sub>x</sub> or NH<sub>3</sub> consumed within the 1 SCR brick for the spray and 4% gas are compared. Based on the differences between the two results, the ammonia that passes through 1 SCR brick in the form of droplets can be found. This plot is shown in figure 4.5.3.



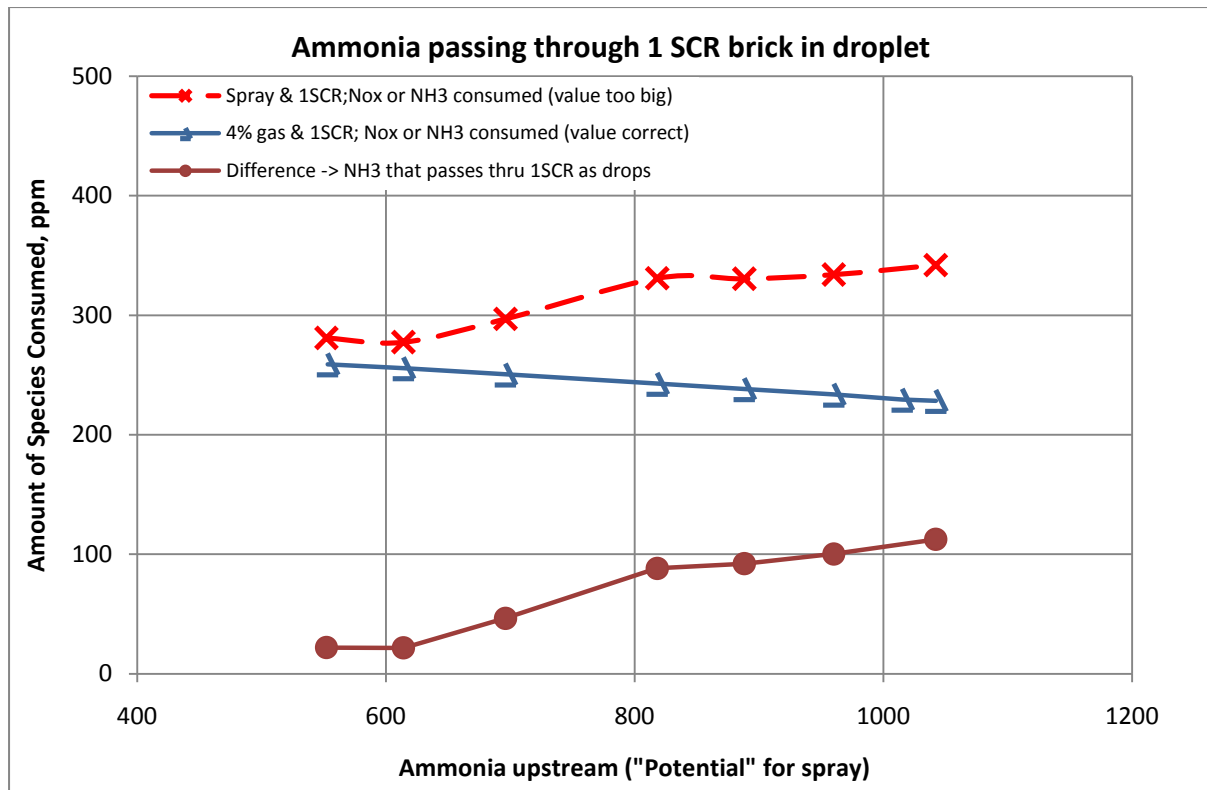


Figure 4.5.3 Ammonia passing through 1 SCR brick in droplets form.

It is observed from the differences that approximately 10 to 100 ppm of potential ammonia from the urea spray did pass through the 1 SCR brick. The information shown here also indicates, more droplets passing through as the urea flow rate increased.

#### 4.6 Analysis of NO and NO<sub>2</sub> conversion efficiency and ammonia slip.

Three significant parameters in SCR system are NO, NO<sub>2</sub> conversion efficiency and ammonia slip. The analysis of NO and NO<sub>2</sub> conversion efficiency requires the NO and NO<sub>2</sub> inlet condition and the exit NO, NO<sub>2</sub> measurements. From the summary of data only five sets of results (see table 4.1.5, 4.1.6, 4.2.5, 4.2.8 and 4.2.9) can be analysed for NO and NO<sub>2</sub> conversion efficiency. Two sets of result are from the 1 SCR and 4 SCR spray, another two from 1 SCR and 4 SCR with 5% gas and one set from 1 SCR with 4% gas

#### 4.6.1 NO conversion efficiency

In this section the NO conversion efficiency can be plotted against the calculated potential ammonia input from the spray, 4% gas and 5% gas with respect to the SCR brick length as shown in figure 4.6.1. NO conversion efficiency can be defined as below:

$$NO \text{ conversion efficiency} = \frac{NO \text{ in} - NO \text{ out}}{NO \text{ in}} \times 100\%$$

From figure 4.6.1, the excessive urea spray setting only results in a NO conversion of approximately 30 % for the 1 SCR brick (shown in red and blue). The reason for this is due to the high space velocity (low residence time) of around 182k/hour for the 1 SCR brick at a temperature in the region of 590K. As a result of the high space velocity, unconverted droplets can survive through the SCR brick unreacted. The 1 SCR with spray and 4% gas shows a perfect match of NO conversion from around 400 to 1100 ppm ammonia input while the 5% gas shows NO conversion slightly higher for lower range of ammonia input (less than 500 ppm).

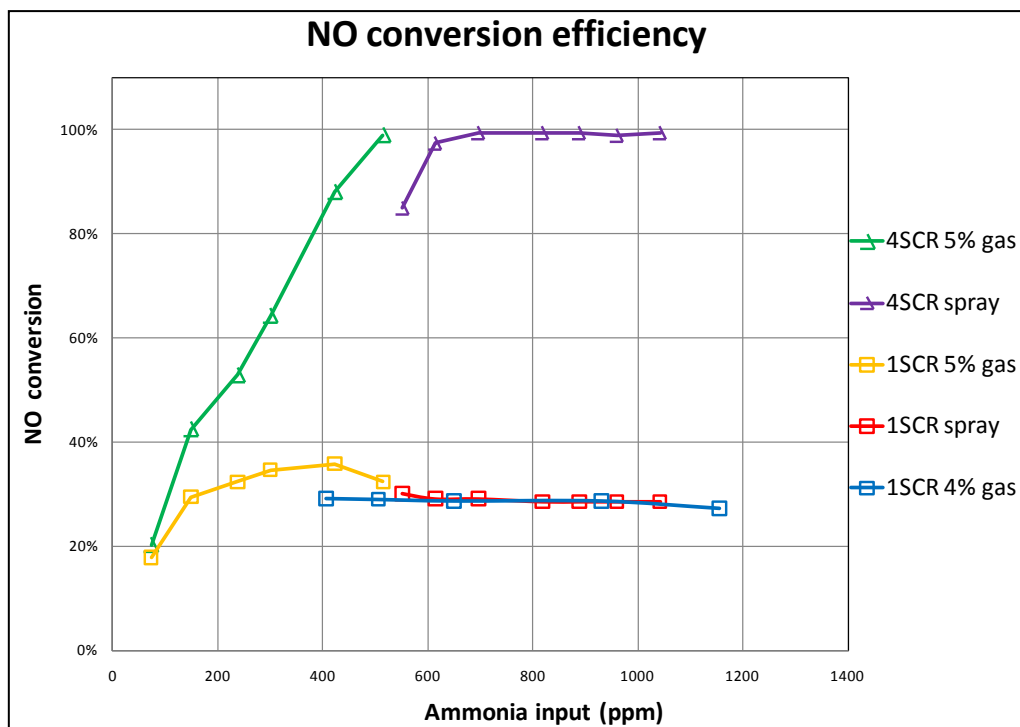


Figure 4.6.1 NO conversion with respect to SCR length.

In contrast, the 4 SCR brick conversion efficiency was very high and close to 100% when ammonia input was sufficient (shown in green and purple). The space velocity for 4 SCR is reasonably low at around 45.5 k/hour, which gives higher residence time of the ammonia in the SCR bricks. The SCR bricks space velocity at approximately 590 K is summarized in table 4.6.1

Table 4.6.1 Space velocity for SCR bricks used in the investigation.

Number of SCR brick	Brick Length, mm	Space Velocity, k/hour
1	91	182
2	182	91
3	273	61
4	364	45.5

#### 4.6.2 NO<sub>2</sub> conversion efficiency

Similarly the NO<sub>2</sub> conversion efficiency was performed with the results from 1 and 4 SCR with urea spray, 1 and 4 SCR with 5% gas and 1 SCR with 4% gas. The NO<sub>2</sub> conversion efficiency is shown in figure 4.6.2

The NO<sub>2</sub> conversion efficiency is defined using the following equation:

$$NO_2 \text{ conversion efficiency} = \frac{NO_2 \text{ in} - NO_2 \text{ out}}{NO_2 \text{ in}} \times 100\%$$

The conversion efficiency for the 1 SCR spray case is too high based on the assumption that all droplets are converted within the bricks. The conversion efficiency for 4 SCR spray is over 100% based on the negative NO<sub>2</sub> out (table 4.1.6) due to experimental error.

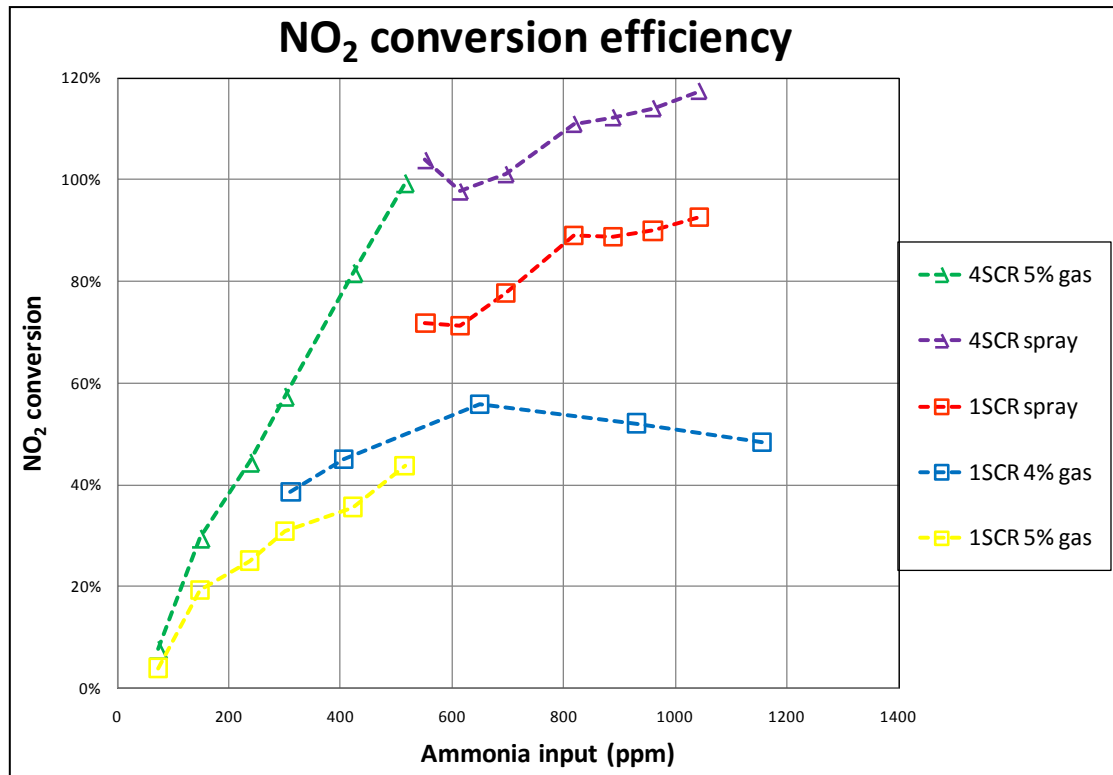
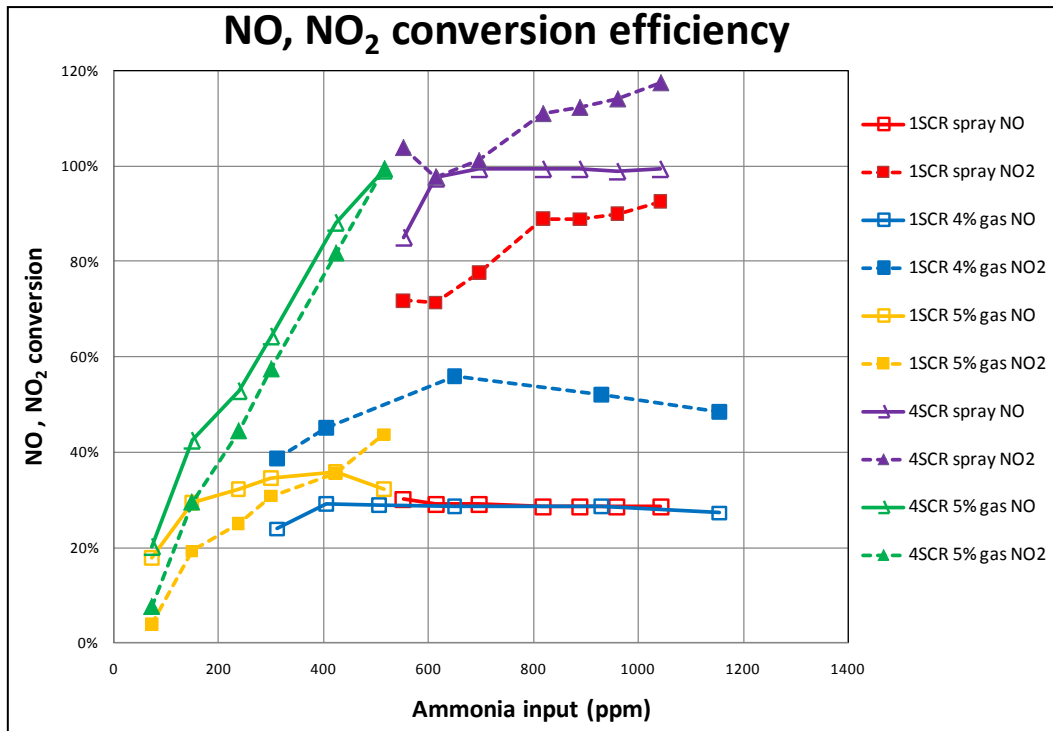


Figure 4.6.2 NO<sub>2</sub> conversion with respect to SCR brick length.

The NO<sub>2</sub> conversion was higher for the 4 SCR spray (purple) and 4 SCR 5% gas (in green) followed by the 1 SCR spray (red). The 4 SCR 5% gas efficiency increased linearly from 0 to reach 100% at ammonia input of 500 ppm. The NO<sub>2</sub> efficiency for 4 SCR spray ranged from 80 to 100% and reached the peak at ammonia input of 700 ppm. The 4% gas with 1 SCR NO<sub>2</sub> conversion shows slightly higher conversion as compared to the 5% with 1 SCR. The NO<sub>2</sub> conversion efficiency for 1 SCR spray is also higher from 70 to 90% as compared to 40 to 55% for 1 SCR 4% (blue) and below 45% for 1 SCR 5% (yellow). Even with the high space velocity in the 1 SCR spray case, the NO<sub>2</sub> reaches up to 90% conversion. This will be discussed further in the following section.

#### 4.6.3 Comparison of NO and NO<sub>2</sub> conversion.

To summarize the NO and NO<sub>2</sub> conversion efficiency for along the SCR length, the results from the previous two sections are plotted together in figure 4.6.3 Dashed lines show NO<sub>2</sub> conversion and solid lines show NO conversion. The 4 SCR is shown with symbol (Δ) and the 1 SCR with symbol (□) in the legend.

Figure 4.6.3 Comparison of NO and NO<sub>2</sub> conversion efficiency

Comparing the NO and NO<sub>2</sub> conversion efficiency for the 4 SCR bricks (purple and green lines) shows NO<sub>2</sub> conversion efficiency for the spray and gas were similar in all test cases as compared with the NO. However for 1 SCR brick NO<sub>2</sub> conversion, the 4% gas (blue-dash line) and the spray (red-dash line) are much higher than the NO conversion. The spray NO<sub>2</sub> conversion (red-dashed line) is high due to droplets passing through unaccounted for, as discussed earlier. The 5% gas results (in yellow), however at low ammonia input are closer but by 500 ppm ammonia input, again the NO<sub>2</sub> conversion exceed the NO conversion.

This is considered as one of the most significant finding in this study. Whilst, NO<sub>2</sub> and NO react at equal amount with NH<sub>3</sub> for the fast kinetic scheme reviewed earlier (equation 2.1e in section 2.1), this contradicts with findings from the NO, NO<sub>2</sub> conversion observed in the studies here where NO<sub>2</sub> conversion level are significantly higher than NO after 1 SCR brick.

#### 4.6.4 Ammonia slip.

High concentration of ammonia released from the spray poses another problem associated with ammonia slip. At the time of this investigation, the actual NH<sub>3</sub> slip measurement could not be performed due to the interference problem with the MEXA analyser as previously discussed. However, the methodology described in this thesis allows the ammonia slip to be deduced as summarized in table of results (refer to table 4.1.5, 4.1.6, 4.2.5, 4.2.6, 4.2.7, 4.2.8 and 4.2.9) earlier.

The highest ammonia slips are from the 1 SCR brick clearly due to the high space velocity, see figure 4.6.4. The 4 SCR spray also gives high ammonia slippage due to the excess spray used. However the slippage for both spray cases are too high because it include droplet. The 4 SCR spray study shows slip because excess potential ammonia, > 550 ppm, was supplied. For 1 SCR brick, the difference between the spray and 4% gas gives the amount of ammonia slippage in droplet form (shown in orange). The 2, 3 and 4 SCR with 5% gas produced almost no slippage clearly due to most of the supplied ammonia having reacted with the engine out NO<sub>x</sub> up to supplied ammonia input levels of 500 ppm.

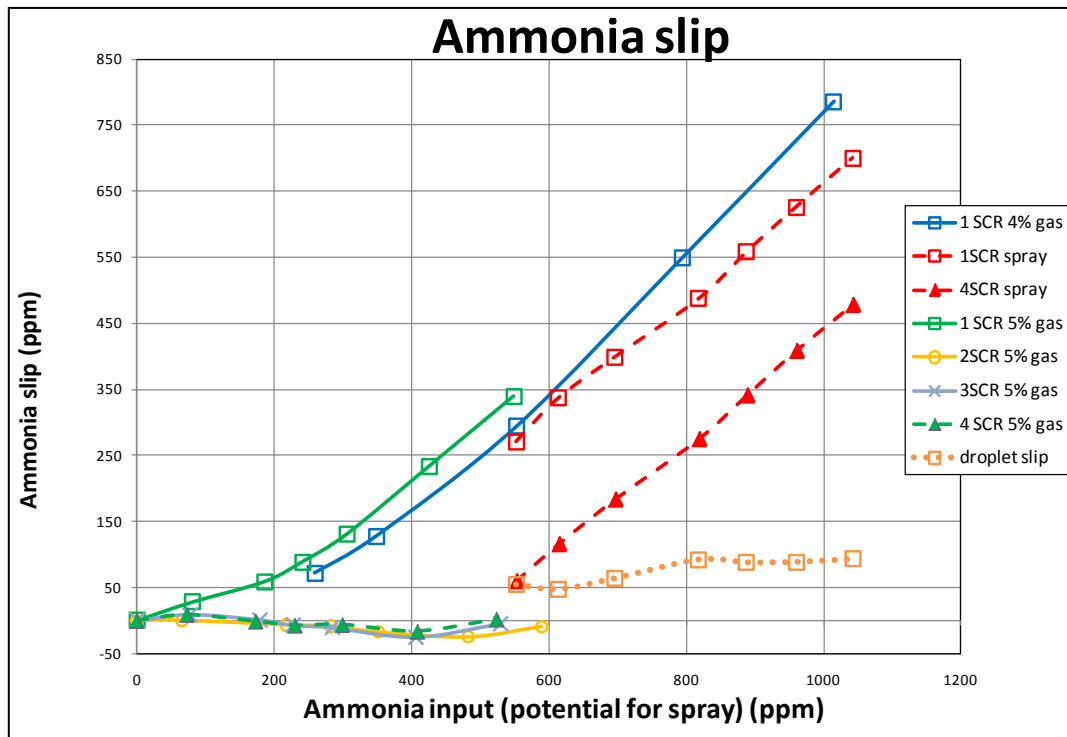


Figure 4.6.4 Ammonia slip against potential ammonia input with respect to SCR brick length.

#### 4.7 CFD modelling analysis comparison with measurements.

CFD simulations were performed to compare with the results for 1 and 4 SCR with 5% gas. Only the 1 SCR data was available for the 4% gas. The CFD package Star-CD version 3.26 was used and all of the CFD modelling results were presented and compared with the experimental data from this study in the published paper (Tamaldin et al. 2010). The CFD work described here was undertaken by Dr. C.A. Roberts following discussions regarding inlet boundary conditions derived from the experiments. In some cases, experiments were repeated to recheck data and to supply additional information for the CFD model.

#### 4.7.1 CFD data comparison with ammonia gas injection for 1 SCR and 4 SCR bricks.

In this analysis, the data from 1 SCR and 4 SCR with the 4% and 5% gas are plotted against the ammonia input separately. For the 1 SCR with 4% and 5% gas, the results for NO and NO<sub>2</sub> + NH<sub>3</sub> are plotted against the inlet ammonia. The CFD and measurement results are compared as shown in figure 4.7.1a.

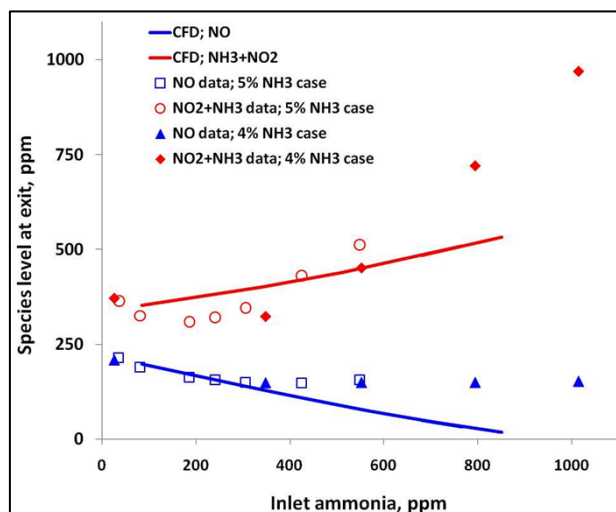


Figure 4.7.1a CFD and data comparison for species level at exit from 1 SCR brick.

Direct comparison of NO and NH<sub>3</sub>+ NO<sub>2</sub> measurements at the exit of the SCR bricks for 4% and 5% gas with CFD result are shown. At low level ammonia input, approximately less than 400 ppm, CFD and measurement match reasonably. At higher ammonia input level, above 400 ppm CFD and measurement do not acceptably match. A similar comparison was performed with the 4 SCR bricks shown in figure 4.7.1b. The results for NO and NH<sub>3</sub>+ NO<sub>2</sub> at the exit of the 4 SCR bricks is plotted against ammonia input.

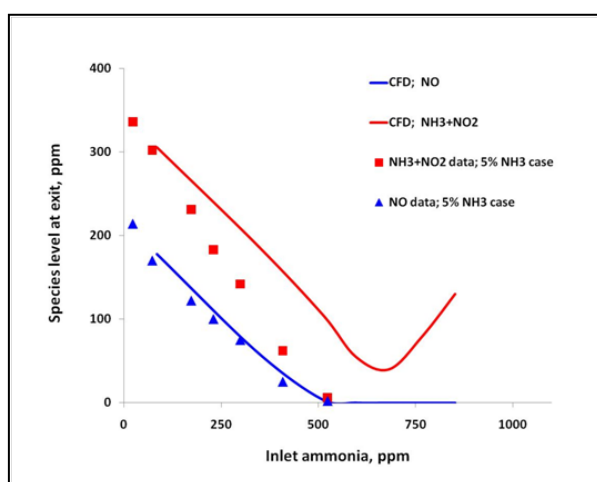


Figure 4.7.1b CFD and data comparison for species levels at exit from 4 SCR bricks.

Similar to the 1 SCR result, the agreement between CFD and measurement for 4 SCR bricks is fairly good at low ammonia input, approximately less than 500 ppm. The NO level measured and the CFD for 4 SCR matched much better than the 1 SCR comparison. At high ammonia input, greater than 500 ppm CFD prediction and measurement deviate for  $\text{NH}_3 + \text{NO}_2$ .

#### 4.8 Comparison of CFD prediction with $\text{NO}_2$ , NO and $\text{NH}_3$ at the SCR exit.

The final analysis involves comparison of the exhaust species at exit from the SCR bricks. For this analysis, three different cases will be discussed and presented separately. Results are plotted with respect to the individual level of  $\text{NH}_3$  gas injected.

##### 4.8.1 CFD prediction comparison of $\text{NO}_2$ with measurement results.

Measurement and CFD simulation are plotted against SCR brick length. CFD prediction and measurement for  $\text{NO}_2$  exiting the SCR bricks is shown in figure 4.8.1. The legend described the ammonia input used. In this comparison, it is observed that fairly good agreement between simulation and measurements is achieved after one SCR brick. Past the two SCR bricks agreement is poorer.

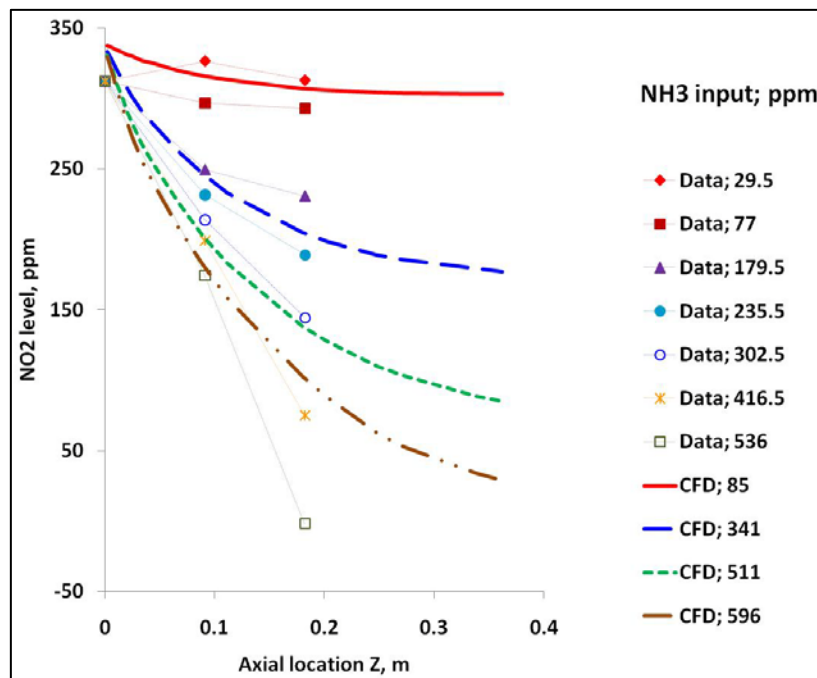


Figure 4.8.1 Simulations of  $\text{NO}_2$  against measurements at SCR exit.



#### 4.8.2 CFD prediction comparison of NO with measurement results.

CFD prediction and measurement comparison for NO exiting the SCR bricks is shown in figure 4.8.2. The NO results comparison to simulation shows good agreement after two bricks but poorly agree after the one SCR brick. Similarly the experimental and CFD ammonia input are shown in the legend.

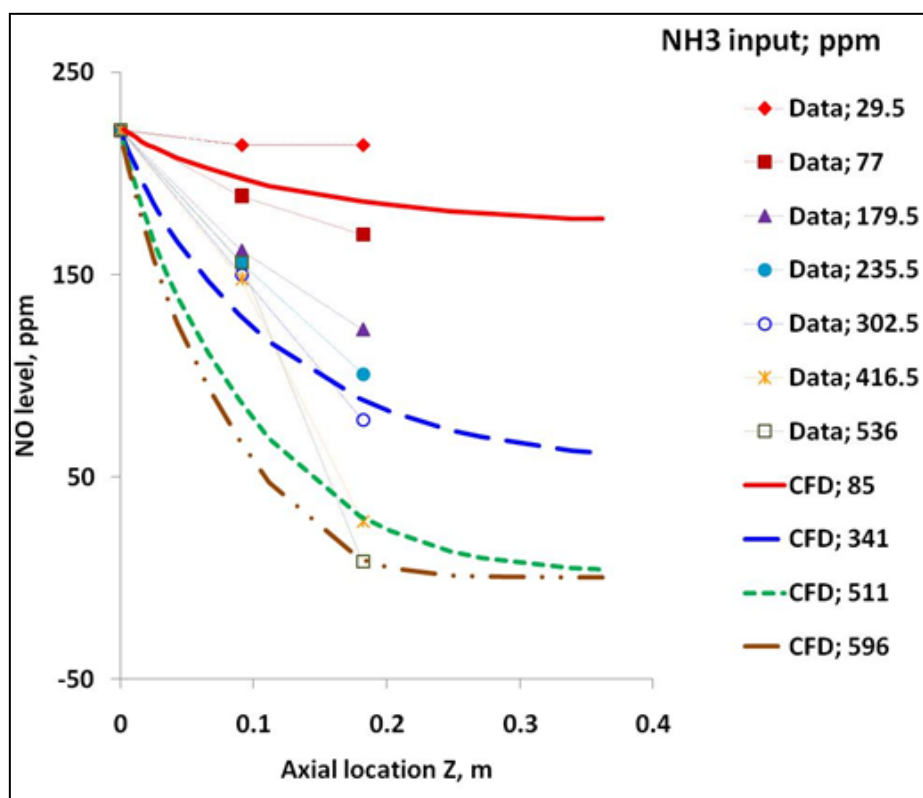


Figure 4.8.2 Simulations of NO against measurements at SCR exit.

#### 4.8.3 CFD prediction comparison of NH<sub>3</sub> with measurement results.

CFD prediction and measurement for NH<sub>3</sub> exiting the SCR bricks is shown in figure 4.8.3. The most significant observation from the NH<sub>3</sub> simulation is the NH<sub>3</sub> slip predicted after the two bricks but not observed in the measurements. Ammonia input for the experiments and CFD are shown in the legend.

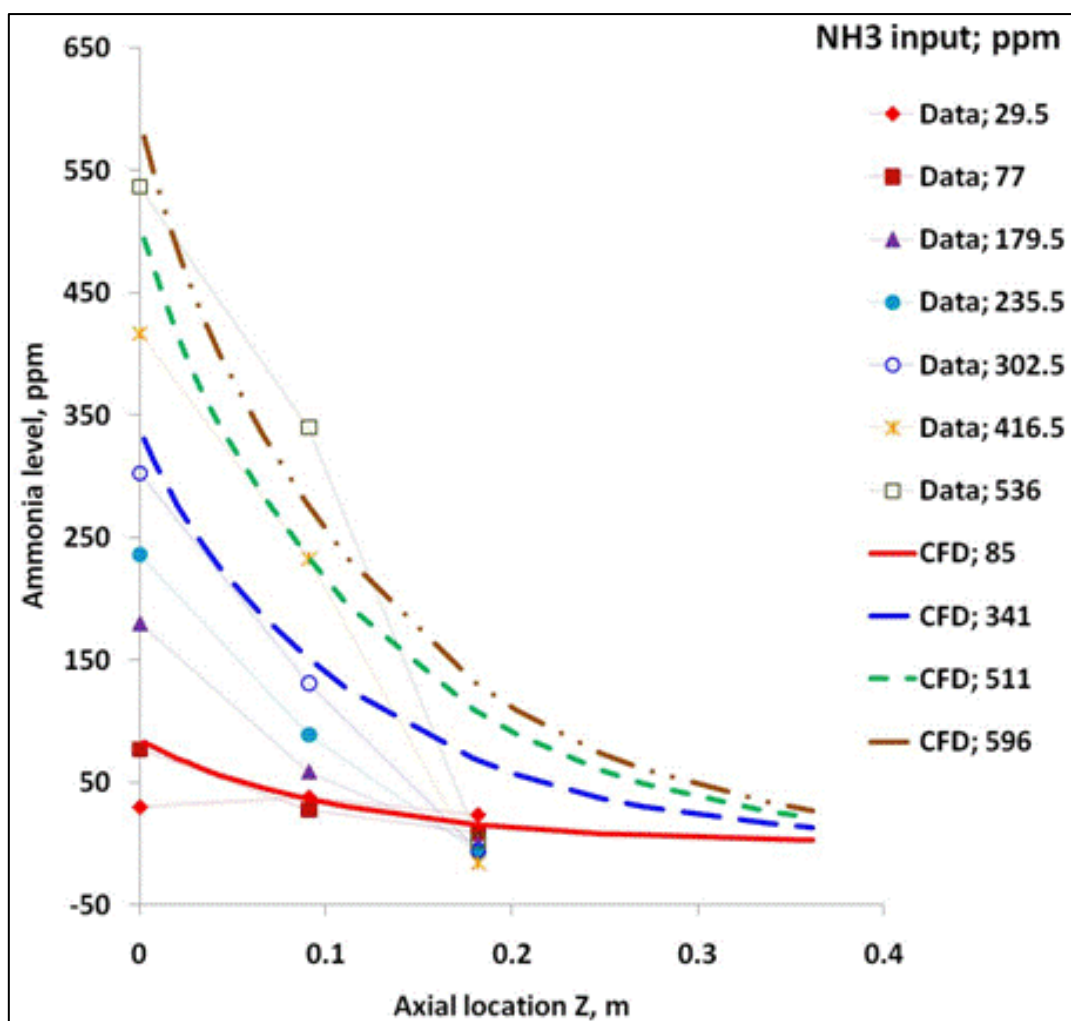


Figure 4.8.3 Simulations of NH<sub>3</sub> against measurements at SCR exit.

#### 4.8.4 Overall remark from CFD comparison with measurements.

Generally the agreement between the comparisons of CFD prediction to the measurements is fairly good. Measurements showed that reactions were complete after two SCR bricks. The kinetic scheme applied in this simulation was based on the kinetic presented by Olsson et al, 2008. However, it is not known how similar the catalysts used in Olsson are to those of this investigation. Some changes were made to the total ammonia storage capacity suitable for the catalysts used in these experiments. Thus, good overall agreement was achieved even simulation do not show full agreement with the model.

#### 4.9 Transient analysis in the investigation.

In this investigation transient behaviour of the NO<sub>x</sub> reduction SCR reaction with urea spray or ammonia gas injection was observed. The transient behaviour observed was slightly different when using urea spray as compared with ammonia gas.

##### 4.9.1 Transient analysis of 4 SCR bricks with 4% NH<sub>3</sub> gas.

This was a 4% NH<sub>3</sub> gas study with 4 SCR bricks. NO<sub>x</sub> at a level of 611 ppm from the engine as measured by EXSA, 557 ppm as measured by MEXA, was supplied to the SCR. NH<sub>3</sub> gas was injected at input level of 1045 ppm at approximately 900 seconds. The NO<sub>x</sub> readings were completely reduced when the ammonia gas injection started, with no ammonia slip present despite excess ammonia injected. This can be seen in time between 900 to 1100 seconds in the figure 4.9.1

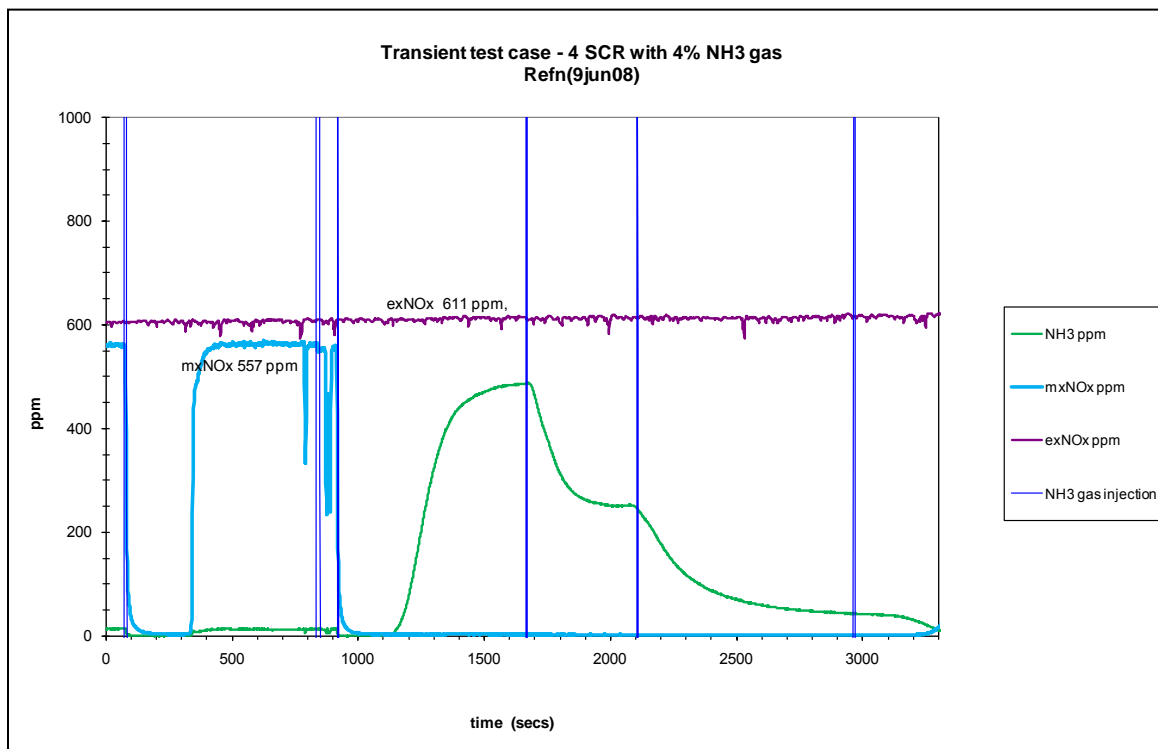


Figure 4.9.1 Sample of transient response in 4 SCR bricks with 4% NH<sub>3</sub> gas.

Part of the ammonia trace for the 4 SCR brick with 4% gas is shown again in figure 4.9.1a. On this figure the area is separated into three regions. Region A represents the reacted  $\text{NH}_3$ . Region B describes the ammonia storage or absorption of the SCR bricks and region C represents the ammonia slipped at the back of the 4 SCR bricks.

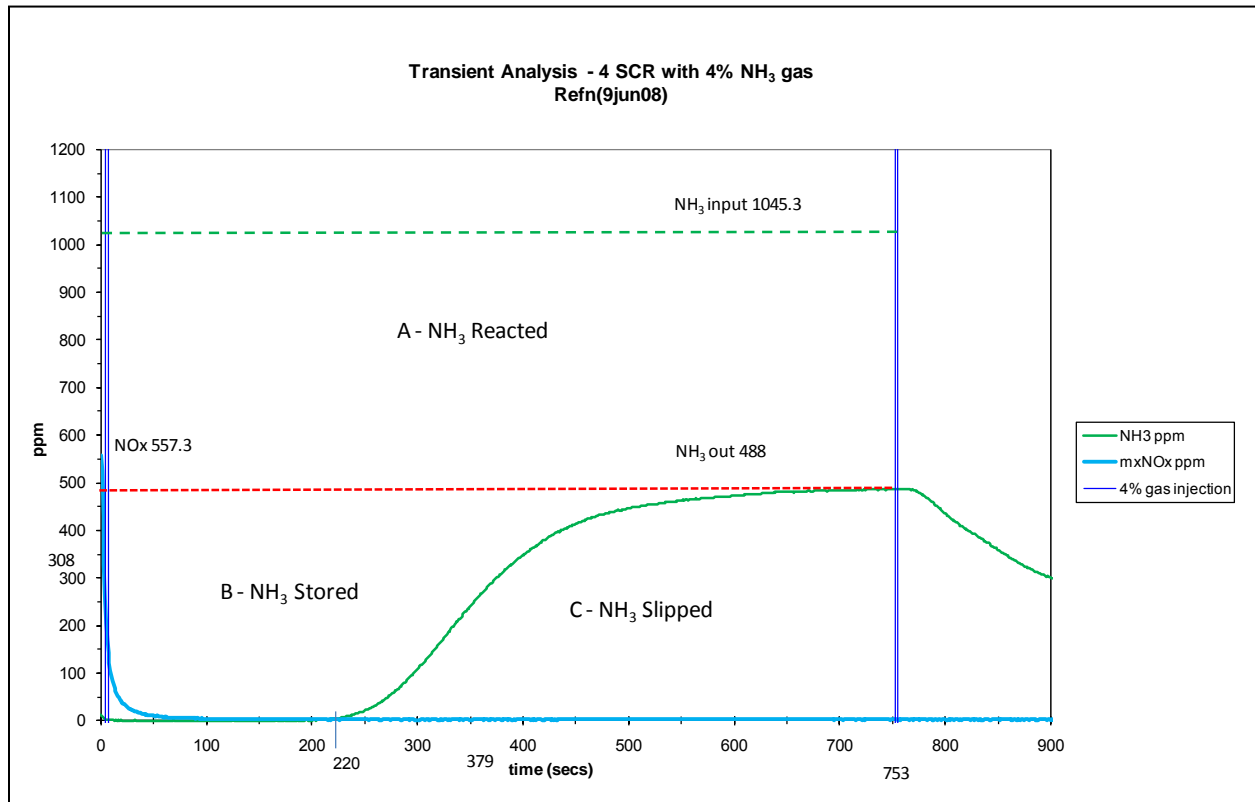


Figure 4.9.1a Transient Analysis for 4% gas with 4 SCR

The  $\text{NO}_x$  out level initially was 557.3 ppm before the ammonia gas injection started and it rapidly dropped to zero as soon as ammonia gas was injected. The  $\text{NO}_x$  level remains zero from the beginning of the 4% ammonia gas injection until the end of the trace because it was reacting with the excess ammonia supplied. The ammonia gas injection setting used in this region was calculated to be 1045 ppm.

The total  $\text{NH}_3$  reacted is matched by the amount of  $\text{NO}_x$  reacted and can be found using the following;

$$\text{Area for region A} = \text{Total } \text{NH}_3 \text{ reacted} = (1045.3 - 488) \text{ ppm} \times 753 \text{ seconds}$$

$$= 419\,647 \text{ ppm.secs} \approx 7.02 \text{ grams}^{*\text{Note}}$$

\*Note :

To convert an area in  $\text{NH}_3$  ppm.s to a mass in grams.

$$\text{Multiply by } \frac{17}{28.96} \times \frac{28.5}{1000\ 000} = 0.00001673$$

Where 17 is the Molecular weight for  $\text{NH}_3$  and

28.96 is Molecular weight for exhaust.

28.5 is exhaust mass flow rate in grams/seconds

Area of B + C = 488 ppm x 753 seconds

= 367 464 ppm.secs  $\approx$  6.15 grams

Although excess ammonia was supplied the slip remains zero for a period of 220 seconds until it begins to emerge at the back of the 4 SCR. During this period, the ammonia is continuously reacting with  $\text{NO}_x$  but it has also been stored in the 4 SCR bricks. Then, when the ammonia storage within the 4 SCR bricks approached its maximum capacity, the surplus ammonia started to exit the bricks at about 220 seconds. Region C starts as the ammonia slip begins to rise after the 220 seconds. As suggested by **Olsson et al. (2007)** as the maximum storage capacity is reached, the ammonia desorption will occur at a rate faster than the ammonia absorption of the bricks. This effect together with the continuous 4% ammonia gas injection caused the ammonia slip to rise exponentially until a steady value was reached, in this case, ammonia slip at 488 ppm. At this stage, the excess ammonia supplied to the bricks just passed through because there was no  $\text{NO}_x$  to react and no free storage capacity. The area above the ammonia slippage line until maximum ammonia slippage at 488 ppm will give the ammonia storage of the bricks.

The time taken to reach the steady value of ammonia slip was approximately 533 seconds from the onset of slip. The area under the ammonia slip curve can be found by integrating the curve within the 220 to 753 seconds time period. This can be achieved numerically within an excel spreadsheet as shown in appendix 4.9.1a. The area was converted to mass and found to be around 3.14 grams slipped between 220 to 753 seconds.

Finally the ammonia stored which is represented by the area of Region B,

$$\begin{aligned}\text{Stored ammonia} &= (\text{Area of B} + \text{C}) - \text{NH}_3 \text{ slip (Region C)} \\ &= (6.15 - 3.14) \text{ grams} \\ &\approx 3.01 \text{ grams}\end{aligned}$$

Ammonia Stored in the 4 SCR bricks  $\approx 3.01$  grams

The ammonia reacted was found to be 7.02 grams a further 3.01 grams was stored while 3.14 grams slipped at the back.

#### 4.9.1.1 Time constants for gas.

The time constant for NO<sub>x</sub> falling from its initial value (557.3 ppm) in figure 4.9.1a can be found from the falling curve. Starting from the NO<sub>x</sub> reading of 557.3 ppm, it dropped rapidly as soon as ammonia gas at 4% was injected. The time constant for this reaction could be found as the following, defining the fall to 36.79% as the time constant.

$$\begin{aligned}[C] &= 0.3679 [C]_0 \\ [C] &= 0.3679 [557.3 \text{ ppm}] = 205 \text{ ppm} \\ \text{time at 205 ppm} &= 5 \text{ seconds} \\ \text{The time constant for NO}_x \text{ falling} &\text{ was about 5 seconds.}\end{aligned}$$

This time constant is mainly from the time response of the MEXA analyzer. The chemical reactions themselves are very much faster.

The time constant for ammonia rising during the slip is found at 63.3 % of the final steady value. In this case it was found that time taken was approximately 159 seconds for NH<sub>3</sub> to rise to 308 ppm.

#### 4.9.2 Transient analysis of 4 SCR brick with urea spray

The transient analysis was performed on the 4 SCR with urea spray in a similar way to the transient analysis for 4 SCR with 4%  $\text{NH}_3$  gas. An example of a typical transient observation with urea spray and 4 SCR is shown in figure 4.9.2. In this case, the spray setting was adjusted and the incoming ammonia was estimated at around 929, then 857 and then 785 ppm. The spray was potentially capable of supplying more ammonia than this but some remained as urea droplets and was not available for reaction. From the figure shown, the incoming  $\text{NO}_x$  was 539 ppm throughout and this was fully reacted as there was no  $\text{NO}_x$  slip detected at the exit of the SCR. The trace up to 956 seconds can be divided into three different regions.

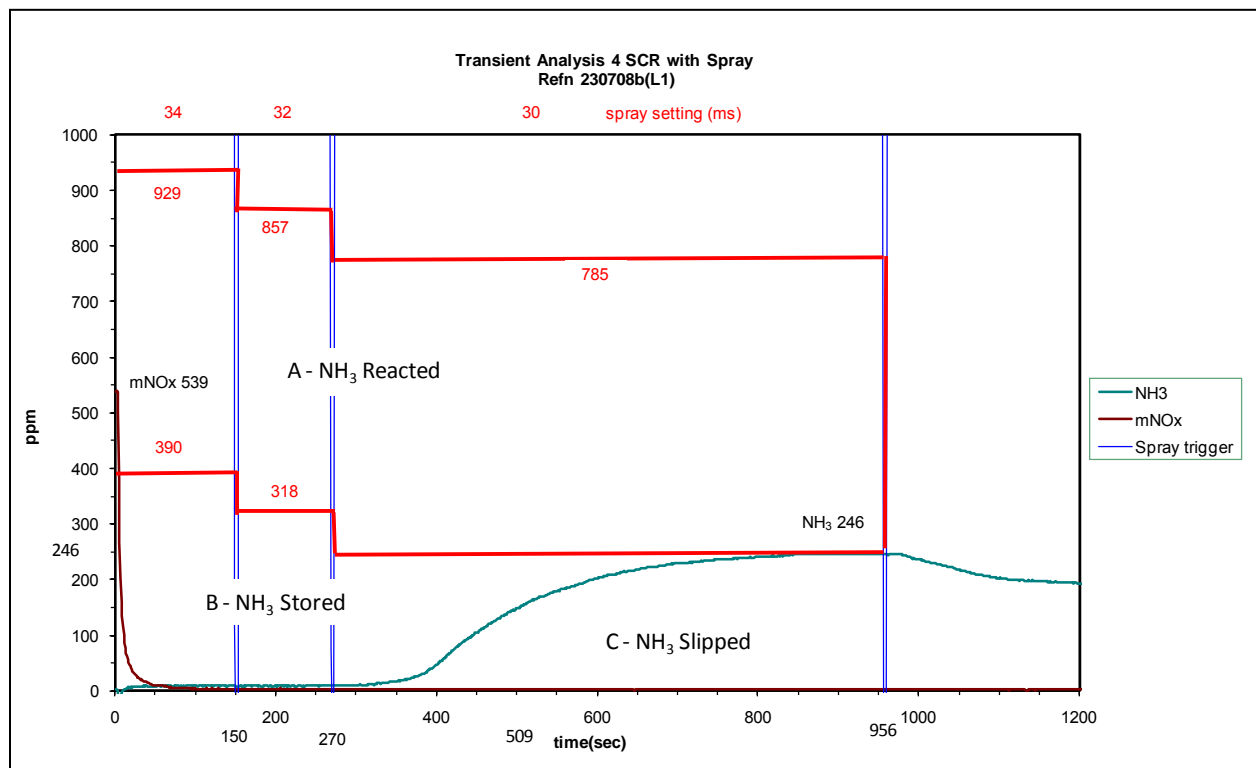


Figure 4.9.2 Transient Analysis for urea spray with 4 SCR

Region A, represents the overall  $\text{NH}_3$  reacted. The area under region A starts from the first urea spray injection and the spray rate changed twice until time reached 956 seconds. In this region, all of the incoming  $\text{NO}_x$  at 539 ppm was reacted. The ammonia slip was observed just after the 270 seconds. The total  $\text{NH}_3$  reacted in this case can be found using;

$$\begin{aligned}
 \text{Area for region A} = \text{Total NH}_3 \text{ reacted} &= 539 \text{ ppm} \times 956 \text{ seconds} \\
 &= 515\,284 \text{ ppm.secs} \\
 &\approx 8.62 \text{ grams}
 \end{aligned}$$

$$\begin{aligned}
 \text{Area for region B + C} \\
 &= (390 \times 150) + 318(270-150) + 246(956-270) \\
 &= 265\,416 \text{ ppm.secs} \\
 &\approx 4.44 \text{ grams}
 \end{aligned}$$

Region B represents the amount of ammonia being stored by the 4 SCR bricks. The ammonia slip started rising around 270 seconds. It took another 686 seconds to reach the ammonia slip steady value of 246 ppm.

Region C represents the ammonia slipped at the exit of the 4 SCR bricks. The steady value of 246 ppm is reached at about 956 seconds. The amount of ammonia slippage can be found by integration of the area under ammonia slip curve between 270 to 956 seconds. This is obtained using numerical integration in excel spreadsheet and converted to mass as shown in appendix 4.9.2a. The amount of ammonia slip was calculated and found to be 1.93 grams.

Similarly to the 4% ammonia gas study, at 270 seconds ammonia storage is approaching its maximum and ammonia desorption started. This is clearly shown by the exponential rise in the ammonia slip curve in figure 4.9.2.

$$\begin{aligned}
 \text{Finally the ammonia stored under Region B} &= \text{Area (B+C)} - \text{Area C} \\
 &= 4.44 - 1.93 \text{ grams}
 \end{aligned}$$

$$\text{Ammonia Stored in the 4 SCR bricks} \approx 2.5 \text{ grams}$$

The total ammonia reacted in the SCR system was found to be 8.62 grams, 2.5 grams was stored in the bricks while 1.93 grams slip at the back.



#### 4.9.2.1 Time constants for urea spray.

The time constant for NO<sub>x</sub> reduction in this case is defined as the time where the concentration has fallen 0.3679 from its initial value.

$$[C] = 0.3679 [C]_0$$

$$[C] = 0.3679 [539 \text{ ppm}] = 198.3 \text{ ppm}$$

$$\text{Time @198.3 ppm} = 7.5 \text{ seconds}$$

Therefore time constant for NO<sub>x</sub> reduction is 7.5 seconds. However, this time constant is dominated by the time response from the MEXA analyzer since the NO<sub>x</sub> and NH<sub>3</sub> reaction in the SCR is occurring at a much faster rate.

The time constant for the ammonia rise is the time from where the ammonia slip just begins until 0.632 of its final steady value as described in the rising curve analysis. Therefore the time constant for ammonia rise in this case is as follows:

$$\text{NH}_3 \text{ begin slip @ after 270 seconds}$$

$$0.632 \times 246 \text{ ppm} = 155.5 \text{ ppm @ 509 seconds}$$

$$\text{Time constant for ammonia rise} = 509 - 270 = 239 \text{ seconds.}$$

#### 4.9.3 Comparison of the urea spray and ammonia gas transients.

In order to compare the transient behaviour of the gas with the urea spray study, the results from sections 4.9.1 and 4.9.2 are compared. The summary of comparison between the two cases is shown in table 4.9.3.

Table 4.9.3 Comparison of the 4% gas with urea spray transient analysis.

Properties	4% gas with 4 SCR bricks	Urea spray with 4 SCR bricks
1. NO <sub>x</sub> reduction time constant.	5 seconds	7.5 seconds
2. Ammonia storage time to onset of slip.	220 seconds	270 seconds
3. Time constant of rise in ammonia slip	159 seconds	239 seconds
4. Amount of ammonia reacted	7.02 grams	8.62 grams
5. Amount of ammonia stored	3.01 grams	2.50 grams
6. Amount of ammonia slipped	3.14 grams	1.93 grams

From the table 4.9.3, it was observed that the NO<sub>x</sub> reduction time constant for gas is slightly less than the urea spray case, but both times were attributable to the response time of MEXA analyser and should be instantaneous. The ammonia storage, rise and slip times were different with 4 % gas as compared with urea spray. In urea spray case droplet conversion is necessary while the 4% gas is readily available for SCR reaction. The amount of stored and slipped are slightly higher with 4% gas case compared with the urea spray case.

#### 4.10 Summary of the experimental and simulation results.

This investigation has compared the performance of SCR system with urea spray injection and ammonia gas. These studies involved the NO<sub>2</sub>/NO ratio of approximately 60/40 and shows all reactions with ammonia were complete after the two SCR bricks at a length of 182 mm.

To summarize the results the following concluding remarks could be made:

- Some precaution and concern is needed when interpretations are made based on measurements reading from a CLD based analyser involving NO and NO<sub>2</sub>. This is needed especially in the presence of ammonia. The methodology suggested in this investigation however enables amount consumed to be extracted. From known amounts of input from individual measurements upstream and downstream of the SCR, the data for NO, NO<sub>2</sub> and NH<sub>3</sub> can be extracted.

- In the urea spray studies, when the urea in the form of AdBlue solution was injected, about 200 ppm of  $\text{NH}_3$  were released from the droplets of urea spray and reacting with  $\text{NO}_x$  within the SCR bricks.
- From estimation, it was observed that in the range of 10 to 100 ppm of potential ammonia manage to pass through one SCR at a length of 91 mm in droplets form.
- From the CFD simulations using the porous medium approach and kinetics scheme published in the open literature, have shown some ability to predict the steady state tests investigated here.
- The model has been used to predict individual species along the SCR bricks length and some moderate agreement with the measurement has been achieved especially with the long bricks. For short brick, space velocity was high and there were breakthrough of all species.
- A transient analysis showed that the time constant for  $\text{NO}_x$  reduction are quite close for gas and spray but for the time constant for ammonia slip is higher in spray than gas.
- $\text{NO}_2$  conversion efficiency was found higher than  $\text{NO}$  in all test cases which contradict with fast reaction kinetic.

## CHAPTER 5: CONCLUSIONS AND FUTURE WORK

### 5.0 Conclusions and Future work: Introduction.

Despite the limitations of the MEXA gas analyser, and the need to derive a strategy for interpretation of the measurements made by it, a thorough investigation of SCR process has been made in a specially designed exhaust system on an experimental test bed. The conclusion from the investigation include the development of the experimental techniques, the interference of  $\text{NO}_2$  and  $\text{NH}_3$ , the methodology, the transient response, the SCR and spray system performance and the significance of the main findings from the result chapter.

### 5.1 DPF-DOC Arrangement.

The DOC-DPF arrangement was tested for  $\text{NO}_2$  to  $\text{NO}$  ratio to assist the SCR reactions. With this arrangement, the  $\text{NO}$  coming out from the engine was oxidized by the DOC but later reacted with the trapped soot in the DPF, leaving less  $\text{NO}_2$  out than before. With less  $\text{NO}_2$ , the SCR reactions taking place were at the minimal level and leaving  $\text{NO}_x$  out passing the system still at higher readings. In the final arrangement used in this investigation, DPF-DOC was identified as the acceptable sequence upstream of the SCR. Utilizing this arrangement, higher  $\text{NO}_2$  to  $\text{NO}$  ratio was achieved. In the literature, 50:50  $\text{NO}_2$  to  $\text{NO}$  ratio or higher was shown as the preferred condition to optimize the SCR reactions. Subsequently, in this investigation, a higher  $\text{NO}_2$  to  $\text{NO}$  ratio was studied.

### 5.2 Experimental techniques.

The biggest obstacles in the beginning of this investigation were to establish suitable experimental techniques in order to complete the steady state study with the SCR system. Interferences within the analysers were a particular problem because the continuous injection of the urea or ammonia gas was necessary in this investigation. The use of both urea spray and ammonia gas were investigated. Interference and reaction between  $\text{NO}_2$  and  $\text{NH}_3$  on the  $\text{NO}_x$  converter within the MEXA has resulted in significant loss of reliable directly measured test data.

This was overcome by a methodology that allowed all required parameters to be deduced. The spray used in this study was designed for heavy-duty application with the lowest possible setting utilized. This caused intermittent problems especially with the low settings involved in light duty

investigation. Due to the formation of white deposit (polymeric complexes such as melamine, ammelide and ammeline) spray blockage can occur and hinder SCR catalyst performance as described by Fang et al. 2003. Therefore a rigorous procedure for spray monitoring and cleaning was incorporated to ensure the spray was working properly in the experiment. All of the challenges and obstacles were overcome to develop a methodology for obtaining reliable data in this study.

### **5.3 Behaviour of urea droplet from spray.**

One of the important findings with the spray test cases, was the proportion of urea droplet decomposed before entering the SCR brick for NO<sub>x</sub> reduction reaction to occur. This detail was described in section 4.5 of the results chapter. It shows that more than half of the actual ammonia was still in the droplet form upstream of the SCR brick. It was observed approximately around 200 ppm ammonia was released from the droplet in the first SCR bricks and consumed for the NO<sub>x</sub> reduction reactions. The final finding shows between 10 -100 ppm of potential ammonia passed through the first brick as droplets under circumstances from NO<sub>x</sub> matched spray input to excess spray.

### **5.4 Space Velocity and Resident Time Effect.**

The SCR space velocity role for the NO<sub>x</sub> reduction efficiency was a very important observation in this investigation. The variation of space velocity had immediate effect on the residence time of the exhaust gases and ammonia within the SCR. It was found that, the 2, 3 and 4 SCR bricks had a similar effect on the SCR reactions taking place. All the NO<sub>x</sub> reduction had apparently completed in the 2 SCR bricks, therefore in the results shown for 4 SCR bricks could be assumed similar to the 2 SCR bricks. Conversion was incomplete in 1 SCR but it was notable that NO<sub>2</sub> conversion was greater than NO conversion. This is significant finding because it cannot be explained by the fast SCR reaction acting alone.

### **5.5 Transient observation and storage.**

Transient response observation during NO<sub>x</sub> reduction and ammonia slippage also reveals about the ammonia absorption by the SCR bricks. The amount of NH<sub>3</sub> stored was about 3 grams on 4 SCR bricks for both gas and spray cases as described earlier in section 4.9.3.

### 5.6 Significant of findings in chapter 4

- NO<sub>x</sub> and NH<sub>3</sub> reaction were completed after the 2 SCR bricks.
- The 2, 3 and 4 SCR bricks show similar NO<sub>x</sub> or NH<sub>3</sub> consumed.
- Meticulous cleaning of the urea spray was necessary for well-controlled operation.
- The gas and the spray results were similar in both 1 and 4 SCR bricks.
- With 1 SCR spray, droplets were passing through unconverted.
- Repeatability with gas test cases was excellent.
- Droplet released ammonia more at the SCR sites rather than upstream of the SCR.
- Droplet converted to ammonia much better in 4 SCR than 1 SCR.
- For 1 SCR cases, after about 400 ppm NH<sub>3</sub> consume, no further NO<sub>x</sub> reduction was taking place.
- Agreement overall was fairly good although predicted NH<sub>3</sub> slip after two bricks was not observed in the experiments. Agreement for NO was good after 2 SCR bricks but not good after 1 SCR brick. NO<sub>2</sub> agreement was better after 1 SCR brick than 2 SCR bricks.
- Transient response of the spray and gas cases was studied and provided measured values of NH<sub>3</sub> storage.
- NO<sub>2</sub> conversion was higher than NO for 1 SCR brick which does not agree with fast SCR kinetics suggest other reaction occurred.

Overall urea spray results showed similar trends to the ammonia gas results. The 5% ammonia gas results covered the lower range of ammonia gas used and the urea spray injected higher ammonia. This can clearly be seen section 4.4.2 comparison of all NO<sub>x</sub> and NH<sub>3</sub> consumed. The NO<sub>x</sub> or NH<sub>3</sub> consumed from the 1 SCR test with spray closely matched the 1 SCR test with gas. The 4 SCR test with the spray matched as the continuation of the 4 SCR test with gas line.

### 5.7 Contributions to the knowledge

- Measurement of NO<sub>2</sub> in the presence of high concentrations of NH<sub>3</sub> is clearly erroneous due to interference effect using the MEXA CLD based analyser. Despite this problem, a unique methodology was developed in this thesis to extract useful information to describe the SCR reaction in this investigation.

- The comparative analysis of the investigation with the use of urea spray and ammonia gas was described and lead to NO and NO<sub>2</sub> conversion efficiency with the use of different SCR bricks length.
- Insight into the behaviour of the urea droplets in the investigation was obtained. It show that from half to three quarter of droplet from spray remained unconverted to ammonia gas at the entry of first SCR brick. About 200 ppm ammonia released from droplet react in the SCR brick and between 10 to 100 ppm of potential ammonia passed through the first bricks as droplets. This occurs from the conditions of NO<sub>x</sub> matched spray input to excess spray.
- The CFD model for gas provide reasonable predictions for the long bricks while the short brick shows breakthrough of all species due to high space velocity. The reaction kinetics used from literature was able to show some ability to describe the species profiles within the SCR bricks.
- The most significant findings in this study is the higher NO<sub>2</sub> conversion efficiency for 1 SCR brick compared to NO. This cannot be described by the fast SCR kinetic scheme.

## **5.8 Recommendation for Future Work.**

Throughout the investigations, many areas have been identified for future work in order to optimise the SCR system working in the real application. Some of the identified areas include the exhaust gas analyser, dosing system, more robust spray design, spray position and angle into the exhaust stream, reduced length of the SCR system and also the transient study with the SCR.

### **5.8.1 Improved gas analyser to measure NO<sub>x</sub> in presence of ammonia.**

Most of the time spent in this investigation involved trying to obtain reliable measurements of NO<sub>x</sub>, NO and NH<sub>3</sub> upstream and downstream of the SCR brick. The CLD based analyser clearly causes a lot of setback in this investigation and variations in the results. A FTIR (Fourier Transfer Infra Red) based analyser was recently identified as better candidates for investigation with the use of urea and ammonia of this magnitude. The response time of the analyser was crucial in getting this information as the phase changes of the species within the exhaust gases need to be fully captured.

### **5.8.2 Spray Dosing System.**

Ideally a closed loop feedback spray dosing system would be desirable for this investigation. A manual over-ride system also need to be incorporated, taking into consideration of cold start condition. The system integrated with the engine ECU unit is under heavy development by many automotive suppliers for this purpose.

### **5.8.3 Cleaning of spray or continuous spraying**

To avoid having to clean the spray injector, a more robust spray design is needed to suit the light duty application. Continuous spraying into the exhaust would definitely not be appropriate, but should be covered by the closed loop feedback spray dosing system mention earlier. As for the cleaning, perhaps the solution for this lies with the concentration of urea solution used or a better designed spray to avoid any deposit build up.

### **5.8.4 Improved warm up and system using sequential program.**

The control software for the engine test bed is capable of programming of the sequence for setting up the engine warm up and cool down period, calibrating the analyser, periodic parameters logging and many other task. As the investigations were conducted, very limited time was spent on this side of the program due to other difficulties and challenges faced with the analyser and the spray system. The analysers control from the test bed program was not configured for this investigation. In the future, this should be seriously considered to have better control and monitoring sequence.

### **5.8.5 Signal trigger improvement with level differentiation of spray pulses and gas settings.**

Current spray and gas injection system was manually control by adjusting the signal generator for the spray and the gas flow meter for the gas. The spray signal generator was also connected as a voltage input to the engine test bed data logger. As for the logging the gas flow into the main engine test bed program, was done manually by pressing the trigger switch when the gas started.

For improvement of this system, the spray or gas injection system should have a signal input to the main engine data logger. Therefore, every spray sequence should be seen in the result plot similar to the exhaust gas data showing when the injector started and by how much is being injected.



#### **5.8.6 Investigation of Effect of Spray Angle and Positions.**

In this investigation, only the generic position of the spray is being explored which is upstream of the SCR brick into the expansion chamber for proper mixing. Other possibility was not explored such as spraying into a narrow pipe close to the SCR brick. The spray position and angle into the exhaust should be investigated to further improve this system. As in the real application, the effect of spray angle is crucial due to the confined spaces and angle existing in the real exhaust system in a light duty vehicle.

#### **5.8.7 Moving from 1D to 3D flow (change from long cone to short cone after the spray)**

As previously described in the methodology section 3.2.6 a long cone diffuser after the expansion chamber was used to ensure uniform single dimensional flow of the exhaust gas mixed with the ammonia entering the SCR brick. In the future, this long diffuser cone could be replaced with a short diffuser cone which would be closer in geometry to a real system. This changes the flow from single dimensional to three dimensional flow, therefore a more complex CFD model would be required for this case.

#### **5.8.8 Transient study (acceleration and deceleration)**

This study only considered very simple transient but future transient study with the SCR system would be necessary. As the engine going through the series of acceleration and deceleration as prescribed in the European Transient Cycle (ETC), the SCR performance results would be highly valuable.

#### **5.8.9 Engine Mass flow rate measurement and logging.**

The engine mass flow rate measurement in this investigation was conducted using external Ricardo mass flow meter as described in section 3.1.3 and manual data was logged from the digital manometer. Ideally, this information should be directly logged from the engine ECU either with the use of engine management system such as Gredi and dSpace. Getting information logged to the engine data logger would improve the experimental procedure for this type of investigation in the future.

## REFERENCES

- 1 Abu-Jrai, A. and Tsolakis, A.(2007) - *The Effect of H<sub>2</sub> and CO on the Selective Catalytic Reduction of NO<sub>x</sub> under Real Diesel Engine Exhaust Conditions over Pt/Al<sub>2</sub>O<sub>3</sub>*, International Journal of Hydrogen Energy, 57. Vol. 32, Issue 12, pp2073-2080.
- 2 Abu-Jrai, A., Tsolakis, A. and Megaritis, A. (2007) - *The influence of H<sub>2</sub> and CO on Diesel Engine Combustion Characteristics, Exhaust Gas Emissions, and Aftertreatment Selective Catalytic NO<sub>x</sub> Reduction*, International Journal of Hydrogen Energy, Vol. 32, Issue 15, pp3565-3571.
- 3 Albonetti, S., Mengou, J.E. and Trifiro, F.(2007) - *Polyfunctionality of DeNO<sub>x</sub> Catalysts in other Pollutant Abatement*, Catalysis Today, Vol. 119, Issue 1-4, pp295-300.
- 4 Alimin, A. J., Roberts C. A. and Benjamin S.F.(2006) - *A NO<sub>x</sub> Trap Study using Fast Response Emission Analyzers for Model Validation*, SAE2006-01-0685, SAE 2006 World Congress, Detroit, Michigan, 3-6 April 2006.
- 5 Alkemade, U. G. and Schumann, B.(2006) - *Engines and Exhaust Aftertreatment Systems for Future Automotive Applications*, Solid State Ionics, Vol. 177, Issues 26-32, 31 October 2006, pp2291-2296.
- 6 Alvarez, R., Weilenmann, M. and Favez, J.-Y. (2008) - *Evidence of increased mass fraction of NO<sub>2</sub> within real-world NO<sub>x</sub> emissions of modern light vehicles - derived from a reliable online measuring method*, Atmospheric Environment, Vol. 42, Issue 19, pp4699-4707.
- 7 Amin, N.A.S. and Chong, C.M. (2005) - *SCR of NO with C<sub>3</sub>H<sub>6</sub> in the presence of excess O<sub>2</sub> over Cu/Ag/CeO<sub>2</sub>-ZrO<sub>2</sub> catalyst*, Chemical Engineering Journal, Vol. 113, Issue 1, pp13-25.
- 8 Amon, B., Keefe, G. (2001) - *On-Road Demonstration of NO<sub>x</sub> Emissions Control for Heavy Duty Trucks using SINOx<sup>TM</sup> Urea SCR Technology- Long Term Experiment and Measurement Results*, SAE 2001-01-1931, International Spring Fuels and Lubricants Meeting and Exposition, Orlando, Florida, May 7-9, 2001.
- 9 Amon, B., Stefan, F., Hofman, L. and Jurgen, Z. (2004) - *SCR-A Technology for Global Emissions Control of Diesel Engines*, F2004V160, Fisita 2004 World Automotive Congress, Barcelona Spain, May 23-27, 2004.
- 10 Anunziata, O.A., Beltramone, A.R. and Requejo, F.G. (2007) - *In-containing BEA Zeolite for Selective Catalytic Reduction of NO<sub>x</sub>: Part I: Synthesis, Characterization and Catalytic Activity*, Journal of Molecular Catalysis A: Chemical, Vol. 267, Issue 1-2, pp194-201.
- 11 Anunziata, O.A., Beltramone, A.R., Juric, Z., Pierella, L.B. and Requejo, F.G. (2004) - *Fe-containing ZSM-11 zeolites as active catalyst for SCR of NO<sub>x</sub>: Part I. Synthesis, characterization by XRD, BET and FTIR and catalytic properties*, Applied Catalysis A: General, Vol. 264, Issue 1, pp93-101.
- 12 Anunziata, O.A., Beltramone, A.R., Ledes, E.J. and Requejo, F.G. (2007) - *In-containing BEA Zeolite for Selective Catalytic Reduction of NO<sub>x</sub>: Part II. Relation between In Active Sites and Catalytic Activity*, Journal of Molecular Catalysis A: Chemical, Vol. 267, Issue 1-2, pp272-279.

- 13 Baraket, L., Ghorbel, A. and Grange, P. (2007) - *Selective Catalytic Reduction of NO by Ammonia on V<sub>2</sub>O<sub>5</sub>-SO<sub>4</sub><sup>2-</sup>/TiO<sub>2</sub> Catalysts Prepared by the Sol-Gel Method*, Applied Catalysis B: Environmental, Vol. 72, Issue 1-2, pp37-43.
- 14 BASF (2003) - *Urea solution 32.5% AdBlue*, Technical Leaflet, BASF AG, Ludwigshafen, Germany, August 2003.
- 15 Beeck, J.O. and E. Joubert (2006) - *Review of SCR Technologies for Diesel Emission Control: European Experiences and Worldwide Perspective~Study Cases of SCR passengers Cars Integration*, 2006 FISITA World Automotive Congress, Yokohama, Japan, October 22-27, 2006.
- 16 Benjamin, S. F., Clarkson, R. J., Haimad, N., Girgis, N. S. (1996) - *An Experimental and Predictive Study of Flow in Axisymmetric Automotive Exhaust Catalyst Systems*, SAE961208, SAE International Spring Fuels and Lubricants Meeting and Exposition, Vol. 105, pp1008 - 1019, Dearborn, Michigan, May 6-8 1996
- 17 Benjamin, S. F., Roberts, C. A. (2007) - *The Porous Medium Approach Applied to CFD Modelling of SCR in an Automotive Exhaust with Injection of Urea Droplets*, IMechE Conference Internal Combustion Engines: Performance, Fuel Economy and Emissions, London.
- 18 Benjamin, S.F., Roberts, C.A. (2007) - *Three-Dimensional Modelling of NO<sub>x</sub> and Particulate Traps using CFD: A Porous Medium Approach*, Applied Mathematical Modelling, Vol. 31, Issue 11, pp2446 – 2460.
- 19 Beretta, A., Tronconi, E., Groppi, G. and Forzatti, P. (1998) - *Monolithic Catalysts for the Selective Reduction of NO<sub>x</sub> with NH<sub>3</sub> from Stationary Sources*, in: "Structured Catalysts and Reactors"; Editor: Cybulski, A., Dekker, M., New York, pp121-148.
- 20 BOC Special Gas Division (2005) - *Ammonia Safety Datasheet*.
- 21 Bosch, H. and Janssen, F. (1988) - *Catalysis Today* Vol. 2, Issue 4, pV.
- 22 Brandmier, T., Hosp, Schoppe and Ende, U. (1995) - *Model-based control of an SCR-catalyst for the NO<sub>x</sub>-reduction of diesel-engines*, IEEE Control Systems Magazine, Vol. 15, Issue 6, pp163-168, Pergamon, Ascona, Switzerland.
- 23 Breedlove, R. et al (2008) - *S,M,L,XL, Optimised Urea Injection*, CTI deNO<sub>x</sub> Forum, Detroit, December 2008.
- 24 Breen, J.P., Burch, R., Hardacre, C., Hill, C.J., Krutzsch, B., Bandl-Konrad, B., Jobson, E., Cider, L., Blakeman, P.G., Peace, L.J., Twigg, M.V., Preis, M. and Gottschling, M. (2007) - *An Investigation of the Thermal Stability and Sulphur Tolerance of Ag/[gamma]-Al<sub>2</sub>O<sub>3</sub> Catalysts for the SCR of NO<sub>x</sub> with Hydrocarbons and Hydrogen*, Applied Catalysis B: Environmental, Vol. 70, Issue1-4, pp36-44.
- 25 Byrne, J. W., Chen, J.M., Speronello, B.K. (1992) - *Selective Catalytic Reduction of NO<sub>x</sub> using Zeolitic Catalysts for High Temperature Applications*, Catalysis Today Vol.13, Issue 1, pp33-42.
- 26 Capek, L., Vradman, L., Sazama, P., Herskowitz, M., Wichterlova, B., Zukerman, R., Brosius, R. and Martens, J.A. (2007) - *Kinetic Experiments and Modeling of NO Oxidation and SCR of NO<sub>x</sub> with Decane over Cu- and Fe-MFI Catalysts*, Applied Catalysis B: Environmental, Vol. 70, Issue 1-4, pp53-57.
- 27 Carslaw, D.C. (2005) - *Evidence of an increasing NO<sub>2</sub>/NO<sub>x</sub> emissions ratio from road traffic Emissions*, Atmospheric Environment, Vol. 39, Issue 26, pp4793-4802.

- 28 Cavataio, G., Girard, J., (2007) - *Laboratory Testing of Urea-SCR Formulations to Meet Tier 2 Bin 5 Emissions*, SAE2007-01-1575, SAE 2007 World Congress, Detroit Michigan, USA, 16-19 April 2007.
- 29 Chaloulakou, A., Mavroidis, I. and Gavriil, I. (2008) - *Compliance with the Annual NO<sub>2</sub> Air Quality Standard in Athens: Required NO<sub>x</sub> Levels and Expected Health Implications*, Atmospheric Environment, Vol. 42, Issue 3, pp454-465.
- 30 Chandler, G. R. and Cooper, B.J.(2000) - *An Integrated SCR and Continuously Regenerating Trap System to meet Future NO<sub>x</sub> and PM Legislation*, SAE2000-01-0188, SAE 2000 World Congress, Detroit Michigan USA, 6-9 March 2000.
- 31 Chatterjee, D., Burkhardt, T., Bandl-Konrad, B., et al., (2005) - *Numerical Simulation of Ammonia SCR Catalytic Converters: Model Development and Application*, SAE2005-01-0965, SAE 2005 World Congress, Detroit Michigan, April 11-14, 2005.
- 32 Chatterjee, D., Burkhardt, T., Weibel, M., et al., (2007) - *Numerical Simulation of Zeolite- and V-Based SCR Catalytic Converters*, SAE 2007-01-1136, SAE 2007 World Congress, Detroit, Michigan, 16-19 April 2007.
- 33 Chen, J.P., Hausladen, M.C., Yang, R.T. (1995) - *Delaminated Fe<sub>2</sub>O<sub>3</sub>-Pillared Clay: Its Preparation, Characterization, and Activities for Selective Catalytic Reduction of NO by NH<sub>3</sub>*, Journal of Catalysis, Vol. 151, Issue 1, pp135-146.
- 34 Chi, J.N. and DaCosta, H.F.M.(2005) - *Modelling and Control of a Urea SCR Aftertreatment System*, SAE2005-01-0966, SAE 2005 World Congress, Detroit Michigan, 11-14 April 2005
- 35 Chmielarz, L., Kustrowski, P., Dziembaj, R., Cool, P. and Vansant, E.F. (2007) - *Selective Catalytic Reduction of NO with Ammonia over Porous Clay Heterostructures Modified with Copper and Iron Species*, Catalysis Today, Vol. 119, Issue 1-4, pp181-186.
- 36 Cho S.M. (1994) - *Properly Apply Selective Catalytic Reduction for NO<sub>x</sub> Removal*, Chemical Engineering Progress, pp39-45, January 1994.
- 37 Ciardelli, C., Nova, I., Tronconi, E., Chatterjee, D., Bandl-Konrad, B., Weibel, M. and Krutzsch, B. (2007) - *Reactivity of NO/NO<sub>2</sub>-NH<sub>3</sub> SCR System for Diesel Exhaust Aftertreatment: Identification of the Reaction Network as a Function of Temperature and NO<sub>2</sub> Feed Content*. Applied Catalysis B: Environmental, Vol. 70, Issue 1-4, pp80-90.
- 38 Ciardelli, C., Nova, I., Tronconi, E., Chatterjee, D., Burkhardt, T. and Weibel, M. (2007) - *NH<sub>3</sub> SCR of NO<sub>x</sub> for Diesel Exhausts Aftertreatment: Role of NO<sub>2</sub> in Catalytic Mechanism, Unsteady Kinetics and Monolith Converter Modelling*, Chemical Engineering Science, Vol. 62, Issue 18-20, pp5001-5006.
- 39 Ciardelli, C., Nova, I., Tronconi, E., Konrad, B., Chatterjee, D., Ecke, K. and Weibel, M.(2004) - *SCR-DeNO<sub>x</sub> for Diesel Engine Exhaust Aftertreatment: Unsteady-State Kinetic Study and Monolith Reactor Modelling*, Chemical Engineering Science, Vol. 59, Issue 22-23, pp5301-5309.
- 40 Clapp, L.J. and Jenkin, M.E. (2001) - *Analysis of the relationship between ambient levels of O<sub>3</sub>, NO<sub>2</sub> and NO as a function of NO<sub>x</sub> in the UK*, Atmospheric Environment, Vol. 35, Issue 36, pp6391-6405.
- 41 Colombo, M., Nova, I. and Tronconi, E. (2010) - *A Comparative Study of the NH<sub>3</sub>-SCR Reactions over a Cu-Zeolite and a Fe-Zeolite Catalyst*, Catalysis Today, Vol. 151. Issue 3-4, pp223-230.

- 42 Cooper, B.J., McDonnald, A.C., Walker, A.P. and Sanchez, M. (2003) - *The Development and On-Road Performance and Durability of the Four-Way Emission Control SCRT System*, US DOE, 9th Diesel Engine Emissions Reduction Conference (DEER), Newport, RI, August 2003, [http://www.eere.energy.gov/vehiclesandfuels/pdfs/deer\\_2003/session8/2003\\_deer\\_walker.pdf](http://www.eere.energy.gov/vehiclesandfuels/pdfs/deer_2003/session8/2003_deer_walker.pdf)
- 43 Costa, C.N. and Efstathiou, A.M. (2007) - *Low-Temperature H<sub>2</sub>-SCR of NO on a Novel Pt/MgO-CeO<sub>2</sub> Catalyst*, Applied Catalysis B: Environmental, Vol.72, Issue 3-4, pp240-252.
- 44 Craig, R., Robinson, G. and Hatfield, P. (1992) - *Performance of High Temperature SCR Catalyst System at Unocal's science and Technology Division*, pp423-426 (Published by ASME, New York, NY, USA, Houston, TX, USA,).
- 45 Devadas, M., Krocher, O., Elsener, M., et al. (2006) - *Influence of NO<sub>2</sub> on the SCR of NO with Ammonia over Fe-ZSM5*, Applied Catalysis B:Environmental, Vol. 67, pp187 – 196.
- 46 Devadas, M., Krocher, O., Elsener, M., Wokaun, A., Mitrikas, G., Soger, N., Pfeifer, M., Demel, Y. and Mussmann, L. (2007) - *Characterization and catalytic investigation of Fe-ZSM5 for urea-SCR*, Catalysis Today, Vol. 119, Issue 1-4, pp137-144.
- 47 Devadas, M., Krocher, O., Elsener, M., Wokaun, A., Soger, N., Pfeifer, M., Demel, Y. and Mussmann, L. (2006) - *Influence of NO<sub>2</sub> on the Selective Catalytic Reduction of NO with Ammonia over Fe-ZSM5*, Applied Catalysis B: Environmental, Vol. 67, Issue 3-4, pp187-196.
- 48 Bosch, R. (2005) - *Diesel Engine Management 4th edition*, GmbH 2005
- 49 DieselNet (2005) - *Selective Catalyst Reduction*, DieselNet Update, Available online <http://www.dieselnet.com>
- 50 DieselNet (2006) - *Tailpipe Emission Standards*, DieselNet Update, Available online, <http://www.dieselnet.com>
- 51 Dong, H., Shuai, S., Li, R., Wang, J., Shi, X. and He, H. (2008) - *Study of NO<sub>x</sub> Selective Catalytic Reduction by ethanol over Ag/Al<sub>2</sub>O<sub>3</sub> catalyst on a HD diesel engine*. Chemical Engineering Journal, Vol.135, Issue 3, pp195-201.
- 52 Dorado, F., Romero, R., Cruz, J., Garci'a, P.B., Romero, A. and Valverde, J.L. (2007) – *Selective Catalytic Reduction of NO by Propene in the Presence of Oxygen and Water over Catalysts Prepared by the Modified Sol-Gel Method*, Catalysis Communications, Vol. 8, Issue 4, pp736-740.
- 53 Dzwigaj, S., Janas, J., Machej, T. and Che, M. (2007) - *Selective catalytic reduction of NO by alcohols on Co- and Fe-Si[beta] catalysts*, Catalysis Today, Vol. 119, Issue 1-4, pp133-136.
- 54 Eberhard, H., et al., (2006) - *The Time Behaviour of Surface Applied Fluorine Inducing the Formation of an Alumina Scale on Gamma-TiAl during Oxidation at 900 °C in Air*, Intermetallics, October-November 2006, Vol. 14, Issues 10-11, , pp1136-1142.
- 55 Eberhard, J., J. Kreutmair, (1994) - *Verfahren und Vorrichtung zur selectiven katalytischen Reduktion von NO<sub>x</sub> in sauerstoffhaltigen Gasen, (Translated- Method and Apparatus for Selective Catalytic Reduction of NO<sub>x</sub> in Oxygen-Containing Gases)*, European Patent, EP 0 615 777 A1
- 56 Elmoe, T. D., Sorenson, R.Z., Quaade, U., Christensen, C.H., Norskov J.K., Johannessen, T., (2006) - *A high Density Ammonia Storage/delivery System based on Mg(NH<sub>3</sub>)<sub>6</sub>Cl<sub>2</sub> for SCR-DeNO<sub>x</sub> in vehicles*, Chemical Engineering Science, Vol. 61, pp2618-2625.
- 57 EUBusiness Magazine (2006) - *EU to introduce legislation as car makers fail on emission targets*, November 2006, Available online, <http://www.eubusiness.com/Environ/>

- 58 European Commission Directive 1999/96/EC-B1(2005) –*Standard for Exhaust Emission, Heavy Duty vehicle with gross vehicle weight exceeding 3.5 tonnes*, for Motor Vehicle Registered on or after 1<sup>st</sup> October 2006.
- 59 European Commission Directive 91/542/EEC/Stage II –*Standard for Exhaust Emission for Heavy Duty Vehicle with Gross Vehicle Weight Exceeding 3.5 tonnes*, for Diesel Driven Motor Vehicle registered on or after 1<sup>st</sup> January 2001 but before 1<sup>st</sup> October 2006.
- 60 European Commission Directive 96/69/EC - *Standard for exhaust emission for Passenger car and Light commercial vehicle with gross vehicle weight not exceeding 3.5 tonnes*, For diesel driven motor vehicles registered on or after 1<sup>st</sup> January 2001 but before 1<sup>st</sup> October 2006.
- 61 European Commission Directive 98/69/EC-B(2005) - *Standard for exhaust emission Passenger Car and Light commercial vehicle with gross vehicle weight not exceeding 3.5 tonnes*, For diesel driven motor vehicles registered on or after 1<sup>st</sup> October 2006.
- 62 European Parliament Text (2005) - *Winning the Battle Against Global Climate Change*, 16 November 2005, Strasbourg, France, available online, <http://www.europarl.europa.eu>
- 63 Fang, H.L. and DaCosta H.F.M. (2003) - *Urea Thermolysis and NO<sub>x</sub> Reduction with and without SCR Catalysts*, Applied Catalysis B. Environmental, Vol. 46, pp17-34
- 64 Farias, F. and ApSimon, H. (2006) - *Relative contributions from traffic and aircraft NO<sub>x</sub> emissions to exposure in West London*, Environmental Modelling & Software, Vol. 21, Issue 4, pp477-485.
- 65 Ferreira, A.P., Capela, S., Da Costa, P., Henriques, C., Ribeiro, M.F. and Ribeiro, F.R. (2007) – *CH<sub>4</sub>-SCR of NO over Co and Pd ferrierite catalysts: Effect of preparation on catalytic performance*, Catalysis Today, Vol. 119, Issue 1-4, pp156-165.
- 66 Fischer, S., Hofmann, L., et al. (2004) - *SCR~A Technology for Global Emissions Control of Diesel Engines*, 2004 FISITA World Automotive Congress, Barcelona, Spain.23-27 May 2004
- 67 Fissore, D., Penciu, O.M. and Barresi, A.A. (2006) - *SCR of NO<sub>x</sub> in Loop Reactors: Asymptotic Model and Bifurcational Analysis*, Chemical Engineering Journal, Vol. 122, Issue 3, pp175-182.
- 68 Fissore, D., Pisano, R. and Barresi, A.A. (2007) - *Observer Design for the Selective Catalytic Reduction of NO<sub>x</sub> in a Loop Reactor*, Chemical Engineering Journal, Vol.128, Issue 2-3, pp181-189.
- 69 Focus on Catalysis (2006) - *AdBlue distributors in Europe*, Issue 2, p3.
- 70 Focus on Catalysts (2005) - *Blueprint for AdBlue*, Issue 8, p2.
- 71 Forzatti, P., Lietti, L., Nova, I. and Tronconi, E. (2010) - *Diesel NO<sub>x</sub> Aftertreatment Catalytic Technologies: Analogies in LNT and SCR Catalytic Chemistry*, Catalysis Today, Vol. 151, Issue 3-4, 19 Jun 2010, pp202-211.
- 72 Gaffney, J.S. and Marley, N.A. (2009) - *The Impacts of Combustion Emissions on Air Quality and Climate - from Coal to Biofuels and Beyond*, Atmospheric Environment, Vol. 43, Issue 1, pp23-36.
- 73 Garcia Cortes, J.M., Illan Gomez, M.J. and Salinas Martinez de Lecea, C. (2007) - *The Selective Reduction of NO<sub>x</sub> with Propene on Pt-beta Catalyst: A Transient Study*, Applied Catalysis B: Environmental, vol. 74 Issue 3-4, pp313-323.
- 74 Garcia-Bordeje, E., Pinilla, J.L., Lazaro, M.J. and Moliner, R. (2006) - *NH<sub>3</sub>-SCR of NO at Low Temperatures over Sulphated Vanadia on Carbon-Coated Monoliths: Effect of H<sub>2</sub>O and SO<sub>2</sub> Traces in the Gas Feed*, Applied Catalysis B: Environmental, Vol. 66, Issue 3-4, pp281-287.

- 75 Gieshoff, J., A. Schäfer-Sindlinger, et al. (2000), *Improved SCR Systems for Heavy-Duty Applications*, SAE2000-01-0189, SAE 2000 World Congress, Detroit, Michigan, 6-9 March-2000.
- 76 Gieshoff, J., M. Pfeifer, et al. (2001) - *Advanced Urea SCR Catalysts for Automotive Applications*, SAE2001-01-0514, SAE 2001 World Congress, March 2001, Detroit, MI, Session: Diesel Exhaust Emissions Control (Part C&D), March 2001.
- 77 Giovanni, C., Girard, J., Patterson, J.E., Montreuil, C., Cheng, Y. and Lambert, C.K. (2007) – *Laboratory Testing of Urea SCR Formulations to Meet Tier 2 Bin 5 Emission*, SAE2007-01-1575, SAE 2007 World Congress, Detroit, Michigan, April 14-19 2007.
- 78 Girard, J., R. Snow, et al. (2007) - *The Influence of Ammonia to NOx Ratio on SCR Performance*, SAE World Congress & Exhibition, Detroit, Michigan, April 16-19, 2007.
- 79 Gorbach, A (2009) - *Urea Preparation in Exhaust System of Commercial Vehicles*, CTI Emission Control Forum, Nuertigen, January 2009.
- 80 Grossale, A., Nova, I. and Tronconi, E. (2009) - *Ammonia Blocking of the "Fast SCR" Reactivity over a Commercial Fe-Zeolite Catalyst for Diesel Exhaust Aftertreatment*, Journal of Catalysis, Vol. 265, Issue 2, pp141-147.
- 81 Grossale, A., Nova, I. and Tronconi, E. (2008) - *Study of a Fe-Zeolite-based System as NH<sub>3</sub>-SCR Catalyst for Diesel Exhaust Aftertreatment*, Catalysis Today, Vol. 136, Issue 1-2, pp18-27.
- 82 Grossale, A., Nova, I., Tronconi, E., Chatterjee, D. and Weibel, M. (2008) - *The chemistry of the NO/NO<sub>2</sub>-NH<sub>3</sub> "fast" SCR reaction over Fe-ZSM5 Investigated by Transient Reaction Analysis*, Journal of Catalysis, Vol. 256, Issue 2, pp312-322.
- 83 Guo G., Warner, J., Cavataio, G., Dobson, D., Badillo, E. and Lambert, C. (2010) - *The Development of Advanced Urea-SCR Systems for Tier 2 Bin 5 and Beyond Diesel Vehicles*, SAE2010-01-1183, SAE 2010 World Congress, Detroit Michigan, April 13-15, 2010.
- 84 Gurupatham, A., He, Y. (2008) - *Architecture Design and Analysis of Diesel Engine Exhaust Aftertreatment System and comparative Study with Close Couple DOC-DPF System*, SAE2008-01-1756, SAE International Powertrains, Fuels and Lubricants Congress Shanghai, China, June 23-25, 2008.
- 85 Guyon, M., Blanche, P., et al., (2000) - *NOx-Trap System Development and Characterization for Diesel Engines Emission Control*, SAE2000-01-2910, SAE International Fall Fuels and Lubricants Meeting and Exhibition, Baltimore, Maryland, October 16-19, 2000.
- 86 Hamada, I., Kato, Y., Imada, N., Kikkawa, H. and Yamada, A. (2005) - *A Unique Titania-Based SCR NOx Catalyst for Diesel Exhaust Emission Control*, SAE2005-01-1859, SAE World Congress, Detroit, Michigan, April 11-14, 2005.
- 87 Hammerle, R., (2003) - *Urea SCR and DPF System for Diesel Sport Utility Vehicle Meeting Tier II Bin 5*, US DOE, 9th Diesel Engine Emissions Reduction Conference (DEER), Newport, Rhode Island, August 2003, [http://www.eere.energy.gov/vehiclesandfuels/pdfs/deer\\_2003/session10/2003\\_deer\\_hammerle.pdf](http://www.eere.energy.gov/vehiclesandfuels/pdfs/deer_2003/session10/2003_deer_hammerle.pdf)
- 88 Heck, R. M. and Farrauto R. J. (2003) - *Catalytic Air Pollution Control: Commercial Technology*, Focus on Catalysts, Vol. 2003, Issue 9, p8.
- 89 Heck, R. M., Farrauto R. J., Gulati, S.T. (2009) - *Catalytic Air Pollution Control: Commercial Technology*, 3<sup>rd</sup> Edition John Wiley March 2009.

- 90 Heck, R.M., et al., (1994) - *Operating Characteristics and Commercial Operating Experience with High Temperature SCR NO<sub>x</sub> Catalyst*, Environmental Progress, Vol.13, issue 4, pp 221-225
- 91 Hevia, M.A.G., Ordonez, S. and Diez, F.V. (2007) - *Effect of the Catalyst Properties on the Performance of a Reverse Flow Reactor for Methane Combustion in Lean Mixtures*, Chemical Engineering Journal, Vol. 129, Issue1-3, pp1-10.
- 92 Hirata, K., N., Masaki, N., Ueno, H. and Akagawa, H. (2005) - *Development of Urea-SCR System for Heavy-Duty Commercial Vehicles*, SAE2005-01-1860, SAE 2005 World Congress & Exhibition, Detroit, Michigan, April 11-14, 2005.
- 93 Hoffman, J.(1996) - *Process for the Selective Catalytic Reduction of Nitrogen Oxides*, International Patent Application, WO 96/06674 (Nako)
- 94 Hunnekes, E.V.,and Patchett, J., (2006) - *Ammonia oxidation catalysts for mobile SCR Systems*, SAE2006-01-0640, SAE 2006 World Congress, Detroit Michigan, April 3-6, 2006.
- 95 Irfan, M.F., Goo, J.H., Kim, S.D. and Hong, S.C. (2007) - *Effect of CO on NO Oxidation Over Platinum based Catalysts for Hybrid Fast SCR Process*, Chemosphere, Vol. 66, Issue 1, pp54-59.
- 96 JAMA-Japan Automobile Manufacturers Association Newsletter (2006), vol. 18, February 2006, available online, <http://www.jama-english.jp/asis/news/vol18.pdf>
- 97 Janssen, J.J., (1997) - *Environmental Catalysis - Stationary Sources*, in: Handbook of Heterogeneous Catalysis, G. Ertl et al. (editors), Wiley 1997, pp1636-1644
- 98 JARI, (2004) - *Advanced Clean-Energy Vehicles (ACEVs)*, Project Summary, Japan Automobile Research Institute.
- 99 Johannessen, T., Schmidt, H., Svagin, J. et al. (2008) - *Ammonia Storage and Delivery Systems for Automotive NO<sub>x</sub> Aftertreatment*, SAE2008-01-1027, SAE 2008 World Congress, Detroit, Michigan, April 14-17, 2008.
- 100 Johansson, C., Burman, L. and Forsberg, B. (2009) - *The Effects of Congestions Tax on Air Quality and Health*, Atmospheric Environment, Vol. 43, Issue 31, pp4843-4854.
- 101 Johnson, T. V., (2006) - *Diesel Emission Control in Review*, SAE2006-01-0030, 2006 World Congress, Detroit, Michigan, April 3-6, 2006.
- 102 Johnson, T. V., (2007) - *Diesel Emission Control in Review*, SAE2007-01-0233, 2007 World Congress, Detroit, Michigan, April 16-19, 2007.
- 103 Johnson, T. V., (2008) - *Diesel Emission Control in Review*, SAE2008-01-0069, 2008 World Congress, Detroit, Michigan, April 14-17, 2008.
- 104 Johnson, T. V., (2009) - *Diesel Emission Control in Review*, SAE2009-01-0121, 2009 World Congress, Detroit, Michigan, April 20-23, 2009.
- 105 Johnson, T. V., (2010) - *Review of Diesel Emission and Control*, SAE 2010-01-0301, 2010 World Congress, Detroit, Michigan, April 13-15, 2010.
- 106 Jossen, R., Heine, M.C., Pratsinis, S.E., Augustine, S.M. and Akhtar, M.K. (2007) - *Thermal Stability and Catalytic Activity of Flame-Made Silica-Vanadia-Tungsten Oxide-Titania*, Applied Catalysis B: Environmental, Vol. 69, Issue 3-4, pp181-188.
- 107 Joubert, E., Courtois, X., Marecot, P., Canaff, C. and Duprez, D. (2006) - *The Chemistry of DeNO<sub>x</sub> Reactions over Pt/Al<sub>2</sub>O<sub>3</sub>: The Oxime Route to N<sub>2</sub> or N<sub>2</sub>O*, Journal of Catalysis, Vol. 243, Issue 2, pp252-262.



- 108 Jung, S.M., Demoulin, O. and Grange, P. (2005) - *The Study of a Synergetic Effect over a H-ZSM-5/V<sub>2</sub>O<sub>5</sub> Hybrid Catalyst on SCR Reaction*, Journal of Molecular Catalysis A: Chemical, Vol. 236, Issue 1-2, pp94-98.
- 109 Kang, M., Kim, D.J., Park, E.D., Kim, J.M., Yie, J.E., Kim, S.H., Hope-Weeks, L. and Eyring, E.M. (2006) - *Two-Stage Catalyst System for Selective Catalytic Reduction of NO<sub>x</sub> by NH<sub>3</sub> at Low Temperatures*, Applied Catalysis B: Environmental, Vol. 68, Issue 1-2, pp21-27.
- 110 Karvosenoja, N. and Johansson, M. (2003) - *Cost Curve Analysis for SO<sub>2</sub> and NO<sub>x</sub> Emission Control in Finland*, Environmental Science & Policy, Vol. 6, Issue 4, pp329-340.
- 111 Kelly, J.F., Stanculec, M., Charland, J.P. (2006) - *Evaluation of Amines for the Selective Catalyst Reduction (SCR) of NO<sub>x</sub> from Diesel Engine Exhaust*, Fuel, September 2006, Vol.85, Issue 12-13, pp1772-1780.
- 112 Keuken, M.P., Jonkers, S., Wilmkink, I.R. and Wesseling, J.(2010) - *Reduced NO<sub>x</sub> and PM<sub>10</sub> emissions on urban motorways in The Netherlands by 80 km/h speed management*, Science of The Total Environment, Vol. 408, Issue 12, pp2517-2526.
- 113 Kim, Y.W. and Nieuwstadt, M.V. (2006) - *Threshold Monitoring of Urea SCR System*, SAE2006-01-3548, Commercial Vehicle Engineering Congress and Exhibition, Chicago, Illinois, Oct 31-Nov 02, 2006.
- 114 Knox E. G. (2008) - *Atmospheric Pollutants and Mortalities in English Local Authority Areas*, Journal of Epidemiol Community Health, Vol. 62, Issue 5, pp442-447.
- 115 Koebel, M., Elsener, M., and Kleemann, M. (2000) - *Urea-SCR: A Promising Technique to Reduce NO<sub>x</sub> Emissions from Automotive Diesel Engines*, Catalysis Today, Vol. 59, pp335-345.
- 116 Koebel, M., Elsener, M., et al.(2001) - *Recent Advances in the Development of Urea-SCR for Automotive Applications*, SAE 2001-01-3625, SAE International Fall Fuels and Lubricants Meeting and Exhibition, San Antonio Texas, September 24-27, 2001.
- 117 Koebel, M., Elsener, M. and Madia, G. (2001) - *Reaction Pathways in the Selective Catalytic Reduction Process with NO and NO<sub>2</sub> at Low Temperature*, Industrial & Engineering Chemistry Research, Vol. 40, Issue 1, pp52 -59.
- 118 Koebel, M., Madia, G., et al., (2002) - *Selective Catalytic Reduction of NO and NO<sub>2</sub> at Low Temperatures*, Catalysis Today, 15 April 2002, Vol. 73, Issues 3-4, pp239-247.
- 119 Komatsu, T., Tomokuni, K. and Yamada, I. (2006) - *Outstanding low temperature HC-SCR of NO<sub>x</sub> over Platinum-group Catalysts Supported on Mesoporous Materials Expecting Diesel-Auto Emission Regulation*, Catalysis Today, Vol. 116, Issue 2, pp244-249.
- 120 Konova, P., Arve, K., Klingstedt, F., Nikolov, P., Naydenov, A., Kumar, N. and Murzin, D.Y. (2007) - *A combination of Ag/alumina and Ag modified ZSM-5 to remove NO<sub>x</sub> and CO during lean conditions*, Applied Catalysis B: Environmental, Vol.70, Issue 1-4, pp138-145.
- 121 Konstandopoulos, A., Kostoglou, M.,Skaperdas, E., Papaioannou, E., Zarvalis, D., and Kladopoulou, E. (2000) - *Fundamental Studies of Diesel particulate filter: Transient loading, Regeneration and Aging*, SAE2000-01-1016, SAE 200 World Congress, Detroit, Michigan, March 6-9, 2000.
- 122 Kotsifa, A., Kondarides, D.I. and Verykios, X.E. (2007) - *Comparative Study of the Chemisorptive and Catalytic Properties of Supported Pt Catalysts Related to the Selective Catalytic Reduction of NO by Propylene*, Applied Catalysis B: Environmental, Vol. 72, Issue 1-2, pp136-148.

- 123 Kousoulidou, M., Ntziachristos, L., Mellios, G. and Samaras, Z. (2008) - *Road-Transport Emission Projections to 2020 in European Urban Environments*, Atmospheric Environment, Vol. 42, Issue 32, pp7465-7475.
- 124 Krishnamurthy, M., Carder, D.K., Thompson, G. and Gautam, M. (2007) - *Cost of Lower NO<sub>x</sub> Emissions: Increased CO<sub>2</sub> Emissions from Heavy-Duty Diesel Engines*, Atmospheric Environment, Vol. 41, Issue 3, pp666-675.
- 125 Krocher, O., Devadas, M., Elsener, M., Wokaun, A., Soger, N., Pfeifer, M., Demel, Y. and Mussmann, L. (2006) - *Investigation of the Selective Catalytic Reduction of NO by NH<sub>3</sub> on Fe-ZSM5 Monolith Catalysts*, Applied Catalysis B: Environmental, Vol.66, Issue 3-4, pp208-216.
- 126 Lambert, C., Cavataio, G., et al. (2006) - *Urea SCR and DPF System for Tier 2 Diesel Light-Duty Trucks*, Department of Energy (DOE) Presentation, Diesel Exhaust Aftertreatment Ford Research & Advance Engineering.
- 127 Lambert, C., Hammerle, R., McGill, R. Khair, M., Sharp, C.(2004) - *Technical Advantages of Urea SCR for Light Duty and Heavy Duty Diesel Vehicle Applications*, SAE2004-01-1292, SAE 2004 World Congress and Exhibition, Detroit, Michigan, March 8-11, 2004.
- 128 Larsson, A.-C., Einvall, J., Andersson, A. and Sanati, M. (2006) - *Targeting by Comparison with Laboratory Experiments the SCR Catalyst Deactivation Process by Potassium and Zinc Salts in a Large-Scale Biomass Combustion Boiler*, Energy and Fuels, Vol. 20, Issue 4, pp1398-1405.
- 129 Lazaro, M.J., Galvez, M.E., Ruiz, C., Juan, R. and Moliner, R. (2006) - *Vanadium Loaded Carbon-Based Catalysts for the Reduction of Nitric Oxide*, Applied Catalysis B: Environmental, Vol. 68, Issue 3-4, pp130-138.
- 130 Lepperhoff, G. and J. Schommers, (1988) - *Verhalten von SCR-Katalysatoren im Dieselmotorischen Abgas*", MTZ Motortechnische Zeitschrift (*English- Behavior of SCR Catalysts in Diesel Exhaust*, MTZ Motor Technical Journal), Vol. 49, p1.
- 131 Liu, Z., Millington, P.J., Bailie, J.E., Rajaram, R.R. and Anderson, J.A.(2007) - *A Comparative Study of the role of the support on the behaviour of iron based ammonia SCR catalysts*, Microporous and Mesoporous Materials, 23 August 2007, Vol.104, Issues 1-3, pp159-170.
- 132 Lonyi, F., Valyon, J., Gutierrez, L., Ulla, M.A. and Lombardo, E.A. (2007) - *The SCR of NO with CH<sub>4</sub> over Co-, Co,Pt-, and H-Mordenite Catalysts*, Applied Catalysis B: Environmental, Vol.73, Issue 1-2, pp1-10.
- 133 Madia, G., Elsener, M., et al.,(2002) - *Thermal Stability of Vanadia-Tungsta-Titania Catalysts in the SCR Process*, Applied Catalysis B: Environmental, 28 November 2002, Vol. 39, Issue 2, pp181-190
- 134 Magdi, K., Dale, L.M. (1999) - *Performance Evaluation of Advance Emission Control Technologies for Diesel Heavy Duty Engines*, SAE 1999-01-3564, SAE International Fall Fuel and Lubricant Meeting and Exhibition, Ontario, Canada.
- 135 Martin, J.A., Yates, M., Avila, P., Suarez, S. and Blanco, J. (2007) - *Nitrous Oxide Formation in Low Temperature Selective Catalytic Reduction of Nitrogen Oxides with V<sub>2</sub>O<sub>5</sub>/TiO<sub>2</sub> catalysts*, Applied Catalysis B: Environmental, Vol.70, Issue 1-4, pp330-334.
- 136 MECA white paper (2005) - *Diesel Particulate Filter Maintenance: Current Practices and Experience*, Available online, <http://www.meca.org>.
- 137 MECA white paper (2007) - *Emission Control Technologies for Diesel-Powered Vehicles*, December 2007, Available online, <http://www.meca.org>.

- 138 Ministry of the Environment Government of Japan, (2007) - *Air Pollution Control Law*, Available online, <http://www.env.go.jp/en/laws/air/air/index.html>
- 139 Mironyuk, T.V. and Orlyk, S.N. (2007) - *Effect of Rhodium on the Properties of Bifunctional  $MxOy/ZrO_2$  Catalysts in the Reduction of Nitrogen Oxides by Hydrocarbons*, Applied Catalysis B: Environmental, Vol. 70, Issue1-4, pp58-64.
- 140 Mutin, P.H., Popa, A.F., Vioux, A., Delahay, G. and Coq, B.( 2006) - *Nonhydrolytic Vanadia-Titania Xerogels: Synthesis, Characterization, and Behavior in the Selective Catalytic Reduction of NO by  $NH_3$* , Applied Catalysis B: Environmental, Vol. 69, Issue 1-2, pp49-57.
- 141 Nacken, M., Heidenreich, S., Hackel, M. and Schaub, G. (2007) - *Catalytic Activation of Ceramic Filter Elements for Combined Particle Separation, NO<sub>x</sub> removal and VOC total Oxidation*, Applied Catalysis B: Environmental, Vol.70, Issue1-4, pp370-376.
- 142 Nakayama, R., T. Watanabe, et al. (2006) - *Control Strategy for Urea-SCR System in Single Step Load Transition*, Powertrain and Fluid Systems Conference and Exhibition, Toronto, Ontario, Canada. Oct 16-19, 2006.
- 143 Narayanaswamy, K., He, Y. (2008) - *Modelling of Copper-Zeolite and Iron-Zeolite SCR Catalysts at Steady State and Transient Conditions*, SAE 2008-01-0615, SAE 2008 World Congress, Detroit, Michigan, April 14-17, 2008.
- 144 Naser, T.M., Kanda, I., Ohara, T., Sakamoto, K., Kobayashi, S., Nitta, H. and Nataami, T. (2009) - *Analysis of traffic-related NO<sub>x</sub> and EC concentrations at various distances from major roads in Japan*, Atmospheric Environment, Vol.43, Issue 15, pp2379-2390.
- 145 Nejar, N. and Illan-Gomez, M.J. (2007) - *Potassium-Copper and Potassium-Cobalt Catalysts supported on Alumina for Simultaneous NO<sub>x</sub> and Soot Removal from Simulated Diesel Engine Exhaust*, Applied Catalysis B: Environmental, Vol. 70, Issue 1-4, pp261-268.
- 146 Nobukawa, T., Sugawara, K., Okumura, K., Tomishige, K. and Kunitomi, K. (2007) - *Role of Active Oxygen Transients in Selective Catalytic Reduction of  $N_2O$  with  $CH_4$  over Fe-Zeolite Catalysts*, Applied Catalysis B: Environmental, Vol. 70, Issue 1-4, pp342-352.
- 147 Nojima, S., Iida, K., Kobayashi, N. and Naito, O. (2001) - *Development of NO<sub>x</sub> Removal SCR Catalyst for Low  $SO_2$  Oxidation*, Technical Review - Mitsubishi Heavy Industries, Vol.38, Issue 2, pp87-91.
- 148 Nova, I., Ciardelli, C., Tronconi, E., Chatterjee, D. and Bandl-Konrad, B. (2006) -  *$NH_3$ -SCR of NO over a V-based Catalyst: Low-T Redox Kinetics with  $NH_3$  Inhibition*, AIChE Journal, Vol.52, Issue 9, pp3222-3233.
- 149 Nova, I., Ciardelli, C., Tronconi, E., Chatterjee, D. and Bandl-Konrad, B. (2006) -  *$NH_3$ -NO/NO<sub>2</sub> Chemistry over V-based Catalysts and its Role in the Mechanism of the Fast SCR Reaction*, Catalysis Today, Vol.114, Issue 1, pp3-12.
- 150 Nova, I., Lietti, L., Tronconi, E. and Forzatti, P. (2000) - *Dynamics of SCR reaction over a  $TiO_2$ -Supported Vanadia-Tungsta Commercial Catalyst*, Catalysis Today, Vol. 60, Issue 1, pp73-82.
- 151 Nova, I., Lietti, L., Tronconi, E. and Forzatti, P. (2001) - *Transient Response Method Applied to the Kinetic Analysis of the DeNO<sub>x</sub>-SCR Reaction*, Chemical Engineering Science, Vol. 56, Issue 4, pp1229-1237.
- 152 Nova, I., Lietti, L., Tronconi, E., Forzatti, P., Avelino Corma, F.V.M.S.M. and José Luis, G.F.(2000) - *Concentration Programmed Adsorption-Desorption/Surface Reaction Study of the SCR-DeNO<sub>x</sub> Reaction*, Studies in Surface Science and Catalysis, pp623-628.

- 153 OEHHA, (2005) - *Chemicals Known To The State To Cause Cancer Or Reproductive Toxicity*, California Environmental Protection Agency, Office of Environmental Health Hazard Assessment (OEHHA), Safe Drinking Water and Toxic Enforcement Act of 1986 (Proposition 65), Updated May 27, 2005.
- 154 Olsson, L., Sjövall, H. and Blint, R.J. (2008) - *A Kinetic Model for Ammonia Selective Catalytic Reduction over Cu-ZSM-5*, Applied Catalysis B: Environmental, Vol. 81, Issue 3-4, pp203-217.
- 155 Parche, M., (2006) - *Euro V and VI Global Emission Strategies Conference*, Amsterdam, June 2006.
- 156 Pieterse, J.A.Z. and Booneveld, S. (2007) - *Catalytic reduction of NO<sub>x</sub> with H<sub>2</sub>/CO/CH<sub>4</sub> over PdMOR Catalysts*, Applied Catalysis B: Environmental, Vol.73, Issue 3-4, pp327-335.
- 157 Pieterse, J.A.Z., Top, H., Vollink, F., Hoving, K. and van den Brink, R.W. (2006) - *Selective Catalytic Reduction of NO<sub>x</sub> in Real Exhaust Gas of Gas Engines Using Unburned Gas: Catalyst Deactivation and Advances Toward Long-Term Stability*, Chemical Engineering Journal, Vol.120, Issue 1-2, pp17-23.
- 158 Qi, G. and Yang, R.T. (2005) - *Low-Temperature SCR of NO with NH<sub>3</sub> over Noble Metal Promoted Fe-ZSM-5 Catalysts*, Catalysis Letters, Vol. 100, Issue 3-4, pp 243-246.
- 159 Rahkamaa-Tolonen, K., Manula, T., Lomma, M., Huuhtanen, M., Keiski, R.L.(2005) - *The Effect of NO<sub>2</sub> on the Activity of Fresh and Aged Zeolite Catalysts in the NH<sub>3</sub>-SCR Reaction*, Catalysis Today, Vol. 100, pp217-222.
- 160 Reuters News Services (2007) - *European Carmakers Reduced Carbon Dioxide (CO<sub>2</sub>) Emissions from New Cars by only 0.2 percent in 2006, Far Off an Agreed Goal*, Brussels September 2007, Available online, <http://www.planetark.com/dailynewsstory.cfm/newsid/44167/story.htm>
- 161 Schaber, P.M., Colson, J., Higgins, S., Thielen, D., Anspach, B., and Brauer, J.,(2004) - *Thermal Decomposition (Pyrolysis) of Urea in an Open Reaction Vessel*, Thermochemica Acta 424: pp131-142.
- 162 Schmeig, S.J., Lee, J-H.(2005) - *Evaluation of Supplier Catalyst Formulations for the SCR of NO<sub>x</sub> with Ammonia*, SAE 2005-01-3881, Powertrain and Fluid Systems Conference and Exhibition San Antonio, Texas, October 24-27, 2005.
- 163 Shah, S.D., Mauti, A., Richert, J.F.O., Loos, M.J., Chase, R.E. (2007) - *Measuring NO<sub>x</sub> in the Presence of Ammonia*, SAE2007-01-0331, SAE 2007 World Congress, Detroit, Michigan, 2007.
- 164 Shibata, J., Hashimoto, M., Shimizu, K.-I., Yoshida, H., Hattori, T. and Satsuma, A. (2004) - *Factors Controlling Activity and Selectivity for SCR of NO by Hydrogen over Supported Platinum Catalysts*, Journal of Physical Chemistry B, Vol.108, Issue 47, pp18327-18335.
- 165 Snyder, J. D., Subramaniam, B.(1998) - *Numerical Simulation of a Reverse flow NO<sub>x</sub>-SCR Reactor with Side Stream Ammonia Addition*, Chem Eng Sci Vol. 53, Issue 4, pp727-734.
- 166 Song, Q. and G. Zhu, (2002) - *Model-based, Closed-Loop Control of Urea SCR Exhaust Aftertreatment System for Diesel Engine*, SAE2002-01-0287, SAE 2002 World Congress. March 4-7, 2007.
- 167 Spurk (2000) US EPA-United States, Environmental Protection Agency, - *Federal and California Exhaust and Evaporative Emission Standards for Light-Duty Vehicles and Light-Duty Trucks*, Document No: EPA420-B-00-001, February 2000.

- 168 Spurk, D.C., Pfeifer, M., Gieshoff, J, Lox, E. (2001) - *Ein SCR Katalysator auch fuer den Einsatz im PKW*, 10<sup>th</sup> Aachener Kolloquium Fazu.(translated)- *A SCR Catalyst for the use in Passenger Cars*, 10<sup>th</sup> Aachen Colloquium on Automobile and Engine Technology 2001.
- 169 Spurk, P.C., M. Pfeifer, et al., (2007) – *Challenges for the Future Diesel Engines Exhaust Gas Aftertreatment System*, SAE2007-01-0040, Fuels & Emission Conference, Cape Town, South Africa, January 23-25, 2007
- 170 Sullivan, J.A. and Keane, O. (2007) - *A Combination of NO<sub>x</sub> Trapping Materials and Urea-SCR Catalysts for use in the Removal of NO<sub>x</sub> from Mobile Diesel Engines*, Applied Catalysis B: Environmental, Vol. 70, Issue 1-4, pp205-214.
- 171 Sullivan, J.A., Doherty, J. A., (2005) - *NH<sub>3</sub> and Urea in the Selective Catalytic Reduction of NO<sub>x</sub> over Oxide-Supported Copper Catalysts*, Applied Catalysis B: Environmental, 10 February 2005, Vol. 55, Issue 3, pp185-194.
- 172 Summers, J.C., Van Houtte, S. and Psaras, D. (1996) - *Simultaneous control of particulate and NO<sub>x</sub> Emissions from Diesel Engines*, Applied Catalysis B: Environmental, Vol.10, Issue 1-3, pp139-156.
- 173 Suzuki, H. and Ishii, H. (2006) - *Emission Characteristics of a Urea SCR System Under Catalyst Activated and De-activated Conditions*, Review of Automotive Engineering, Vol. 27, Issue 2, pp223-228.
- 174 Takada, K., Kusaka, J., Daisho, Y. (2007) - *Empirical and Numerical Study of the Improvements in NO<sub>x</sub> Reduction by a Urea-SCR System Attainable by Controlling the Relative Proportions of NO and NO<sub>2</sub>*, Review of Automotive Engineering, JSAE Technical paper 4-28-1-41.
- 175 Tamaldin, N., Roberts, C.A., Benjamin S.F.(2010) - *Experimental Study of SCR in a Light Duty Diesel Exhaust to Provide Data of a CFD Model Using the Porous Medium Approach*, SAE 2010-01-1177, SAE 2010 World Congress, Detroit, Michigan, April 13-15, 2010.
- 176 Tang, X., Hao, J., Xu, W. and Li, J. (2007) - *Low Temperature Selective Catalytic Reduction of NO<sub>x</sub> with NH<sub>3</sub> over Amorphous MnO<sub>x</sub> Catalysts Prepared by Three Methods*, Catalysis Communications, Vol. 8, Issue 3, pp329-334.
- 177 Tatur, M. (2009) - *Solid SCR Demonstration Truck Application*, presentation at US Department of Energy Directions in Engine Efficiency and Emissions Research (DEER) conference, Dearborn, Michigan, August 2009.
- 178 Technical Report of MECA-Manufacturers of Emissions Controls Association,(1999) - *The Effect of Sulfur in Diesel Fuel on Catalyst*, Emission Control Technology.
- 179 Tennison, P., Lambert, C., Levin, M.(2004) - *NO<sub>x</sub> control development with urea SCR on a Diesel Passenger Car*,SAE 2004-01-1291, SAE 2004 World Congress and Exhibition, Detroit Michigan, March 8-11, 2004
- 180 Theis, J.R. (2009) - *SCR Catalyst Systems Optimized for Light-off and Steady State Performance*, SAE2009-01-0901, SAE 2009 World Congress, Detroit, Michigan, April 20-23, 2009.
- 181 Theis, J.R. and Gulari, E. Estimating the temperatures of the NO<sub>x</sub> storage sites in a lean NO<sub>x</sub> trap during oxidation reactions. Applied Catalysis B: Environmental, In Press, Corrected Proof, 300.

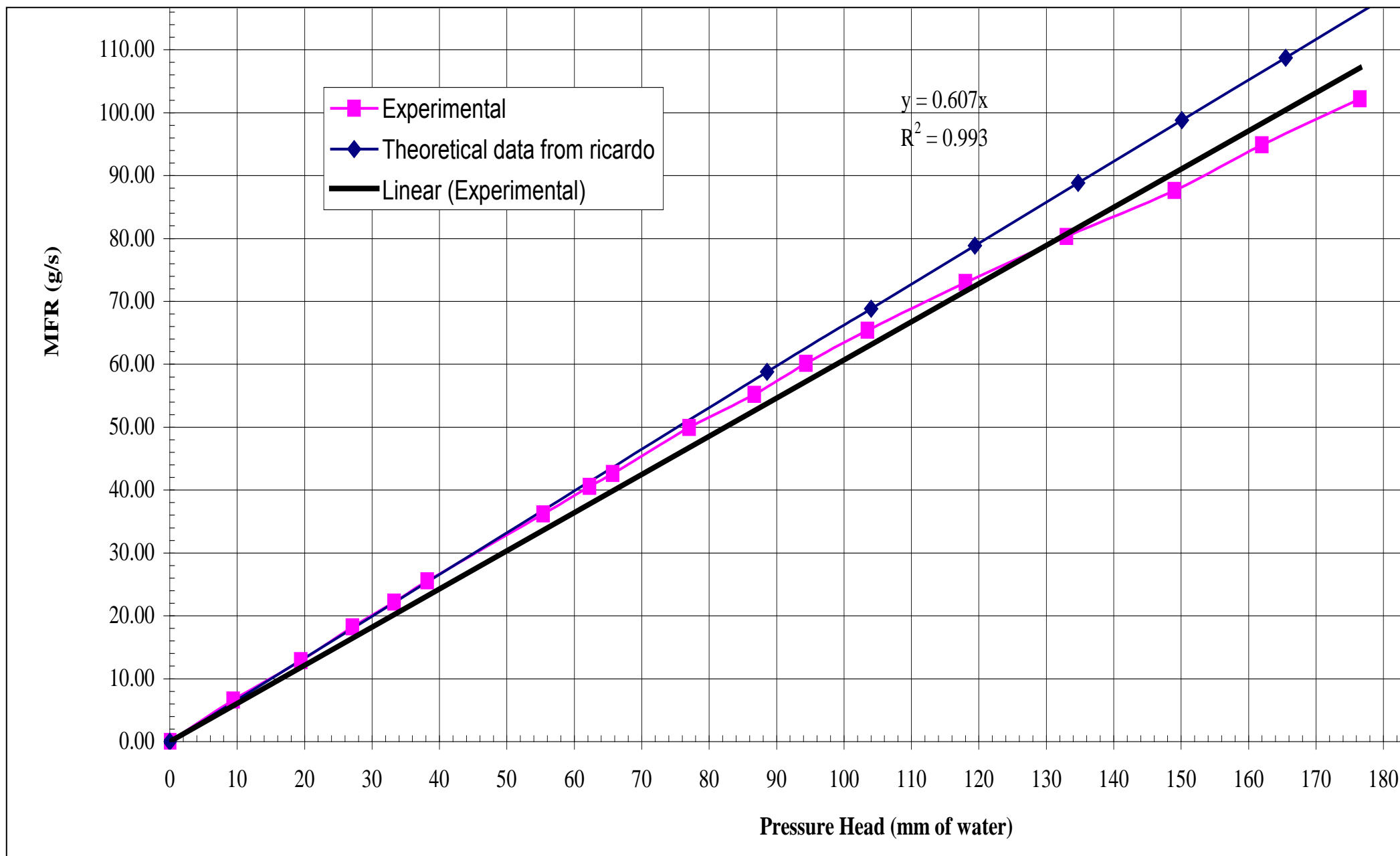
- 182 Thompson, J., Beeck, J.D., Joubert, E., Wilhelm, T. (2008) - *Case studies of urea SCR Integration on Passenger Cars; Monitoring of Urea Inside the Tank During Hot and Cold Environment Test Missions*, SAE 2008-01-1181, SAE 2008 World Congress, Detroit, Michigan, April 14-17, 2008.
- 183 Tomita, A., Yoshii, T., Teranishi, S., Nagao, M. and Hibino, T. (2007) - *Selective catalytic Reduction of NO<sub>x</sub> by H<sub>2</sub> Using Proton Conductors as Catalyst Supports*, Journal of Catalysis, Vol. 247, Issue 2, pp137-144.
- 184 Tranconi, E, Nova, I., Ciardelli, C. et al., (2005) - *Modelling of an SCR Catalytic Converter for Diesel Exhaust After Treatment: Dynamics Effects at Low Temperature*, Catalysis Today, 15 August 2005, Vol.105, pp 529 - 536,
- 185 Tronconi, E. and Beretta, A. (1999) - *The Role of Inter- and Intra-Phase Mass Transfer in the SCR-DeNO<sub>x</sub> Reaction over Catalysts of Different Shapes*, Catalysis Today, Vol. 52, Issue 2-3, pp249-258.
- 186 Tronconi, E., Nova, I., Ciardelli, C., Chatterjee, D., Bandl-Konrad, B. and Burkhardt, T. (2005) - *Modelling of an SCR Catalytic Converter for Diesel Exhaust Aftertreatment: Dynamic Effects at Low Temperature*, Catalysis Today, Vol.105, Issue 3-4, pp529-536.
- 187 Twigg, M.V. (2007) - *Progress and Future Challenges in Controlling Automotive Exhaust Gas Emissions*, Applied Catalysis B: Environmental, Vol. 70, Issue 1-4, pp2-15.
- 188 Uekusa, T, Nakada, T, et al., (2005) - *Emission Reduction Study for Meeting New Requirements with Advance Diesel Engine Technology*, SAE2005-01-2143, Fuels and Lubricants Meeting and Exhibition, Rio de Janeiro, Brazil, May 11-13, 2005.
- 189 United States, Environmental Protection Agency (2006) - *Certification Procedure for Light-Duty and Heavy Duty Diesel Vehicle Using Selective Catalyst Reduction (SCR) Technologies*, Doc no: EPA-HQ-OAR-2006-0886-0002.pdf
- 190 United States, Environmental Protection Agency (2007) - *Draft U.S. Greenhouse Gas Inventory Report, DRAFT INVENTORY OF U.S. GREENHOUSE GAS EMISSIONS AND SINKS: 1990-2005* (February 2007), Available online, <http://www.epa.gov/climatechange/emissions/usinventoryreport07.html>
- 191 Upadhyay, D. and Van Nieuwstadt, M. (2002) - *Control Design of an Automotive Urea SCR Catalyst*, ASME 2002 International Mechanical Engineering Congress and Exposition (IMECE2002), pp699-706, New Orleans, Louisiana, November 17-22, 2002.
- 192 Upadhyay, D. and Van Nieuwstadt, M. (2002) - *Modeling of a Urea SCR Catalyst with Automotive Applications*, ASME 2002 International Mechanical Engineering Congress and Exposition (IMECE2002), pp707-713, New Orleans, Louisiana, November 17-22, 2002.
- 193 US EPA (2006) - *Recommendations for Reducing Emission from the Legacy Diesel Fleet*, Report from Clean Air Act Advisory Committee, April 10, 2006.
- 194 Walker, A. (2005) - *Diesel Emission Control: Past, Present and Future*, 19<sup>th</sup> North American Meeting (NAM), North American Catalysis Society, Philadelphia, Pennsylvania, May 22-27, 2005.
- 195 Wang, Y., Zhu, J. and Ma, R.(2007) - *Macrodynamic Study and Catalytic Reduction of NO by Ammonia under Mild Conditions over Pt-La-Ce-O/Al<sub>2</sub>O<sub>3</sub> Catalysts*, Energy Conversion and Management, July 2007, Vol. 48, Issue 7, pp1936-1942.
- 196 Way, P.(2008) Panel Discussion, *Diesel Emission Control: Urea Deposits and Byproducts* at SAE Commercial Vehicle Conference, Chicago, October 2008

- 197 Willi, R., B. Roduit, R. Koeppel, A. Wokaun, A. Baiker, 1996. "Selective Reduction of NO by NH<sub>3</sub> over Vanadia-Based Commercial Catalyst: Parametric Sensitivity and Kinetic Modeling", Chem. Eng. Sci., 51 (11), pg. 2897-2902
- 198 World Health Organization-WHO (2002) - *Estimated Deaths & DALYs Attributable to Selected Environmental Risk Factors*, by WHO Member State.
- 199 Wu, Z., Jiang, B., Liu, Y., Zhao, W. and Guan, B.(2009) - *Experimental Study on a Low-Temperature SCR Catalyst based on MnOx/TiO<sub>2</sub> Prepared by Sol-Gel Method*, Journal of Hazardous Materials, Vol. 162, Issue 2-3, pp1249-1254.
- 200 Xie, S., Wang, J. and He, H. (2007) - *Poisoning Effect of Sulphate on the Selective Catalytic Reduction of NOx by C<sub>3</sub>H<sub>6</sub> over Ag-Pd/Al<sub>2</sub>O<sub>3</sub>*, Journal of Molecular Catalysis A: Chemical, , Vol. 266, Issue 1-2, pp166-172.
- 201 Yim, S.D., Kim S.J., Baik, J.H., Nam, I.-S., Mok, Y.,S., Lee, J.-H., Cho, B.K., and Oh, S.,H., (2004) - *Decomposition of Urea into NH<sub>3</sub> for the SCR Process*, Industrial and Engineering Chemistry Research Vol. 43, pp4856-4863.
- 202 Yli-Tuomi, T., Aarnio, P., Pirjola, L., Mäkelä, T., Hillamo, R. and Jantunen, M. (2005) - *Emissions of Fine Particles, NOx, and CO from on-road Vehicles in Finland*, Atmospheric Environment, Vol. 39, Issue 35, pp6696-6706.
- 203 Yost, D. M. (2007) - *Systematic Inorganic Chemistry, Ammonia and Liquid Ammonia Solution*, p132, ISBN 1406773026.
- 204 Zhang, C., He, H., Shuai, S. and Wang, J. (2007) - *Catalytic Performance of Ag/Al<sub>2</sub>O<sub>3</sub>-C<sub>2</sub>H<sub>5</sub>OH-Cu/Al<sub>2</sub>O<sub>3</sub> System for the Removal of NOx from Diesel Engine Exhaust*, Environmental Pollution, Vol.147, Issue 2, pp415-421.
- 205 Zhang, F., Zhang, S., Guan, N., Schreier, E., Richter, M., Eckelt, R. and Fricke, R. (2007) - *NO SCR with Propane and Propene on Co-based Alumina Catalysts Prepared by Co-Precipitation*, Applied Catalysis B: Environmental, Vol. 73, Issue 3-4, pp209-219.
- 206 Zhu, L., Zhang, W., Liu, W. and Huang, Z. (2010) - *Experimental Study on Particulate and NOx Emissions of a Diesel Engine Fueled with Ultra Low Sulfur Diesel, RME-Diesel Blends and PME-Diesel Blends*, Science of The Total Environment, Vol.408, Issue 5, pp1050-1058.

# APPENDICES










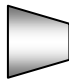
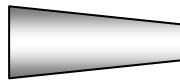



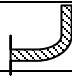

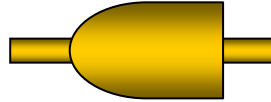


Appendix 3.1.1 – Power curve for Ford 2.0 litre diesel engine  
(complementary of Ford powertrain development division, 2001



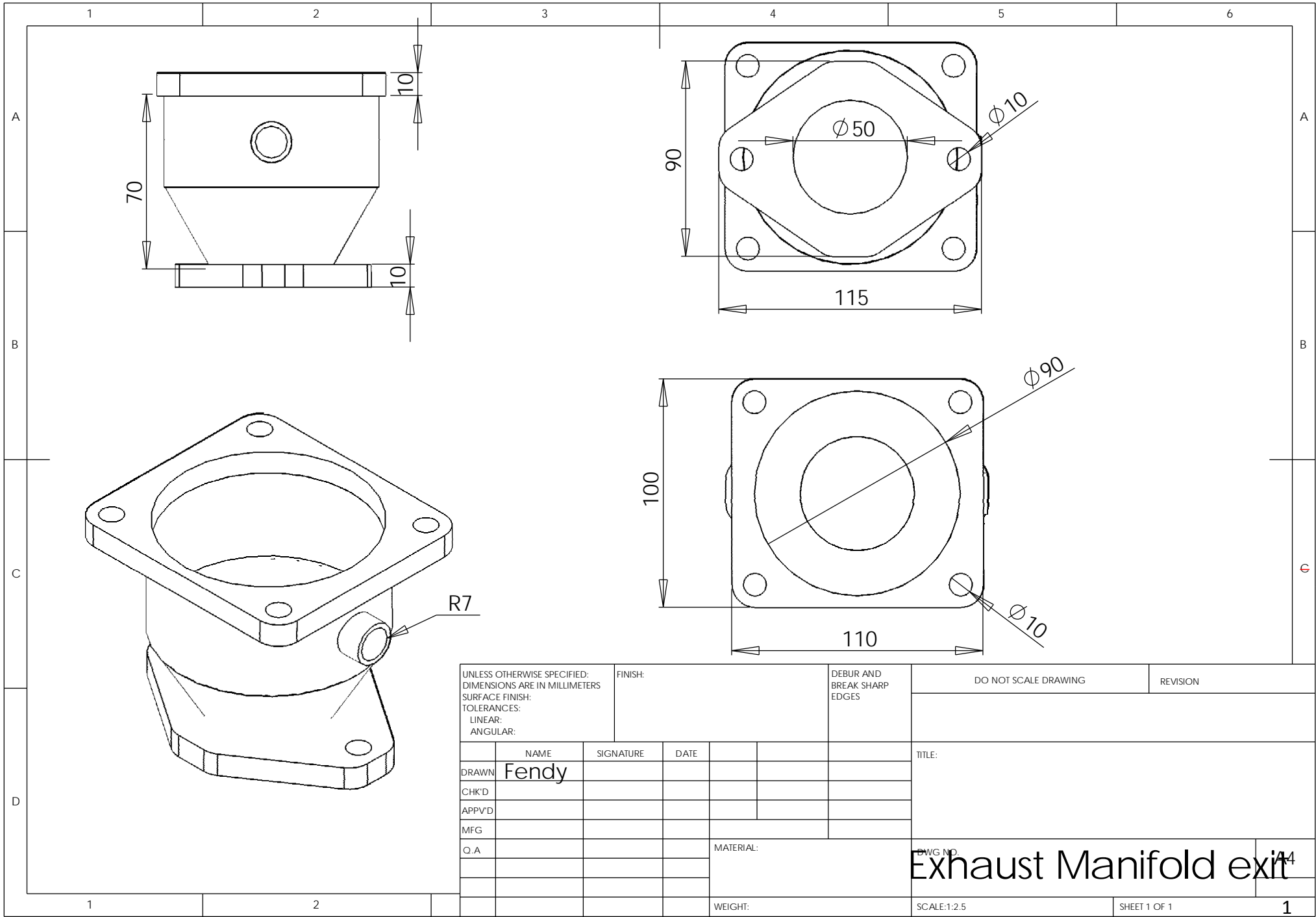
Appendix 3.1.3 - Ricardo Mass flow meter calibration chart.

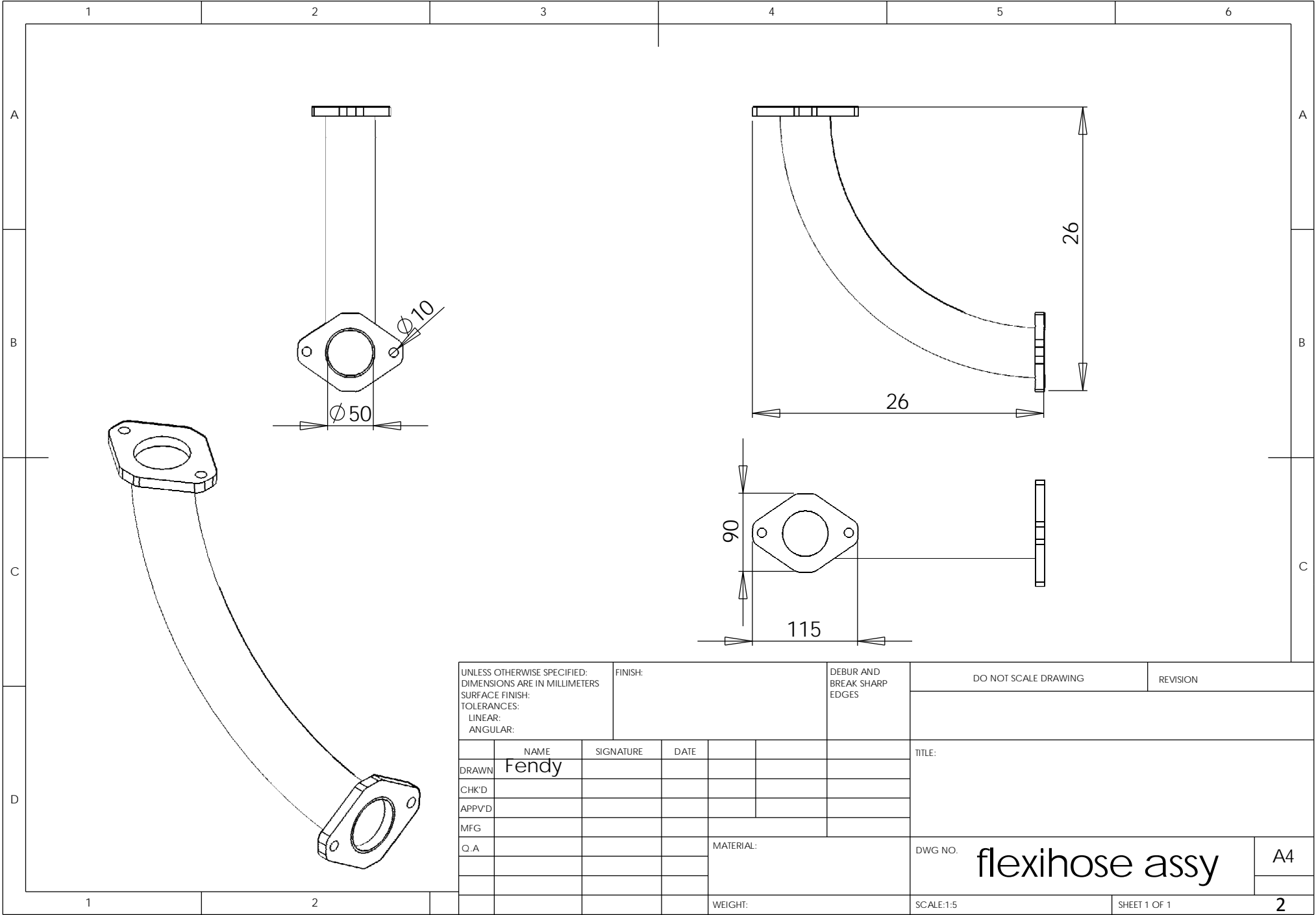
### Appendix 3.2 Supplied parts for SCR exhaust build.

No	Parts Description	Quantity	Size
1	Flange 	20 pcs	125 x 80 mm Centre hole 50 mm diameter
2	Flange Cover 	4 pcs	115 x 85 mm
3	Hex bolts 	100 pcs	10 mm diameter
4	Nuts 	100 pcs	10 mm inside diameter
5	Washer 	200 pcs	11 mm inside diameter
6	Ring Flange 	20 pcs	Diameter <sub>out</sub> =190 mm Diameter <sub>in</sub> =115mm 8 x 1mm holes
7	Gasket – 2 hole 	20 pcs	125 x 80 mm Centre hole 50 mm diameter
8	Gasket – 8 hole 	20 pcs	Diameter <sub>out</sub> =190 mm Diameter <sub>in</sub> =115mm 8 x 1mm holes
9	Inlet cone 	1 unit	Diameter <sub>small</sub> =50 mm Diameter <sub>large</sub> = 115 mm Length = 150 mm
10	2 <sup>nd</sup> cone 	1 unit	Diameter <sub>small</sub> =50 mm Diameter <sub>large</sub> = 115 mm Length = 900 mm
11	Expansion duct/ 3 <sup>rd</sup> cone 	1 unit	Diameter <sub>small</sub> =50 mm Diameter <sub>large</sub> = 115 mm Length = 410 mm
12	Exit cone / 4th cone 	1 unit	Diameter <sub>small</sub> =50 mm Diameter <sub>large</sub> = 115 mm Length = 90 mm
13	DOC Assembly 	3 unit	1 unit 95 mm length 2 unit 190 mm length
14	DPF Assembly 	1 unit	155 mm length
15	SCR Assembly 	3 unit	1 unit 92.5 mm length 2 unit 185 mm length
16	Flexible hose 	1 unit	50 mm x 1 m length
17	Straight pipe 	1 unit	50 mm x 2m length
18	Expansion box assembly 	1 unit	Refer to drawing in appendix 3.2b

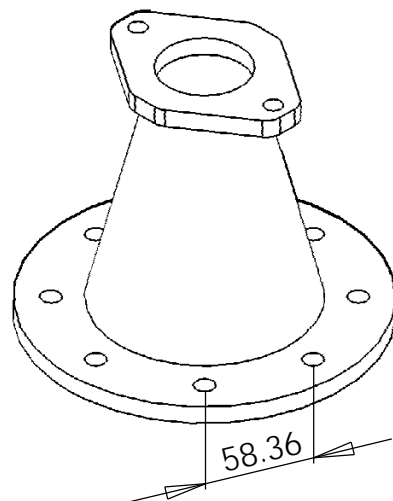
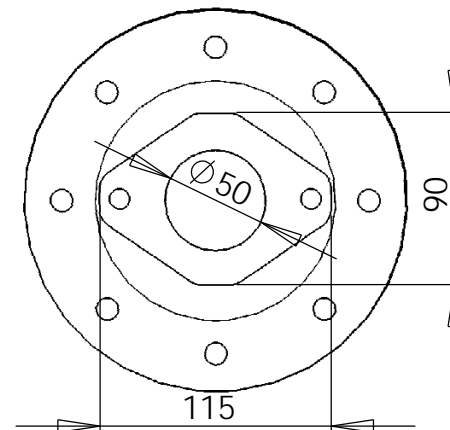
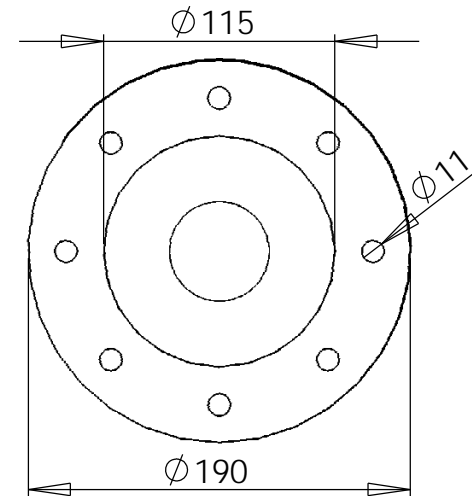
## Appendix 3.2b List of drawing for SCR Exhaust System

- 1 - Exhaust Manifold exit
- 2 - Flexi hose assembly
- 3 - 1<sup>st</sup> cone 150 mm
- 4 - DPF Assembly
- 5 - DOC Assembly
- 6 - Instrumentation module assembly – 110 mm
- 7 - 2<sup>nd</sup> cone – 90 mm
- 8 - Expansion box assembly
- 9 - Instrumentation pipe assembly – 200 mm
- 10 - 3<sup>rd</sup> cone – 410 mm
- 11 - SCR assembly
- 12 - Instrumentation module assembly – 90 mm
- 13 - Last cone assembly
- 14 - T-piece assembly
- 15 - Final assembly front view
- 16 - Final assembly isometric view

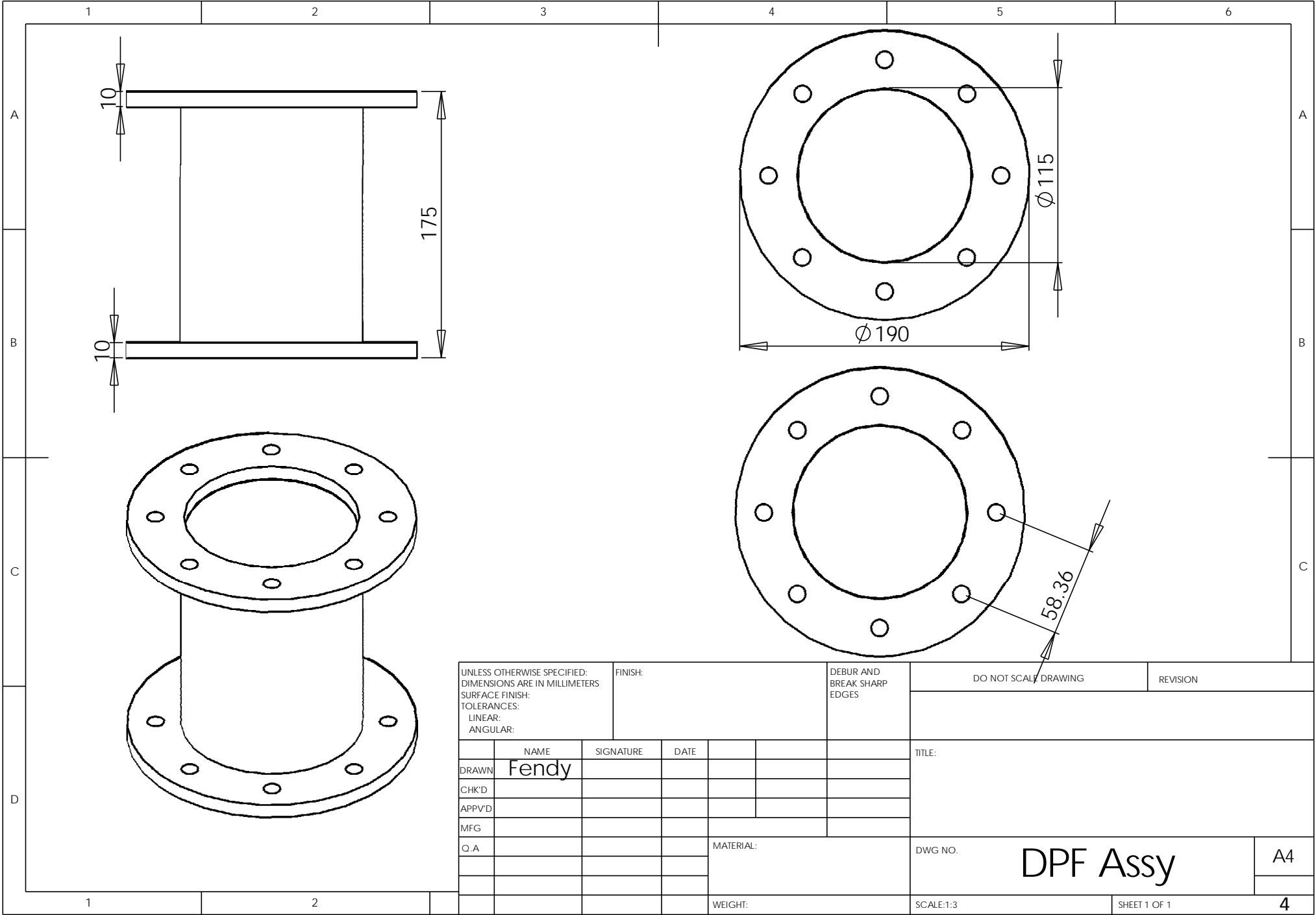




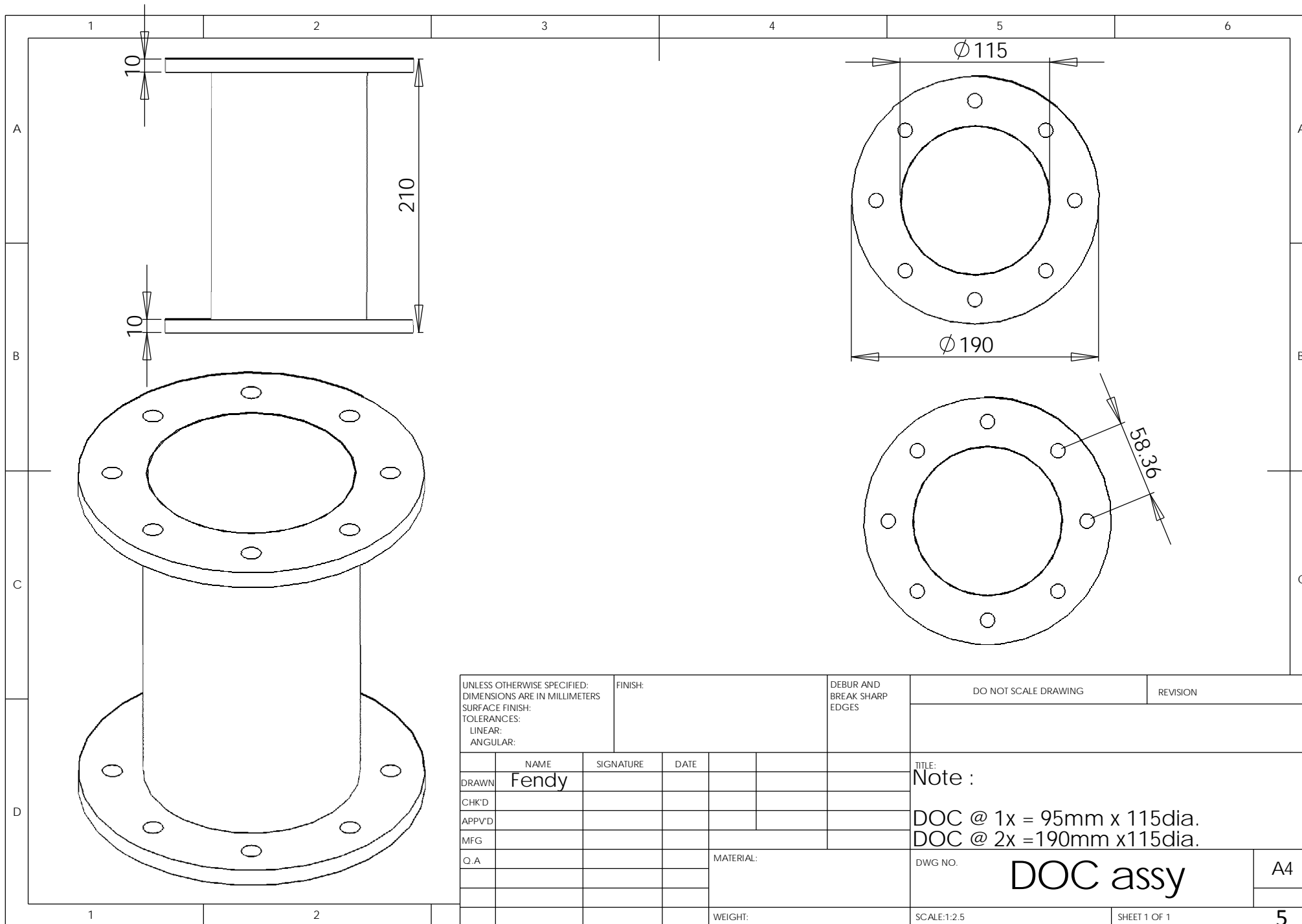
UNLESS OTHERWISE SPECIFIED: DIMENSIONS ARE IN MILLIMETERS SURFACE FINISH: TOLERANCES: LINEAR: ANGULAR:				FINISH:				DEBUR AND BREAK SHARP EDGES		DO NOT SCALE DRAWING				REVISION				
	NAME		SIGNATURE		DATE				TITLE:									
DRAWN	Fendy																	
CHK'D																		
APPV'D																		
MFG																		
Q.A					MATERIAL:				DWG NO.				flexihose assy		A4			
									SCALE:1:5				SHEET 1 OF 1					
					WEIGHT:								2					

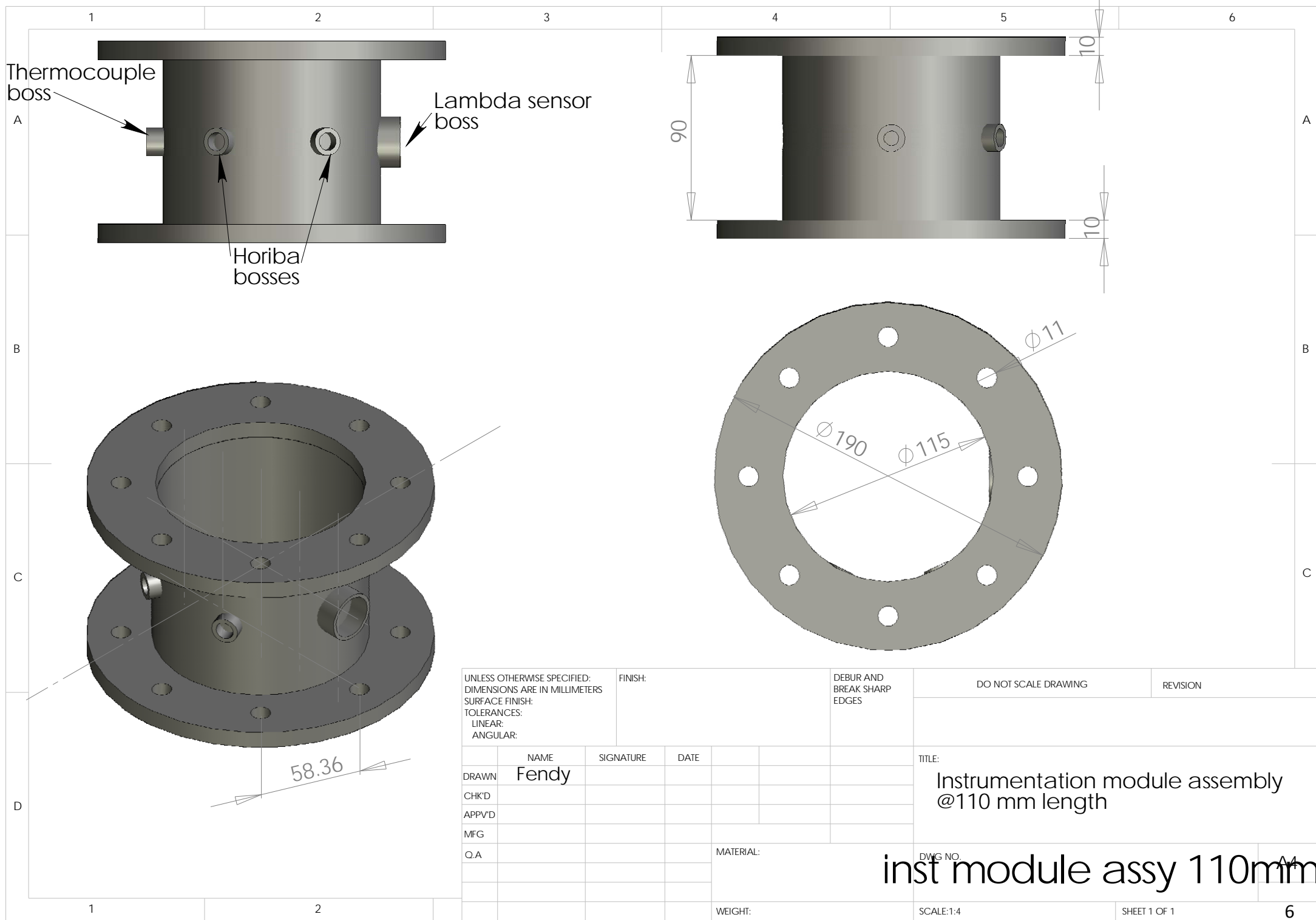


UNLESS OTHERWISE SPECIFIED: DIMENSIONS ARE IN MILLIMETERS SURFACE FINISH: TOLERANCES: LINEAR: ANGULAR:				FINISH:		DEBUR AND BREAK SHARP EDGES		DO NOT SCALE DRAWING		REVISION	
	NAME		SIGNATURE		DATE				TITLE:		
DRAWN	Fendy										
CHK'D											
APPV'D											
MFG											
Q.A						MATERIAL:		DWG NO		1st cone 150 mm	
										A4	
						WEIGHT:		SCALE:1:3.5		SHEET 1 OF 1	
										3	









UNLESS OTHERWISE SPECIFIED:  
DIMENSIONS ARE IN MILLIMETERS  
SURFACE FINISH:  
TOLERANCES:  
LINEAR:  
ANGULAR:

FINISH:

DEBUR AND  
BREAK SHARP  
EDGES

DO NOT SCALE DRAWING

REVISION

DRAWN  
CHK'D  
APPV'D  
MFG  
Q.A

NAME  
Fendy

SIGNATURE

DATE

MATERIAL:

WEIGHT:

TITLE:

Instrumentation module assembly  
@110 mm length

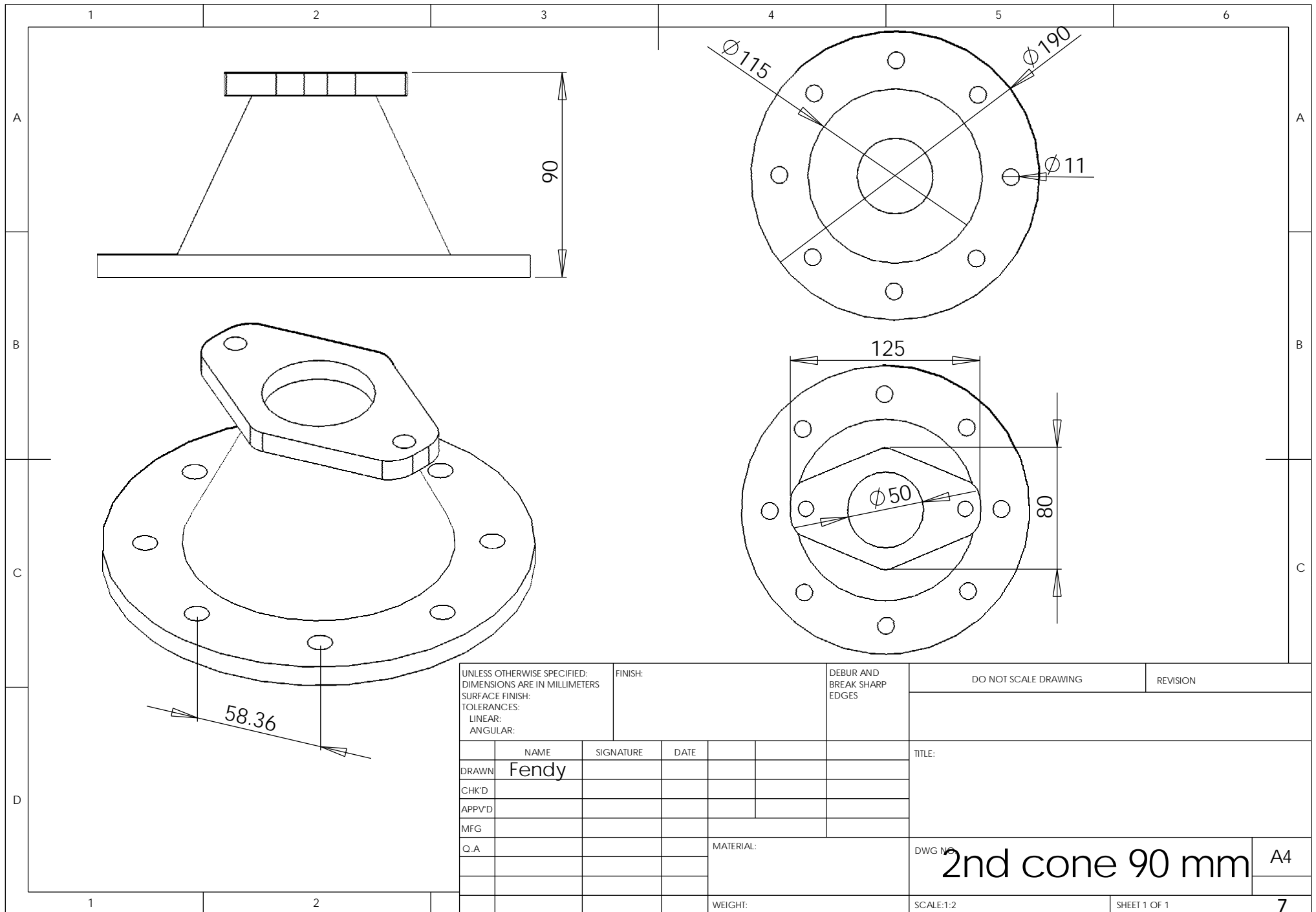
DWG NO.

inst module assy 110mm

SCALE:1:4

SHEET 1 OF 1

6



UNLESS OTHERWISE SPECIFIED:  
DIMENSIONS ARE IN MILLIMETERS  
SURFACE FINISH:  
TOLERANCES:  
LINEAR:  
ANGULAR:

FINISH:

DEBUR AND  
BREAK SHARP  
EDGES

DO NOT SCALE DRAWING

REVISION

	NAME	SIGNATURE	DATE			
DRAWN	Fendy					
CHK'D						
APPV'D						
MFG						
Q.A						

TITLE:

MATERIAL:

DWG NO.

2nd cone 90 mm

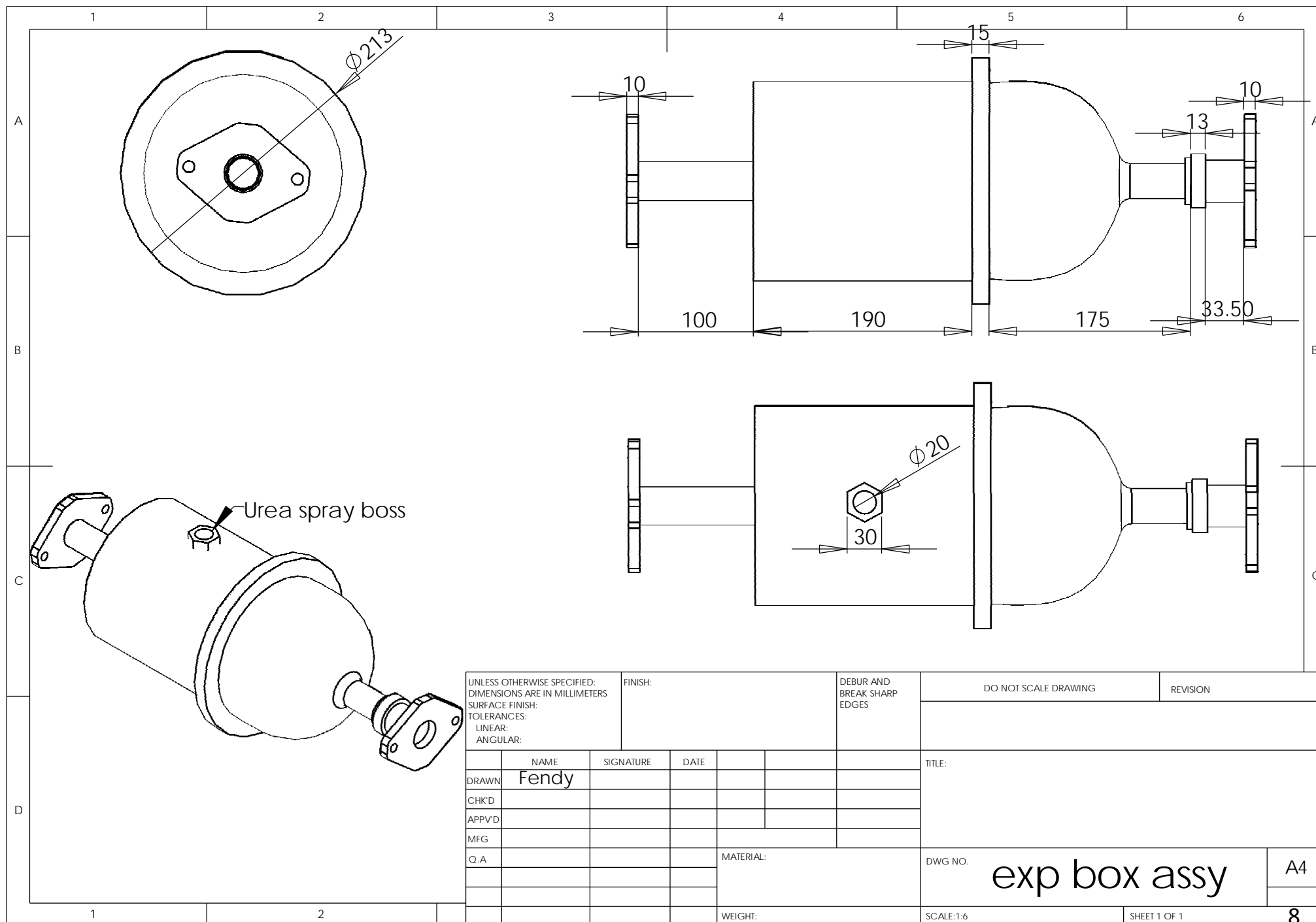
A4

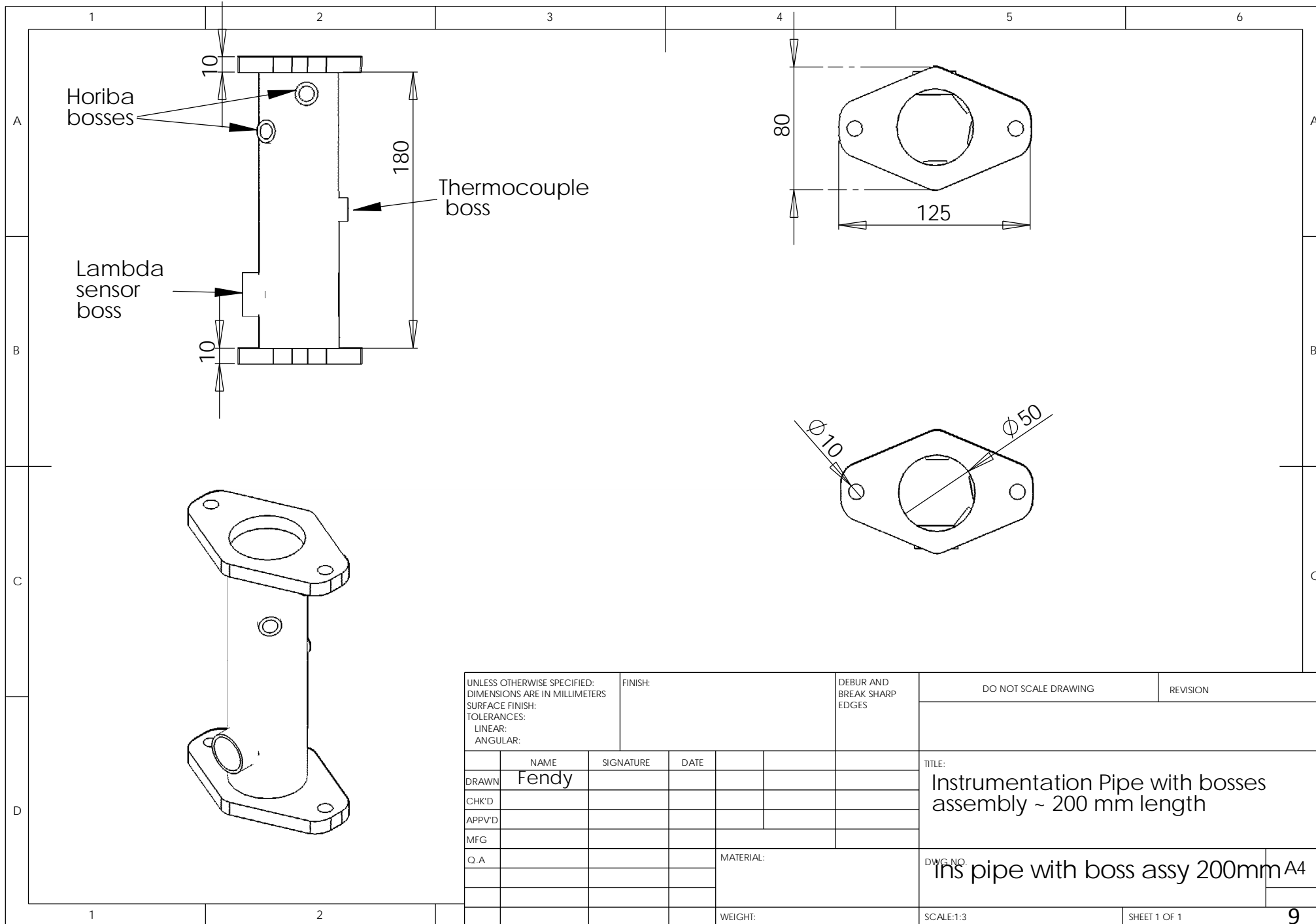
WEIGHT:

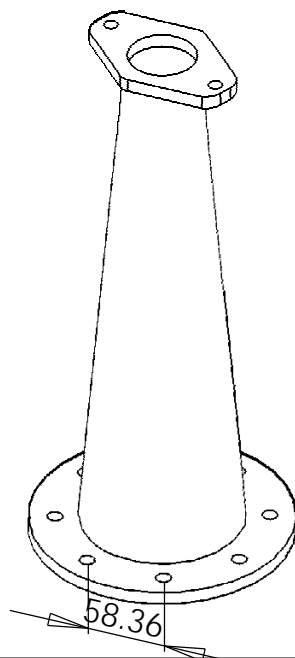
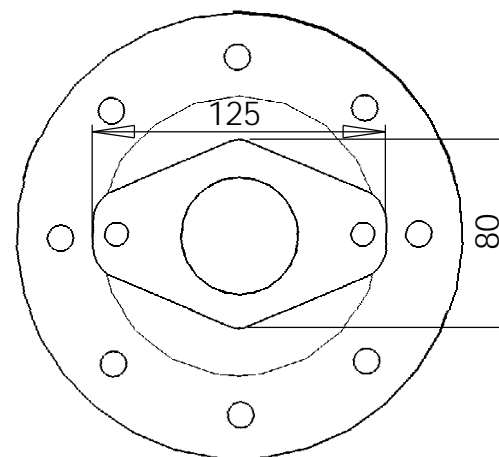
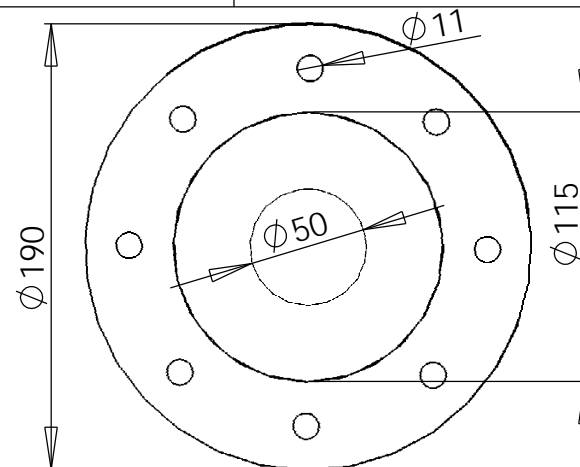
SCALE:1:2

SHEET 1 OF 1

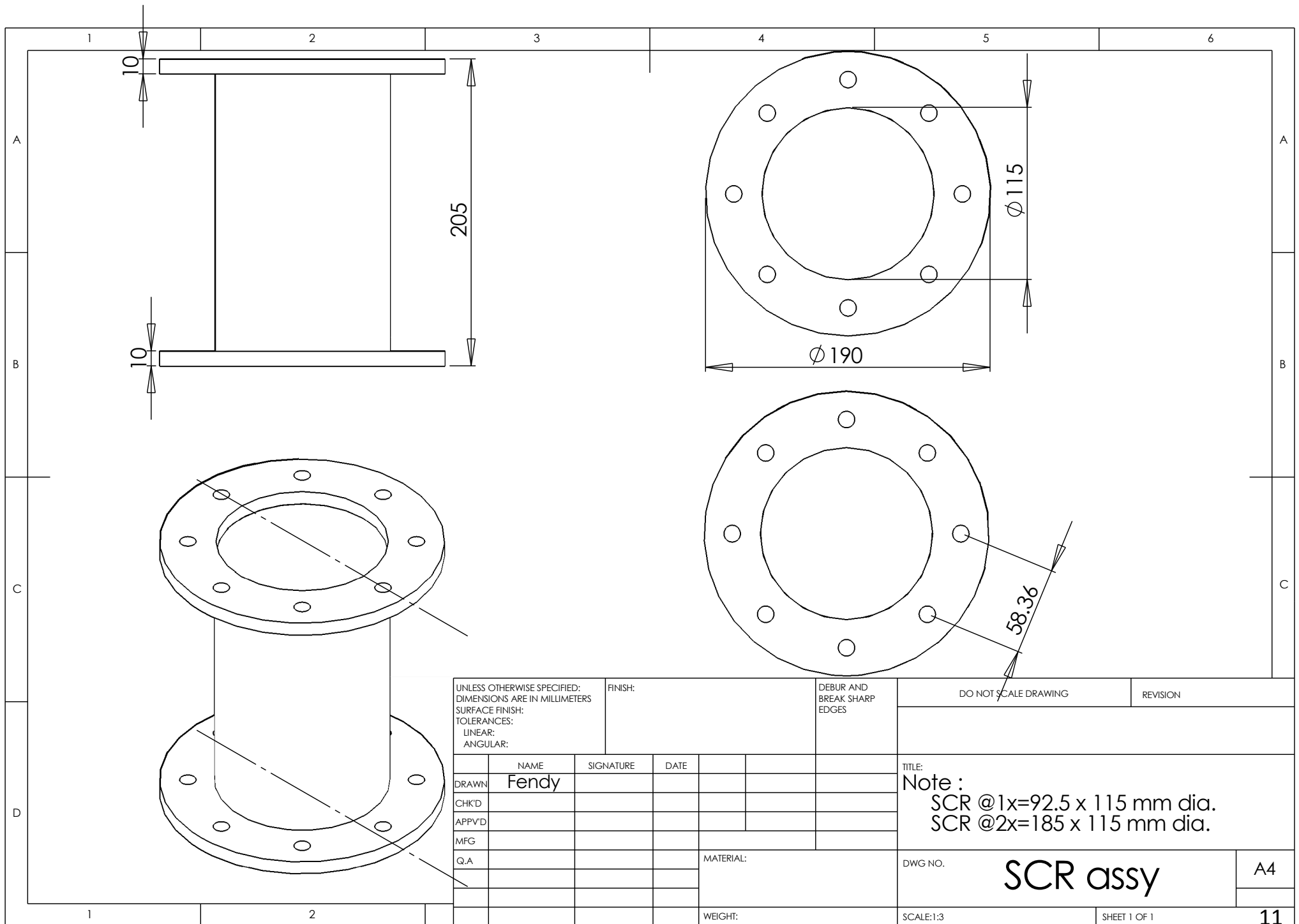
7





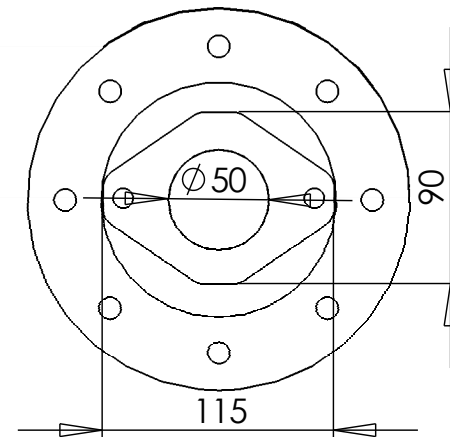
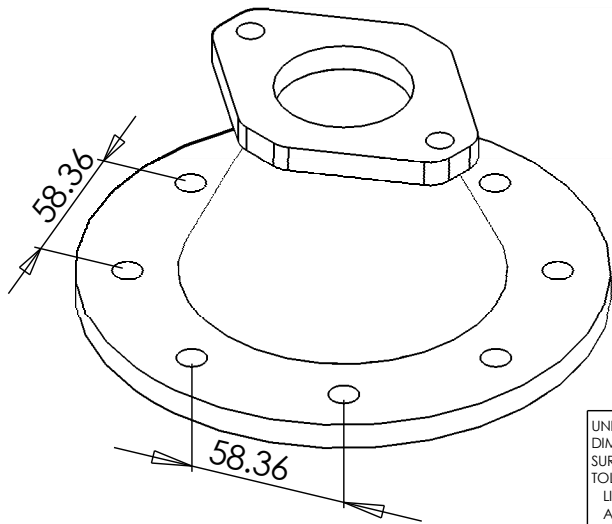
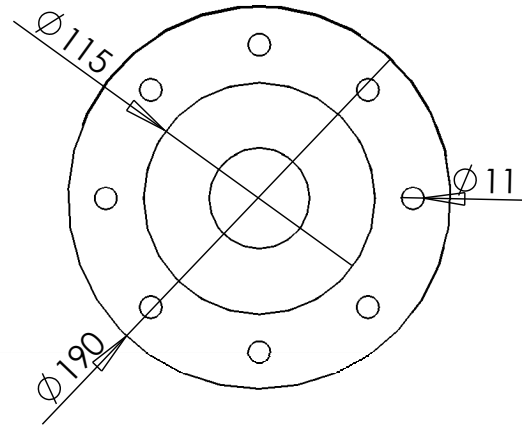
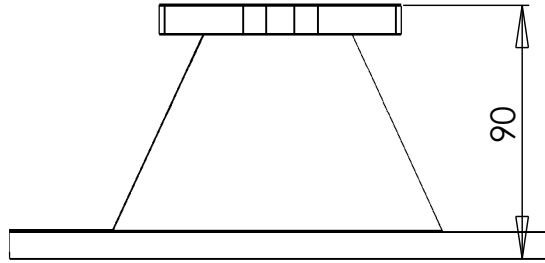


UNLESS OTHERWISE SPECIFIED: DIMENSIONS ARE IN MILLIMETERS SURFACE FINISH: TOLERANCES: LINEAR: ANGULAR:				FINISH:			DEBUR AND BREAK SHARP EDGES		DO NOT SCALE DRAWING		REVISION	
	NAME		SIGNATURE		DATE				TITLE:			
DRAWN	Fendy											
CHK'D												
APPV'D												
MFG												
Q.A					MATERIAL:			DWG NO.				
								3rd cone 410 mm				
					WEIGHT:			SCALE:1:3				
								SHEET 1 OF 1				
												10



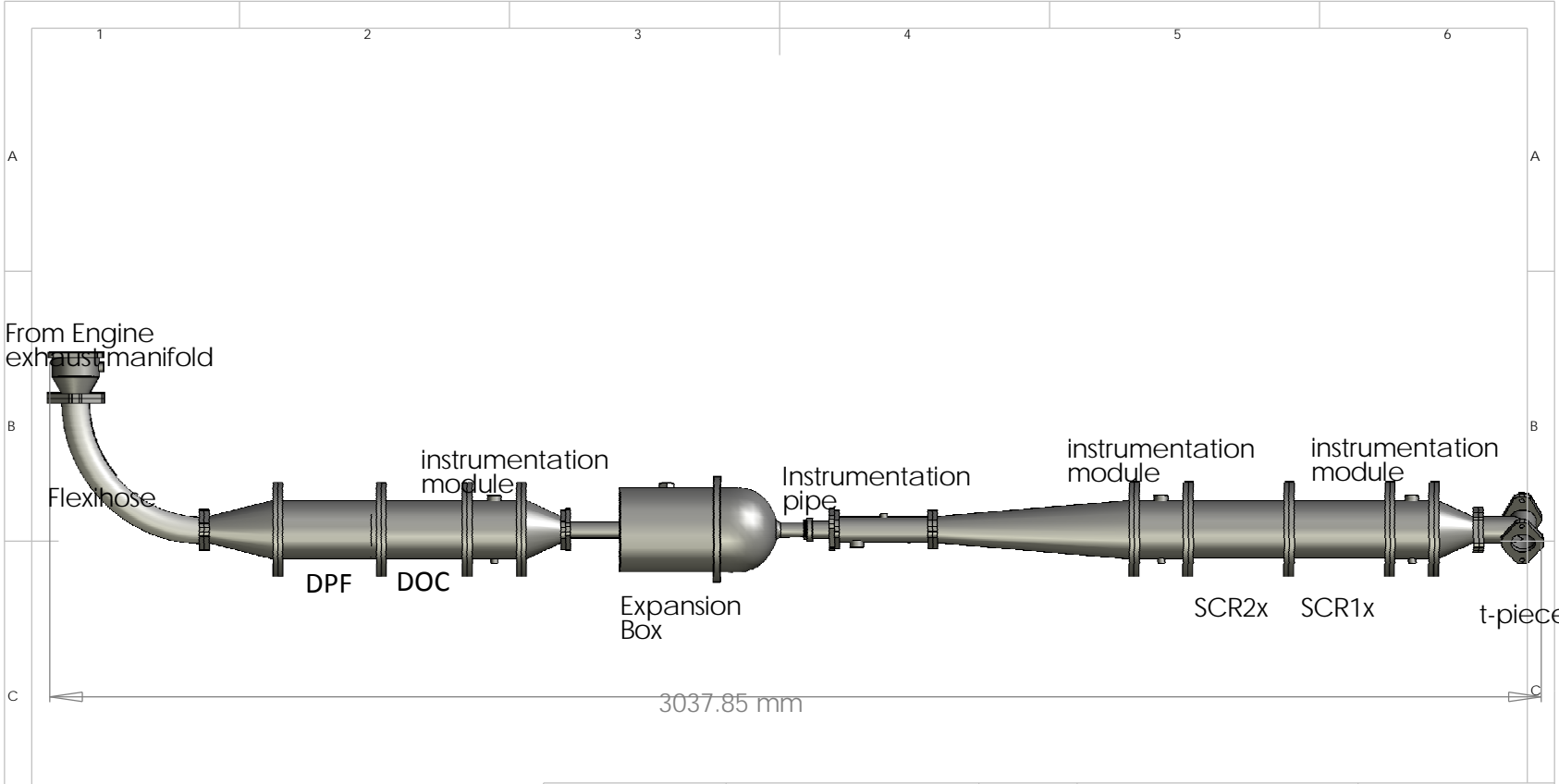






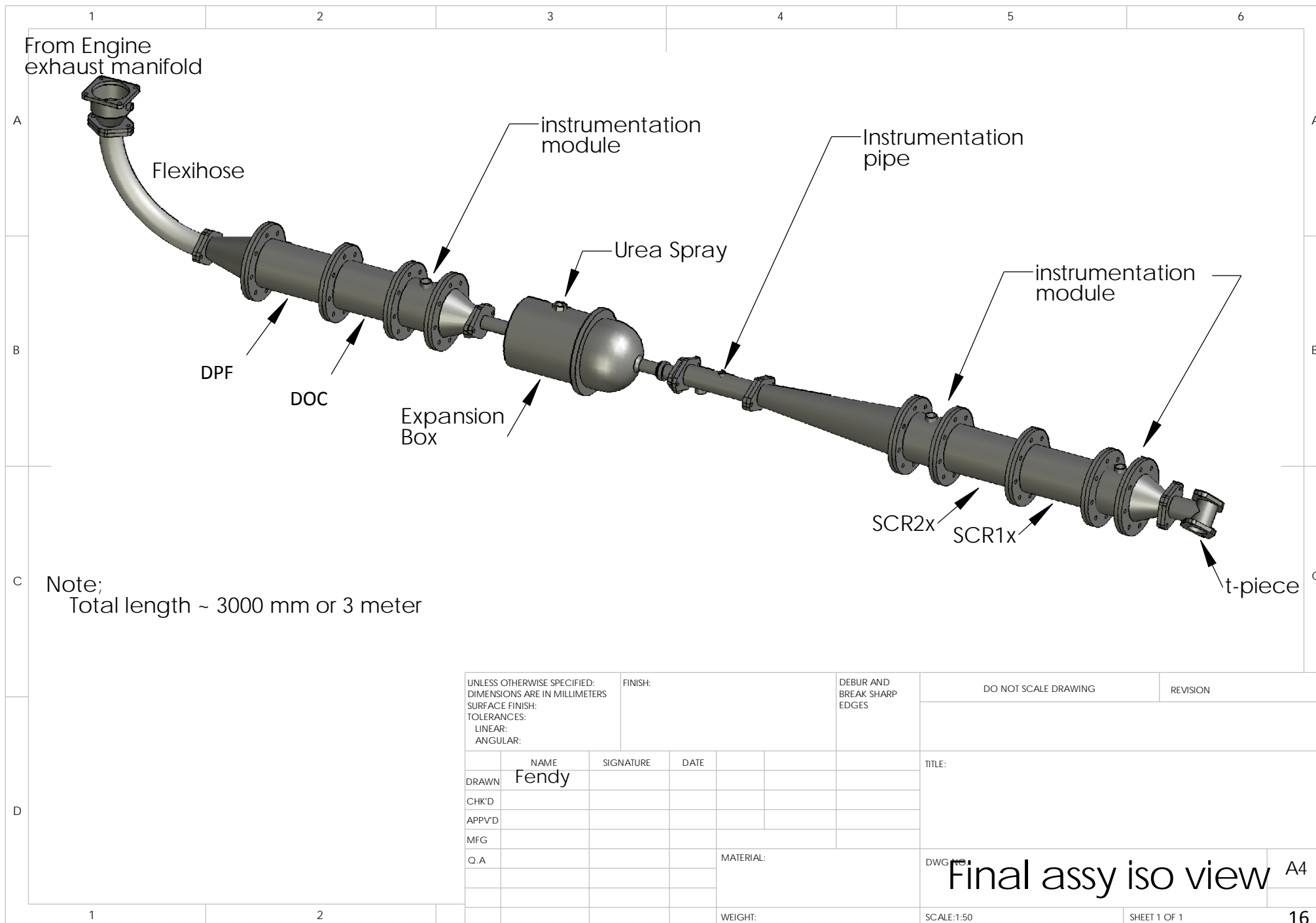
UNLESS OTHERWISE SPECIFIED: DIMENSIONS ARE IN MILLIMETERS SURFACE FINISH: TOLERANCES: LINEAR: ANGULAR:				FINISH:		DEBUR AND BREAK SHARP EDGES		DO NOT SCALE DRAWING		REVISION	
DRAWN <b>Fendy</b>				SIGNATURE		DATE		TITLE:			
CHK'D											
APPV'D											
MFG											
Q.A											
						MATERIAL:		DWG NO. <b>last cone assy</b>			
								A4			
						WEIGHT:		SCALE:1:2.5			
								SHEET 1 OF 1			
								<b>13</b>			





UNLESS OTHERWISE SPECIFIED: DIMENSIONS ARE IN MILLIMETERS SURFACE FINISH: TOLERANCES: LINEAR: ANGULAR:						FINISH:		DEBUR AND BREAK SHARP EDGES		DO NOT SCALE DRAWING				REVISION	
DRAWN		NAME		SIGNATURE		DATE						TITLE:			
CHK'D		Fendy													
APP'VD															
MFG															
Q.A						MATERIAL:				DWS NO.		Final assy front view			
												A4			
												15			

A4  
15



### Appendix 3.4.1 MEXA 1170Nx Ammonia Analyser Specifications

#### a. Analyser Outline

Model	MEXA-1170NX
Approved standards	CE, FCC
Application	Exhaust gases from engines
Target components	NO <sub>x</sub> , NH <sub>3</sub>
Principle	Chemi-luminescence detection (heated)
Measuring range of NO <sub>x</sub>	NO <sub>x</sub> : 0 - 10/20/50/100/500/1000/2000/5000/10000 ppm (9 ranges)
Measuring range of NH <sub>3</sub>	0 - 10/20/50/100/500/1000 ppm (Display range for NH <sub>3</sub> is range agreed with the current range of NO <sub>x</sub> .)
Outputs/ Inputs	<ul style="list-style-type: none"> <li>● Monitoring on LCD panel</li> <li>● Analog output: 0 - 1 V/ 0 - 10 V (to be specified when ordering)</li> <li>● Digital input-output: RS-232C communication (by AK protocol) LAN communication (by AK protocol)</li> <li>● Communication with the MEXA-7000 series (optional): can be connected to the main control unit (MCU)</li> </ul>
Sample line temperature	120°C ±20°C
Sample gas flow rate	3.0 L/min ±0.5 L/min
Sample gas pressure	Between -5 kPa to 30 kPa
Environment for operation	Ambient temperature: from 5°C to 40°C Ambient humidity: under 80% as relative humidity

#### b. Optional

Cabinet	For mounting MEXA-1170NX, 570(W) × 710(D) × 1000(H) mm
Heated filter	HF-04, with sampling probe (0.3 m)
Recorder cable	For analog output (3 channels), max. 10 m
RS-232C cable	For host communication, D-sub 9 pin, cross cable, max. 15 m
LAN cable	For host communication or MCU communication, 10baseT, max 50m
Checker	For leak check and delay check, with specified cable (max. 7 m)
Remote controller	For panel operation, with specified cable (max. 55 m)
Communication with MEXA-7000 *4	Following functions on MEXA-7000 MCU are available: <ul style="list-style-type: none"> <li>● Display of concentration</li> <li>● Range selection</li> <li>● Status switching between Stand-by and Pause</li> <li>● Control of gas sampling (ZERO/SPAN/CAL/MEAS/PURGE/RESET)</li> <li>● Calendar time function (Stand-by and Pause only)</li> <li>● Analog output (optional function of MEXA-7000)</li> <li>● Trend chart (optional function of MEXA-7000)</li> <li>● Post trend chart (optional function of MEXA-7000)</li> </ul>
NO <sub>2</sub> measurement	Can be used as NO <sub>x</sub> , NO, NO <sub>2</sub> analyzer

\*4: A MCU of Ver. 3.00 or more is required for this optional function. Contact to HORIBA group company office for updating MCU.

c. System configuration

Configuration	<p>Consists of the following units:</p> <ul style="list-style-type: none"> <li>● Analyzer unit (including two NO detectors)</li> <li>● Sampling unit (including NH<sub>3</sub> oxidizing furnace)</li> <li>● VPU (vacuum pump unit)</li> </ul>
Control temperature of furnace	850°C
Gas inlets and outlets	<ul style="list-style-type: none"> <li>● Sample inlet: 6 mm O.D./ 4 mm I.D. heated tube, max. 6 m</li> <li>● Span inlet: 6 mm O.D./ 4 mm I.D. PTFE tube</li> <li>● Zero gas inlet: 6 mm O.D./ 4 mm I.D. PTFE tube</li> <li>● NH<sub>3</sub> gas inlet: 6 mm O.D./ 4 mm I.D. PTFE tube</li> <li>● O<sub>2</sub> inlet: 3 mm O.D./ 2 mm I.D. SUS tube</li> <li>● Check gas inlet: specified coupler</li> <li>● Purge air inlet: 6 mm O.D./ 4 mm I.D. PTFE tube</li> <li>● Exhaust outlets: hose ends (× 3; 10 mm, 10 mm and 16 mm dia.)</li> </ul>
Utilities	<ul style="list-style-type: none"> <li>● NO/N<sub>2</sub> (for span gas): 100 kPa ±10 kPa, approx. 3 L/min</li> <li>● NH<sub>3</sub>/N<sub>2</sub> (for efficiency check of NH<sub>3</sub> oxidation): 100 kPa ±10 kPa, approx. 3 L/min</li> <li>● N<sub>2</sub> (for zero gas): purity more than 99.99% 100 kPa ±10 kPa, approx. 3 L/min,</li> <li>● O<sub>2</sub> (for O<sub>3</sub> generation and NH<sub>3</sub> oxidation): purity more than 99.99% 100 kPa ±10 kPa, approx. 0.7 L/min</li> <li>● Compressed air or N<sub>2</sub> (for line purge): 100 kPa ±10 kPa, approx. 5 L/min</li> </ul>
Power supply	100/110/115/120/200/230/240 V AC (±10%, max. 250 V), 50/60 Hz (±1 Hz), single phase (To be specified when ordering. It cannot be changed after purchasing.)
Power capacity	Approx. 2.5 kVA as maximum (approx. 1.5 kVA at stable state)
Dimensions	<ul style="list-style-type: none"> <li>● Analyzer unit: 498(W) × 612(D) × 188(H) mm</li> <li>● Sampling unit: 498(W) × 691(D) × 232(H) mm</li> <li>● Vacuum pump unit: 300(W) × 550(D) × 340 (H) mm</li> </ul> <p>(excluding protruding objects)</p>
Mass	<ul style="list-style-type: none"> <li>● Analyzer unit: approx. 25 kg</li> <li>● Sampling unit: approx. 35 kg</li> <li>● Vacuum pump unit: approx. 20 kg</li> </ul>

d. Analyser performance

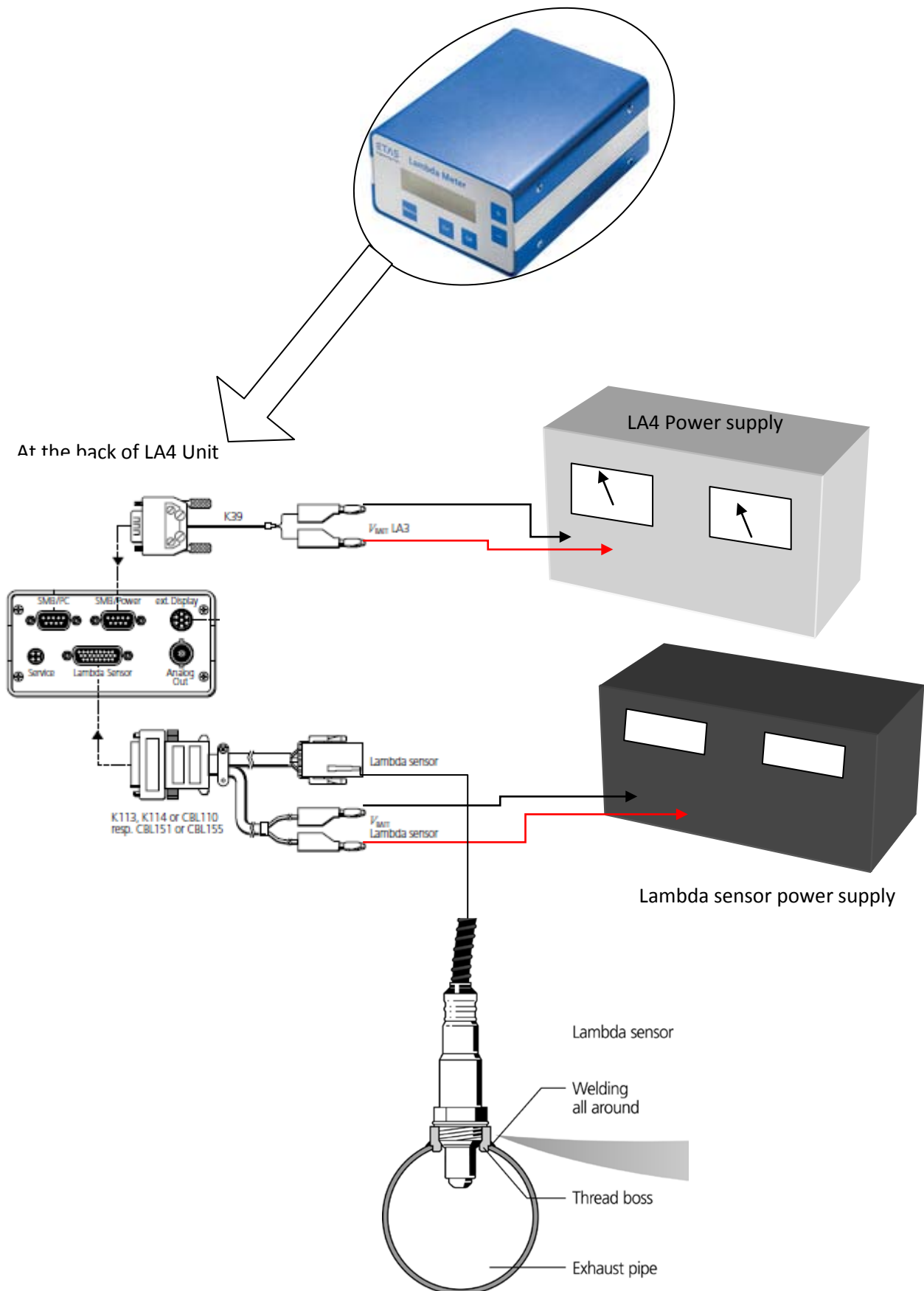
Response time of calibration line ( $T_{5-90}$ ) *1	From ZERO/SPAN inlet, at flow rate of 3.0 L/min, <ul style="list-style-type: none"> <li>• NO<sub>x</sub>: within 1.5 s (by switching N<sub>2</sub> to NO)</li> <li>• NH<sub>3</sub>: within 3.0 s (by switching N<sub>2</sub> to 50 ppm NH<sub>3</sub>)</li> </ul>
Response time of sample line ( $T_{5-90}$ ) *1	From inlet of sample probe (6 m), at flow rate of 3.0 L/min, <ul style="list-style-type: none"> <li>• NO<sub>x</sub>: within 3.0 s (switching N<sub>2</sub> to NO)</li> <li>• NH<sub>3</sub>: within 20 s (switching N<sub>2</sub> to 50 ppm NH<sub>3</sub>)</li> </ul>
Noise *2	As NO <sub>x</sub> readings, <ul style="list-style-type: none"> <li>• Zero: less than 2.0% of full scale</li> <li>• Span: less than 2.0% of readings</li> </ul> (as peak-to-peak width in 5 minutes, excluding the spike noise with the frequency of less than once per hour)
Linearity *2	<ul style="list-style-type: none"> <li>• NO<sub>x</sub>: within <math>\pm 1.0\%</math> of full scale</li> <li>• NH<sub>3</sub>: within <math>\pm 2.0\%</math> of full scale</li> </ul> (NH <sub>3</sub> : confirmed by 10 points division of 50 ppm to 1000 ppm NH <sub>3</sub> )
Repeatability *2,3	As NO <sub>x</sub> readings, <ul style="list-style-type: none"> <li>• Zero: within <math>\pm 0.5\%</math> of full scale</li> <li>• Span: within <math>\pm 0.5\%</math> of readings</li> </ul>
Interference (Cross sensitivity) *2	<ul style="list-style-type: none"> <li>• CO<sub>2</sub> interference: within 0 to -2.0% of NO<sub>x</sub> readings (for gas mixture of NO 100 ppm and CO<sub>2</sub> 16 vol%)</li> <li>• H<sub>2</sub>O interference: within 0 to -3.0% of NO<sub>x</sub> indication (for gas mixture of NO 100 ppm and H<sub>2</sub>O 15 vol%)</li> <li>• SO<sub>2</sub> interference: within 0 to -1.0% of NH<sub>3</sub> indication (for gas mixture of NH<sub>3</sub> 50 ppm and SO<sub>2</sub> 10 ppm)</li> </ul>
Drift *2,3	As NO <sub>x</sub> readings, <ul style="list-style-type: none"> <li>• Zero: within <math>\pm 1.0\%</math> of full scale per 8 hours</li> <li>• Span: within <math>\pm 1.0\%</math> of readings per 8 hours</li> </ul> (fluctuation of ambient temperature within $\pm 2^\circ\text{C}$ )
Warm-up time	NO <sub>x</sub> , NH <sub>3</sub> : within 2 hours, until within $\pm 1.0\%$ drift / 30 minutes within 4 hours, until within $\pm 1.0\%$ drift / 8 hours
Calculation error for transient response	NH <sub>3</sub> : within $\pm 10\%$ of full scale (confirmed by switching N <sub>2</sub> to NO 10 ppm at ZERO/ SPAN gas inlet, at flow rate of 3.0 L/min)
NO <sub>x</sub> converter efficiency	More than 90% (for less than 500 ppm NO <sub>2</sub> )
NH <sub>3</sub> oxidation efficiency	More than 80% (for 50 ppm to 1000 ppm NH <sub>3</sub> )

\*1:  $T_{5-90}$  means the time interval from 5% response to 90% response.

\*2: Measurement error of NH<sub>3</sub> tends to become larger when sample gas contains NO<sub>x</sub> of higher concentration.

\*3: Span gas with more than 80% concentration of the full scale shall be used.

## Appendix 3.5: Lambda Sensor Connection Configuration

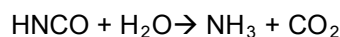
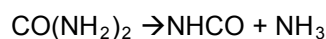




### Appendix 3.6.2 Potential Ammonia Released from Urea Spray Calculation

Calculation of Potential amount of ammonia introduced into exhaust system by urea spray

The disintegration of urea to form ammonia takes place in two stages. First the urea disintegrates at about 137°C to form ammonia and iso-cyanic acid. Then the iso-cyanic acid is hydrolysed to produce ammonia.



The net effect is that for every mol of urea, two mols of ammonia are produced.

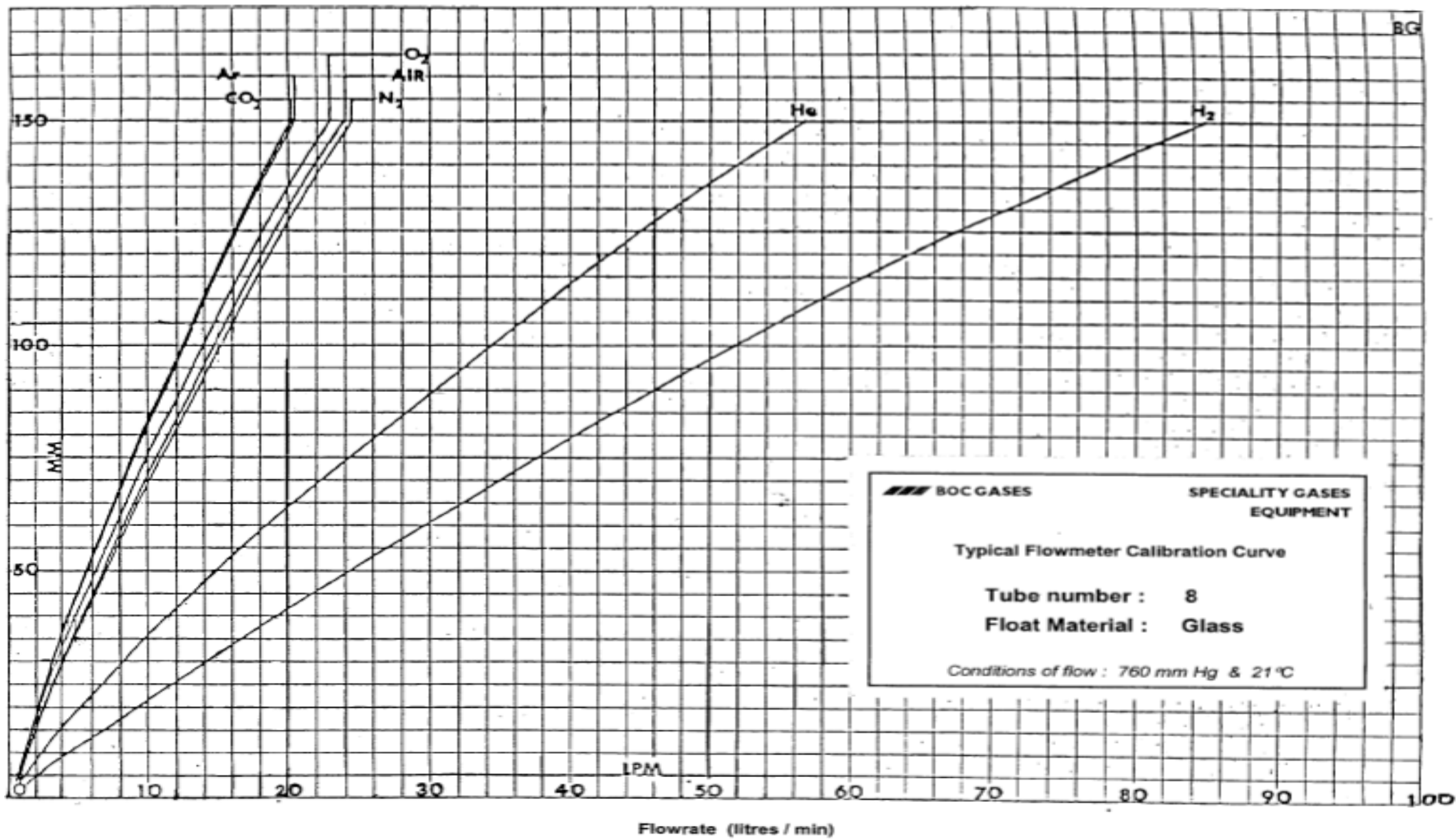
In the experiments described in this thesis, a typical exhaust mass flow rate was 28.5 g/s. An assumption may be made that the mol weight of exhaust is 28.96, the same value as for air. Hence, the rate of exhaust flow may be expressed as 0.984 mol/s.

The spray was calibrated with water. It is assumed that the spray system moves the same volume of aqueous urea as of water. The specific gravity of 32.5% by weight aqueous urea solution is about 1.09. Hence, the spray system flow rate of urea is higher than for water.

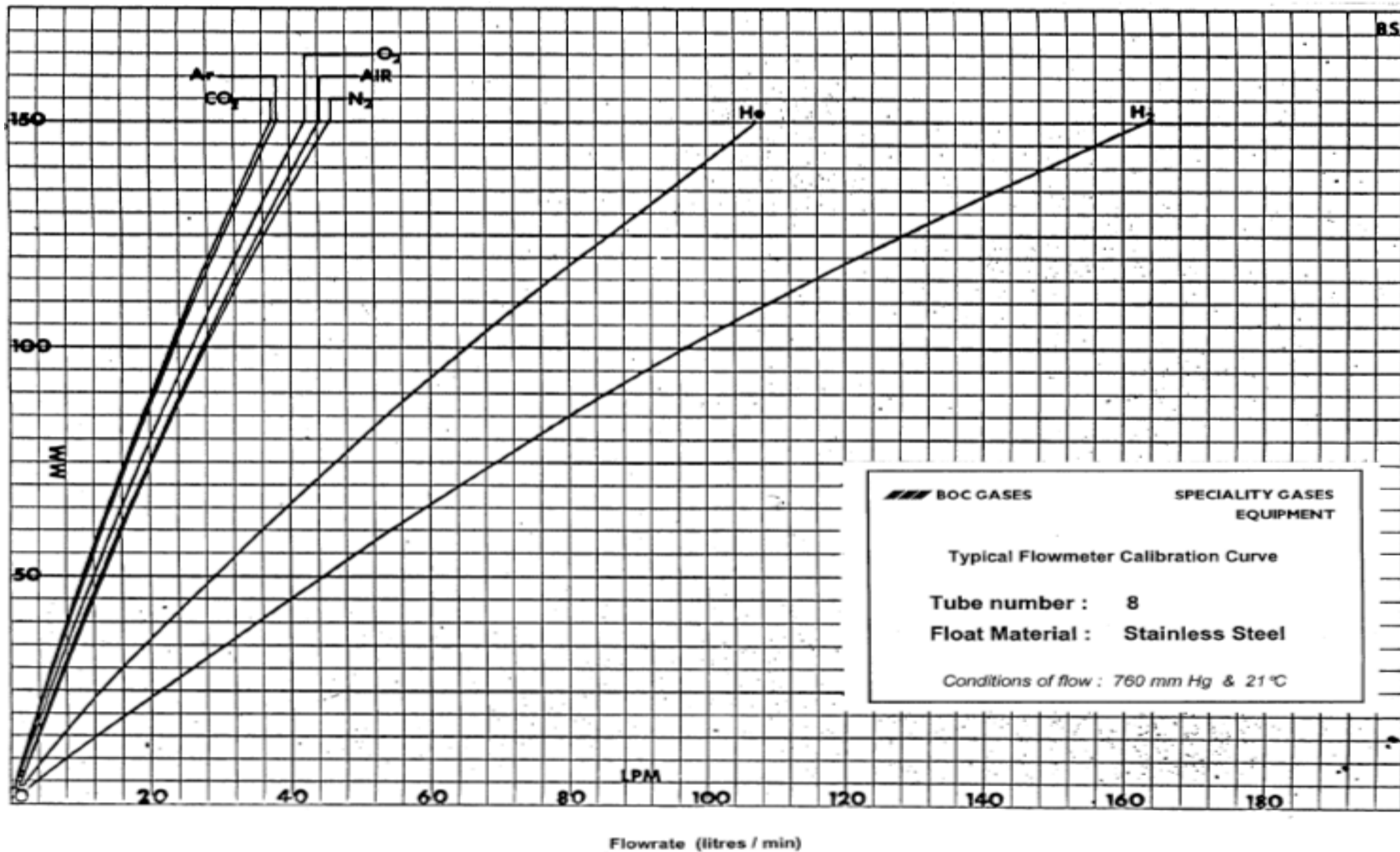
The table below shows Calculation of Potential Ammonia level in exhaust from spray flow rate.

Spray pulse length (ms)	flow rate of water from calibration (mg/s)	Flow rate of urea (mg/s) water x1.09	Flow rate of urea 32.5% by weight (mg/s) fr urea x 32.5%	urea 60g/mol flow rate (mol/s) 1/60.06*1 6.30/1000	urea in 0.984 mol/s exhaust flow (ppm) 0.000271/0.984116 *1 000 000	Potential ammonia (ppm) 1 mol urea = 2 mol ammonia,=2 x 275.6996
24	46	50.1	16.3	0.000271	276	552
26	51	55.6	18.1	0.000301	307	614
* 28	58	63.2	20.5	0.000342	348	696
30	68	74.1	24.1	0.000401	409	818
32	74	80.7	26.2	0.000436	444	888
34	80	87.2	28.3	0.000472	480	960
36	87	94.8	30.8	0.000513	521	1042
40	92	100.3	32.6	0.000543	551	1102

\*Note: The recommended working range for spray injector was from 28 ms upward. Any setting below 28 ms would work intermittently.



Appendix 3.7a Calibration chart for  $\text{NH}_3$  gas flow rate using Glass float



Appendix 3.7b Calibration chart for NH<sub>3</sub> gas flow rate using Stainless Steel float

**Calculation of gas flow rate with 4% & 5% ammonia in N<sub>2</sub> with steel & glass float**

Gas	Mol wt (g)	Sp gravity (SG gas)	Cal Factor
Air	28.96	1.00	1.00
4% ammonia	27.56	0.9517	1.025
5% ammonia	27.45	0.948	1.027

$$CAL\_Factor = \sqrt{\frac{294 \times P_g}{T_g \times 14.7 \times SG}}$$

if T<sub>gas</sub> > 301 K (28 C) changes must be made to avoid error more than 1%

P<sub>gas</sub> > 1 bar (14.7psi)

P<sub>gas</sub> = 1.5 psi 5% error

P<sub>gas</sub> = 3 psi 10 % error

P<sub>g</sub> = gas pressure in flow meter (psi absolute)

T<sub>g</sub> = gas temperature in flow meter (degree absolute)

assume 300 K temp

SG = Specific gravity of gas

**4% Steel Float**

steel	psi	calib chart	pressure correction	corrected l/min	PPM
0	0.0	0	0.000	0	0
16	0.1	4	1.003	4.11	124
40	0.3	10	1.010	10.35	311
50	0.5	13	1.017	13.55	406
60	1.0	16	1.033	16.94	506
75	2.0	20	1.066	21.85	650
100	3.0	28	1.097	31.48	930
120	4.0	34	1.128	39.31	1155

**4% Glass Float**

Glass	psi	calib chart	pressure correction	corrected l/min	PPM
0	0.0	0.0	0.000	0	0
16	0.1	2.0	1.003	2.06	62
40	0.3	5.4	1.010	5.59	168
50	0.4	6.7	1.014	6.96	209
60	0.5	8.5	1.017	8.86	267
75	0.7	10.8	1.023	11.32	340
100	1.0	15.0	1.033	15.88	475
120	1.3	18.0	1.043	19.24	574

**5% Glass Float**

Glass	psi	calib chart	pressure correction	corrected l/min	PPM
0	0.0	0.0	0.000	0.00	0
16	0.1	2.0	1.003	2.06	73
32	0.2	4.1	1.007	4.24	149
48	0.4	6.5	1.014	6.77	238
60	0.5	8.2	1.017	8.56	300
80	0.7	11.5	1.024	12.09	423
96	1.0	13.9	1.033	14.75	515

# Appendix 3.7.1a Calculation of gas flow rate with 4% ammonia in N<sub>2</sub> with steel float

## Calculation of gas flow rate with 4% ammonia in N<sub>2</sub> with steel float

Gas	Mol wt (g)	Sp gravity (SG gas)	Cal Factor
Air	28.96	1.00	1.00
4% ammon	27.56	0.9517	1.025
5% ammon	27.45	0.948	1.027

$$CAL\_Factor = \sqrt{\frac{294 \times P_g}{T_g \times 14.7 \times SG}}$$

if T<sub>gas</sub> > 301 K (28 C) changes must be made to avoid error more than 1%

P<sub>gas</sub> > 1 bar(14.7psi)

P<sub>gas</sub> = 1.5 psi 5% error

P<sub>gas</sub> = 3 psi 10 % error

P<sub>g</sub> = gas pressure in flow meter (psi absolute)

T<sub>g</sub> = gas temperature in flow meter (degree absolute)

assume 300 K temp

SG = Specific gravity of gas

4% Steel Float assume temp. 294 K

steel 4%	psi	calib chart	abs P+psi	pressure correction	abs correction	corrected l/min	corrected flow rate m3/s	PPM
0	0.00	0.0	0.0	0	0	0	0.000000	0
16	0.10	4.0	14.8	1.003	1.025	4.11	0.000069	124
40	0.30	10.0	15.0	1.010	1.025	10.35	0.000173	311
50	0.50	13.0	15.2	1.017	1.025	13.55	0.000226	406
60	1.00	16.0	15.7	1.033	1.025	16.95	0.000282	506
75	2.00	20.0	16.7	1.066	1.025	21.85	0.000364	650
100	3.00	28.0	17.7	1.097	1.025	31.49	0.000525	930
120	4.00	34.0	18.7	1.128	1.025	39.31	0.000655	1155

corrected flow rate m3/s	Flow rate NH3 in 4% mix m3/s	occupies 0.0224 m3 @294 K mol/s	injected mixture (NH3+N2) mol/s	in exhaust incl injected gas mol/s	Ammonia level ppm
0.000000	0.0000000	0.000000	0.00000	0.984	0
0.000069	0.0000027	0.000122	0.00306	0.987	124
0.000173	0.0000069	0.000308	0.00770	0.992	311
0.000226	0.0000090	0.000403	0.01008	0.994	406
0.000282	0.0000113	0.000504	0.01261	0.997	506
0.000364	0.0000146	0.000650	0.01626	1.000	650
0.000525	0.0000210	0.000937	0.02343	1.007	930
0.000655	0.0000262	0.001170	0.02925	1.013	1155

## Sample calculation:

For Steel float at 120 & 4 psi

Reading from Calibration chart is 34.0 litre/min

Assume flowing gas mixture temperature ~ 294 K

so no temperature correction is needed.

Corrected flow rate is 34 x 1.128 x 1.025 = 39.31 liter/min = 0.655 litre/s = 0.000655 m<sup>3</sup>/s

Flow rate of ammonia (4% in mixture) = 0.04 x 0.000655 = 0.0000262 m<sup>3</sup>/s

Assume 1 mol of ammonia occupies 22.4 litres = 0.0224 m<sup>3</sup> at 273 K

Correcting for temperature 1 mol occupies 0.0240 m<sup>3</sup> at 293 K

Thus Ammonia flow rate is 0.0000262/0.0224 = 0.00117 mol/s

Flow rate of injected mixture (ammonia + N<sub>2</sub>) is (100/4) x 0.001170 mol/s = 0.02925 mol/s

The engine exhaust flow rate is 28.5 g/s = 28.5/28.96 mol/s = 0.984 mol/s

Total flow rate is exhaust including injected gas = 0.984 + 0.029 = 1.013 mol/s

Ammonia level = 1 000 000 x (mol/s NH3) / (mol/s exhaust) = 0.001170 / 1.013 \* 1 000 000 = 1155 ppm

## Appendix 3.7.1b Calculation of gas flow rate with 4% ammonia in N<sub>2</sub> with glass float

### Calculation of gas flow rate with 4% ammonia in N<sub>2</sub> with glass float

Gas	Mol wt (g)	Sp gravity (SG gas)	Cal Factor
Air	28.96	1.00	1.00
4% ammonia	27.56	0.9517	1.025
5% ammonia	27.45	0.948	1.027

$$CAL\_Factor = \sqrt{\frac{294 \times P_g}{T_g \times 14.7 \times SG}}$$

if  $T_{gas} > 301\text{ K}$  (28 C) changes must be made to avoid error more than 1%

$P_{gas} > 1\text{ bar}$  (14.7psi)

$P_{gas} = 1.5\text{ psi}$  5% error

$P_{gas} = 3\text{ psi}$  10 % error

$P_g$  = gas pressure in flow meter (psi absolute)

$T_g$  = gas temperature in flow meter (degree absolute)

assume 300 K temp

SG = Specific gravity of gas

4% Glass Float assume temp. 294 K

Glass 4%	psi	calib chart	abs P+psi	pressure correction	abs correction	corrected l/min	corrected flow rate m <sup>3</sup> /s	PPM
0	0.00	0.0	0.0	0	0	0	0	0
16	0.10	2.0	14.8	1.003	1.025	2.06	0.000034	62
40	0.30	5.4	15.0	1.010	1.025	5.59	0.000093	168
50	0.40	6.7	15.1	1.014	1.025	6.96	0.000116	209
60	0.50	8.5	15.2	1.017	1.025	8.86	0.000148	267
75	0.67	10.8	15.4	1.023	1.025	11.32	0.000189	340
100	1.00	15.0	15.7	1.033	1.025	15.89	0.000265	475
120	1.30	18.0	16.0	1.043	1.025	19.25	0.000321	574

corrected flow rate m <sup>3</sup> /s	Flow rate NH <sub>3</sub> in 4% mix m <sup>3</sup> /s	1 mol occupies 0.0224 m <sup>3</sup> @294 K mol/s	Flow rate of injected mixture (NH <sub>3</sub> +N <sub>2</sub> ) mol/s	Tot flow rate in exhaust incl injected gas mol/s	Ammonia level ppm
0.000000	0.0000000	0.000000	0.00000	0.984	0
0.000034	0.0000014	0.000061	0.00152	0.986	62
0.000093	0.0000037	0.000166	0.00415	0.988	168
0.000116	0.0000046	0.000207	0.00518	0.989	209
0.000148	0.0000059	0.000264	0.00661	0.991	267
0.000189	0.0000076	0.000338	0.00844	0.992	340
0.000265	0.0000106	0.000473	0.01183	0.996	475
0.000321	0.0000128	0.000573	0.01433	0.998	574

### Sample calculation:

For Glass float at 120 & 1.3 psi

Reading from Calibration chart is 18.0 litre/min

Assume flowing gas mixture temperature ~ 294 K

so no temperature correction is needed.

Corrected flow rate is  $18 \times 1.043 \times 1.025 = 19.25\text{ litre/min} = 0.321\text{ litre/s} = 0.000321\text{ m}^3/\text{s}$

Flow rate of ammonia (4% in mixture) =  $0.04 \times 0.000321 = 0.0000128\text{ m}^3/\text{s}$

Assume 1 mol of ammonia occupies 22.4 litres =  $0.0224\text{ m}^3$  at 273 K

Correcting for temperature 1 mol occupies  $0.0240\text{ m}^3$  at 293 K

Thus Ammonia flow rate is  $0.0000128/0.0224 = 0.000573\text{ mol/s}$

Flow rate of injected mixture (ammonia + N<sub>2</sub>) is  $(100/4) \times 0.000573\text{ mol/s} = 0.01433\text{ mol/s}$

The engine exhaust flow rate is  $28.5\text{ g/s} = 28.5/28.96\text{ mol/s} = 0.984\text{ mol/s}$

Total flow rate is exhaust including injected gas =  $0.984 + 0.01433 = 0.998\text{ mol/s}$

Ammonia level =  $1\,000\,000 \times (\text{mol/s NH}_3) / (\text{mol/s exhaust}) = 0.000573 / 0.998 \times 1\,000\,000 = 574\text{ ppm}$

# Appendix 3.7.1c Calculation of gas flow rate with 5% ammonia in N<sub>2</sub> with glass float

## Calculation of gas flow rate with 5 % ammonia in N<sub>2</sub> with glass float

Gas	Mol wt (g)	Sp gravity (SG gas)	Cal Factor
Air	28.96	1.00	1.00
4% ammon	27.56	0.9517	1.025
5% ammon	27.45	0.948	1.027

$$CAL\_Factor = \sqrt{\frac{294 \times P_g}{T_g \times 14.7 \times SG}}$$

if T<sub>gas</sub> > 301 K (28 C) changes must be made to avoid error more than 1%

P<sub>gas</sub> > 1 bar(14.7psi)

P<sub>gas</sub> = 1.5 psi 5% error

P<sub>gas</sub> = 3 psi 10 % error

P<sub>g</sub> = gas pressure in flow meter (psi absolute)

T<sub>g</sub> = gas temperature in flow meter (degree absolute)

SG = Specific gravity of gas

5% Glass Float assume temp. 294 K

Glass 5%	psi	calib chart	abs P+psi	pressure correction	abs correction	corrected l/min	corrected flow rate	PPM
0	0	0	0	0	0	0	0.000000	0
16	0.1	2	14.8	1.003	1.027	2.06	0.000034	73
32	0.2	4.1	14.9	1.007	1.027	4.24	0.000071	149
48	0.4	6.5	15.1	1.014	1.027	6.77	0.000113	238
60	0.5	8.2	15.2	1.017	1.027	8.56	0.000143	300
80	0.7	11.5	15.4	1.024	1.027	12.09	0.000201	423
96	1.0	13.9	15.7	1.033	1.027	14.75	0.000246	515

corrected flow rate m <sup>3</sup> /s	Flow rate NH <sub>3</sub> in 5% mix m <sup>3</sup> /s	1 mol occupies 0.0240 m <sup>3</sup> @294 K mol/s	Flow rate of injected mixture mol/s	Tot flow rate in exhaust incl injected gas mol/s	Ammonia level ppm
0.000000	0.0000000	0.0000000	0.00000	0.984	0
0.000034	0.0000017	0.0000716	0.00143	0.985	73
0.000071	0.0000035	0.0001472	0.00294	0.987	149
0.000113	0.0000056	0.0002349	0.00470	0.989	238
0.000143	0.0000071	0.0002973	0.00595	0.990	300
0.000201	0.0000101	0.0004197	0.00839	0.992	423
0.000246	0.0000123	0.0005123	0.01025	0.994	515

## Sample calculation:

For Glass float at 96 & 1.0 psi

Reading from Calibration chart is 13.9 litre/min

Assume flowing gas mixture temperature ~ 294 K

so no temperature correction is needed.

Corrected flow rate is 13.9 x 1.033 x 1.027 = 14.75 liter/min = 0.246 litre/s = 0.000246 m<sup>3</sup>/s

Flow rate of ammonia (5% in mixture) = 0.05 x 0.000246 = 0.0000123 m<sup>3</sup>/s

Assume 1 mol of ammonia occupies 22.4 litres = 0.0224 m<sup>3</sup> at 273 K

Correcting for temperature 1 mol occupies 0.0240 m<sup>3</sup> at 293 K

Thus Ammonia flow rate is 0.0000123/0.024 = 0.000513 mol/s

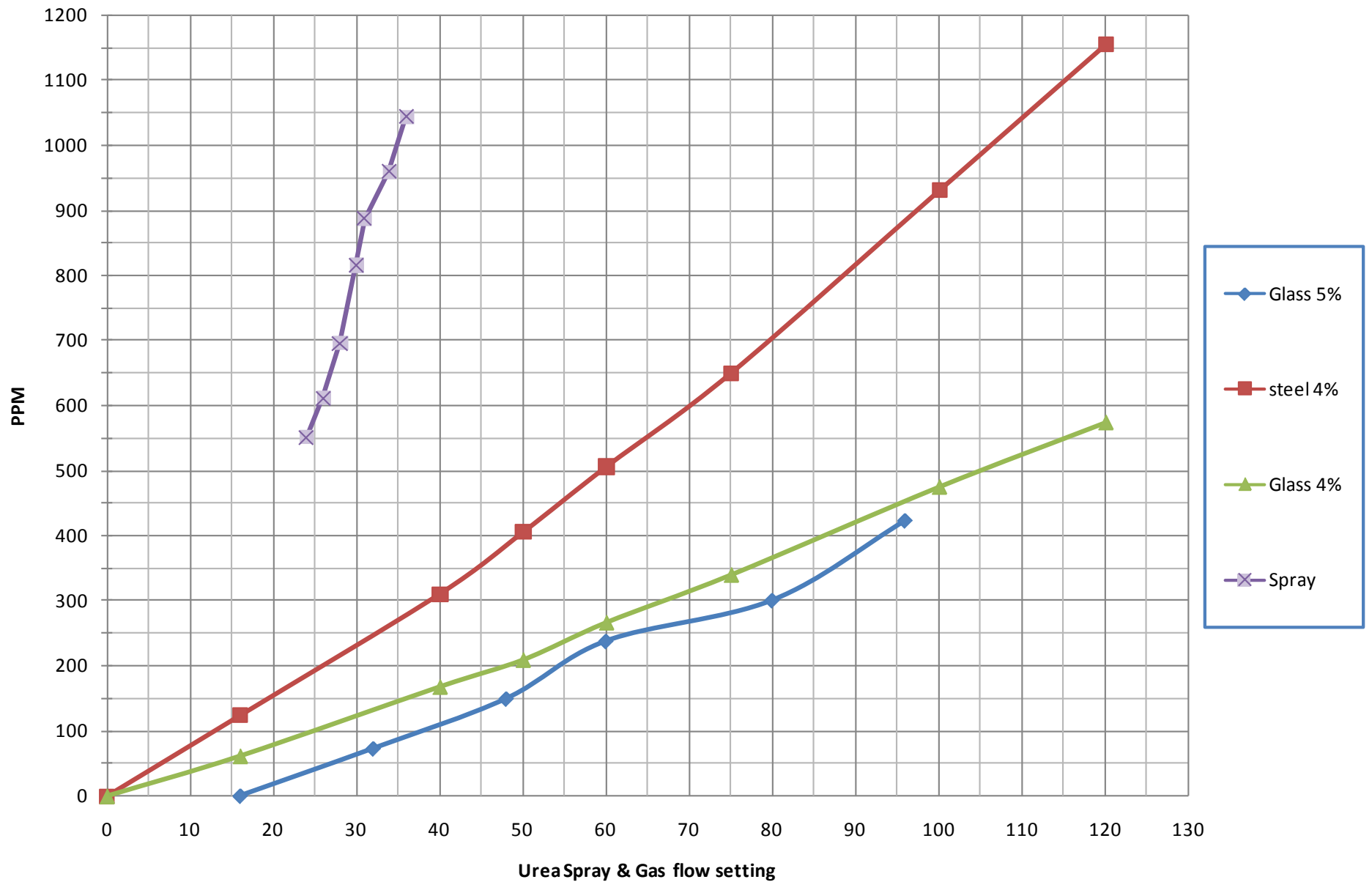
Flow rate of injected mixture (ammonia + N<sub>2</sub>) is (100/5) x 0.000513 mol/s = 0.01025 mol/s

The engine exhaust flow rate is 28.5 g/s = 28.5/28.96 mol/s = 0.984 mol/s

Total flow rate is exhaust including injected gas = 0.984 + 0.010 = 0.994 mol/s

Ammonia level = (mol/s NH<sub>3</sub>) / (mol/s exhaust) x 1 000 000 = 0.000513 / 0.994 x 1 000 000 = 515 ppm

Appendix 3.7.1d Gas and Spray setting vs. Ammonia produced





#### **4.0 - List of appendices for Chapter 4 : Experimental Results**

##### **Appendix 4.1.5 Experimental data for Urea Spray: 1 SCR**

Date: (3, 7, 9 July 2008)

0700708a NO<sub>2</sub> upstream & downstream 1 SCR no spray

090708c NH<sub>3</sub> upstream 1 SCR R

070708b NO<sub>2</sub> downstream 1 SCR

090708b NH<sub>3</sub> downstream 1 SCR L

##### **Appendix 4.1.5b SUM in and SUM out average for 1 SCR with spray**

150708c NH<sub>3</sub> upstream 1 SCR L

150708c NH<sub>3</sub> upstream 1 SCR R

090708c NH<sub>3</sub> upstream 1 SCR L

090708c NH<sub>3</sub> upstream 1 SCR R

070708d NH<sub>3</sub> upstream 1 SCR

150708b NH<sub>3</sub> downstream 1 SCR Left

150708b NH<sub>3</sub> downstream 1 SCR Right

090708b NH<sub>3</sub> downstream 1 SCR L

090708b NH<sub>3</sub> downstream 1 SCR R

070708c NH<sub>3</sub> downstream 1 SCR

#### **Appendix 4.1.6 Experimental data for Urea Spray: 4 SCR**

Date: (1, 7,18,23,24 July 2008)

240708b NO<sub>2</sub> up 4 SCR L-R with spray

240708b NH<sub>3</sub> upstream 4 SCR L1-R1-L1

020708c NO<sub>2</sub> downstream 4 SCR with spray

230708b NH<sub>3</sub> downstream 4 SCR R1

#### **Appendix 4.1.6b SUM in and SUM out average for 4 SCR with spray**

180708c NH<sub>3</sub> upstream 4 SCR spray 34-24 L-R

240708b NH<sub>3</sub> upstream 4 SCR spray L

240708b NH<sub>3</sub> upstream 4 SCR spray R

180708b NH<sub>3</sub> downstream 4 SCR L - R

230708b NH<sub>3</sub> downstream 4 SCR L-R

#### **Appendix 4.2.5 Experimental data for 5% NH<sub>3</sub> gas: 1 SCR**

Date: (5%gas 12, 21 august 2008)

120808b NH<sub>3</sub> upstream 1 SCR 5% gas

120808c NH<sub>3</sub> downstream 1 SCR 5% gas

210808c NO downstream 1 SCR 5% gas

210208 NO downstream 1 SCR 5%-manual log in log book (**Appendix 4.2.5b**)

#### **Appendix 4.2.6** Experimental data for **NH<sub>3</sub> gas: 2 SCR**

Date:(11 august 2008)

110808b NH<sub>3</sub> upstream 2 SCR 5% gas

110808c NH<sub>3</sub> downstream 2 SCR 5% gas

210808c NO downstream 1 SCR 5% gas

#### **Appendix 4.2.7** Experimental data for **NH<sub>3</sub> gas: 3 SCR**

Date:(7 august 2008)

070808b NH<sub>3</sub> upstream 3 SCR 5% gas

070808c NH<sub>3</sub> downstream 3 SCR 5% gas

#### **Appendix 4.2.8** Experimental data for **NH<sub>3</sub> gas: 4 SCR**

Date:(16, 25 jun2008 & 5, 6 august 2008)

060808b NH<sub>3</sub> upstream 4 SCR 5% gas

060808e NH<sub>3</sub> downstream 4 SCR 5% gas

060808c NO<sub>2</sub> upstream 4 SCR 5% gas

060808d NO<sub>2</sub> downstream 4 SCR 5% gas

#### **Appendix 4.2.9** Experimental data for **4% NH<sub>3</sub> gas: 1 SCR**

Date:(Trial 4% 10, 11,12,16,24 jun08/final5%gas 12, 21 august 2008)

100608b NH<sub>3</sub> upstream 1 SCR 4% gas

100608c NO upstream 1 SCR 4% gas

100608b NH<sub>3</sub> downstream 1 SCR 4% gas

100608d NO<sub>2</sub> downstream 1 SCR 4% gas

### **Appendix 4.1.5 Experimental data for Urea Spray: 1 SCR**

**Dates: (3, 7, 9 July 2008)**

0700708a NO<sub>2</sub> upstream & downstream 1 SCR no spray

090708c NH<sub>3</sub> upstream 1 SCR R

070708b NO<sub>2</sub> downstream 1 SCR

090708b NH<sub>3</sub> downstream 1 SCR L

Appendix 4.1.5b SUM in and SUM out average for 1 SCR with spray

150708c NH<sub>3</sub> upstream 1 SCR L

150708c NH<sub>3</sub> upstream 1 SCR R

090708c NH<sub>3</sub> upstream 1 SCR L

090708c NH<sub>3</sub> upstream 1 SCR R

070708d NH<sub>3</sub> upstream 1 SCR

150708b NH<sub>3</sub> downstream 1 SCR Left

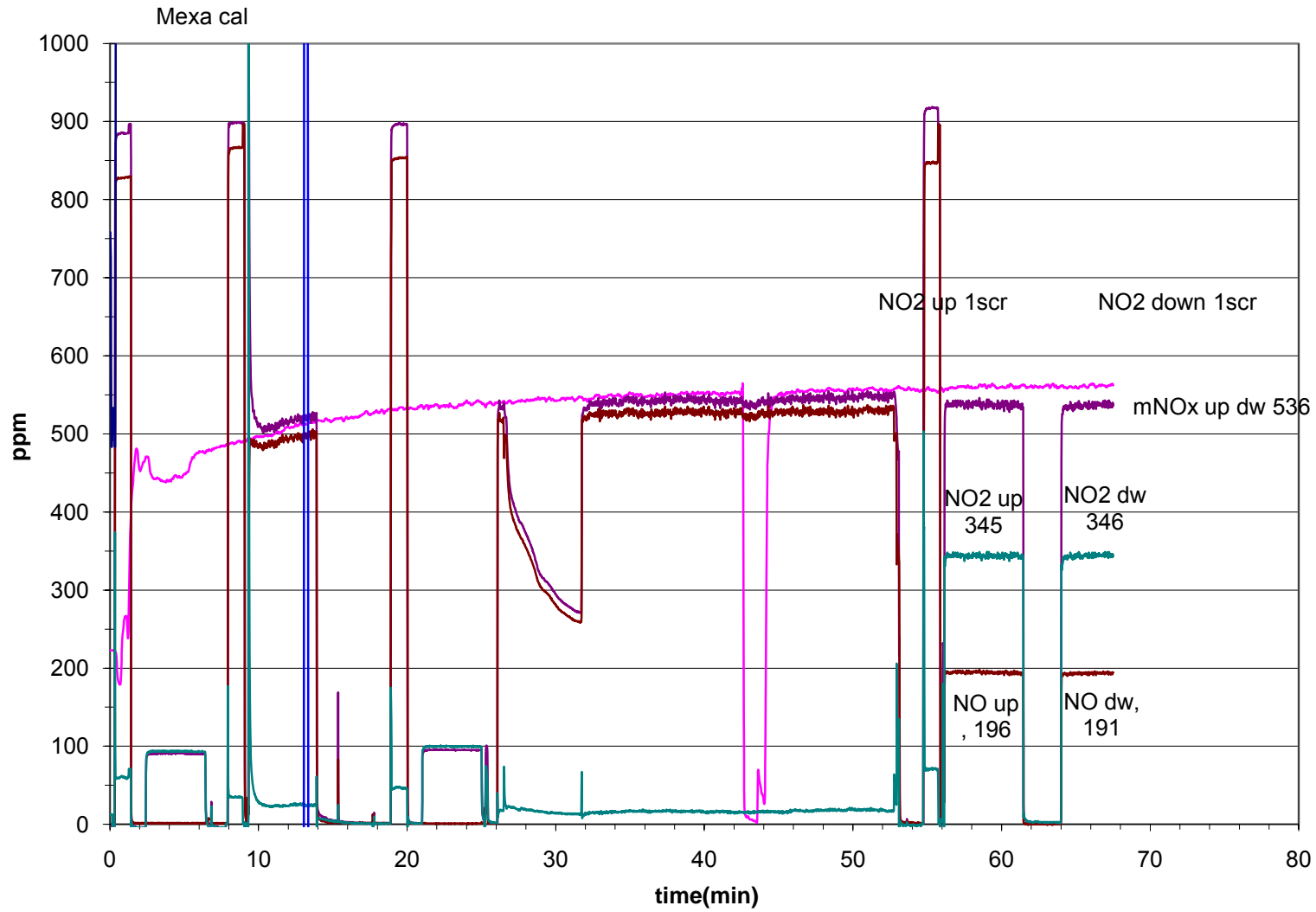
150708b NH<sub>3</sub> downstream 1 SCR Right

090708b NH<sub>3</sub> downstream 1 SCR L

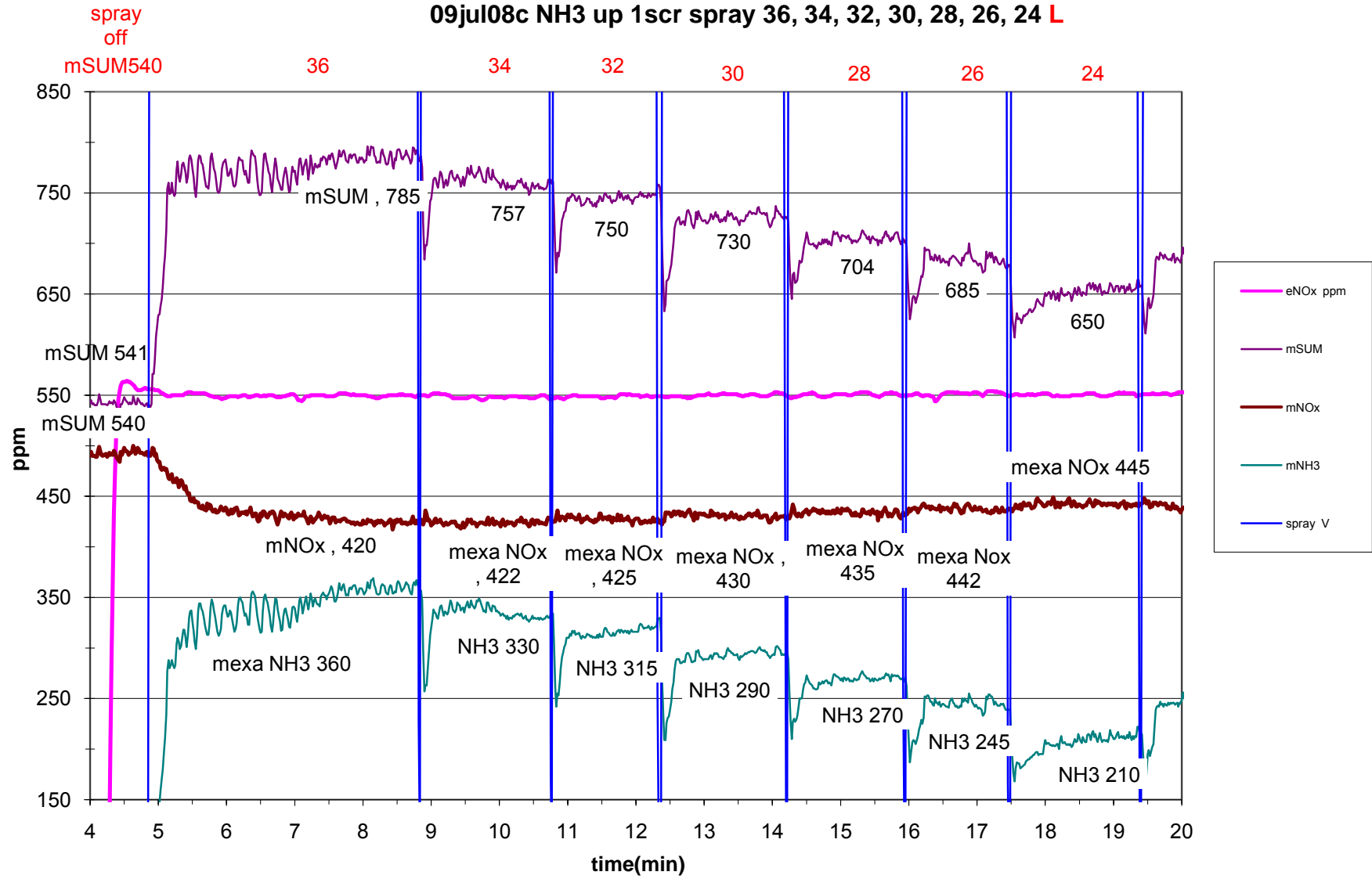
090708b NH<sub>3</sub> downstream 1 SCR R

070708c NH<sub>3</sub> downstream 1 SCR

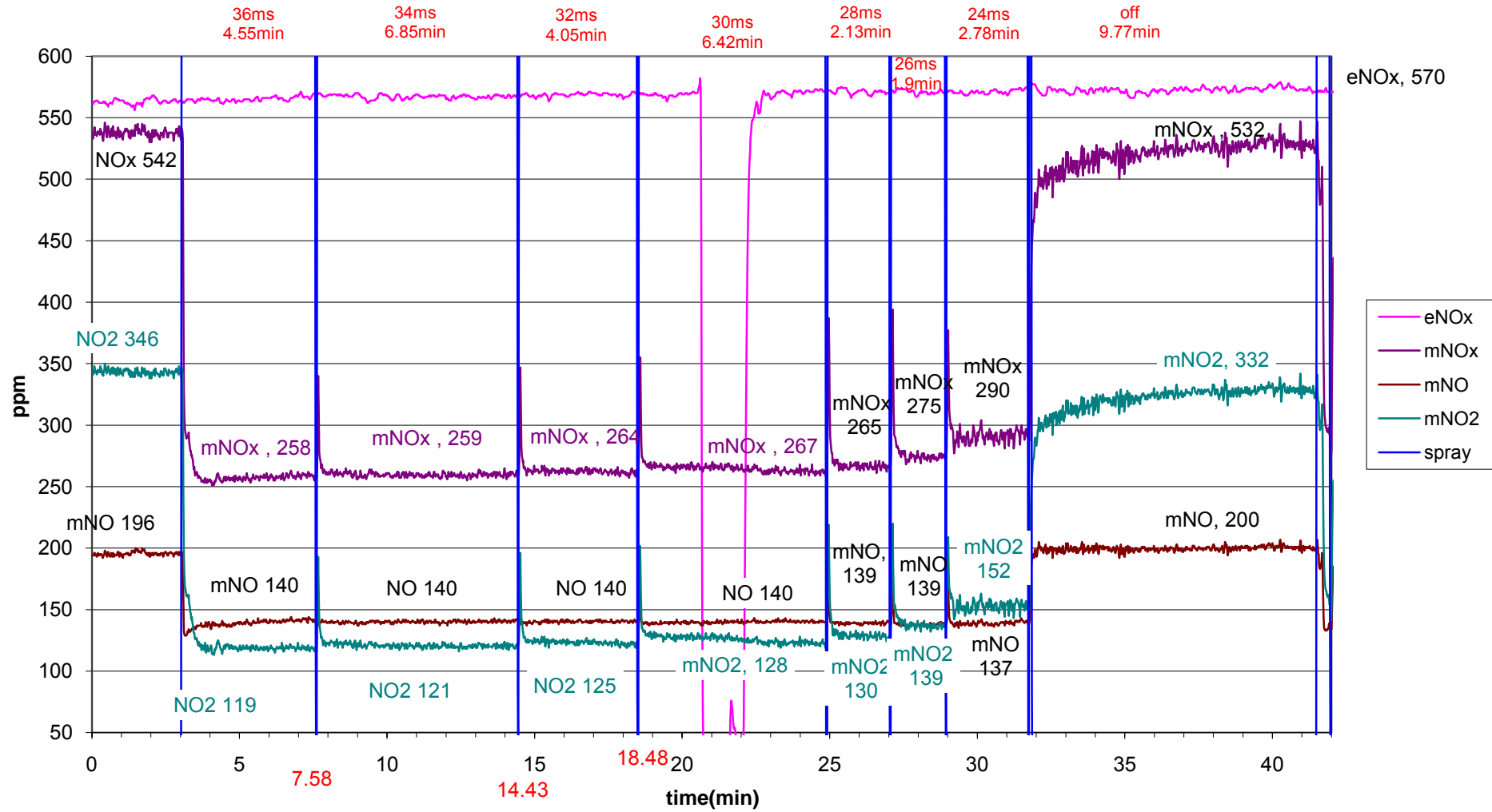
# 7jul08a NO2 up & down 1scr no spray



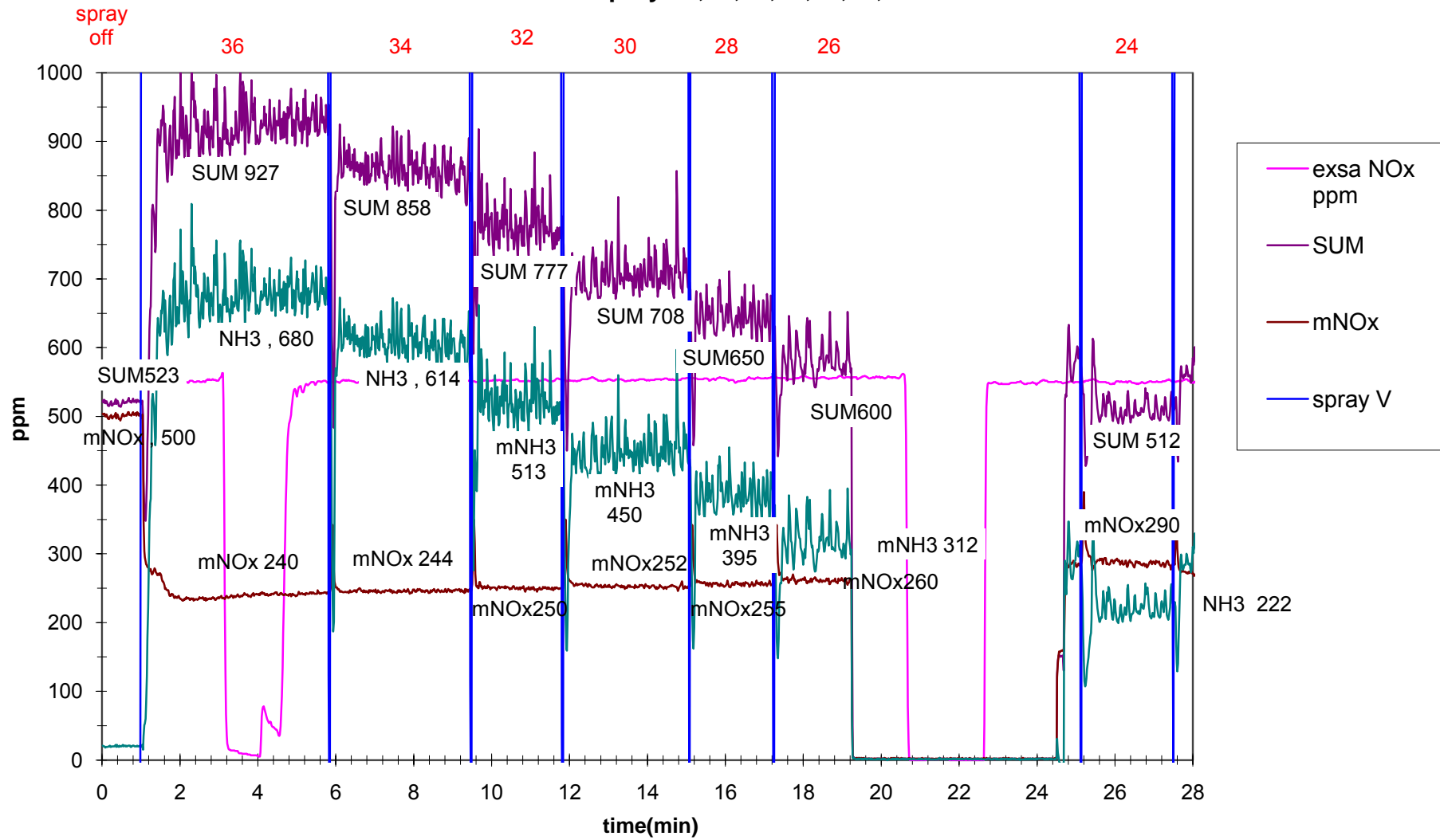
09jul08c NH3 up 1scr spray 36, 34, 32, 30, 28, 26, 24 L



7jul08b NO2 mode  
down 1SCR  
spray 36,34,32,30,24,off



9jul08b NH3 dw 1scr L  
spray 36,34,32,30,28,26,24



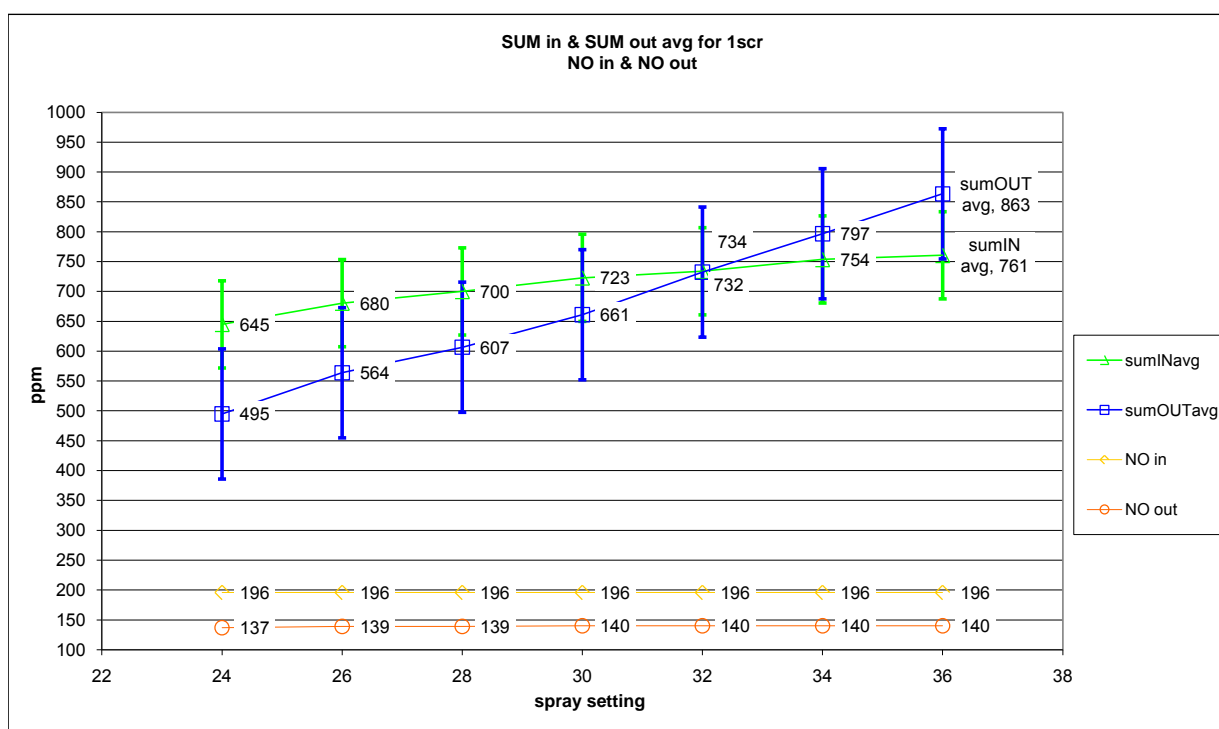


Appendix 4.1.5b SUM in and SUM out average for 1 SCR with spray

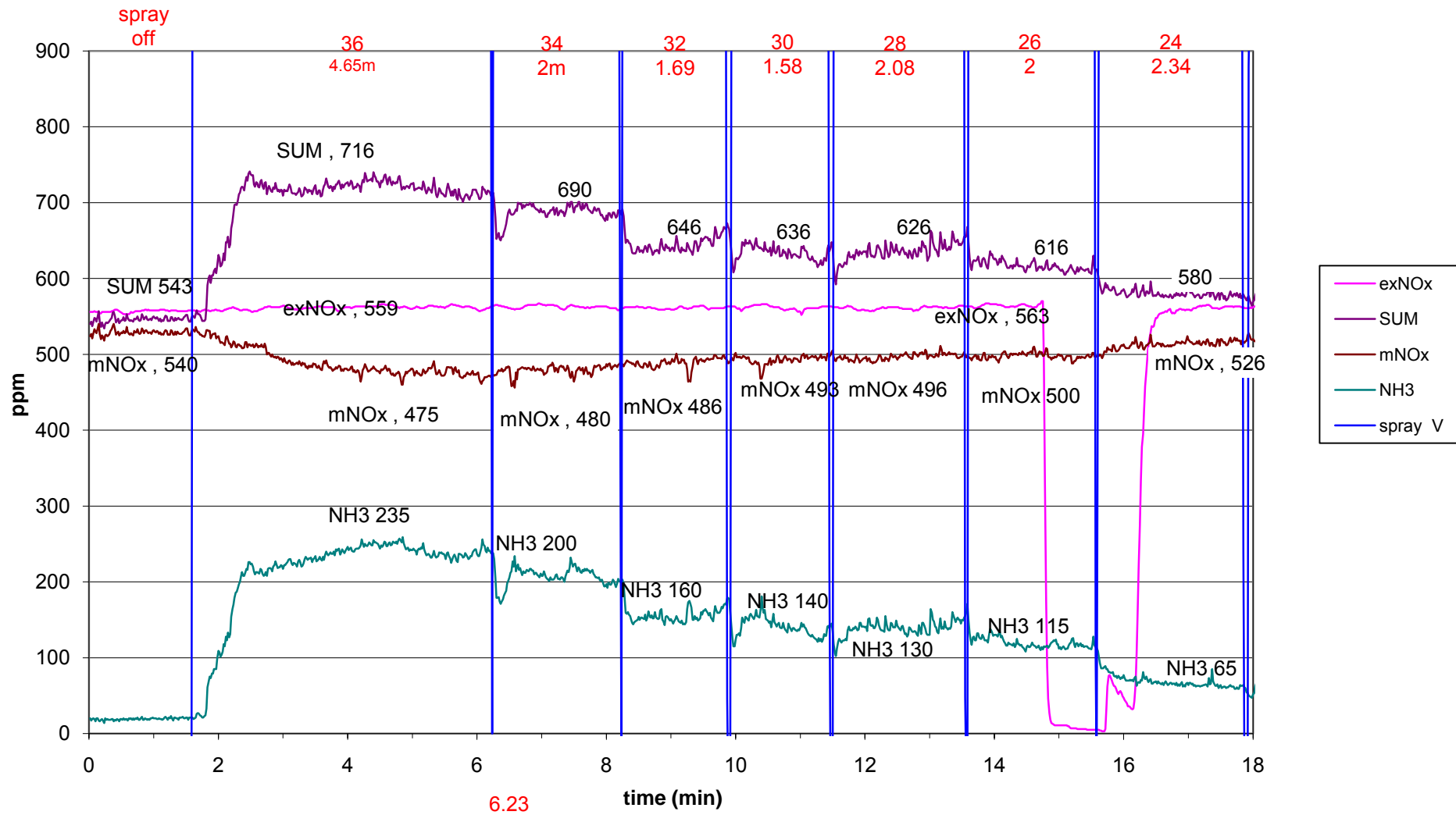
1scr spray variance

SUM IN											
refn	15/7L	15/7R	9/7L	9/7R	7/7d	Data 4 CFD					
	spray	sum1	sum2	sum3	sum4	sum5	sumINavg	std dev	INupper lin	INlower lin	NO in
36	36	716	741	785	800		761	39	799	722	196
34	34	690	720	757	766	835	754	55	808	699	196
32	32	646	700	750	740	833	734	69	803	665	196
30	30	636	670	730	737	841	723	78	801	644	196
28	28	626	650	704	718	802	700	68	768	632	196
26	26	616	616	685	688	797	680	74	755	606	196
24	24	580	591	650	657	746	645	66	711	579	196
off	0	543	565	540	541	563	550	12	563	538	196

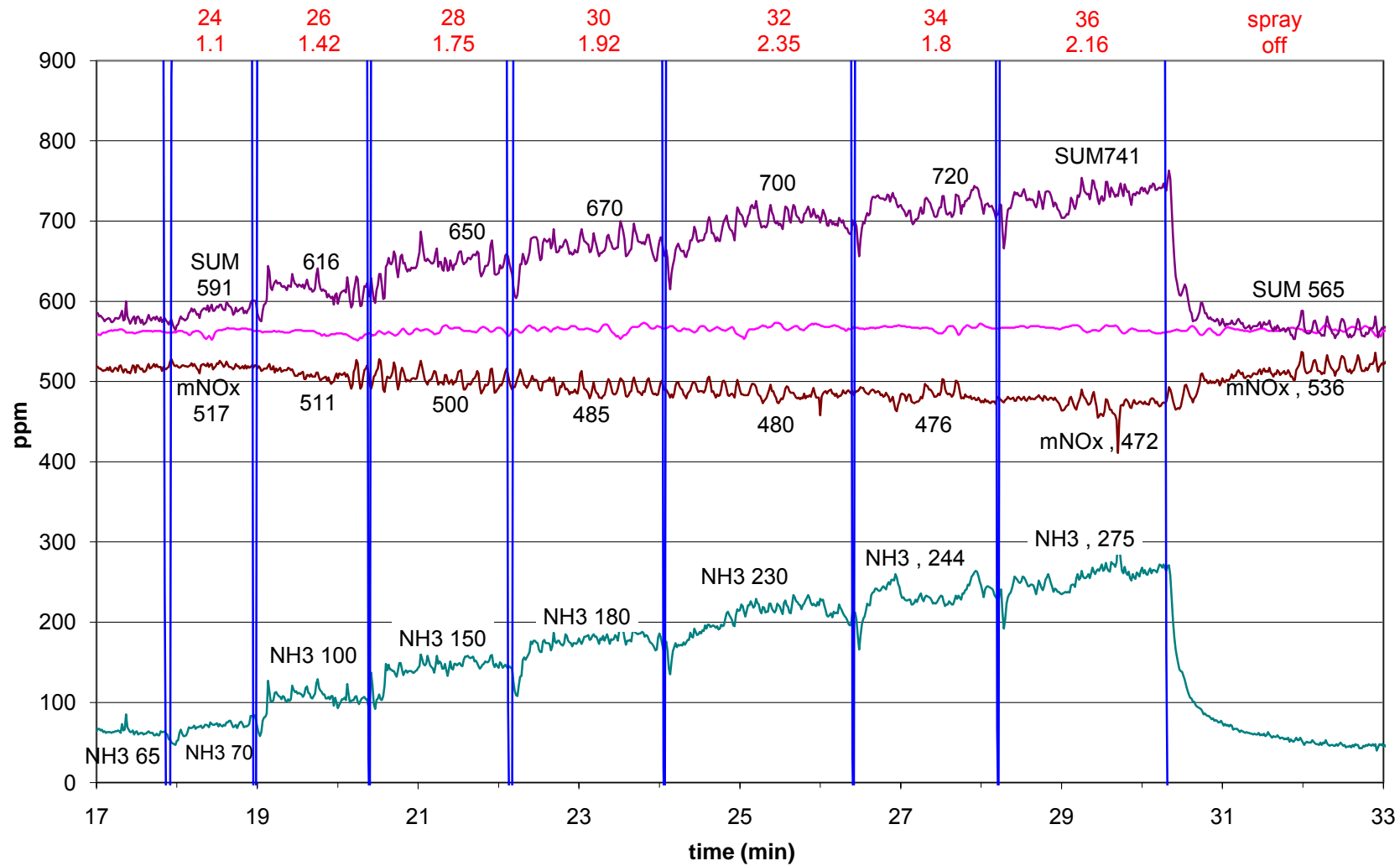
SUM OUT											
refn	15/7L	15/7R	9/7L	9/7R	7/7c	Data 4 CFD					
	spray	sumA	sumB	sumC	sumD	sumE	sumOUTavg	std dev	OUTupper	OUTlower	NO out
36	36	850	750	927	822	968	863	86	950	777	140
34	34	780	700	858	736	909	797	86	883	710	140
32	32	700	635	777	720	830	732	75	807	658	140
30	30	550	590	708	691	766	661	89	750	572	140
28	28	472	534	650	674	703	607	99	705	508	139
26	26	514	470	600	610	625	564	68	632	496	139
24	24	433	440	512	541	548	495	55	550	440	137
off	0	539	550	523	516	562	539	19	558	520	200



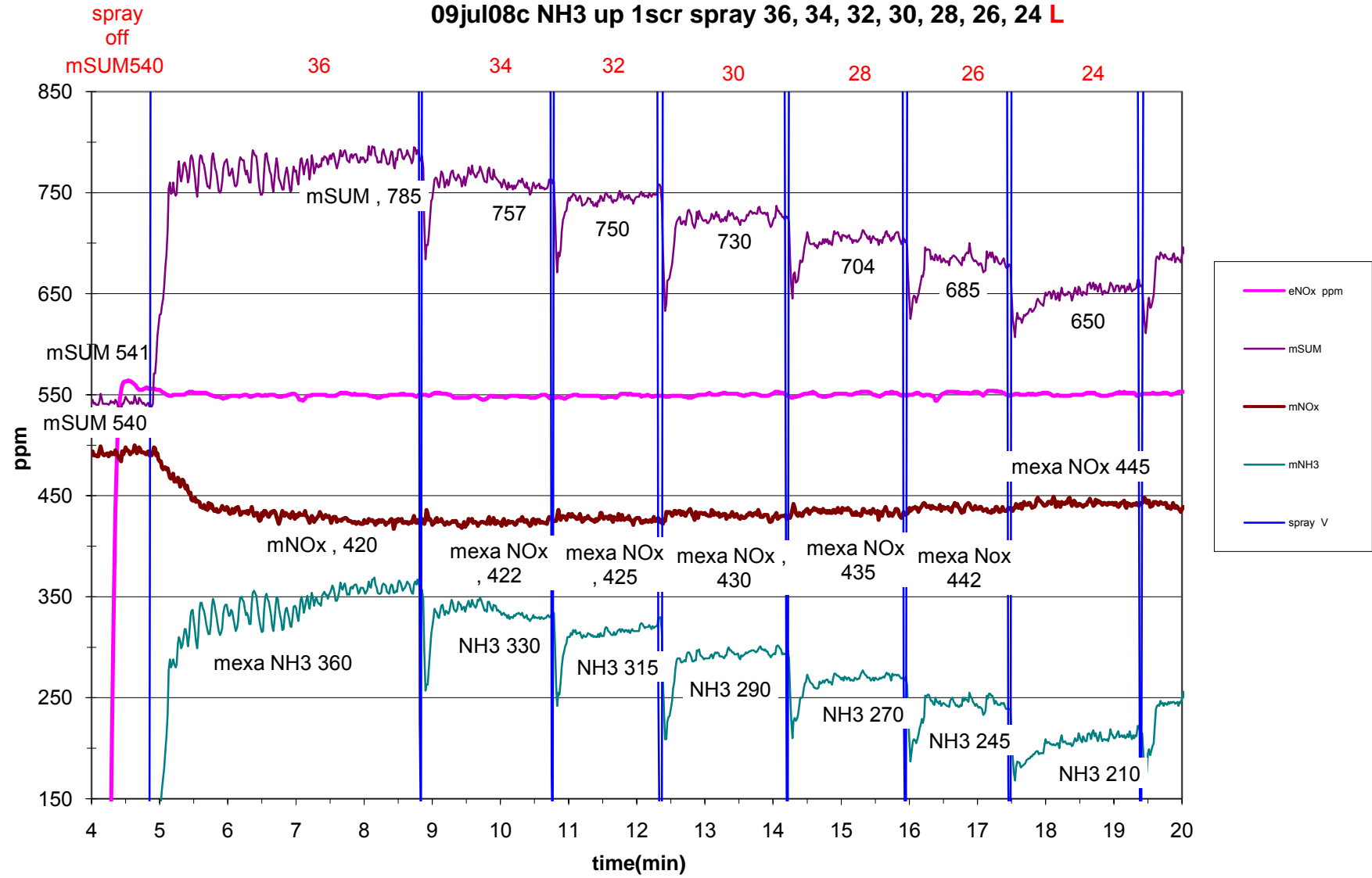
15jul08c L  
spray 36-24 NH3 up1SCR

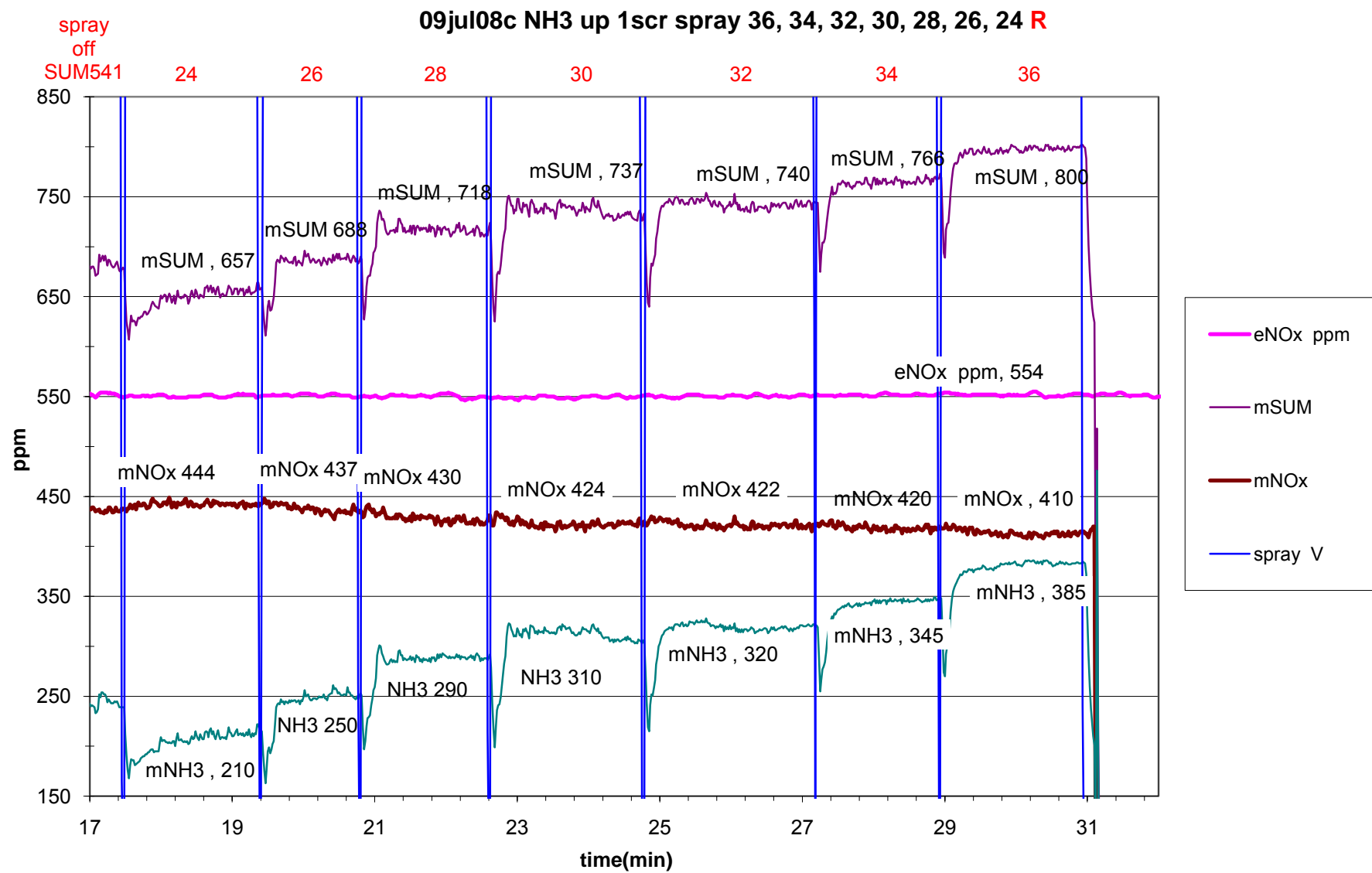


15jul08c R  
spray 24-36 NH3 up1SCR

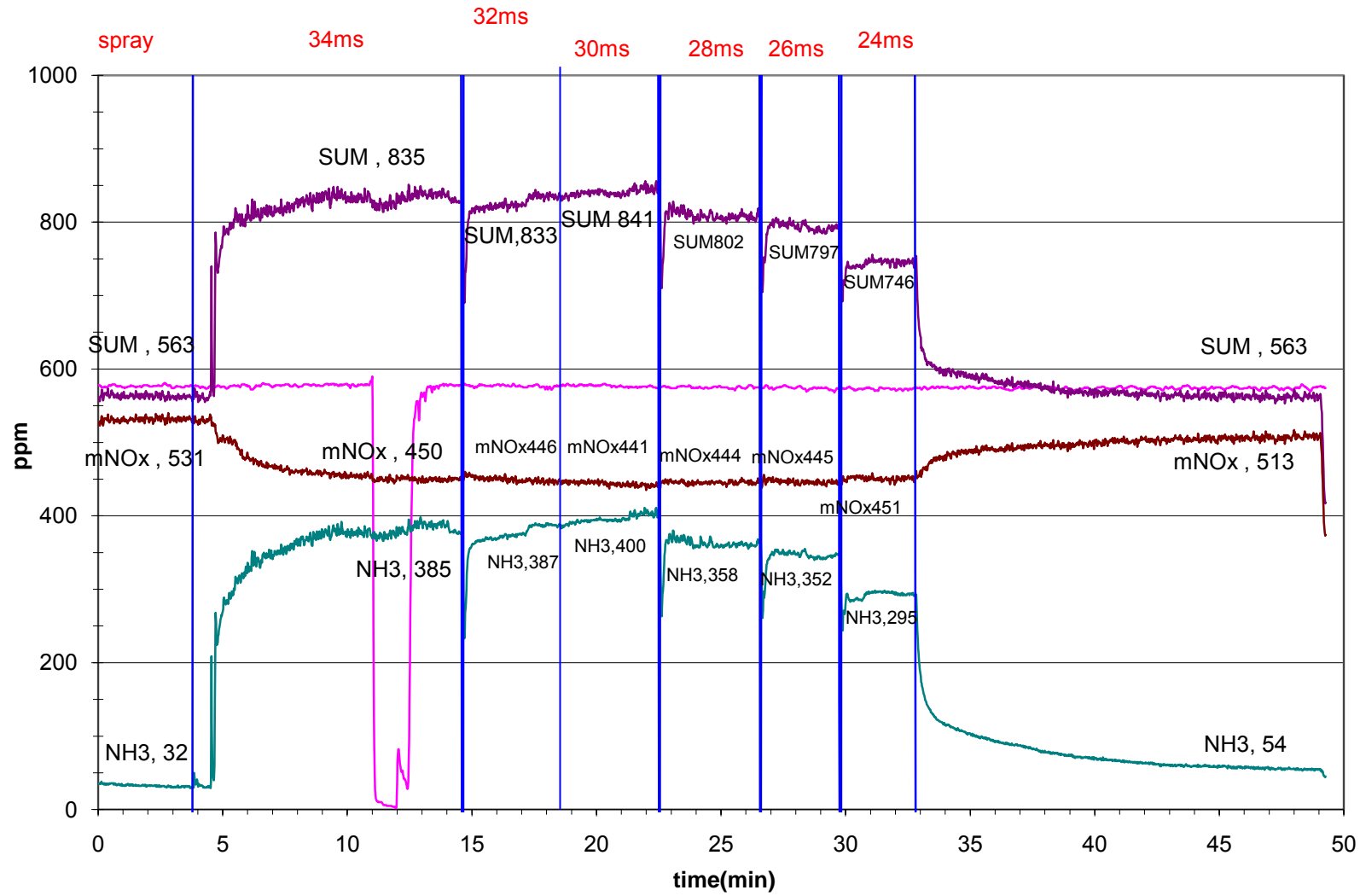


09jul08c NH3 up 1scr spray 36, 34, 32, 30, 28, 26, 24 L

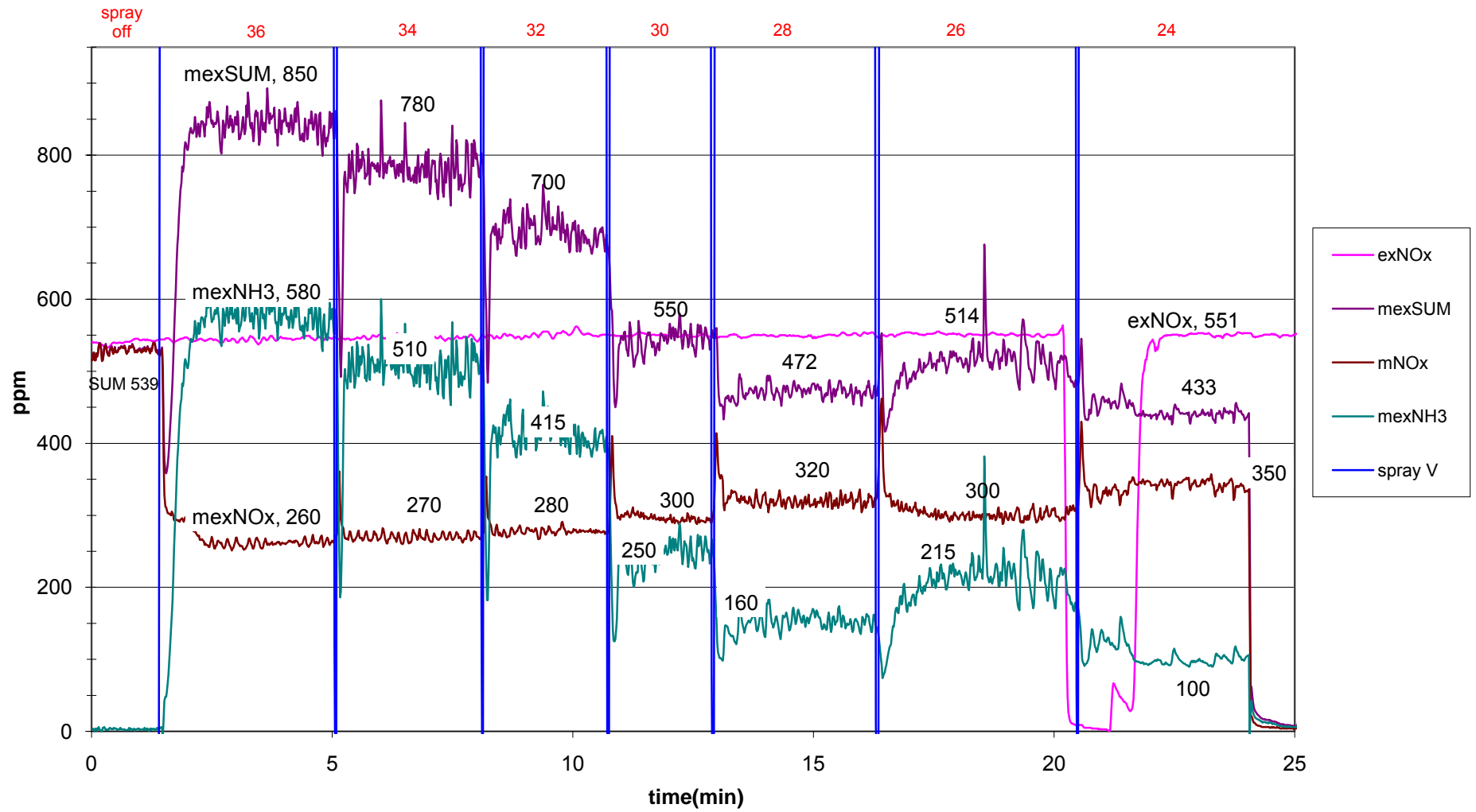




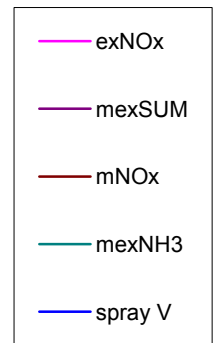
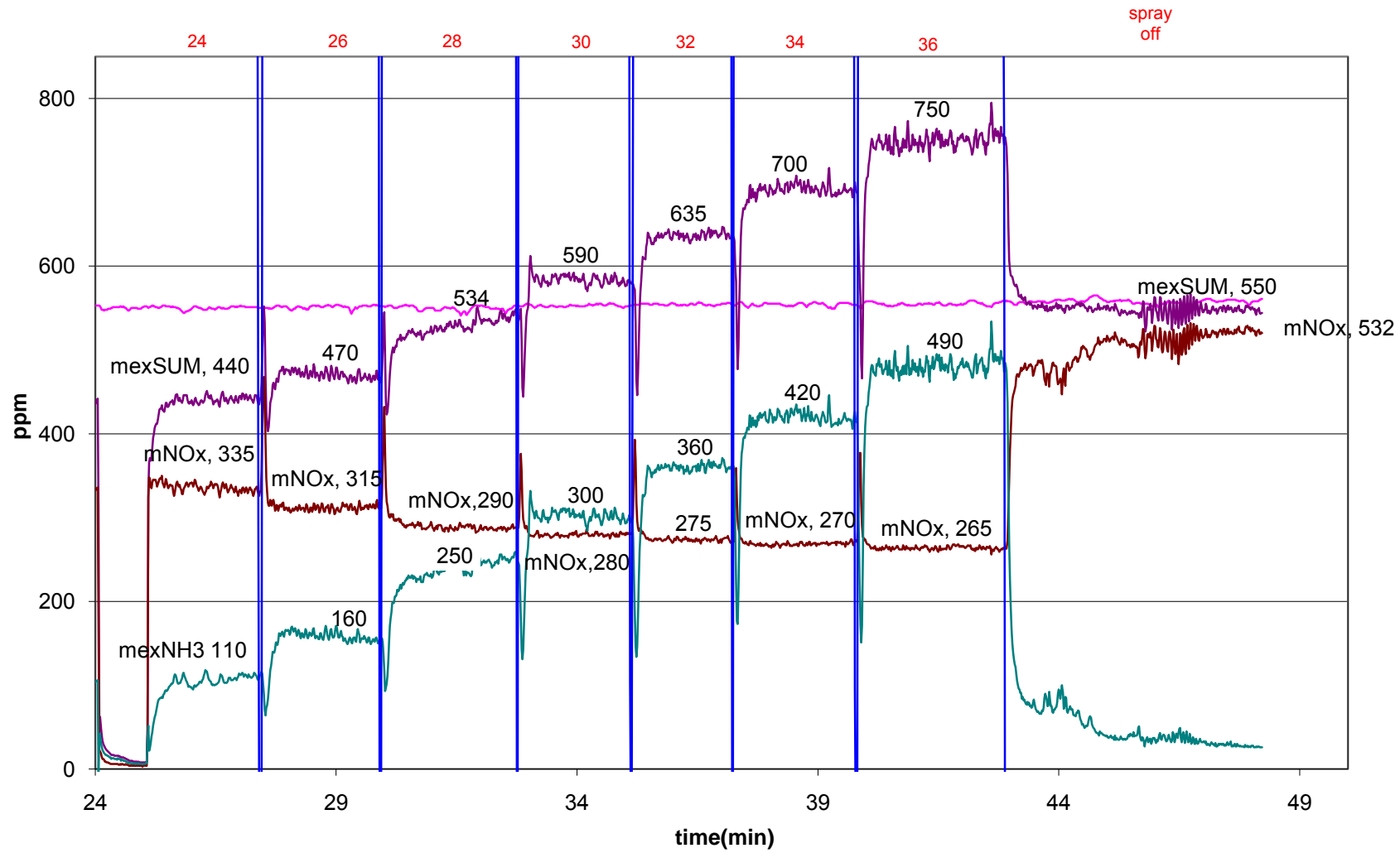
7jul08d nh3 up 1scr  
spray 34,32,30,28,26,24,off



15jul08b NH3 dw 1scr  
spray 36-24 **Left**

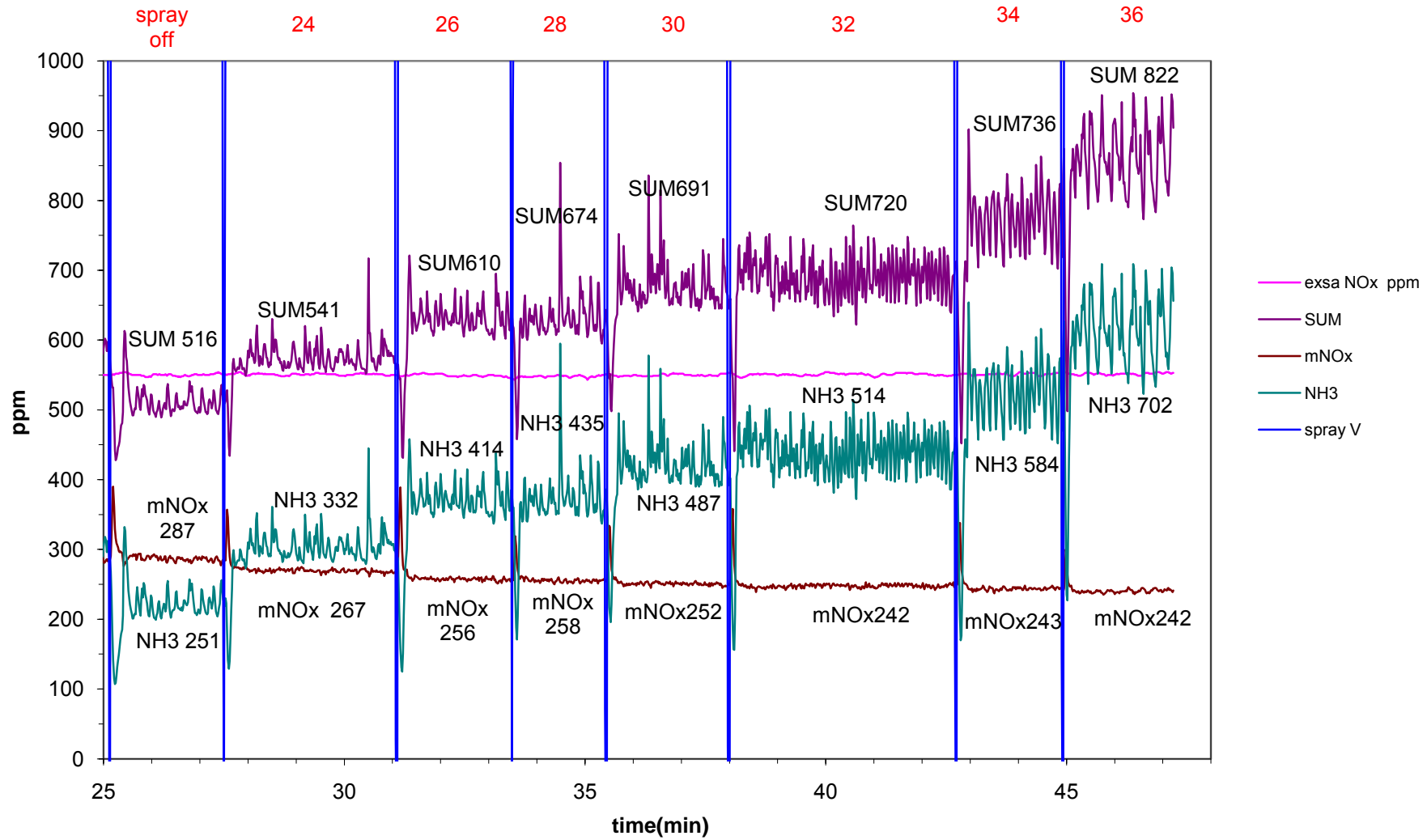


15jul08b NH3 dw 1scr  
spray 24-36 **Right**

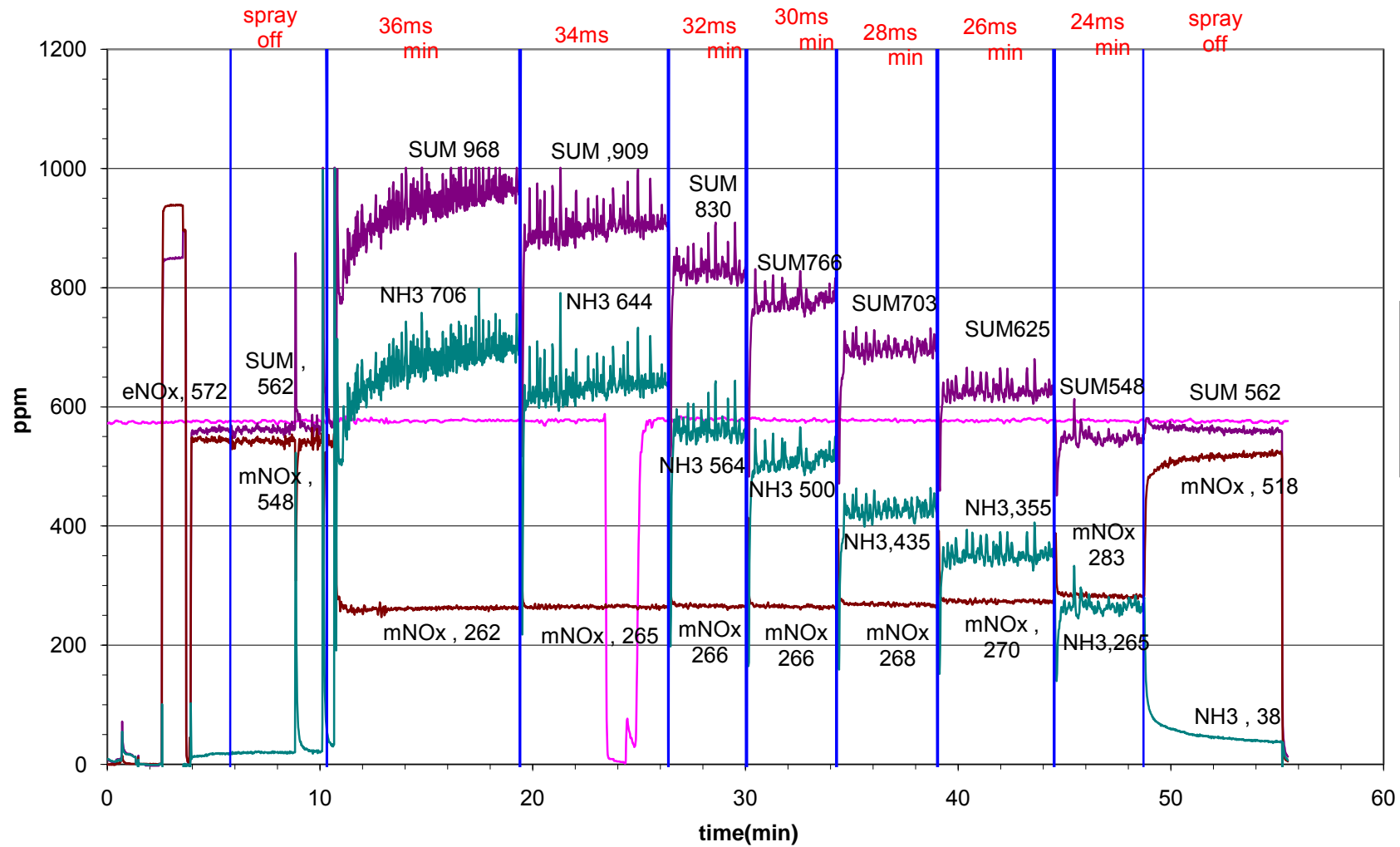




9jul08b NH3 dw 1scr R  
spray 36,34,32,30,28,26,24



7jul08c NH3down 1SCR,  
Spray 36,34,32,30,28,26,24,off



## **Appendix 4.1.6 Experimental data for Urea Spray: 4 SCR**

**Dates: (1, 7,18,23,24 July 2008)**

240708b NO<sub>2</sub> up 4 SCR L-R with spray

240708b NH<sub>3</sub> upstream 4 SCR L1-R1-L1

020708c NO<sub>2</sub> downstream 4 SCR with spray

230708b NH<sub>3</sub> downstream 4 SCR R1

Appendix 4.1.6b SUM in and SUM out average for 4 SCR with spray

180708c NH<sub>3</sub> upstream 4 SCR spray 34-24 L-R

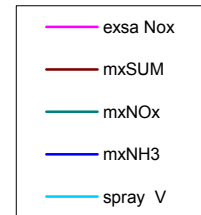
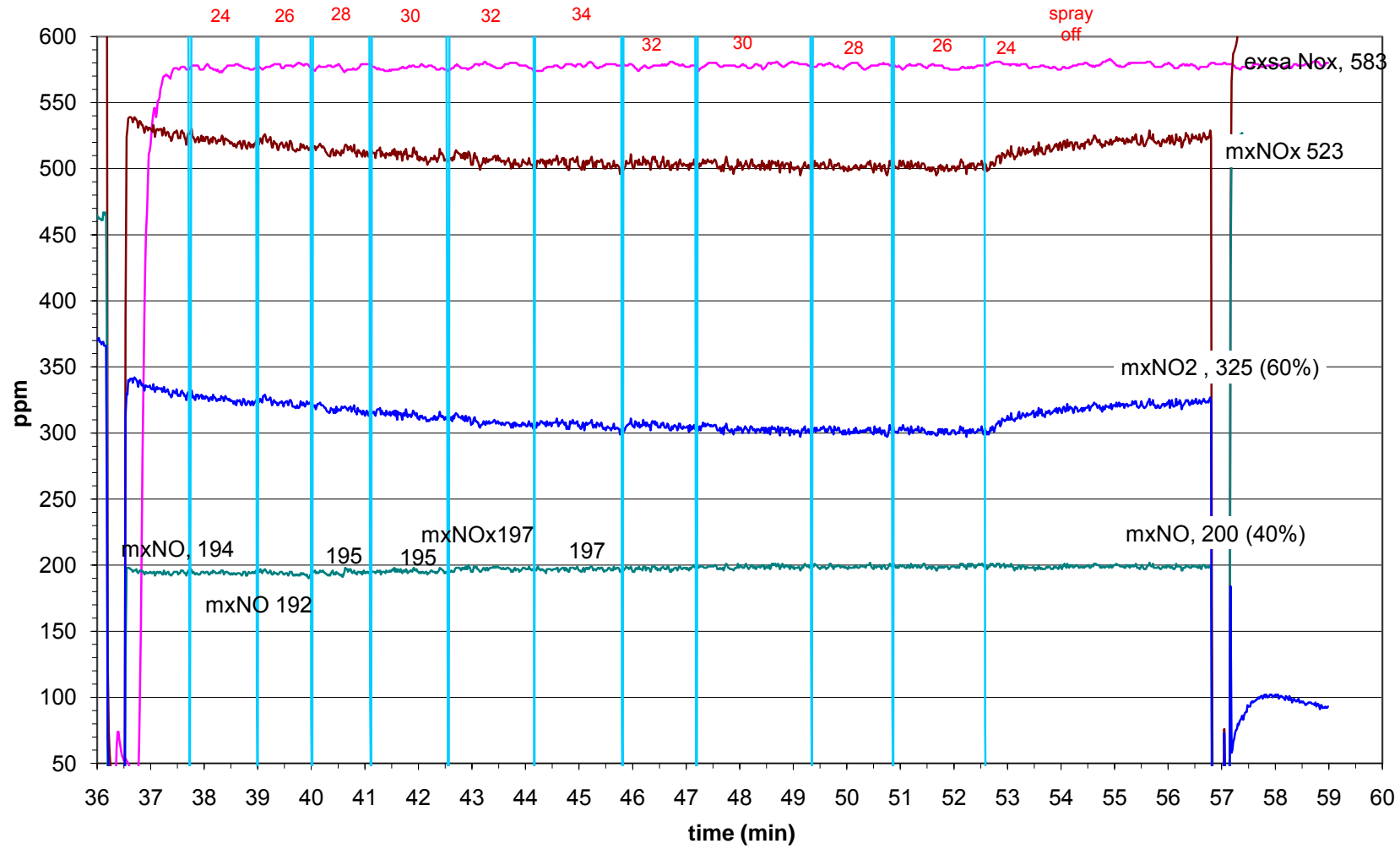
240708b NH<sub>3</sub> upstream 4 SCR spray L

240708b NH<sub>3</sub> upstream 4 SCR spray R

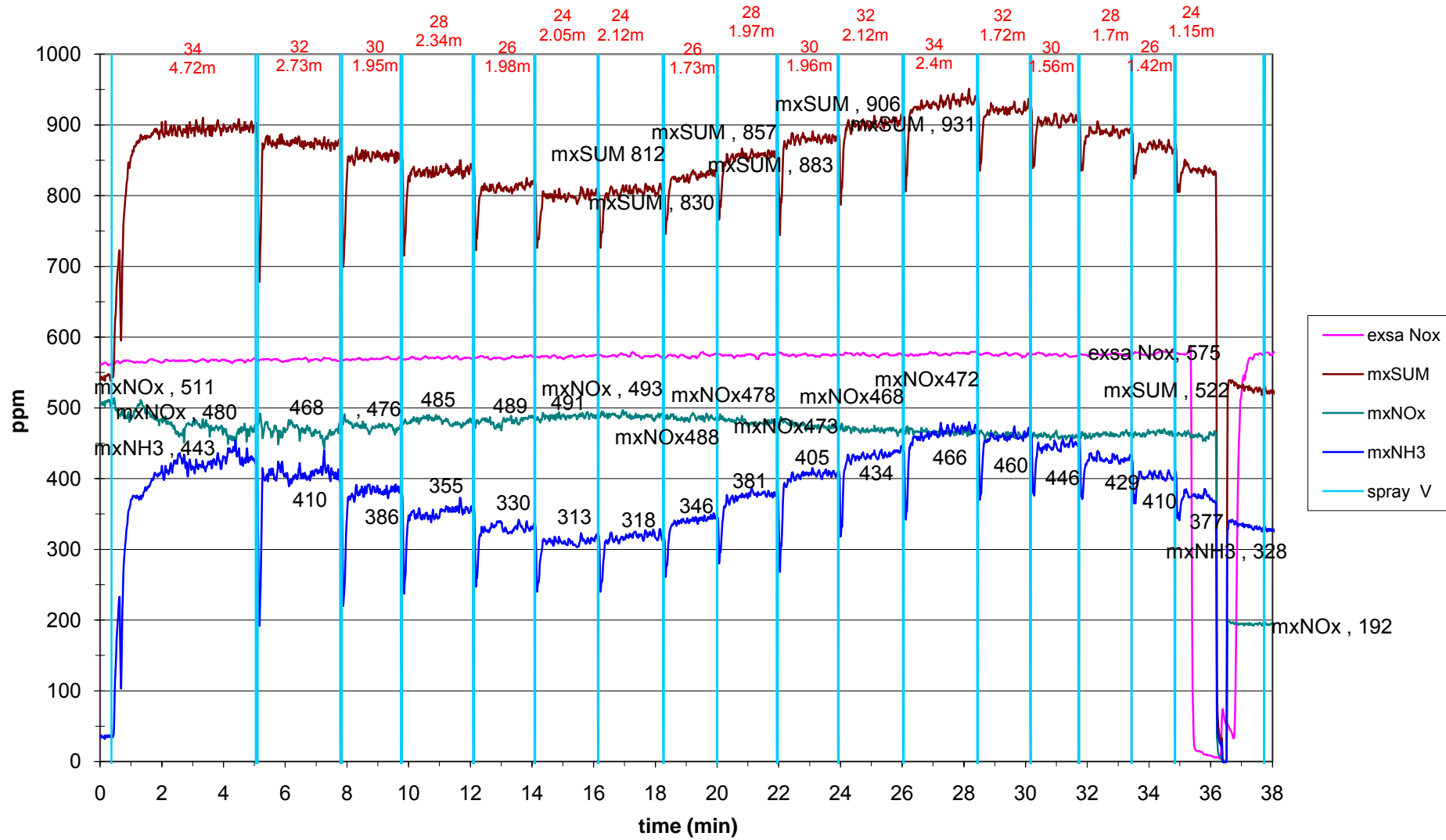
180708b NH<sub>3</sub> downstream 4 SCR L - R

230708b NH<sub>3</sub> downstream 4 SCR L-R

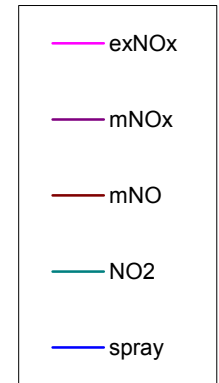
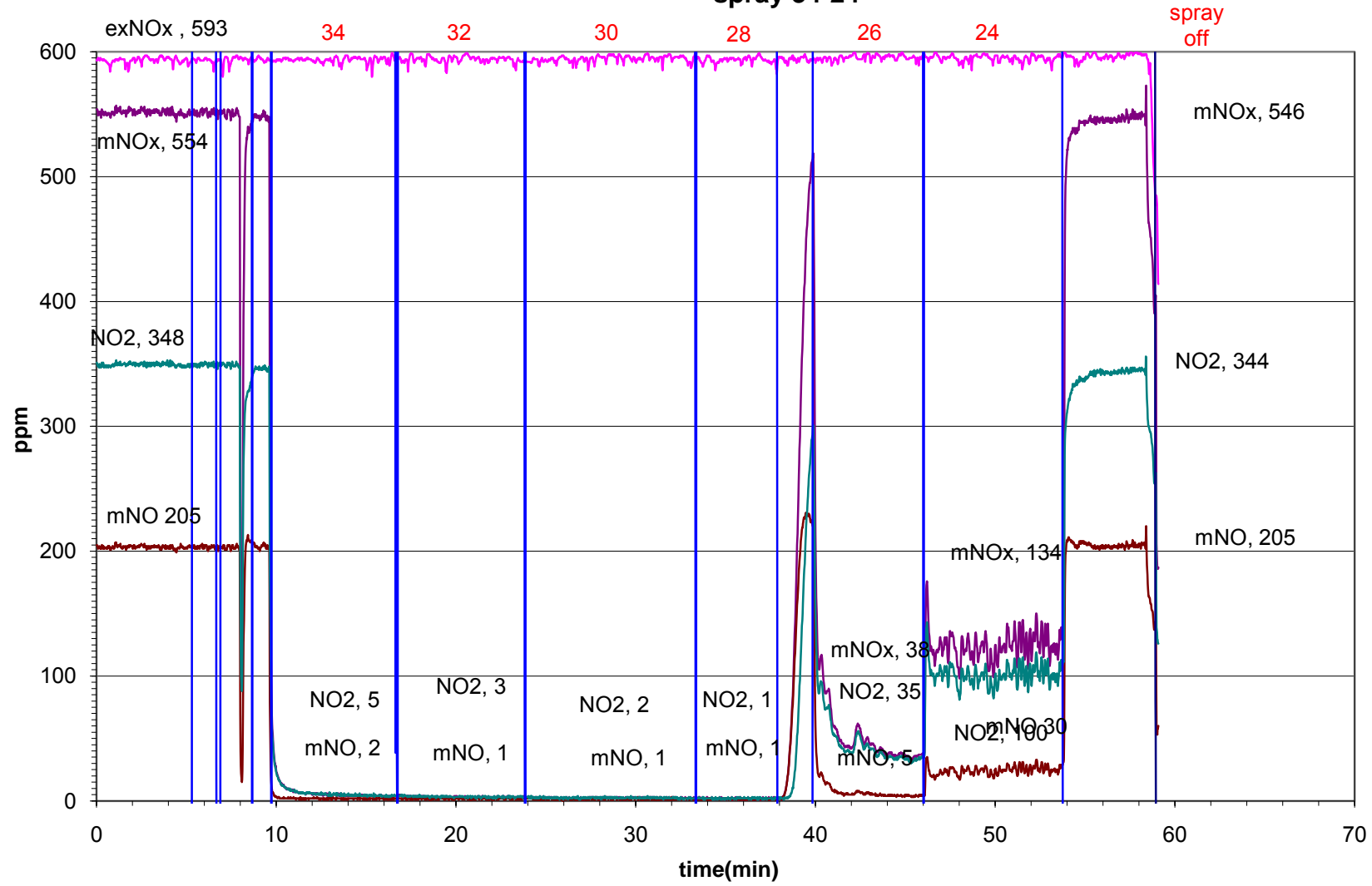
24jul08b no2 up 4SCR L-R  
NO2=60% NO=40%



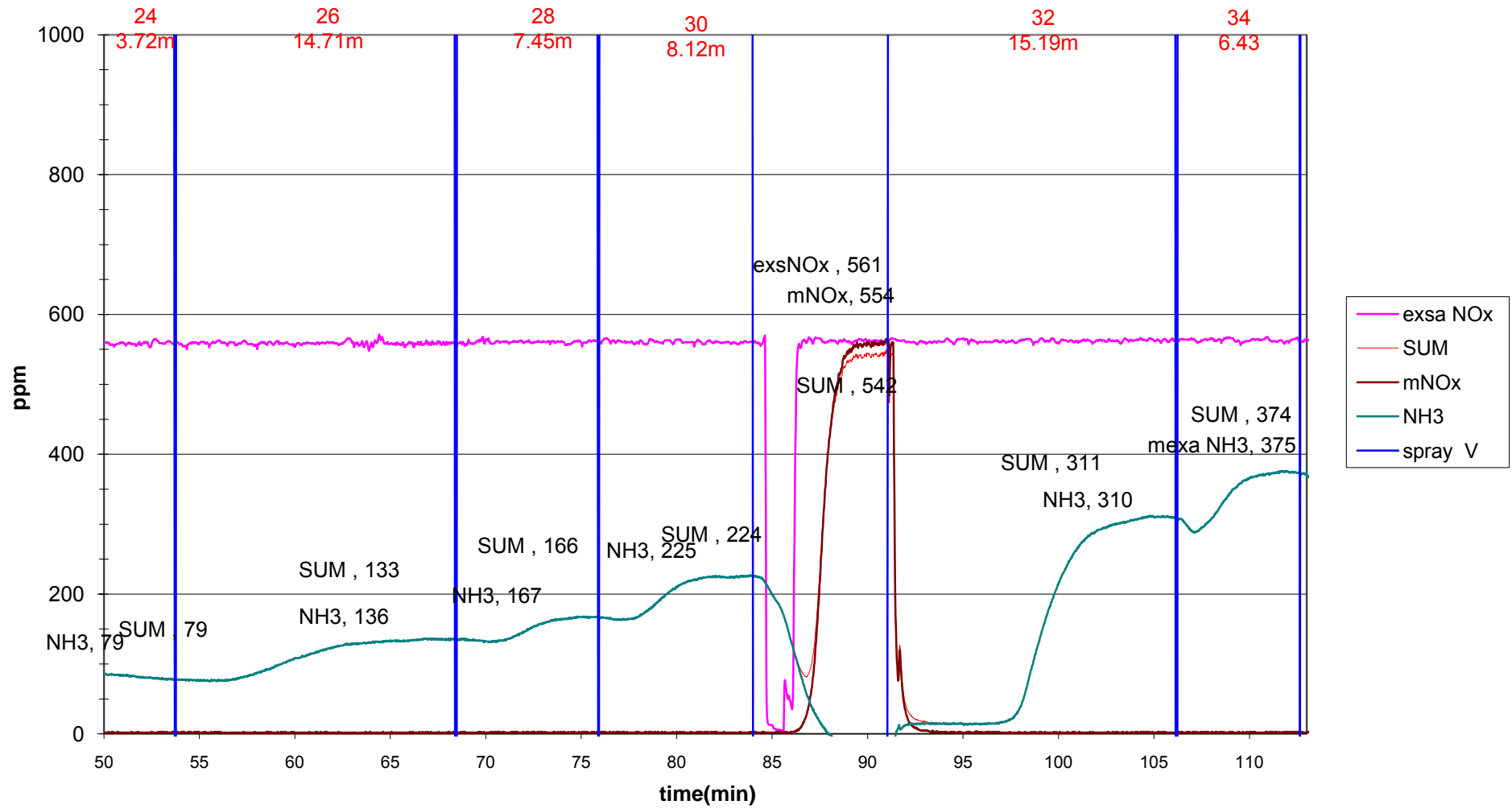
# 24jul08b NH3 up 4SCR L1-R1-L2



020708c NO2 dw 4SCR  
spray 34-24



23jul08b NH3 dw 4SCR R1  
spray 34-24 ms 5 hz

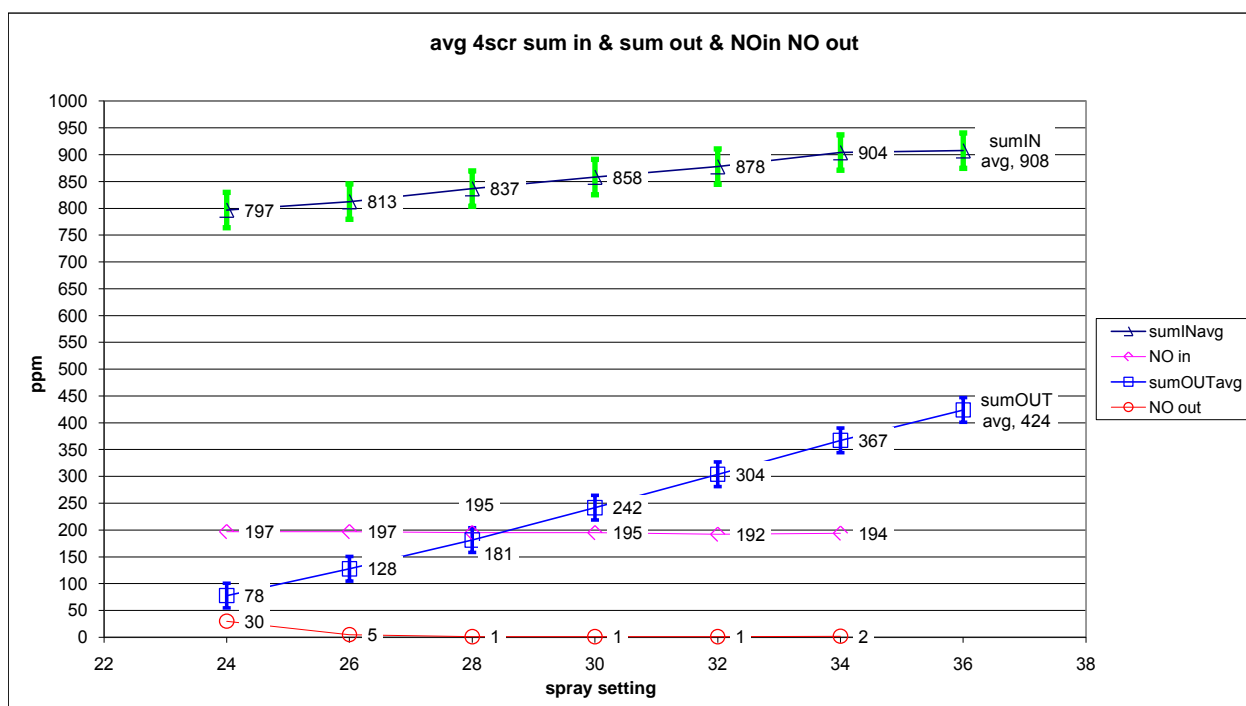


# Appendix 4.1.6b SUM in and SUM out average for 4 SCR with spray

## 4scr spray variance

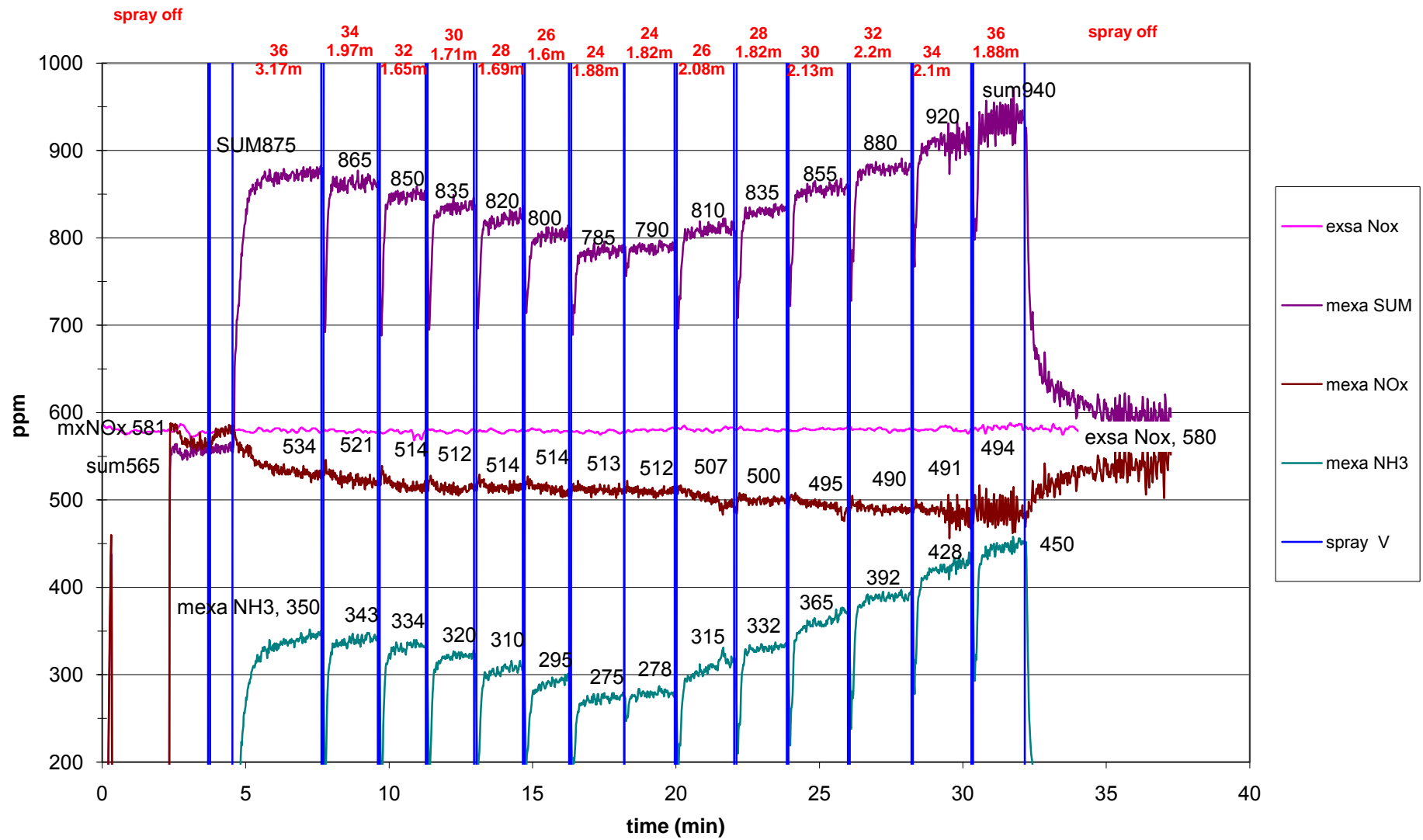
SUM IN										
	refn	18jul08L	18julR	24/7L	24/R	Data 4 CFD				
	spray	sum1	sum2	sum3	sum4	sumINavg	std dev	INupper lin	INlower lin	NO in
36	36	875	940			908	46	953	862	
34	34	865	920	931	900	904	29	933	875	194
32	32	850	880	906	875	878	23	901	855	192
30	30	835	855	883	860	858	20	878	839	195
28	28	820	835	857	835	837	15	852	822	195
26	26	800	810	830	810	813	13	825	800	197
24	24	785	790	812	800	797	12	809	785	197
off	0	565	565	522	522	544	25	568	519	200

SUM OUT										
	refn	18jul08L	18julR	23/7L	23/R	Data 4 CFD				
	spray	sumA	sumB	sumC	sumD	sumOUTavg	std dev	OUTupper	OUTlower	NO out
36	36	447	401			424	33	457	391	
34	34	384	349	375	361	367	15	383	352	2
32	32	326	284	311	295	304	18	322	286	1
30	30	266	242	224	235	242	18	260	224	1
28	28	200	184	166	175	181	15	196	167	1
26	26	141	122	133	115	128	12	139	116	5
24	24	94	78	79	60	78	14	92	64	30
off	0	535	535	540	545	539	5	544	534	205

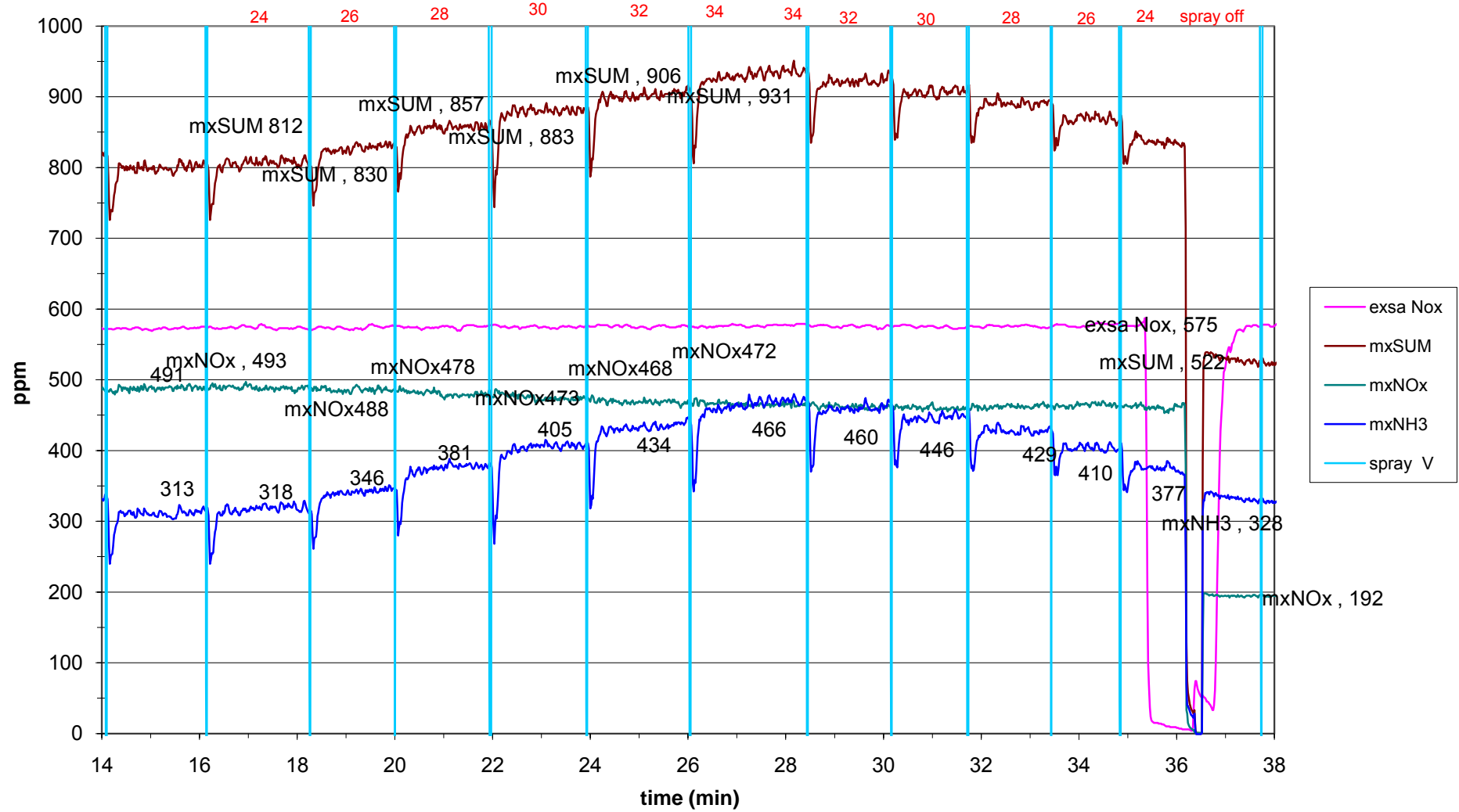




# 18jul08c NH3 up 4scr spray 34-24 L-R

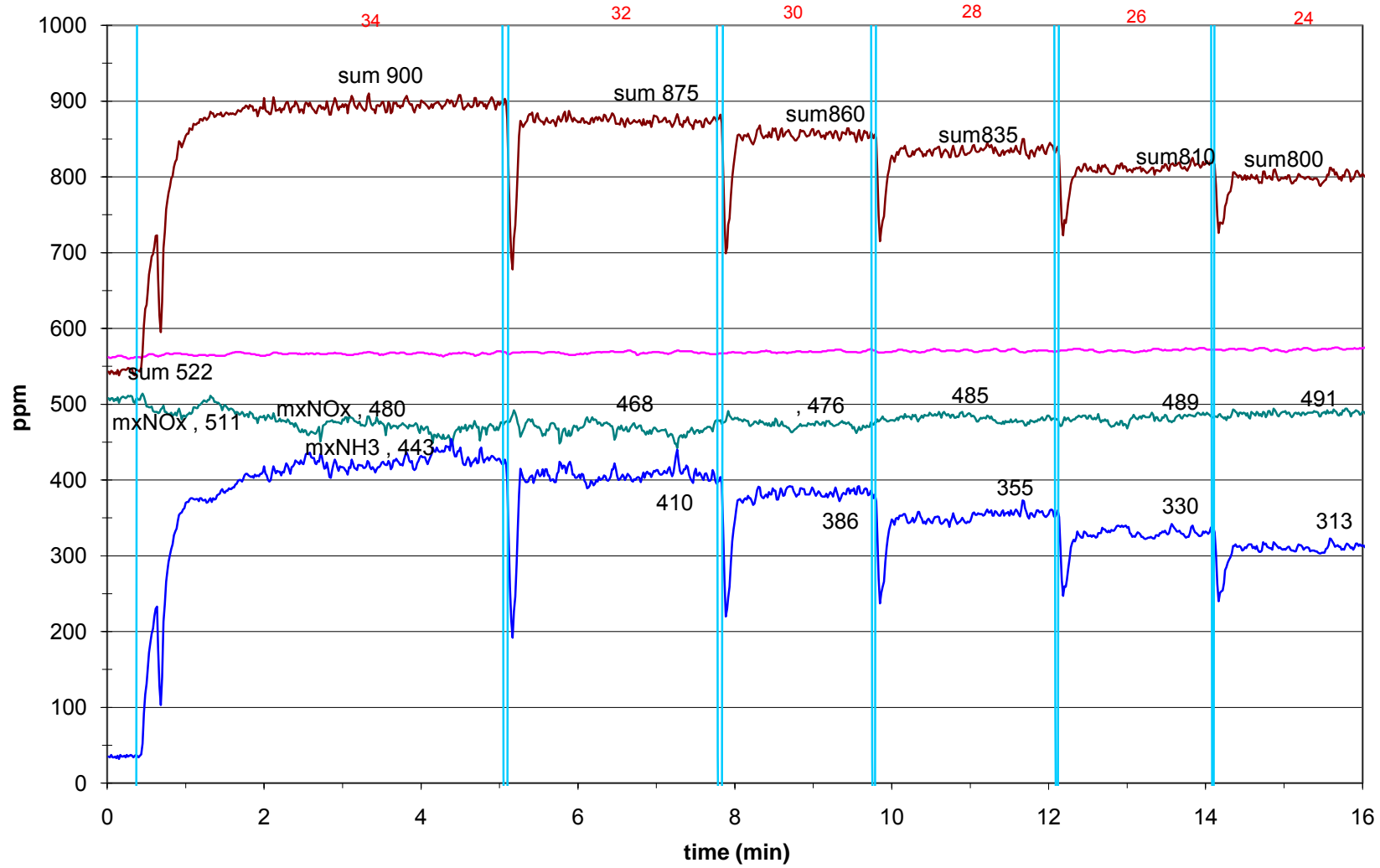


# 24jul08b NH3 up 4SCR L

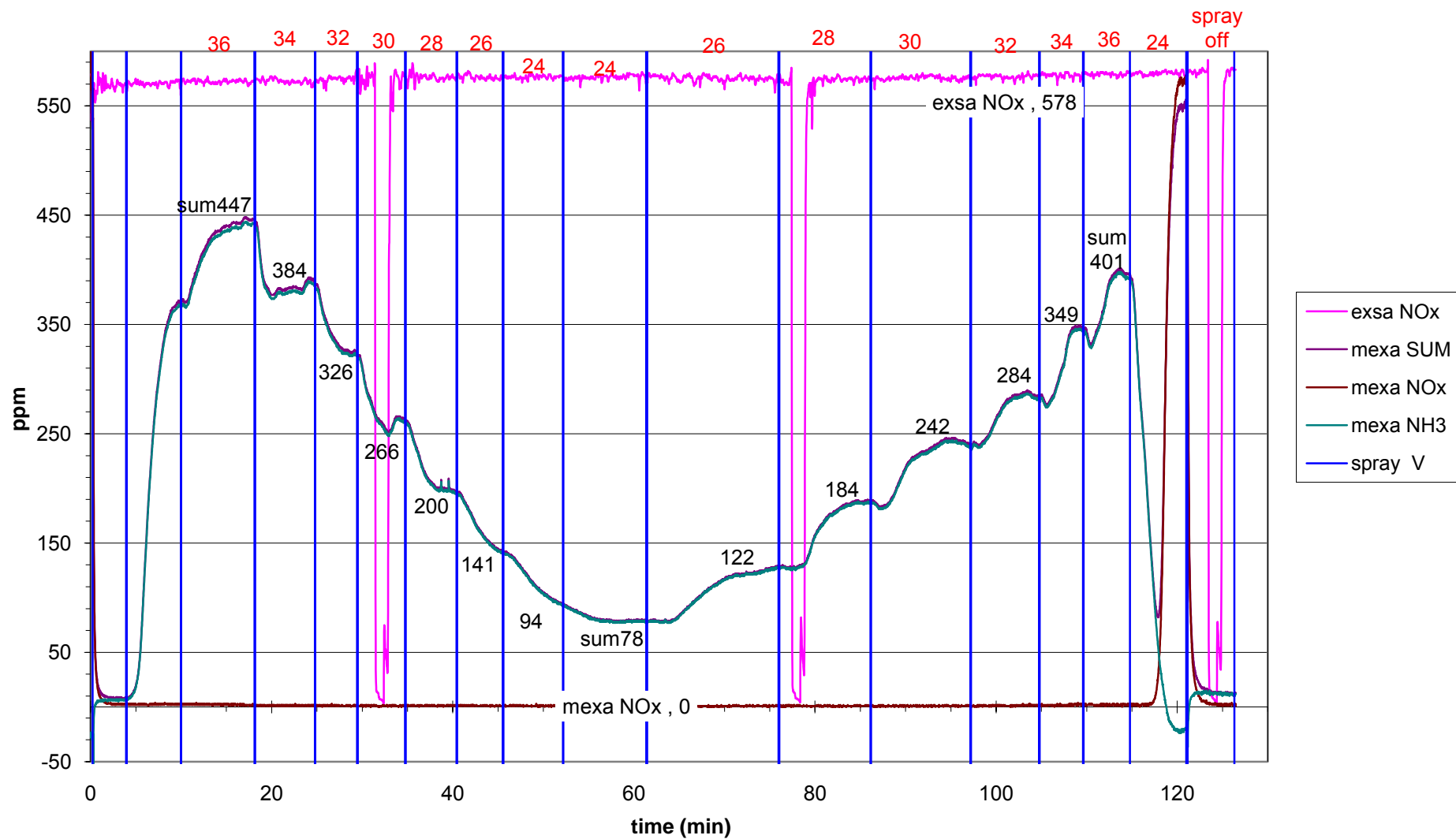


# 24jul08b NH3 up 4SCR R

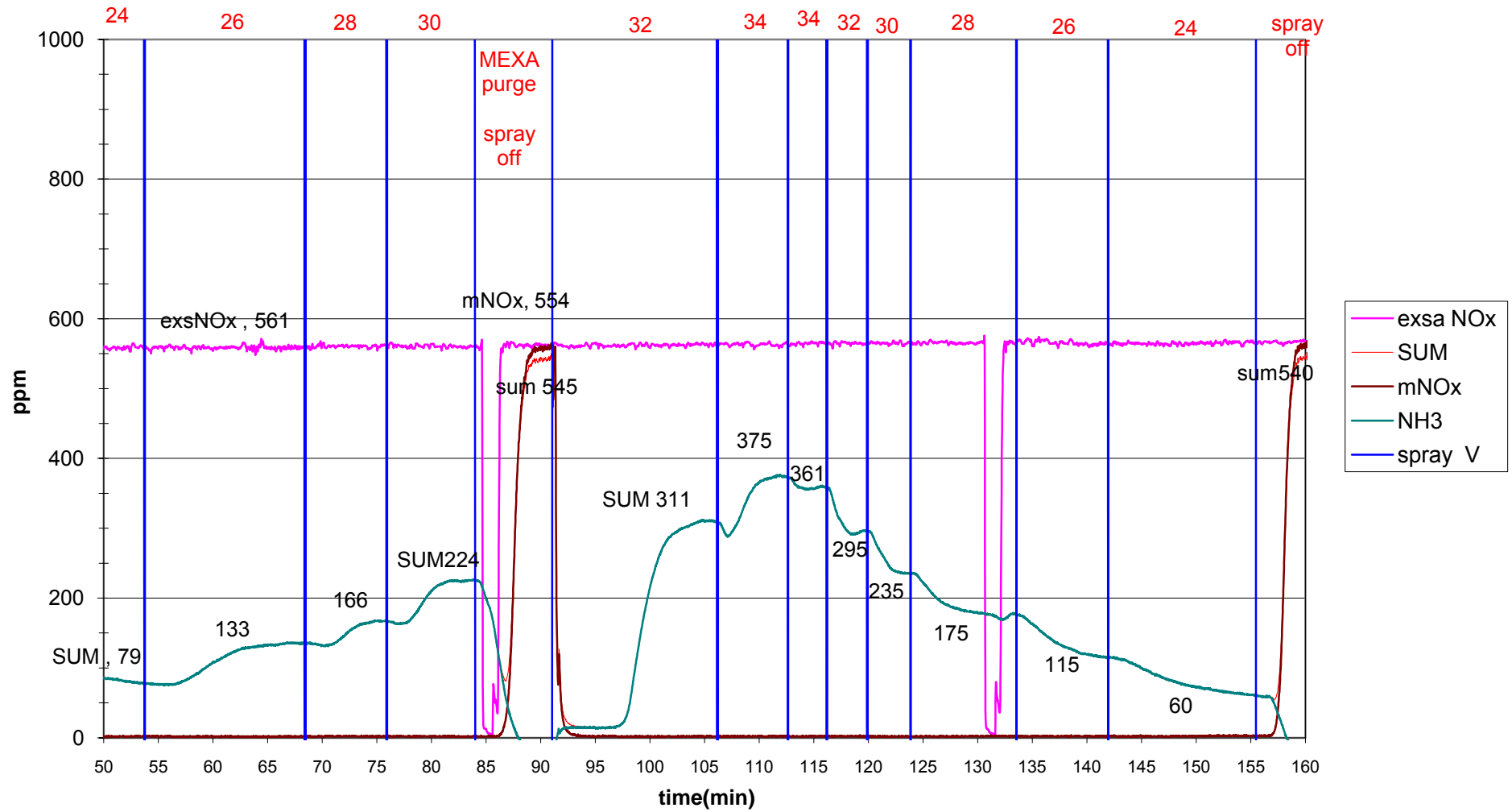
spray off



# 18jul08b NH3 down 4 SCR spray 36-24 L - R



23jul08b NH3 dw 4SCR L - R  
spray 34-24 ms 5 hz



#### **Appendix 4.2.5 Experimental data for 5% NH<sub>3</sub> gas: 1 SCR**

**Dates: (Final 5%gas 12, 21 august 2008)**

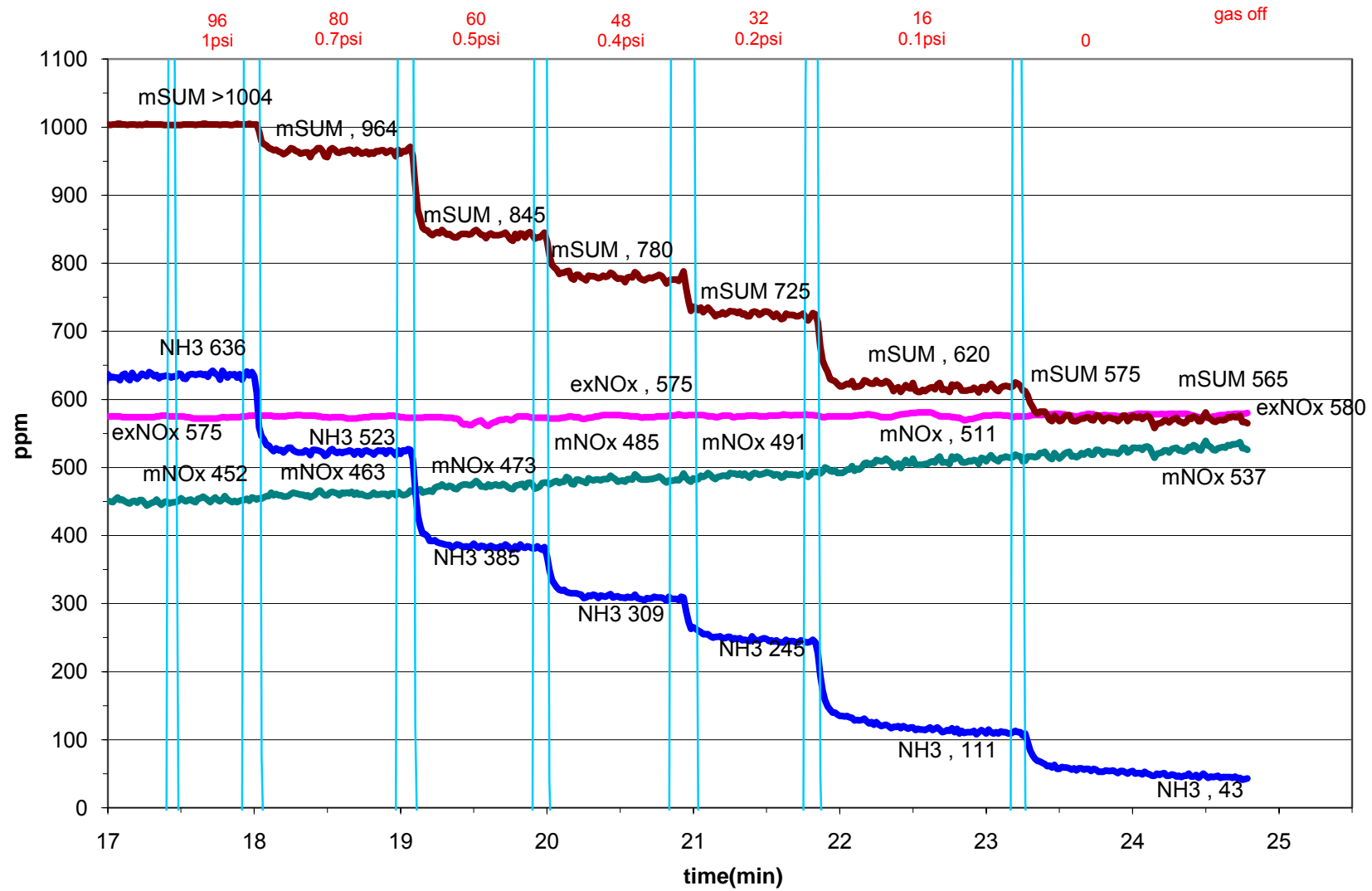
120808b NH<sub>3</sub> upstream 1 SCR 5% gas

120808c NH<sub>3</sub> downstream 1 SCR 5% gas

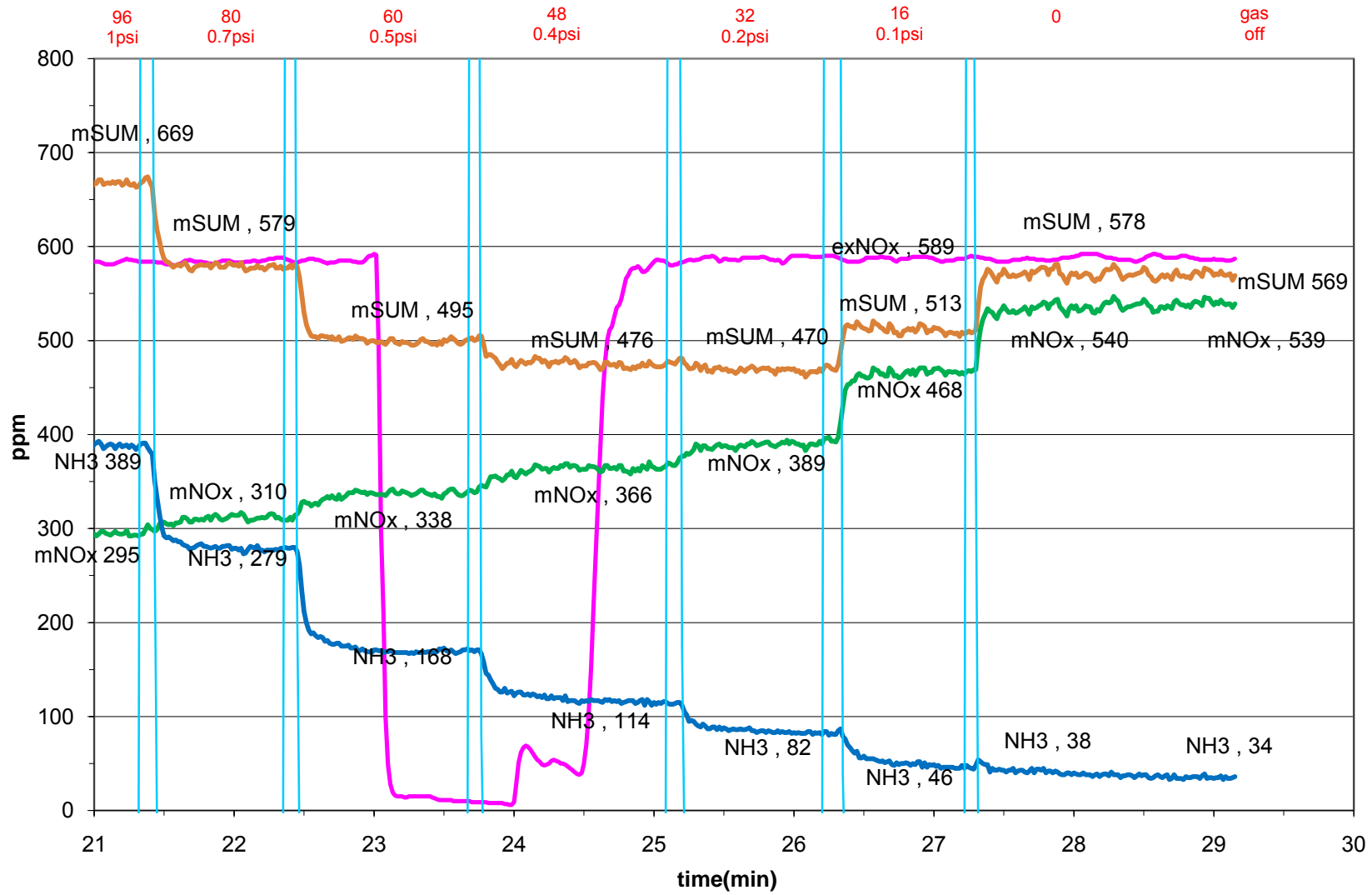
210808c NO downstream 1 SCR 5% gas

210208 NO downstream 1 SCR 5%-manual log in log book (**Appendix 4.2.5b**)

# 12aug08b bNH3 up1SCR 5% L2

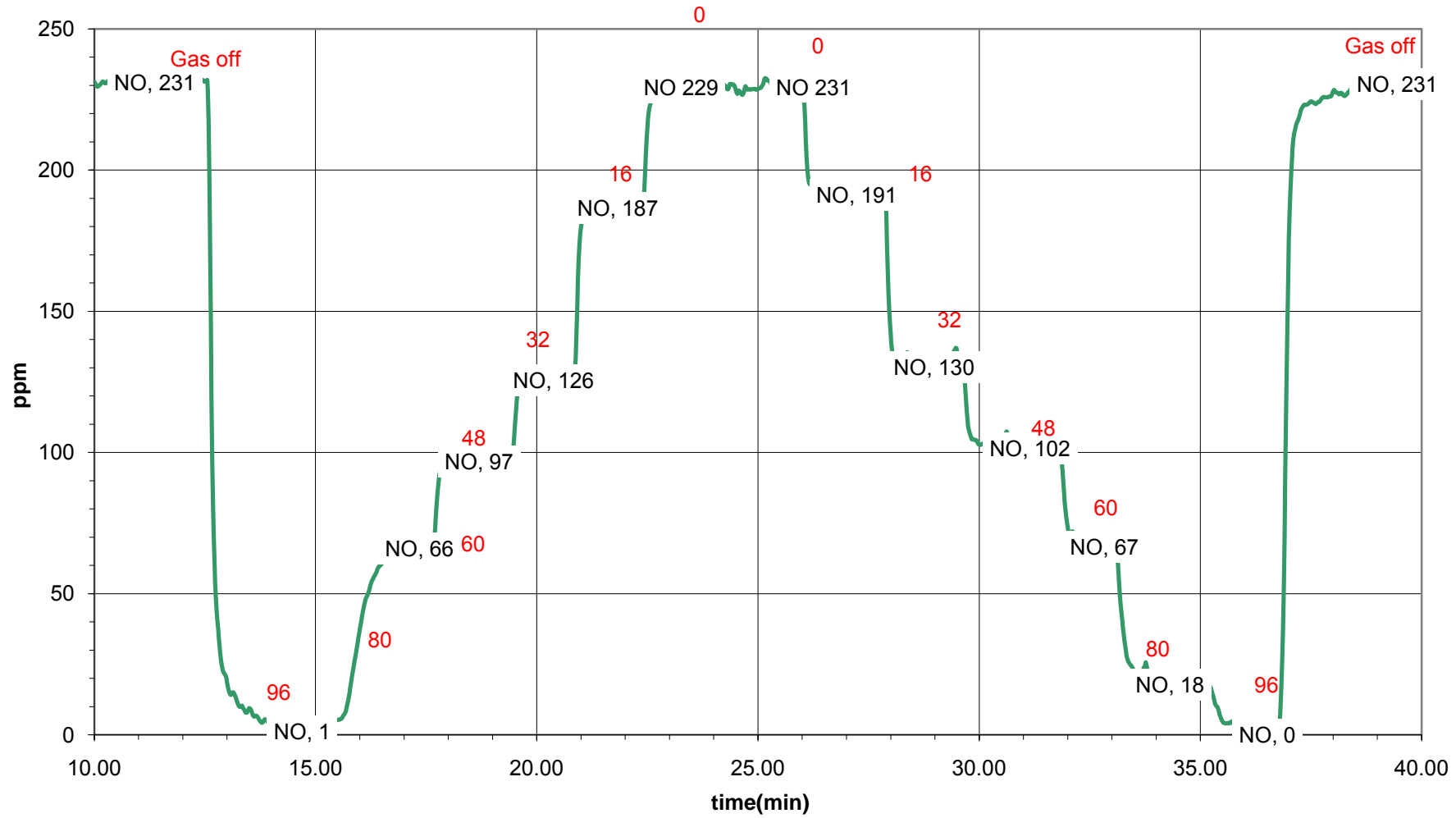


# 12aug08c NH3 dw1scr 5% L2

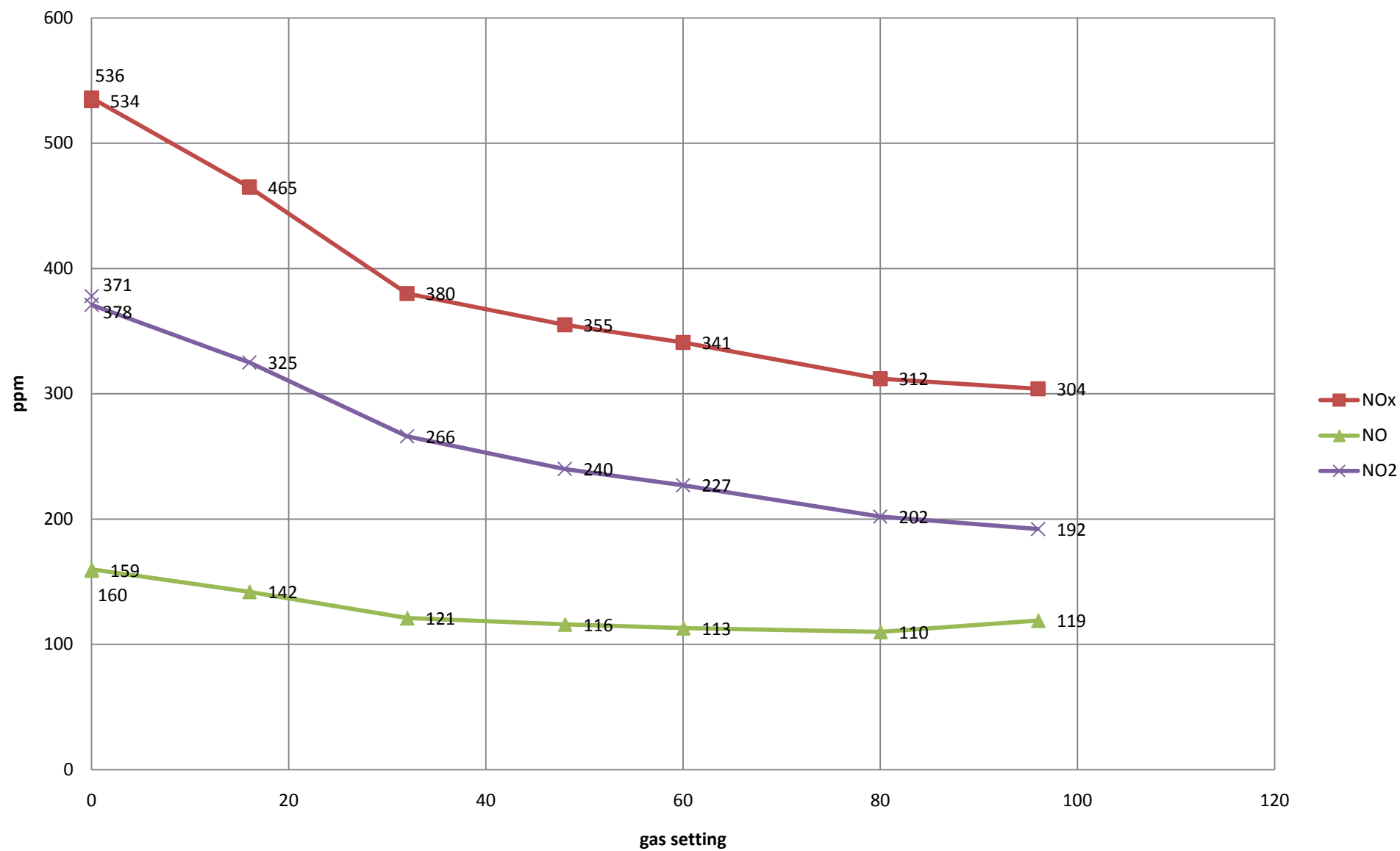




210808c NO dw 1 scr with 5%  
exsa1500 dw1scr Gas flow 96-16(glass float)



21aug08 NO2 down 1SCR 5% gas manual log

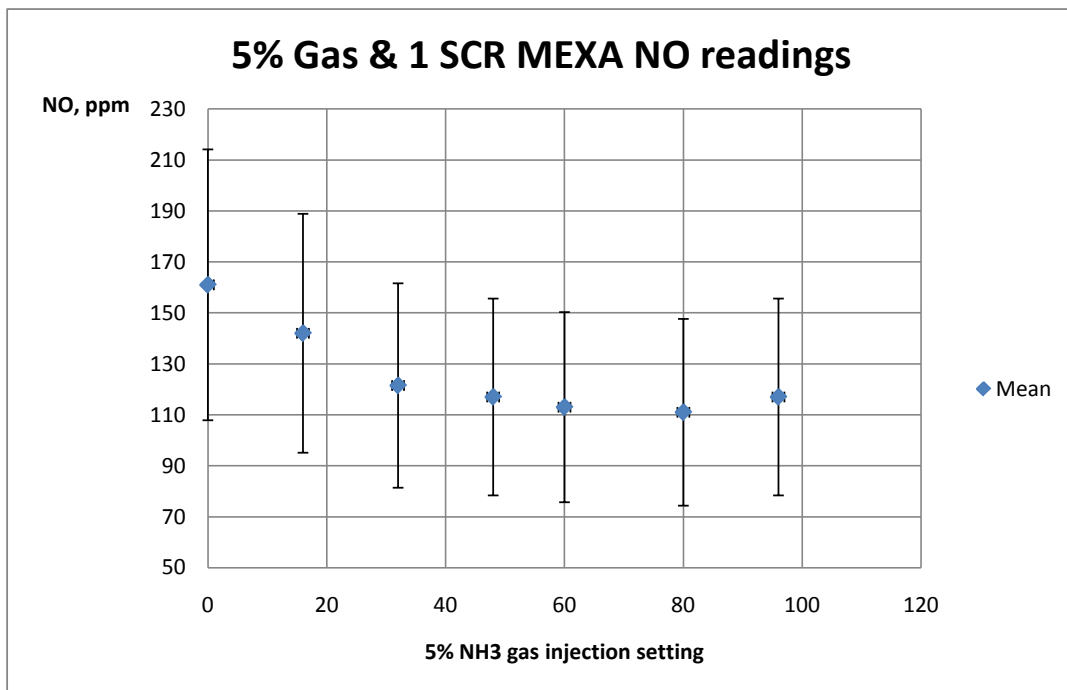


Appendix 4.2.5b NO dw 1 SCR with 5% ammonia gas - Manual log from mexa

Date of test : 210808

Test condition 1500 rpm & 6 Bar bmep

Gas setting	NO reading 1	NO reading 2	Avg	33% var
0	160	162	161	214.13
16	142	142	142	188.86
32	121	122	122	161.60
48	116	118	117	155.61
60	113	113	113	150.29
80	110	112	111	147.63
96	119	115	117	155.61



#### **Appendix 4.2.6 Experimental data for 5% NH<sub>3</sub> gas: 2 SCR**

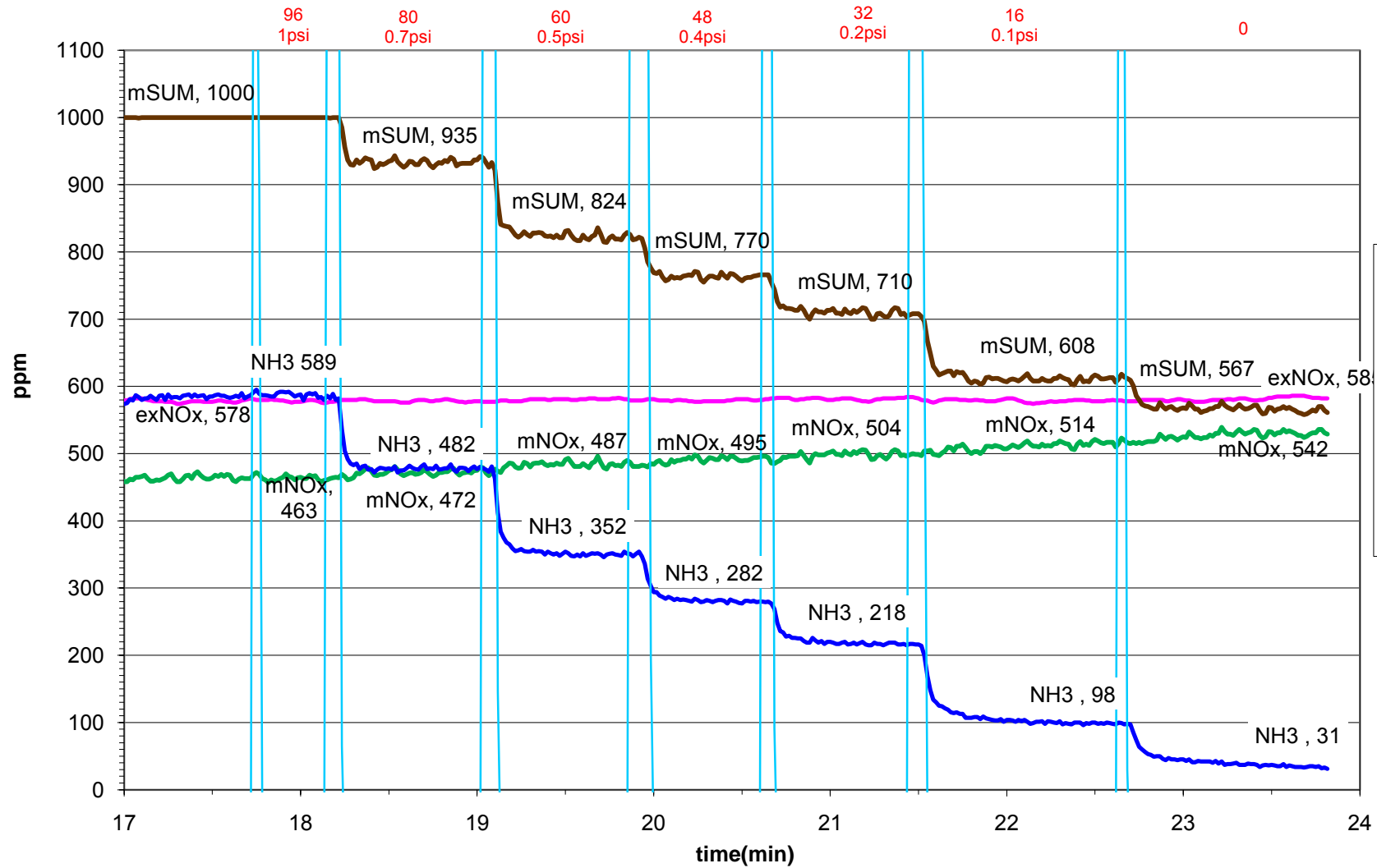
**Date: (11 august 2008)**

110808b NH<sub>3</sub> upstream 2 SCR 5% gas

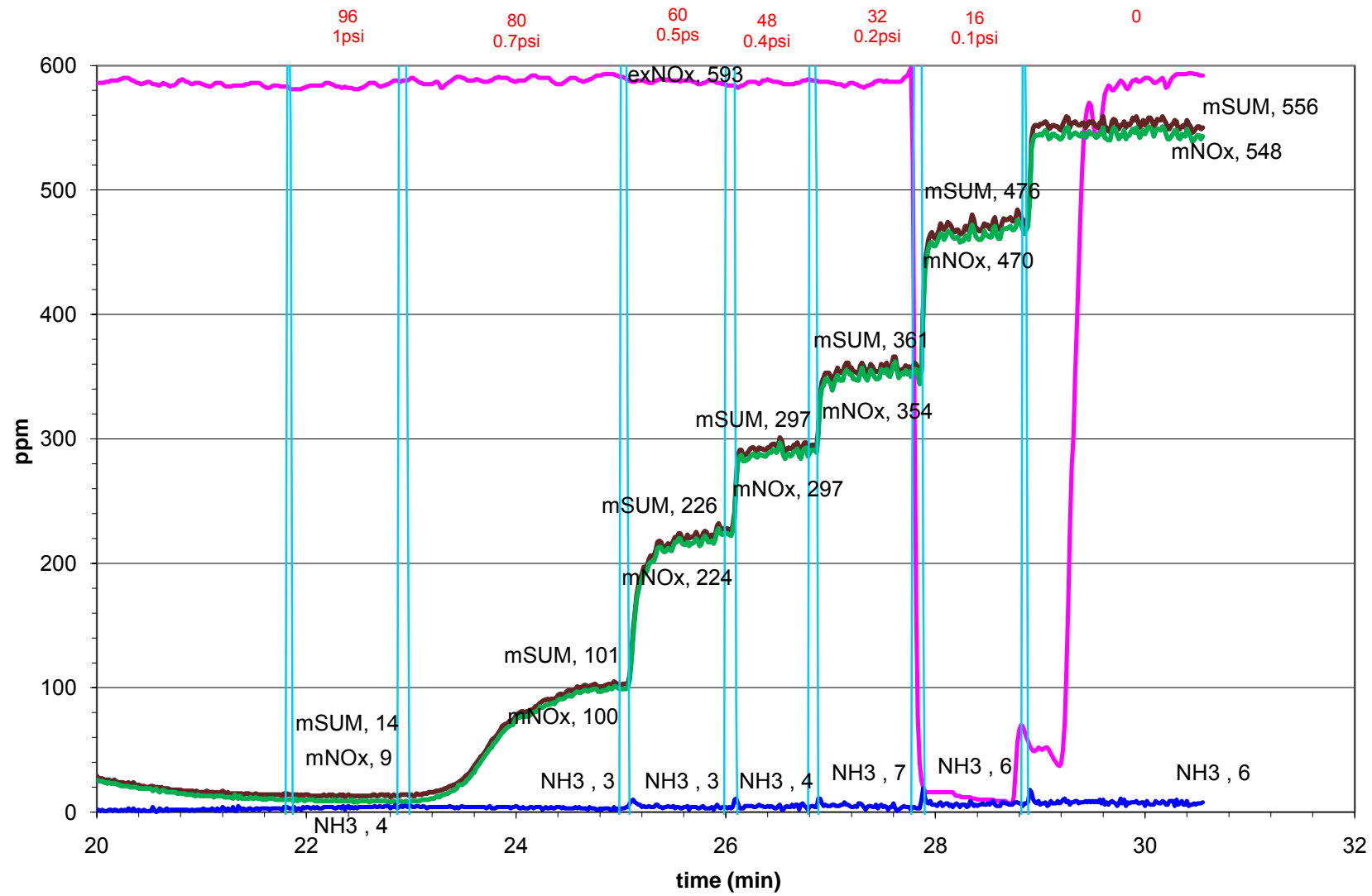
110808c NH<sub>3</sub> downstream 2 SCR 5% gas

210808c NO downstream 1 SCR 5% gas (refer to Appendix 4.2.5)

# 11aug08b NH3 up2SCR 5% gas L2



# 11aug08c NH3 dw2scr 5%



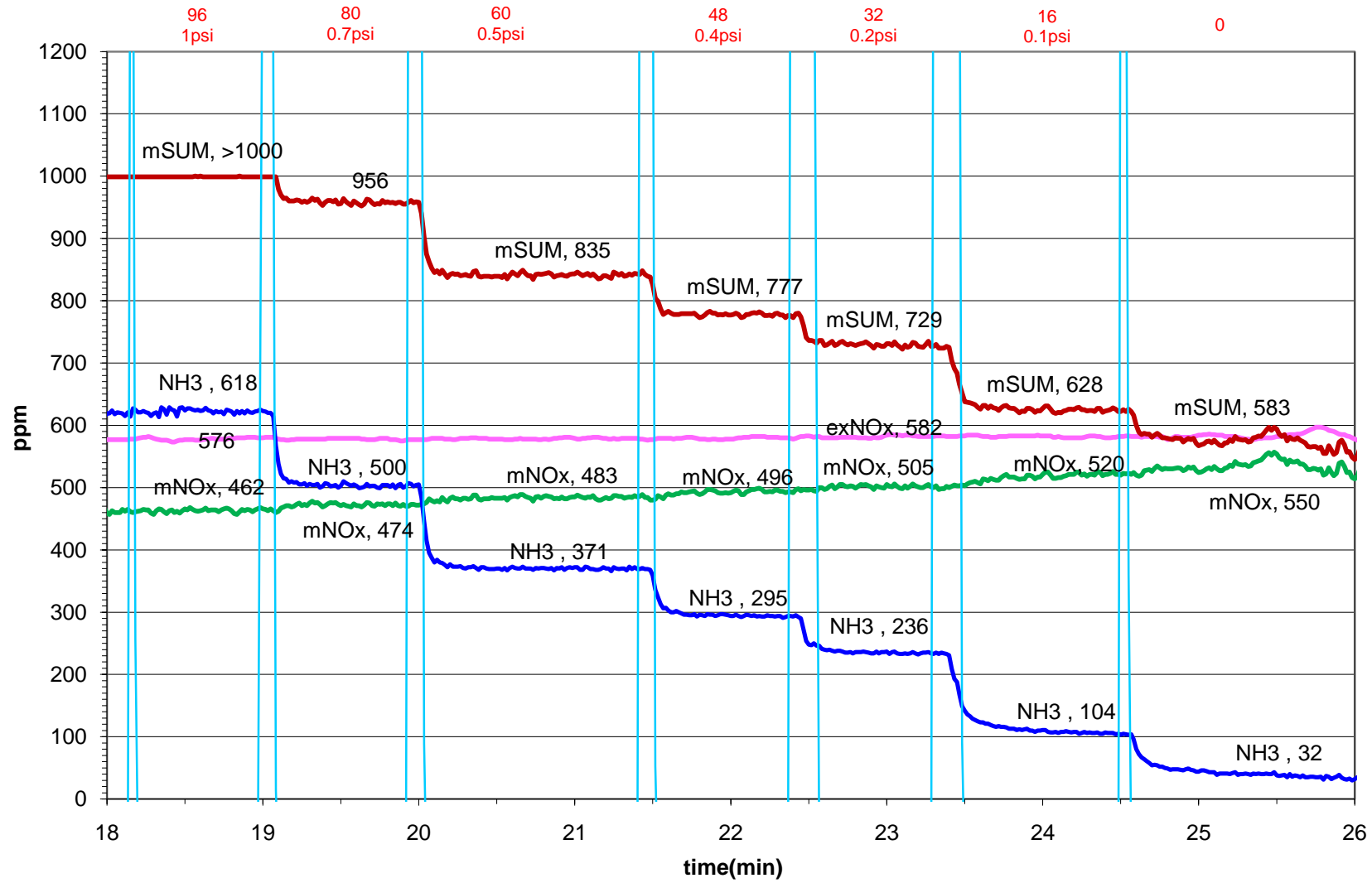
### **Appendix 4.2.7 Experimental data for 5% NH<sub>3</sub> gas: 3 SCR**

**Date: (7 august 2008)**

070808b NH<sub>3</sub> upstream 3 SCR 5% gas

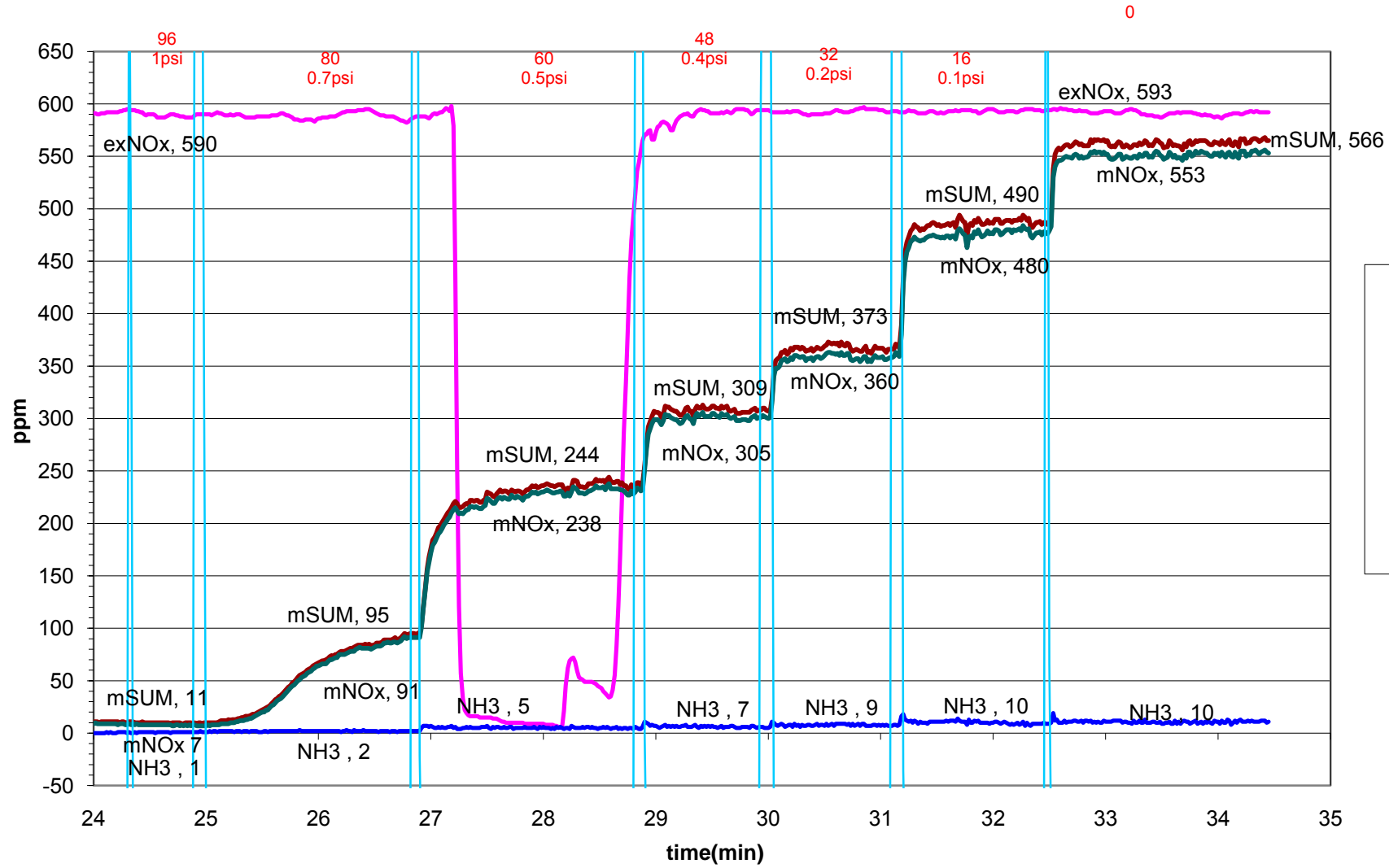
070808c NH<sub>3</sub> downstream 3 SCR 5% gas

# 070808b NH3 up3SCR 5% gas L2





# 070808c NH3 dw3SCR 5% gas L2



### **Appendix 4.2.8 Experimental data for 5% NH<sub>3</sub> gas: 4 SCR**

**Dates: (16, 25 jun2008 & 5, 6 august 2008)**

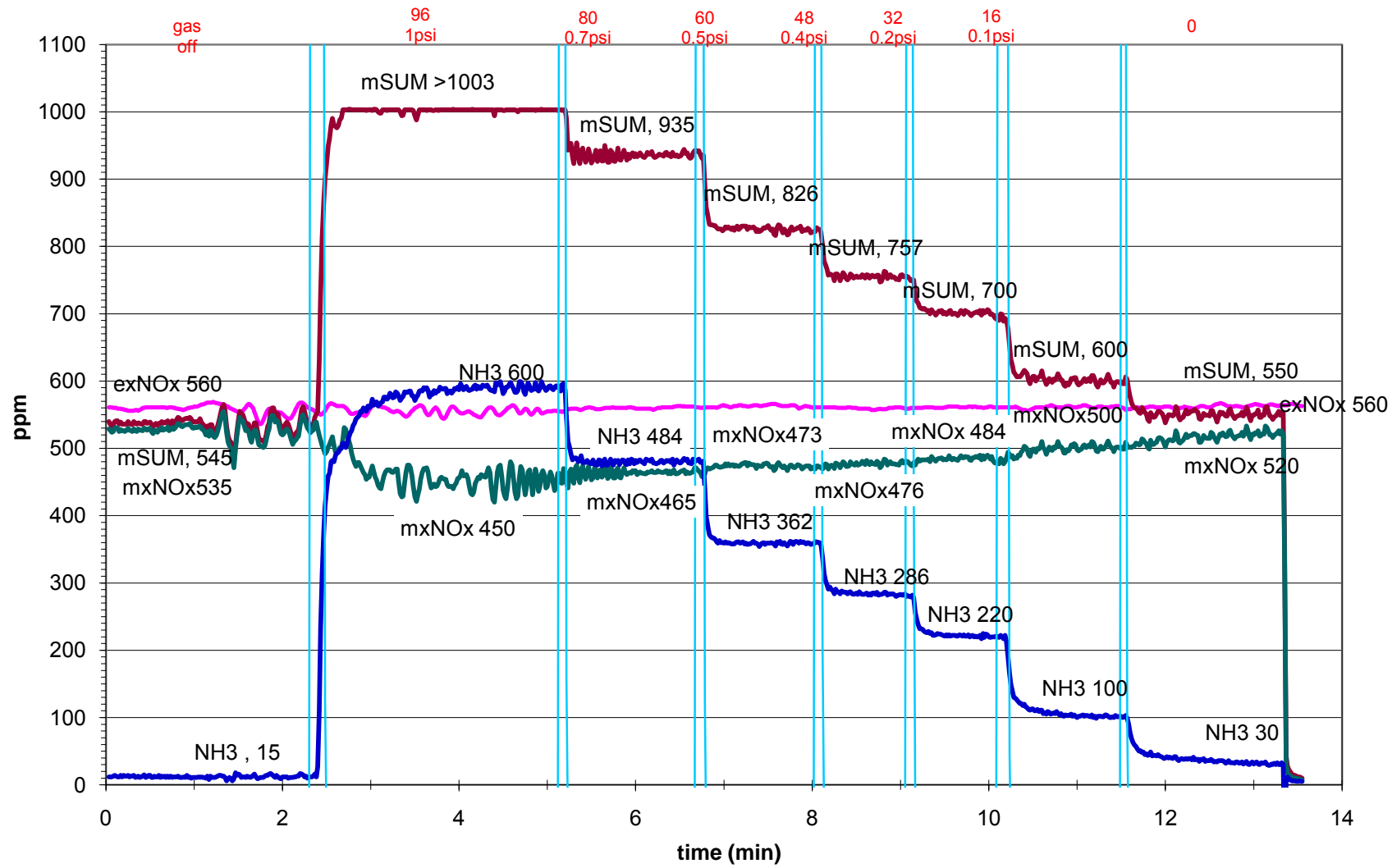
060808b NH<sub>3</sub> upstream 4 SCR 5% gas

060808e NH<sub>3</sub> downstream 4 SCR 5% gas

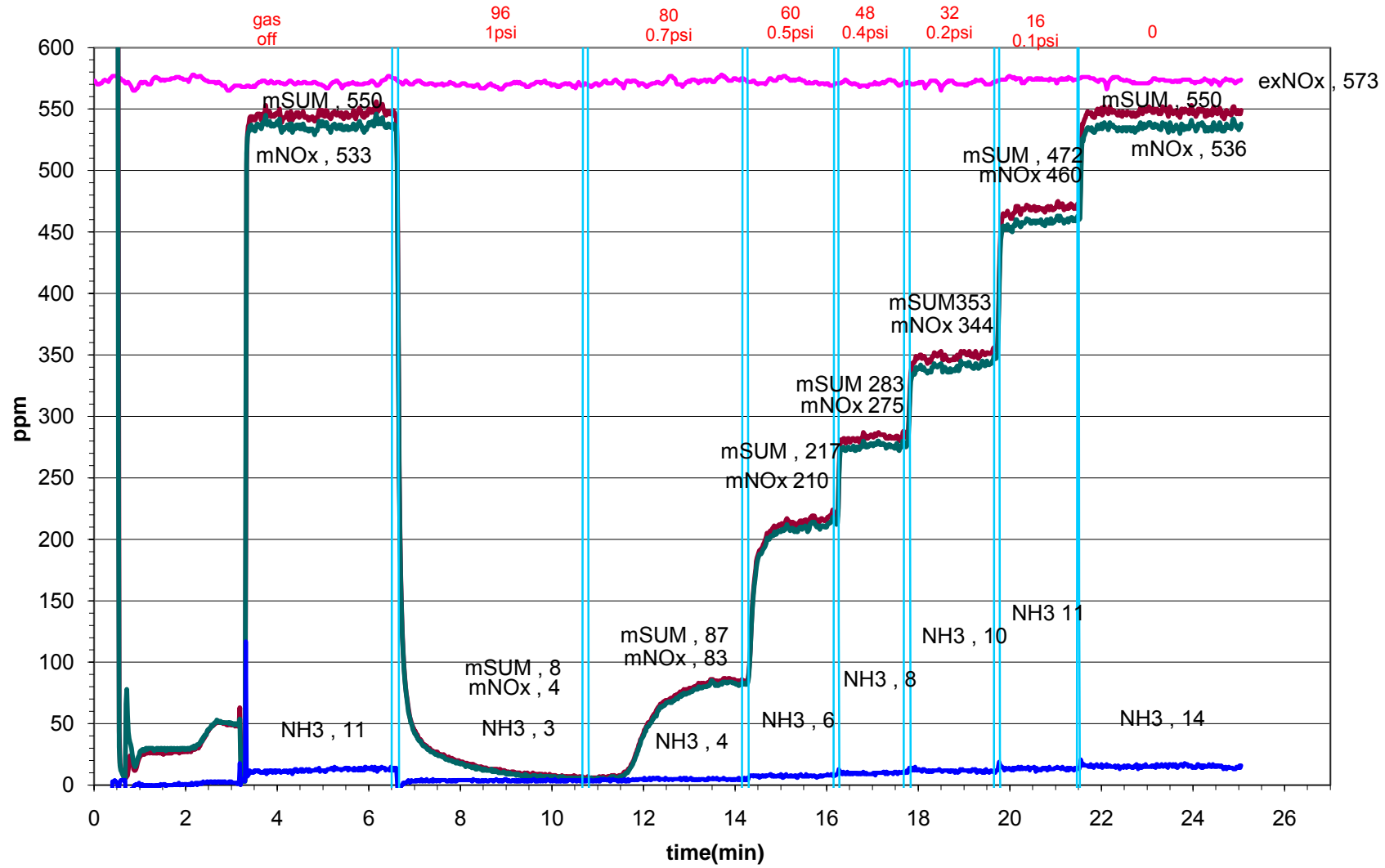
060808c NO<sub>2</sub> upstream 4 SCR 5% gas

060808d NO<sub>2</sub> downstream 4 SCR 5% gas

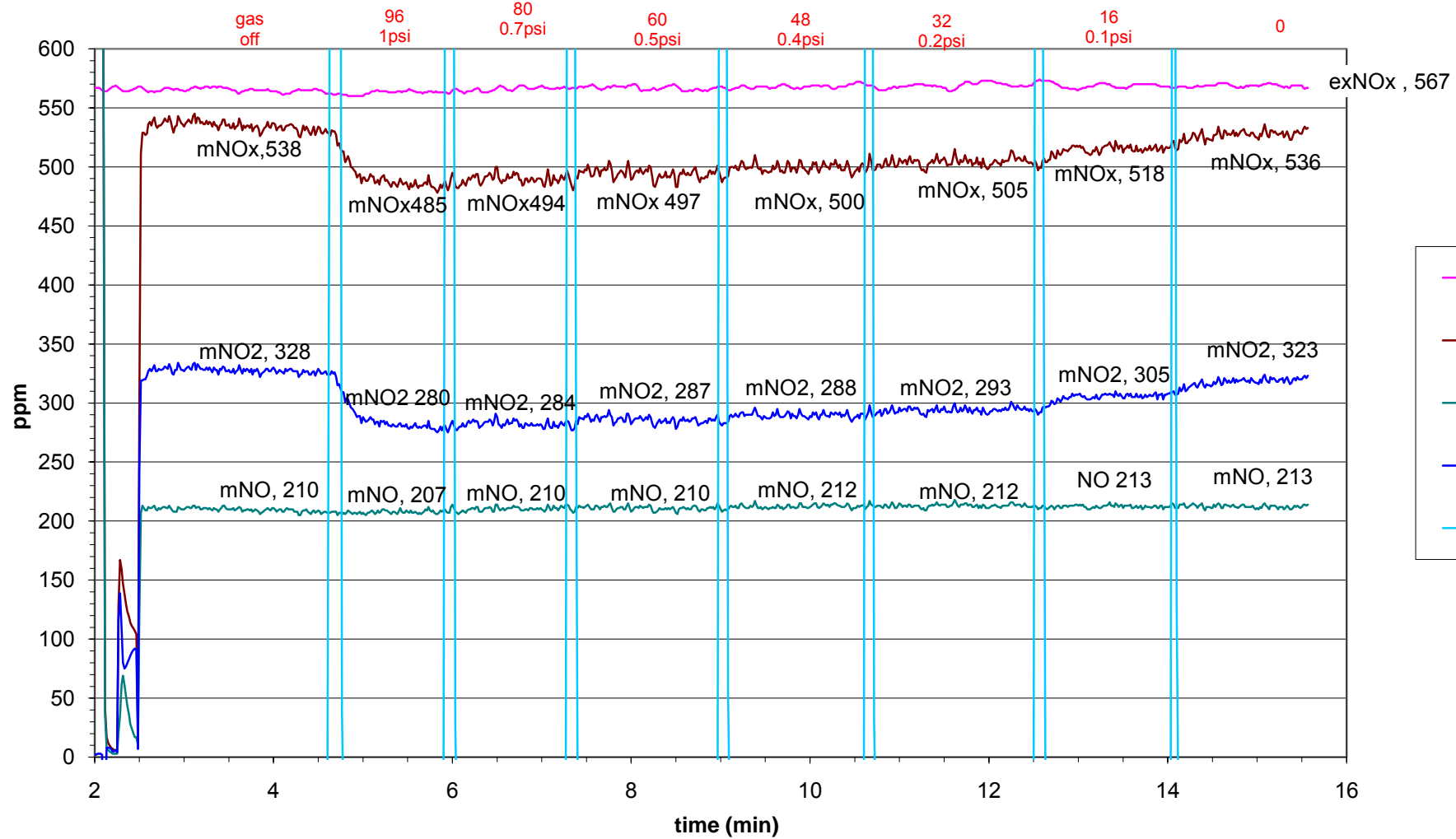
# 060808b NH3 up4SCR( 5% gas) 96-0 glass float



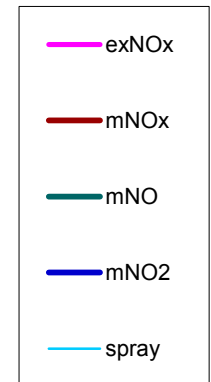
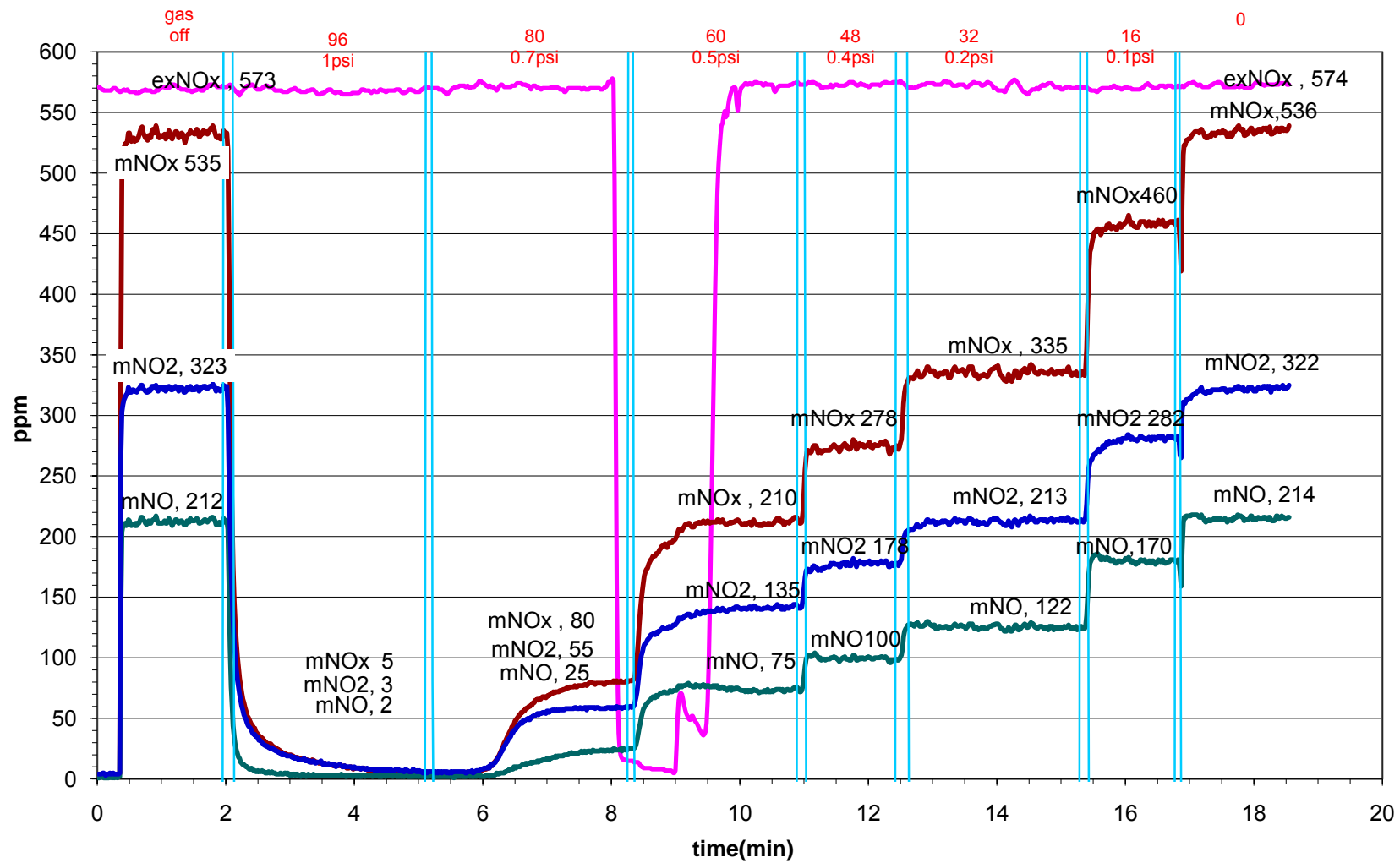
# 060808e NH3 dw4SCR (5%gas)



060808c NO2 up4SCR 5%gas  
NO2=60% NO=40%



060808d NO2 d 4SCR 5%  
NO2=60% NO=40%



### **Appendix 4.2.9 Experimental data for 1 SCR 4% NH<sub>3</sub> gas**

**Dates: (4% gas- 10, 11,12,16,24 jun2008)**

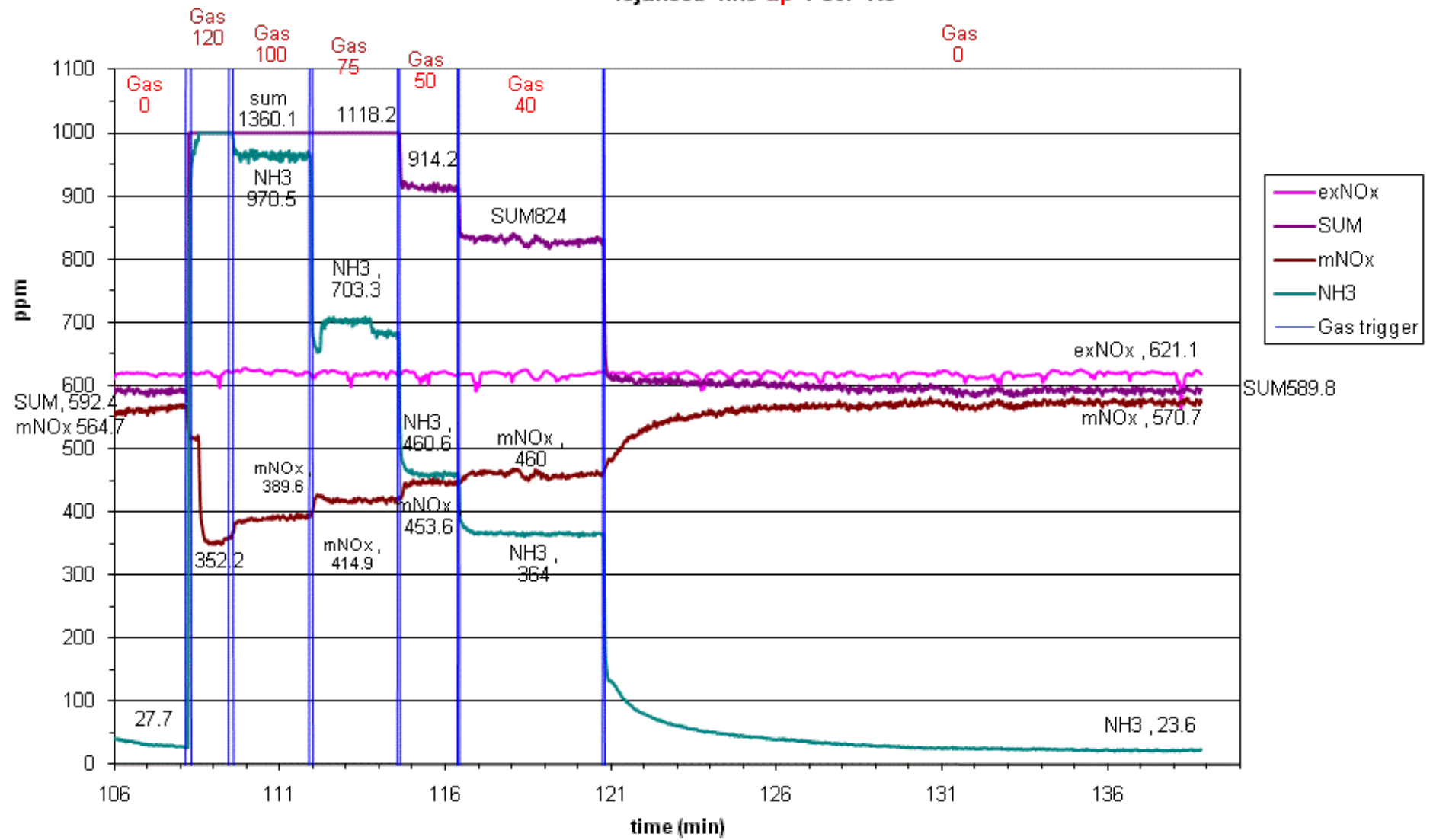
100608b NH<sub>3</sub> upstream 1 SCR 4% gas

100608c NO upstream 1 SCR 4% gas

100608b NH<sub>3</sub> downstream 1 SCR 4% gas

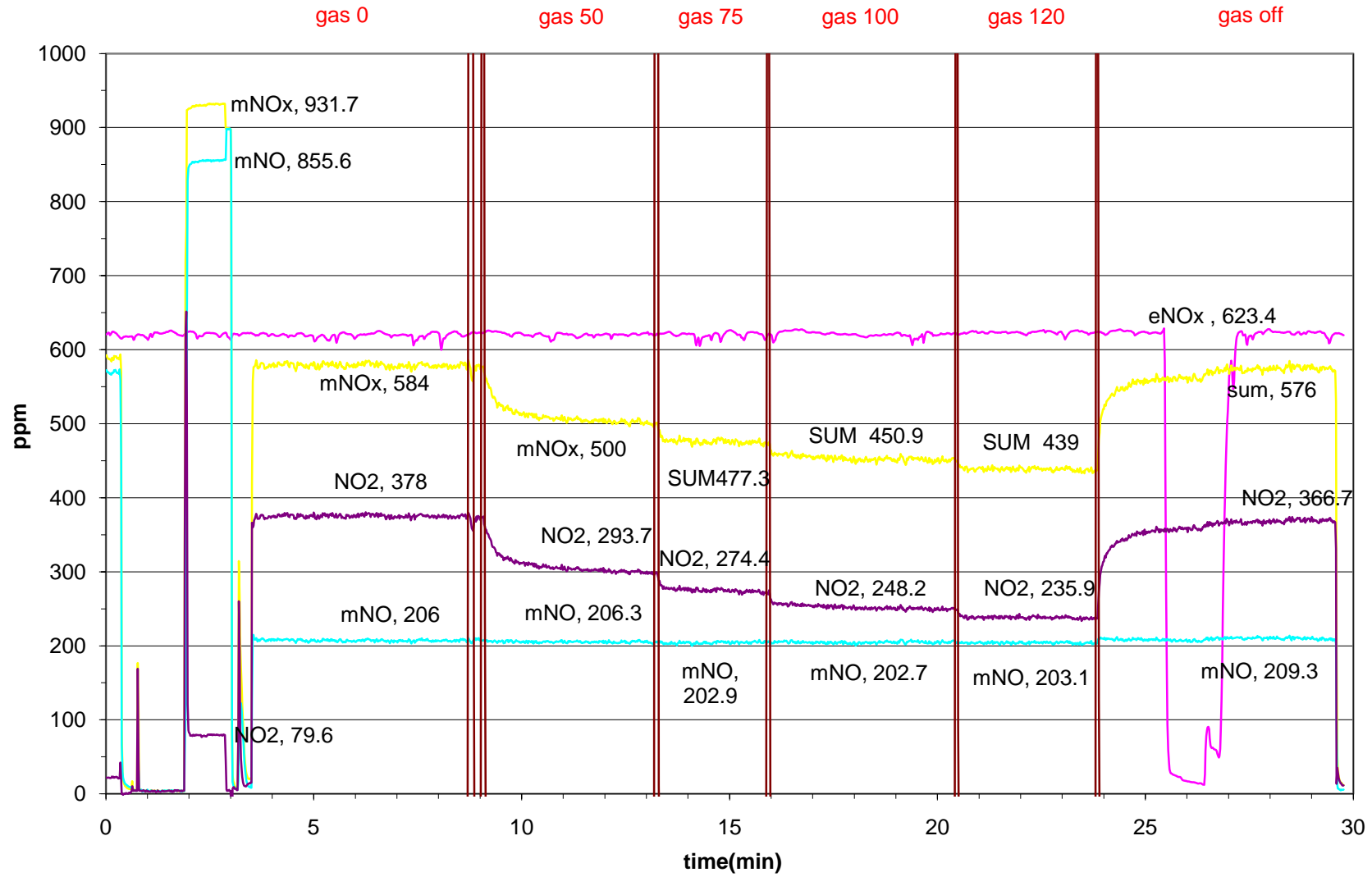
100608d NO<sub>2</sub> downstream 1 SCR 4% gas

# 10jun08b nh3 up 1 scr 4%

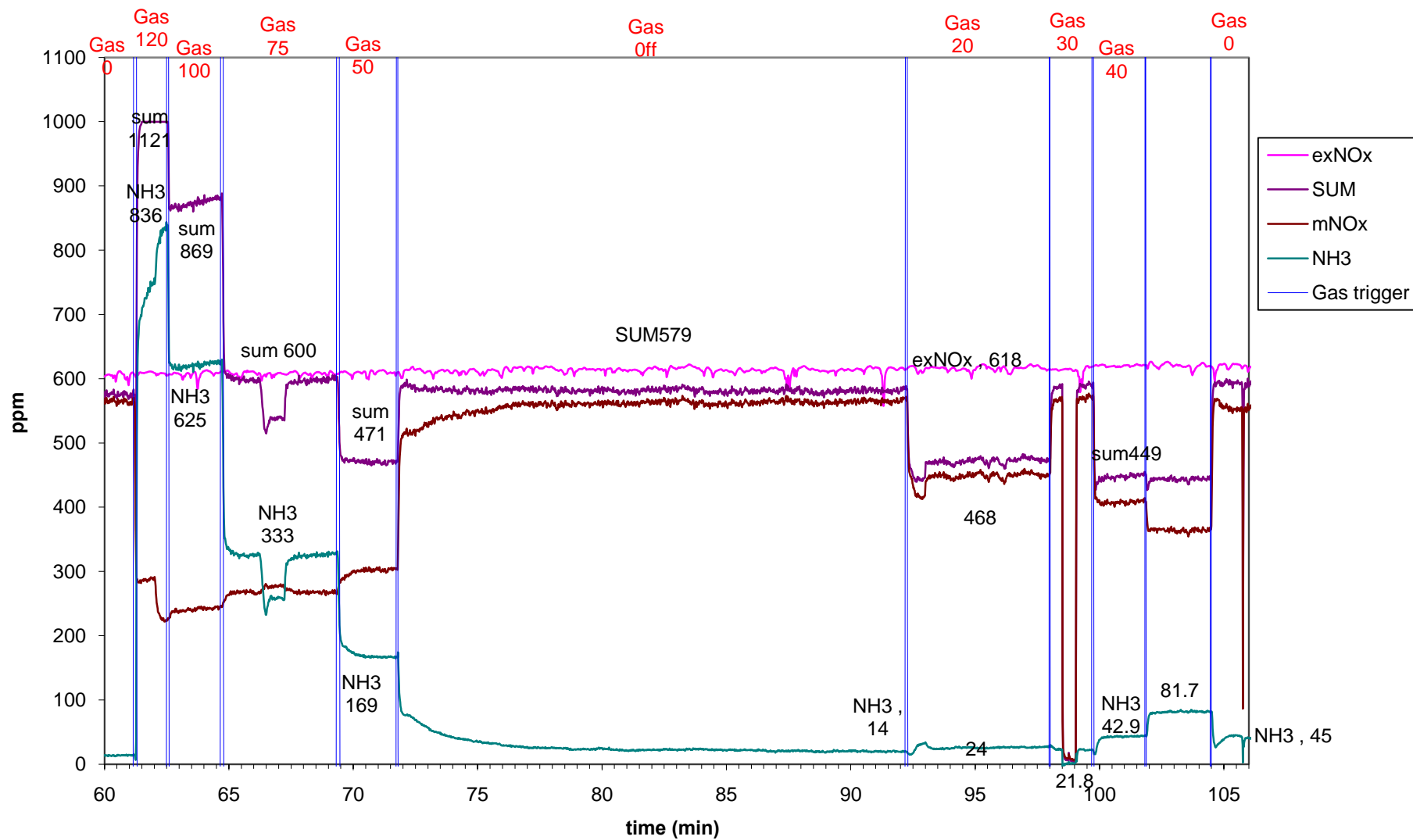




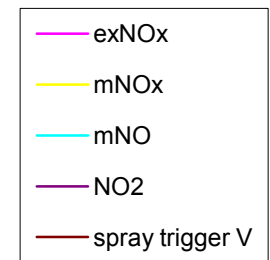
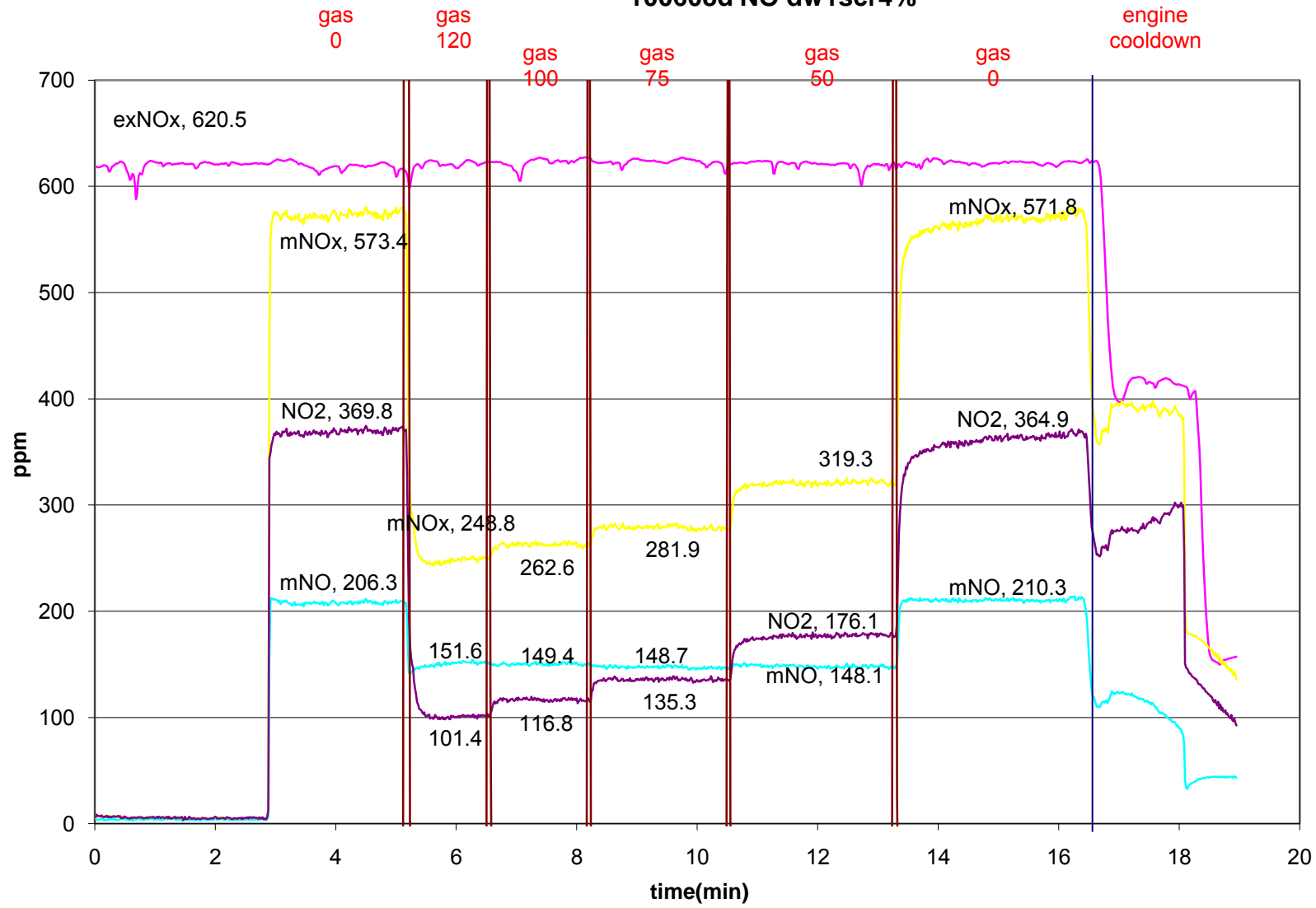
# 100608c NO up1SCR4%



# 10jun08b nh3 downstream 1 scr 4%



# 100608d NO dw1scr4%



# Appendix 4.9.1a Excel numerical integration- 4% gas 4SCR

time	NH3	integration							
sec	ppm	ppm.secs							
0	0	0							
220	4.9	-0.0049	ammonia slip start						
221	4.5	4.6951							
222	5.8	9.8451							
223	4.9	15.1951							
224	5.6	20.4451							
225	5.4	25.9451							
226	5	31.1451							
227	6.2	36.7451							
743	485.9	182811.9951							
744	485.3	183297.5951							
745	486.2	183783.3451							
746	486.6	184269.7451							
747	485.5	184755.7951							
748	485.4	185241.2451							
749	485.6	185726.7451							
750	485.5	186212.2951							
751	485.7	186697.8951							
752	486.3	187183.8951			Area under curve =	187669.85	x	1.67E-05	
753	485.6	187669.8451			=	3.14E+00	grams		

\* In this appendix, portion of the time interval from 227 to 742 was not visible.

The overall time interval involved of ammonia slip was from 220 to 753 seconds

This appendix is just a preview of the whole numerical integration from 220 to 753 seconds

For details of the ammonia slip trace, please refer to figure 4.9.1a

# Appendix 4.9.2a Excel numerical integration- Urea spray 4SCR

	time	NH3	Area under slip						
	s	ppm							
	0	0	0						
slip start fr spray	270	10	1350						
	271	9	1359.5						
	272	10	1369						
	273	9	1378.5						
	274	10	1388						
	275	9	1397.5						
	276	10	1407						
	277	10	1417						
	278	10	1427						
	947	247	113151.5						
	948	247	113398.5						
	949	245	113644.5						
	950	246	113890						
	951	245	114135.5						
	952	245	114380.5						
	953	246	114626						
	954	245	114871.5						
	955	246	115117		Area under curve =	115363	x	1.67E-05	
slip stop	956	246	115363			=	1.93E+00	grams	

\* In this appendix, portion of the time interval from 279 to 946 was not visible.

The overall time interval involved of ammonia slip was from 270 to 956 seconds

This appendix is just a preview of the whole numerical integration from 270 to 956 seconds

For details of the ammonia slip trace, please refer to figure 4.9.2





















# 10jun08b nh3 up 1 scr 4%

